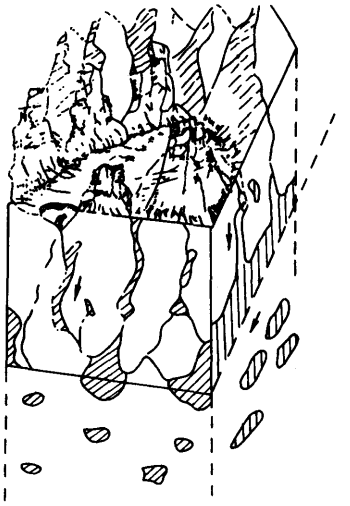

Figure 8. Underground drainage pattern of typical southern China karst. Hachured area indicates underground conduits and arrows show direction of ground-water flow.

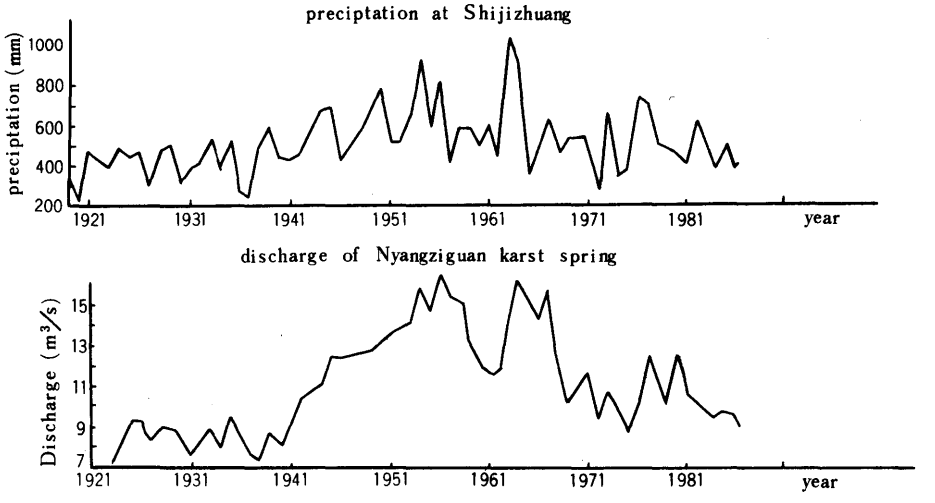

Figure 9. Graphs showing correlation of precipitation and discharge of Nyangziguan karst spring for the past 60 years.

karst systems show that the infiltration rate may be as high as 70 to 90%; for example, the Tisu underground river system has a mean infiltration rate of 0.66, with the low 0.5, and the high 0.8, resulting in a high degree of water table fluctuation (40 m in the lower reach to 100 m in the upper reach). Considering the importance of rapid flow through swallets, vertical shafts, and underground conduits, it is believed that the regulation function of the karst system is poor, as shown by the quick response of output flow to rainfall. After years of effort, hydrogeologists have gradually understood the regulation behavior of the whole system from doline to outlet. During the past couple of decades, through hydrological and hydrochemical analyses of karst springs, karst hydrogeologists, both in China and abroad, have found that the discharge of karst springs is usually a combination of flow in underground passages (conduit flow) and small fissures (diffuse flow). Conduit flow is usually not only fed from a swallow hole, but also regulated by fissure water.

In recent years, studies at the Guilin karst hydrogeological experimental site have revealed that the flow of the outlet is regulated in the system in at least three ways: the soil cover on the slope around a doline, the epikarst zone, and the aeration zone beneath the bottom of the doline (Fig. 8). The behavior is clearly reflected through the storm-response observation data both hydrologically and hydrochemically. Almost every patch of soil on the doline slope has a perched spring, although their discharge is small and changes quickly in response to storm events. Many flow year round and survive the dry season with a discharge of 0.1 L/s and carbonate hardness rising from 110 mg/L during the wet season to 230 mg/L in the dry season.

A humid subtropical doline slope is impressive because of its rough surface, open solutional fissures, and sharp karrens; it appears that this kind of slope surface can absorb all the rainfall and slope runoff and pass it to the underground stream directly. However, drilling data show that the intensely weathered zone is limited to a depth of no more than 10 m. This is similar to the depths determined for the epikarst or subcutaneous zone elsewhere. Deeper than the epikarst zone, the limestone is largely intact; few caves were encountered in boreholes. After a storm, the infiltrated water does not pass directly to the underground stream but forms a flow down the doline slope at a depth of a few meters in the lower part of the epikarst zone.

Many epikarst springs at the bottom of dolines have discharges of 30 L/s and are frequently 100 m higher than the ultimate outlet spring, without any interbedding of impermeable or insoluble rock. Water from epikarst springs is drained by the swallow hole at the bottom of the doline and recharges the main karst hydrologic system. Some epikarst springs can flow through the entire year; in the dry season, epikarst springs comprise about one-half of the total output of the system. The carbonate hardness of these epikarst springs ranges from about 100 mg/L during the storm to about 160 mg/L in the dry season and usually coincides with that of the main outlet spring. These data show the regulation function of the epikarst zone in the hydrologic system.

The regulation effect of the aeration zone below the bottom of doline is reflected in the fluctuation of its water table. Four boreholes ranging from 120 to 250 m in depth were drilled in dolines in the recharge area of the Guilin karst hydrogeological experimental site. The water table in some of the boreholes that hit underground passages has a fluctuation of about 30 m. It rises rapidly after rainfall but falls slowly, indicating that both the underground passage itself and the fissure networks connecting with it play an important role in regulating the hydrographic regime of the karst system. These data regarding the regulation function of a bare karst hydrologic system are useful for a better estimation of karst water resources in a region of this kind; a new mathematical model based on these ideas has been developed.

The most essential characteristic of the interior structure in a karst hydrologic system is its heterogeneity (Yuan, 1985). This feature is more important in mainland China karst because the major carbonate rocks are Pre-Triassic, hard and compact, and with low primary porosity (generally less than 1%; crystalline dolomites may have a porosity of about 5%). Therefore, karst water is mainly stored and flows in various types of karst features in a soluble rock mass rather than in the intergranular or intercrystal porosity. Transmissivity differences between the karst features and wall rock is great; this is the origin for the heterogeneity of karst water. Heterogeneity is always challenging in karst hydrogeological exploration. For example, some wells in karstified strata may yield hundreds of cubic meters of water per hour, but others less than one cubic meter per hour a few meters away. This heterogeneity can be expressed statistically, with the percentage of high-yield wells versus total number of explored wells. For instance, near Wulixu, at western suburb of Guilin, 43 boreholes were drilled in a peak forest plain underlaid by well karstified Lower Carboniferous limestone. The boreholes were in an area 3 km long and 2 km wide; only 14 of them yielded enough water for exploitation. The well completion percentage is 33%; in some extremely heterogeneous examples, the well completion percentage may even be less than 10%.

The karst water heterogeneity is also reflected in the anisotropy of transmissivity in a karst aquifer. This can be seen in the contour map of the water table for the cone of depression around a pumping well; for example, an anisotropic case is in a hydrogeological exploration area near Liuzhou, Guangxi. The middle Carboniferous dolomite aquifer is overlain by silty clay about 10 m thick. When a pumping well had a drawdown of 13.23 m, the cone of depression extended 1,400 m to the northwest, but only 200 to 300 m to the northeast.

The different degrees of karst heterogeneity result from different dimension, direction, density, and degree of integration and connection of karst features in a rock mass. There are many examples of high-well completion in less heterogeneous karst aquifers. For instance, in the Zhaoquing-Fofu synclinal valley, Wumin County, Guangxi, underlain by middle and upper Carboniferous limestone, eight wells, 90 to 120 m in depth, were drilled in an area 5 km long and 2 km wide. Among these, seven are promising, yielding an exploitable discharge ranging from 11.99 to 53.5 L/s. The percentage of well completion for Zhaoging-Fofu area is 88%. An example of less anisotropy is found in Sonkenwu area, Zhejiang Province,

where a pumping test was carried out for the middle Carboniferous limestone aquifer. After 12 hours of pumping, the center well had a drawdown of 30.24 m with a discharge of 23.4 L/s. The cone of depression thus formed was more or less circular, the ratio of the major axis to the minor axis was less than 2.

The heterogeneity of karst can be considered macroscopically (regionally), mesoscopically (for an exploration area), or microscopically (in a hand specimen) (LaFleur, 1984). However, from a practical viewpoint for a hydrogeological exploration area, four degrees of heterogeneity can be distinguished on the basis of two criteria: the percentage of well completion and the ratio of axes for the elliptical cone of depression, as shown in Table 3.

Table 3. Classification of degree of heterogeneity.

Type	Well Completion (%)	Ratio of axes for the cone of depression
Individual cave	5	1
Extremely heterogeneous	20	5
Heterogeneous	20-50	2-5
Relatively homogeneous	80	1-2

The degree of heterogeneity is related to the size and integration of karst features. It is sometimes thought that because there is an evolution sequence from the small, isolated conduit to the integrated network of cave systems, that an extremely heterogeneous type will transform into a relatively homogeneous type in accordance with the intensity or maturity of karstification. This assertion is challenged by the results of field observation. For example, in the humid subtropical southern China karst that has undergone intensive dissolution since the beginning of the Cenozoic or even Late Cretaceous, extensive caves and long underground streams are common. However, their distribution is usually extremely heterogeneous. On the other hand, in the temperate semiarid northern China karst where the karstification process is considered to be less intensive, karst aquifers that are hydrologically more or less homogeneous are not rare. Therefore, the development of different degrees of heterogeneity depend on the manner of karstification rather than only the intensity of karstificaton. There are two categories for karstification: homogeneous karstification and differential karstification. The former can give rise to a relatively homogeneous karst aquifer, whereas the latter usually takes place in a rapid drainage situation and can give rise to an extremely heterogeneous karst aquifer.

The output of a karst hydrologic system is expressed as the discharge, fluid potential, water temperature, hydrochemical composition, air circulation, and other form of energy and material transfer at the outlet of the system. It is the reflection of both the input factors and the regulation functions or reactions occurring within the system. Water is the most important bearer of energy and material and the major

form of output. Many underground streams in southern China rapidly reflect storm events in the monsoon area. The hydrographs not only show good coincidence with the seasonal variation of precipitation but also a short time lag in relation to the storm. For example, the Penshuidong underground stream in Yunnan Province usually has a discharge of 2 to 6 m^3/s during the rainy season from June to September, but in the dry season from October to May, decreases to 0.5 to 1 m^3/s. Moreover, the time lag of its flood peak to the storm event is usually less than five days indicating that the storm pulse is not greatly affected within the system due to the well-developed underground conduits. Some of the extreme cases in southern China have a 1000-fold amplitude of discharge.

The hydrographs of most large karst springs in northern China are different: their discharge is more stable, with high flows no more than twice that of low flows. Peak discharges usually show several months to several years time lag with respect to the relevant rainfall event. For example, the discharge of Lonzhichi karst spring at Linfen County, Shanxi Province, is stable, ranging from 5.4 to 6.7 m^3/s. Moreover, its hydrography usually shows a 6-month lag to the rainfall cycle. The time lag of Nyangziguan karst spring (Shanxi Province) and Baotu karst spring (Jinan, Shandong Province) are seven and three years, respectively. Discharge is delayed in the system because of its large recharge area and the diffuse nature of the flow in the karst aquifer, which is the general case in northern China. This situation is important for water resources estimation and for the exploitation and protection of karst springs, because the systems are acting as big underground reservoirs. For water resources estimation, one needs to consider not only the rainfall of the current year, but also the rainfall of previous years, using as long a record as possible. Additionally, the underground reservoir is more difficult to restore once polluted.

The hydrochemical character of karst water is another important form of output from the karst system. It is a reflection of input factors such as the quantity, intensity, and chemical features of rainfall and surface water flowing into the system, and the chemical reactions occurring within the system. Therefore, the chemical composition of karst water varies with climatic conditions as well as geologic setting. In general, the carbonate hardness increases from colder regions to warmer ones in accordance with lower pH as the carbon dioxide increases. However, geologic factors also play an important part in the formation of hydrochemical features of karst water. For instance, the higher content of the sulfate in northern China karst water is usually from the gypsum present in the Ordovician limestone. The origin of higher magnesium in some regions of northern China and Liuzhou in southern China can be related to the presence of dolomite. If the geologic and topographic settings are favorable for allogenic water to recharge into the karst system, the hydrochemical character can change significantly. The water temperature generally increases with lower latitudes but is modified by topography. For example, some karst springs in Shanxi Plateau have lower temperatures than those at the same latitude in the North China Plain.

ENVIRONMENTAL IMPACTS ON KARST

The exploitation of land, energy, mineral, water, and scenic resources has brought about a series of environmental problems in karst regions, including drought, flooding, deforestation, ground-water pollution, flooding of mine tunnels, surface collapses, and damage to scenic attractions. Almost every problem is related to disturbance of the natural hydrological, chemical, and ecological balance of the karst systems.

The origin of the disturbance is generally human activity. However, because the karst hydrological system is a part of a larger system, it is influenced by characteristics in the lithosphere or the atmospheric circulation system. It is, therefore, sometimes difficult to differentiate between natural and human-induced problems. For instance, there is increasing concern about the discharge decline from all the large karst springs during recent decades in northern China, apparently related to over-exploitation. However, because of the close relation between spring discharge and precipitation, it is reasonable to examine the effect of the multiyear climate trend. The precipitation record of the past 60 years reveals some 20-year cycles. For example, at the Nyangziguan karst spring, 60 km west of the capital of Hebei Province, northern China (Fig. 6 and Fig. 9): from 1923 to 1944 there was a dry period, with a corresponding mean discharge of 8.71 m^3/s (yearly mean discharge ranged between 7.11 and 10.99 m^3/s); the years between 1945 and 1968 were wet, with a corresponding mean discharge of 13.8 m^3/s (yearly mean discharge 11.57 to 16.37 m^3/s); the period since 1969 has been dry, the corresponding mean discharge is 10.27 m^3/s (yearly mean discharge ranging between 8.68 and 12.42 m^3/s) (Zhang Fengqi, 1986). These cycles are important in estimating karst-water resources, especially when a stochastic approach is adopted, and to the decision-makers in charge of long-term planning. Some researchers believe long-term fluctuations in the climate may be related to sunspot activity.

Water pollution from the coal industry which is the major energy source in China is the main environmental problem in Shanxi Province. This is because the coal seams of the Carboniferous System overlie the Middle Ordovician karst aquifer. Again, taking the Nyangziguan karst spring as an example (Fig. 6), it is an important water source for industry, irrigation, and domestic water supply in the northwest part of the great plain in Hebei Province. However, there are important coal industries in its catchment area around Yangquan City (Yuan, 1986a). Downstream from Yangquan, all the surface water, including any industrial waste, is lost along the Taohe River where the water table in the Ordovician limestone is 162 to 193 m beneath the river bed. Thus, the water with high sulfate and high hardness, along with some acid mine water from coal mines, the black water from thermo-electric power station, and all other industrial waste from Yangquan City, recharge the Nyangziguan karst spring and endanger its quality. One of the main environmental effects on karst water is the increase in sulfate and total hardness. The origin of the sulfate may come from the oxidation of pyrite contained in the coal measures or from the gypsum mixed in Ordovician limestone. The $\delta^{34}S$ of the pyrite is -0.8 per mil, while that of the gypsum is 23.8 per mil. The $\delta^{34}S$ of some outlets of the

Nyangziguan karst spring group is 10.9 per mil, while others are 20.1 per mil, indicating that some springs are more affected by the coal industry, whereas other springs are more affected by the dissolution process of the Ordovician limestone and the reduction of discharge in dry years.

In order to use the water resources in karst more efficiently, many water regulating structures have been built to readjust the distribution of water resources in space and time. There are two types of regulating structures: building dams or tunnels along underground streams and building large pumping facilities. Dams and tunnels divert water in the karst system for irrigation or from an underground reservoir to store water in the karst system during the wet season for use during the dry season. There are numerous successful projects of this kind in southern China; however, there are some side effects. One of the problems following the change of a natural drainage system is the flooding of poljes and dolines in the same hydrological system upstream of the dam site. Damage to farmland, villages, and railways has been reported as the result of underground structures. Pumping facilities make use of the underground reservoir in the phreatic zone by pumping more water in the dry season, and letting it be replaced during the wet season. However, the yearly or multiyear water budget must be taken into account or a series of environmental problems, such as lowering of the regional water table, drying up of springs and wells used for water supply, damage to scenic attractions, and surface collapse will take place. An example is Jinan City, the capital of Shandong Province, sometimes called "Spring City" because of its scenic attractions composed of numerous karst springs. The leading one is the Baotu Spring in the downtown area. All the springs have close relations to the major Ordovician limestone karst aquifer underlying the city. In the 1960's, ground-water withdrawal was less than 150,000 m^3/day. In the early 1970's, the total withdrawals in urban areas exceeded 300,000 m^3/day, and was more than 800,000 m^3/day underlying the suburbs. The regional water table declined continuously (Chen, 1984). In 1974, when the water table dropped below the critical level of 27.5 m, the Baotu Spring stopped flowing, and tourism has been seriously endangered. According to preliminary statistics, surface collapse cases resulting from over-pumping of water from karst aquifers have numbered more than 200 in 21 provinces in China; these cases include many thousands of individual collapse points which have caused serious damage (Yuan, 1983).

Buried karst contains oil and natural gas (Sichuan Basin, North China Plain), important brine resources (Sichuan Basin), and geothermal resources, since it is a good reservoir for hot water. In the North China Plain, there are more than 400 geothermal wells 2,200 to 2,600 m in depth, each yielding 1,000 to 2,000 m^3/day of water, with temperature between 45° and 96°C. However, some of these wells have a high fluoride content and become a source of pollution.

In southwestern China, major land resources are on karst plateaus of different elevations, which are usually hydrologically linked by the karst system. Understanding this situation is important to environmental management. For instance, in the Caoba-Kaiyuan area, southern Yunnan Province, there are karst plateaus at elevations of 1,900, 1,300, and 1,100 m above sea level (Fig. 10). All of these are part of a large karst hydrological system. The general outlet of the system

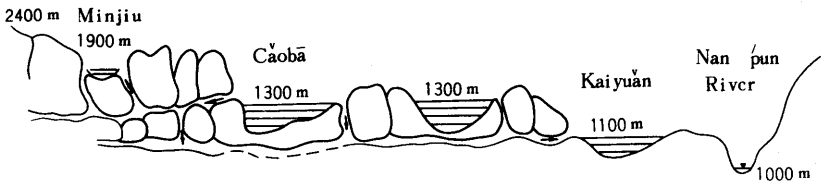

Figure 10. Profile showing the infilling of the Middle Triassic karstified limestone with the less permeable Quaternary and Tertiary sediments (hachured areas) that form plateau farmland. This is an example from Caoba-Kaiyuan area, southern Yunnan Province. Arrows indicate flow direction in the underground drainage conduits.

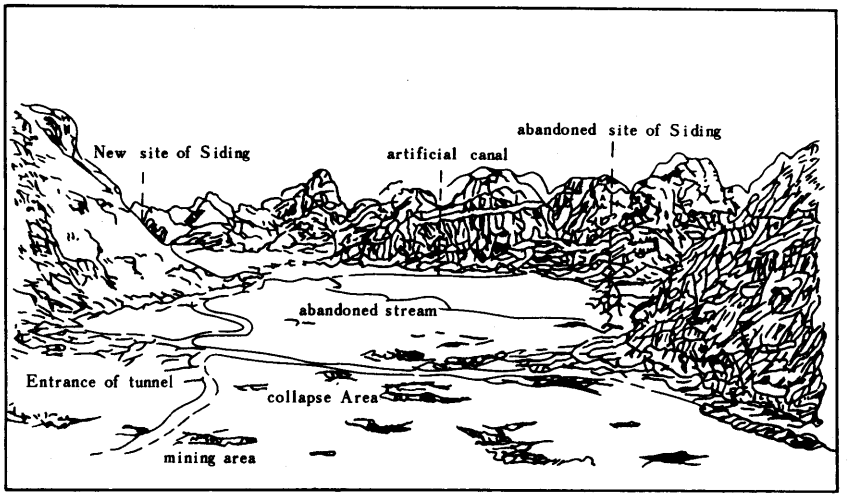

Figure 11. Sketch showing surface collapse in Siding mining area, Guangxi.

is at Nandong, southern suburb of Kaiyuan City, with a maximum discharge of 55.3 m^3/s. It is understandable that water is deficient on the plateau because the vadose zone is 200 to 800 m thick and surface water leakage is serious. However, thanks to the great thickness of impermeable Cenozoic deposits covering the plateau, about 32,400 ha of arable land are around the Caoba area. Moreover, there are important cassiterite deposits on a higher plateau. Along the Nan Pan River gorge, the upper reach of the Pearl River, land resources are limited; this distribution of land and mineral resources causes agriculture, mining, and related industries to be developed in the recharge area of the hydrologic system where the water resources are poor. Meanwhile, the pollution brought about by the waste from mining and the use of pesticides and fertilizers in the recharge area at the Nandong underground stream endanger this important water resource for Kaiyuan City.

Many mineral deposits in China, such as coal, iron, and some non-ferrous mineral deposits, are related to karst aquifers and, consequently, have a series of environmental problems. The most disastrous one is the sudden flooding of mining tunnels with water and mud. This brings about loss of life and property. In past decades, incidents of sudden flooding in karst-related coal mines with discharges more than 1 m^3/min occurred 1,000 times, while those with discharges ranging between 10 m^3/min and 100 m^3/min numbered 120, and 17 incidents were recorded with a discharge of more than 100 m^3/min. Some mines must pump more than 100 m^3 of water to mine one ton of coal. Sudden flooding in mine tunnels may in turn induce many environment problems such as decline of the regional water table, causing springs and wells for water supply to dry up and surface collapse. For example, in the 1960's and 1970's, serious surface collapse took place in the Siding non-ferrous mineral deposit in Guangxi (Fig. 11), which destroyed the Siding village and brought about a loss of about one-third of the stream flow when a discharge of 14.49 m^3/s poured down the mining tunnel (Yuan, 1987).

CONCLUSIONS

This discussion on the karst and karst water in China could be concluded as follows:

1. Karst and its water resources are important in China because of their vast area with rich energy, mineral, land, and tourism resources.

2. Controlled by the framework of soluble rock, the karst water circulates through thousands of hydrological systems of varying sizes. A better understanding of the karst hydrological systems is the key to the proper estimation and use of the water resources to avoid environmental deterioration.

3. A karst hydrological system is composed of soluble rock and its occurrence, karst features, and the water and air circulating through the system and reacting with the karst features. Soluble rock is a prerequisite, but it is the karst features that control the behavior of water in the karst system.

4. The degree of openness of a karst hydrological system decreases from bare karst to covered karst to buried karst. These karst types are the results of different geological history and tectonics.

5. To examine the behavior of karst water in the hydrological system, its storage and flow through the various karst forms, including both surface and subsurface ones, a basic knowledge of karst features and the karst hydrological system is required.

6. The two major factors that affect the development of karst features are geology and climate.

7. The chemical output of karst hydrological system is varied in accordance with climatic conditions but modified by geology and topography.

8. The karst hydrological system is itself a part of a larger system including the atmospheric circulation system and the lithosphere.

9. To use karst water resources reasonably and avoid deterioration of the environment, it is necessary to prepare a comprehensive plan for the use of water and other resources in karst regions.

REFERENCES

Chen Zhengpeng, 1984, Protection of karst springs in Jinan, Shandong: (in Chinese, English abstract), Carsologica Sinica, v. 3.

LaFleur, R.G., 1984, Ground water as a geomorphic agent: Boston, Allen and Unwin Inc., 390 p.

Li Daton, 1983, An estimation on the area of carbonate rock in China: (in Chinese, English abstract), Carsologica Sinica, v. 2.

Yuan Daoxian, 1981, A brief introduction to China's research in karst: The Institute of Karst Geology, 35 p.

Yuan Daoxian, 1983, Problems of environmental protection of karst area: Paper presented to the annual meeting of AAAS, Detroit, Michigan, 15 p.

Yuan Daoxian, 1985, The heterogeneity of karst water: IAHS Publication no. 161, p. 281-292.

Yuan Daoxian, 1986a, Some characteristics of ground-water protection in karst area: IAH memoires, v. XIX, pt. 2, 135-142, Novinar Publishing House.

Yuan Daoxian, 1986b, New observation on tower karst: International Geomorphology, pt. II, p. 1109-1123, John Wiley and Sons, LTD.

Yuan Daoxian, 1987, Keynote address: Environmental and engineering problems of karst geology in China: Karst Hydrogeology, Engineering and Environmental Applications, p. 1-11, A.A. Balkema.

Yuan Daoxian, 1988, On the karst environmental system: Proceedings of the 21st Congress of IAH, Karst Hydrogeology and Karst Environment Protection, Geological Press.

Yang Lizheng, 1985, The underground streams in South China karst: (in Chinese, English abstract), Carsologica Sinica, v. 4.

Zhang Fengqi, 1986, Water resources estimation for Nyangziguankarst spring: (in Chinese) The Institute of Hydrogeology and Engineering Geology.

Zhang Shouyue and others, 1979, Research of karst in China: (In Chinese), Academic Press.

FLOW REGIMES IN KARSTIC SYSTEMS : THE JUDEAN ANTICLINORIUM, CENTRAL ISRAEL

LEVY KROITORU*
and
EMANUEL MAZOR

Geoisotope Group
Weizmann Institute of Science
Rehovot 76100
Israel

and

ARIE ISSAR
Jacob Blaustein Institute of Desert Research
Sede Boqer Campus
Ben-Gurion University of the Negev
Beer Sheva
Israel

ABSTRACT

Recharge in the Judean Mountains anticlinorium is rapid with water moving in the aerated zone, 100 to 350 m deep, primarily in karstic conduits. This interpretation is based on low water temperatures, noble gases-deduced low intake temperatures, and rapid arrival of the bomb tritium signal. Water-rock interactions are completed upon arrival at the saturated zone with no additional water-rock interaction during the downgradient flow in the phreatic zone. The eastern flank of the anticlinorium, the Judean Desert, was found by tritium and ^{14}C data to have a ground-water system that is controlled by karstic conduits with water flow being more rapid in the upper part ("Springs System") than in the confined deeper part ("Wells System"). The springs reveal an intermixing of up to 60-70% old water at the west, close to the recharge area. The western flank of the anticlinorium, the Foot Hills and Shephela Plain, has also a two-fold ground-water system, but with reversed pattern: a deep karstic fast-flowing system, as indicated by low temperatures and high ^{14}C values, and a shallow confined slow-flow system, as reflected by warmer temperatures and lower ^{14}C values. The transition from the central phreatic aquifer to the eastern and western confined systems is abrupt as reflected by disappearance of tritium and significant drop in the ^{14}C values. At the western phreatic-confined contact zone dissolved gases reveal a drastic drop in the dissolved oxygen and nitrogen content, and an increase of H_2S in the confined water. Recent saline water is observed (by dissolved ions, tritium, and ^{14}C data) to intermix with old, confined water in the northeastern wells of the Judean Desert

*Present address: Roy F. Weston, Inc., 955 L'Enfant Plaza, S. W., North Building, 8th Floor, Washington, DC 20024

International Contributions to Hydrogeology, Vol. 13 (1992)
© Verlag Heinz Heise, Hannover, FRG

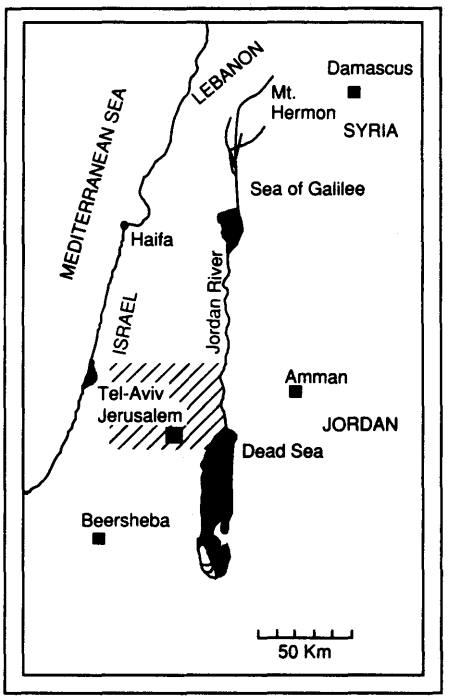

Figure 1. Location map.

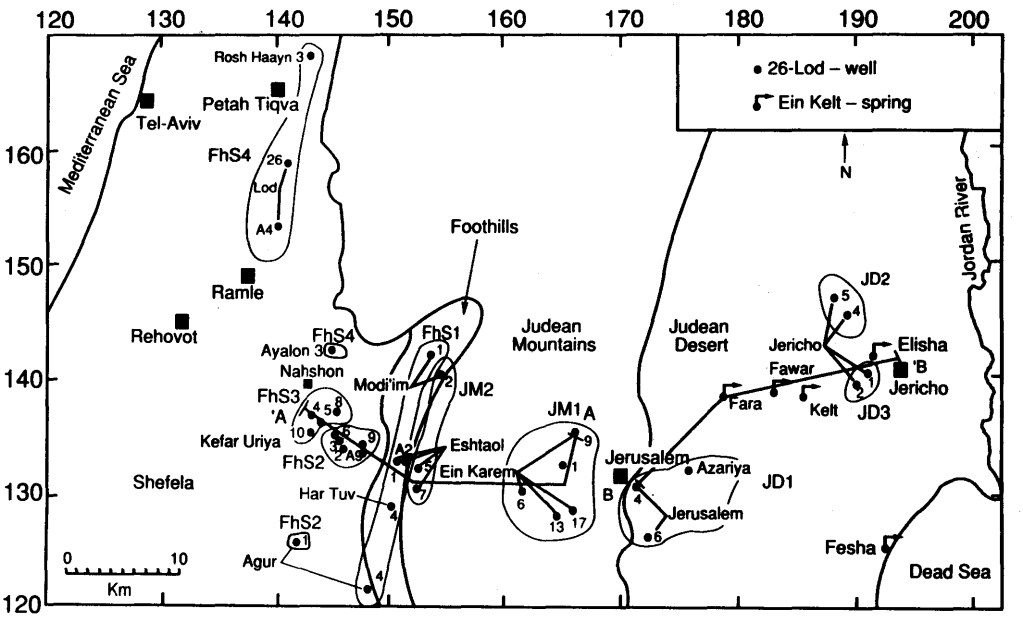

Figure 2. The hydrogeological regions of the study area.

that border upon the Rift Valley, and in a small group of wells in the Shephela plain underlying a phreatic aquifer of Senonian rocks.

INTRODUCTION

Mountainous terrains of limestone and dolomite are commonly karstified, the degree and mode being determined by the local, present and past, climatic and geologic history. As a result, countless combinations are formed of co-existing fast-flowing and slow-flowing sub-systems of the aerated zone and of phreatic and confined sections of regional ground-water systems.

Physical, chemical, and isotopic parameters, monitored in springs and wells, supply the means to understand in detail local ground-water plumbing systems. The research strategy adopted in this study was: 1) ground-water temperatures and noble gas-deduced intake temperatures were used to differentiate slow-flowing water in porous media, equilibrating to local soil temperatures, from fast-flowing water in karstic conduits, with cold winter temperature, 2) fast and slow flows were identified independently by tritium and ^{14}C, 3) dissolved ions were used to recognize types of rocks along the flow path, 4) discordant tritium-^{14}C ages and linear ionic correlation ("mixing lines") were applied to identify intermixing of different water types, and 5) degrees of hydraulic communication between phreatic and confined sections of the ground-water system were verified with the aid of chemical and isotopic transects.

HYDROGEOLOGICAL SETTING

Geography

The area is in the central part of Israel (Fig. 1). It includes a strip 10-15 km wide from the Rift Valley, Jericho area, through the Judean Mountains, Jerusalem area, to the Shefela area, from Har Tuv to Rosh Ha'ayn (Fig. 2). In the study area the elevation ranges from 800 m in the Judean Mountains to approximately 100 m in the Shephela area and to 200 m below sea level in the Rift Valley. The area has a semiarid Mediterranean climate, with a short rainy season from November to March. Precipitation ranges from 600 mm/a in the Judean Mountains to 400 mm/a in the Shefela area and to less than 100 mm/a in the Rift Valley.

The study area has been divided into three regions (Fig. 2) based on structural geology, water levels, and tritium and ^{14}C data. The three areas are 1) the Judean Mountains (JM)--the main recharge area, 2) the Foothills and Shefela (FhS)--western drainage basin, and 3) the Judean Desert (JD)--eastern drainage basin. This subdivision is used throughout the chapter while reporting the results and discussion.

Geohydrology

The most conspicuous geological feature is that of the anticlinal crest of the Judean Mountains of Cretaceous formations, which dip eastward toward the Rift Valley and westward toward the Shephela area where they are overlain by younger formations (Figs. 3 and 4). The Upper Cretaceous formations comprise the regional

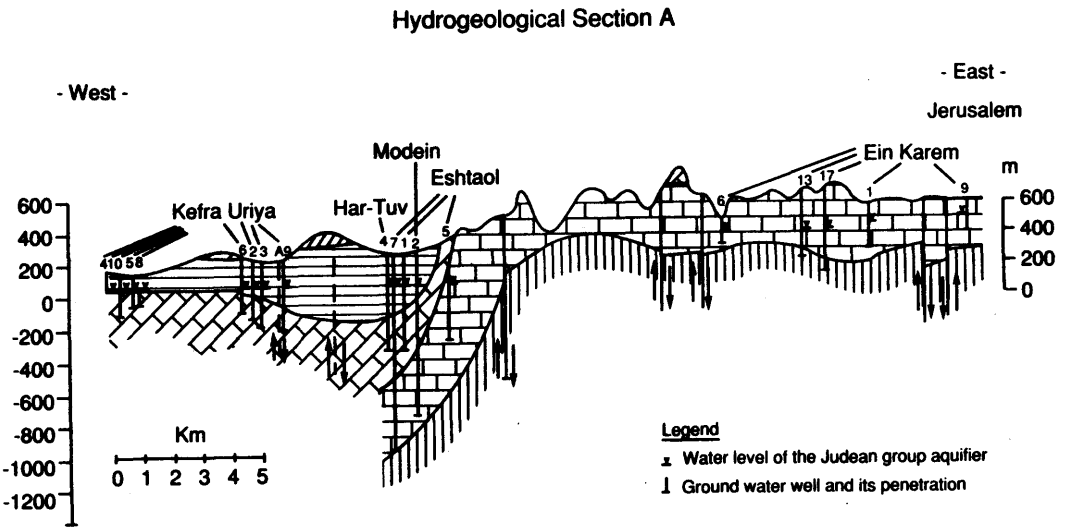

Figure 3. Hydrogeological section A (see legend on Fig. 5).

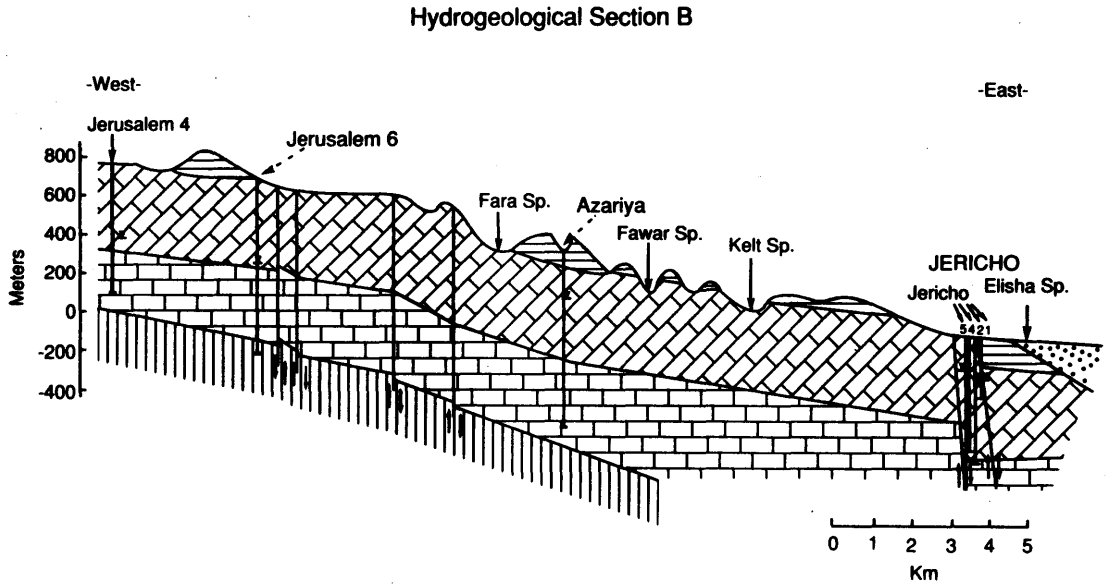

Figure 4. Hydrogeological section B (see legend on Fig. 5).

carbonate Judean Group ground-water system. The thickness of the ground-water system in the study area ranges from 400 to 700 m. The Judean Group ground-water system is underlain by Lower Cretaceous shale, chalk, and marl. The Judean Group rocks crop out in the Judean Mountains, in parts of the Judean Desert, and near Rosh Ha'ayn at the Shephela (Fig. 5). In the rest of the area the Judean Group is covered by Senonian-Pleistocene aquitards and aquicludes.

Shachnai (1980) subdivided the Judean Group ground-water system into two units with leaky communication through a third unit. In the Judean Desert region, Guttman (1980) divided the Judean Group into the lower and upper regional subaquifers.

Hydraulic Properties

The hydraulic properties of the Judean Group ground-water system are not uniform. Of special importance in the Shefela area is the disappearance of the intervening middle-aquitard unit westward, near the facies transition of the platform carbonate to the open-shelf shale units (Talmei Yafe Group). A series of reefs developed along the continental shelf, between the shallow platform to the east, where the Judean Group was deposited, and the deep basin to the west, where the Talmei Yafe chalk-marl formation was deposited (Bein, 1974). The reef-building stage transcended stratigraphic boundaries and resulted in a blurring of the internal subdivision in the Judean Group. The reef structure facilitated dolomitization of the limestone. As a result the Judean Group in the coastal area can be viewed as one dolomitic unit. An almost mirror image of this geologic section is on the eastern flanks of the Judean Mountains in the Judean Desert, except that the aquifer terminates in graben faults, as opposed to a Talmei Yaffe facies analog (Shachnai, 1980).

Recharge and Discharge of the Systems

The main recharge of the ground-water system is through the Judean Group outcrops in the Judean Mountains, estimated to be 352-357 x 10^6 m^3/a (Mercado, 1980). The annual recharge to the Judean Desert is estimated by different authors from 90 to 150 x 10^6 m^3. For the western foothills and Shefela, estimated recharge ranges from 25 to 50% of the total recharge to the lower subaquifer. In the east, estimates as high as 60 to 80% of total recharge have been made for the recharge component entering to the lower subaquifer in the Judean Desert.

The drainage of the Judean Group ground-water system in the Judean Desert is thought to occur through spring discharge in the Judean Desert and along the Dead Sea, mainly at the Fesha springs. The Fesha springs are a major discharge area for most of the deep aquifers (Kroitoru, 1980). The isotopic and chemical composition of the Fesha waters reflect intermixing with the Dead Sea brines (Mazor and Molcho, 1972). The natural drainage of the Judean Group ground-water system in the Shefela plain is primarily by way of discharge of the Rosh Ha'ayn spring complex (Mandel, 1961). This latter discharge ceased in the early 1960's due to extensive pumping.

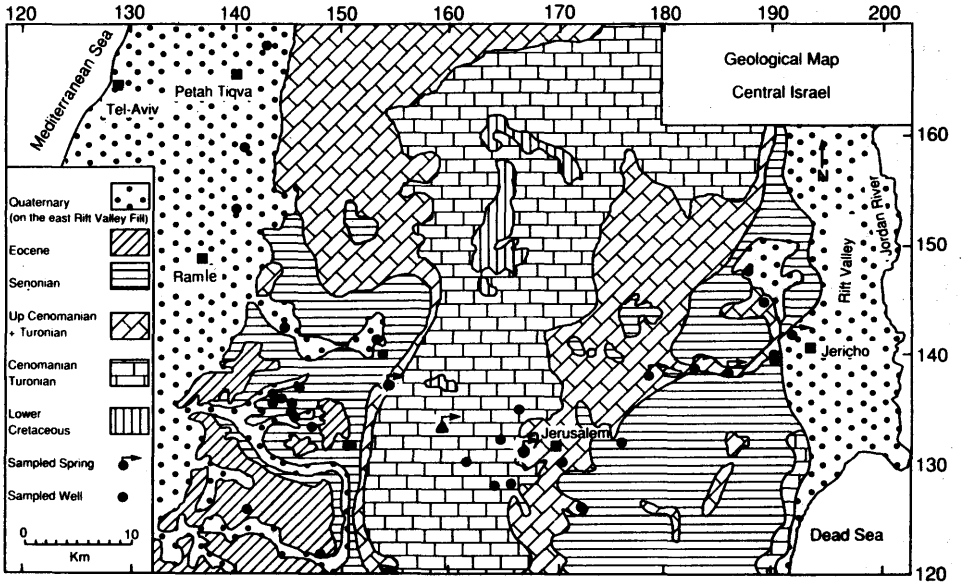

Figure 5. Geological map of central Israel.

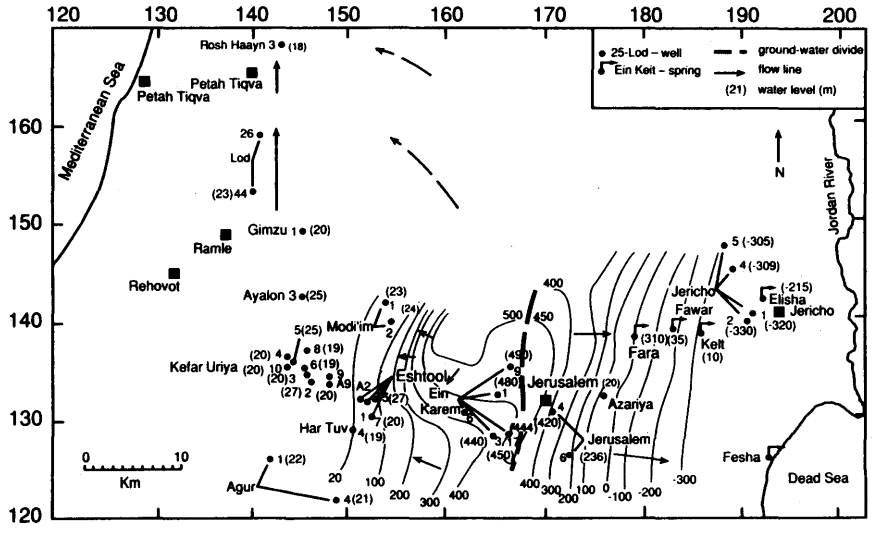

Figure 6. Water levels and flow directions in the Judean Group ground-water system.

Communication Between the Systems

Water levels indicate two main flow directions: eastward to the Rift Valley and westward to the Shefela coastal area (Fig. 6). In the Judean Desert the difference in heads between the two subaquifers is about 60 m higher in the upper unit. In the Shefela area the differences are smaller, the lower aquifer exhibiting higher levels, on the order of 0.5 m (Mero, 1978). The differences in water levels between the two subaquifers in the study area are not sufficient to establish hydraulic communication between them. This is especially true for the Shefela area, where most of the wells were drilled into the upper unit, and extensive pumping since the 1950's has disturbed the natural water levels. In the Judean Desert, the karstic nature of the flow with up to five separate water levels in the Ma'ale Adummim-2 Well complicates identification of hydrologic connection between the subaquifers (Shachnai, 1981).

Mercado (1980) attempted to delineate interconnection between the subaquifers in the Shefela area, using Cl^- content as a tracer. He proposed a conceptual model suggesting that areas of low Cl^- within the upper subaquifer denote upward leakage from the fresher lower aquifer unit. Greitzer (1963) attributed the salinity exhibited by the Upper Cenomanian-Turonian to saline strata (Senonian) overlying the aquifer. He suggested that salty paleo ground water from the Lower Cretaceous can also serve as a salinity source.

Rosenthal and Kronfeld (1982) and Guttman and Kronfeld (1982) defined the two subunits in the eastern drainage basin, the wells system and the springs system, by the use of $^{234}U/^{238}U$ signatures. However, using stable isotopes of carbon and oxygen, these workers were unable to differentiate the two units (Kronfeld and Rosenthal, 1984).

DISCUSSION OF THE FLOW SYSTEMS

The Judean Mountains

The recharge area wells can be divided into two groups (Fig. 2): Group JM1, five wells in the phreatic zone, and Group JM2, three wells at the boundary between the ephratic and confined zone, 15 km downgradient.

Chemical Composition

The wells studied are fresh, the water containing up to 12.7 meq/L of TDS (Fig. 7). The composition of the water (by equivalents) is $Ca^{2+}>Mg^{2+}>Na^+$ and $HCO_3^->Cl^->SO_4^{2-}$. The chemical composition of the water in the eight wells is almost indistinguishable and was found to have been constant over the last 10 years. The exhibited variations in TDS were limited to less than 2 meq/L over this time period. This observation suggests that well groups JM1 and JM2 belong to the same hydrological system. All wells are saturated with respect to dissolved oxygen (DO) at 6-9 mg/L and exhibit redox values in the range of 100-180 mV (Fig. 8). The log P_{CO2} for this area is -2.15 to -1.95.

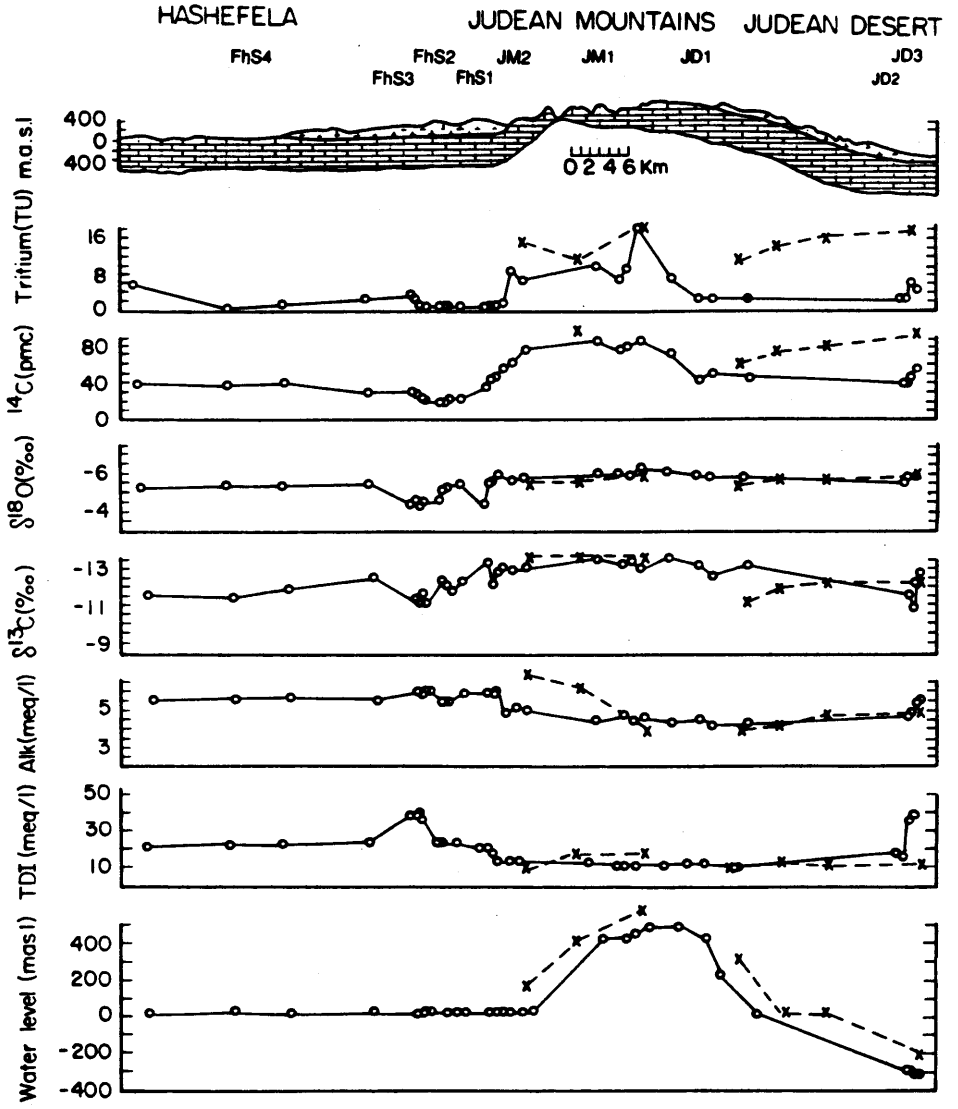

Figure 7. Schematic east-west transect through the Judean Mountains of the Judean Group ground-water system. Isotopic, chemical, and physical parameters of the sampled wells (o) and springs (x) are plotted along the transect.

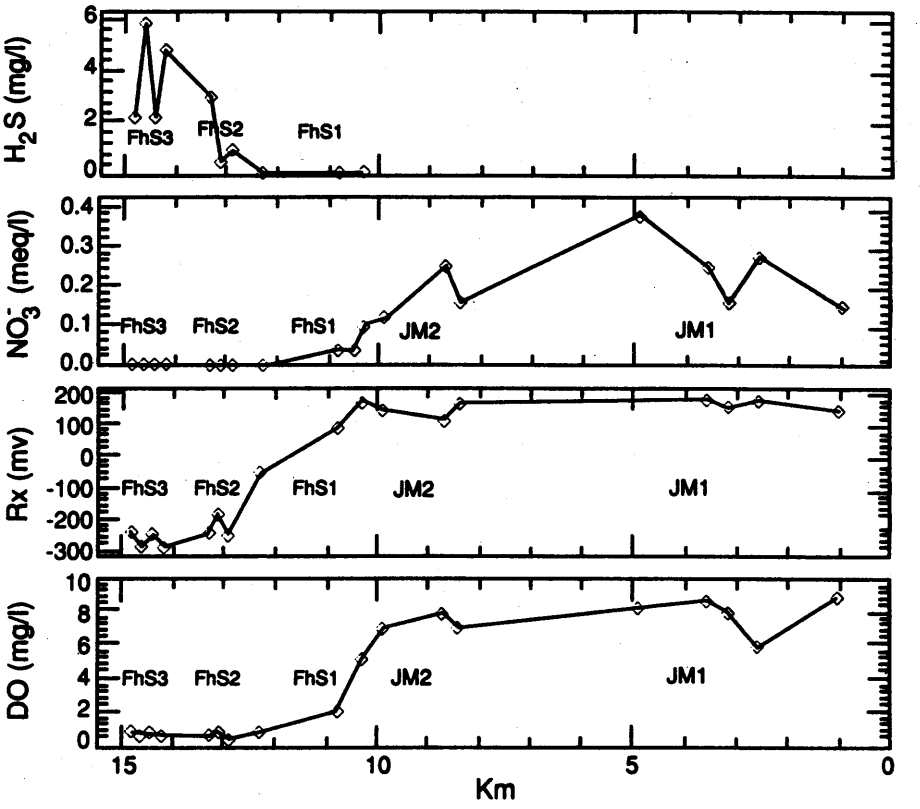

Figure 8. DO (dissolved oxygen), Rx (redox potential), NO_3^-, and H_2S down the hydraulic gradient along hydrogeological section A.

Isotopic Composition

The ^{14}C activity in the ground water of group JM1 is 71-87 pmc. Downgradient, the JM2 group has a ^{14}C activity in the range of 57-79 pmc (Fig. 7). The tritium contents of group JM1 and JM2 are 6-17 TU and 1.5-8 TU. In both groups the ground water $\delta^{13}C$ is -12.6 ± 0.3 per mil. The wells converge around the value of -22.04 ± 1.5 per mil for δD and -5.8 ± 0.2 per mil for $\delta^{18}O$, which lie on the local meteoric water line (Fig. 9) as defined by Gat and Dansgaard (1972). A recharge area common to all the studied waters thus seems plausible.

The chemical and isotopic data indicate that the water attains its chemical composition upon arrival at the saturated zone. From there onwards, during the downgradient flow in the recharge zone and at the transition to the confined zone, no additional water-rock interaction processes are observed, as indicated by the chemical-isotopic similarity of the ground-water composition of groups JM1 and JM2. Geochemical-isotopic mass transfer calculations for the evolution of the recharge area ground water (Kroitoru, 1987) indicated a 40% decrease in ^{14}C concentrations (relative to soil CO_2-^{14}C) due to water-rock interactions. The observed variations in the ^{14}C concentrations of the recharge area wells were interpreted as caused by different contributions of recent water of pre-bomb age (100 pmc) and post-bomb age (>100 pmc).

Karstic Flow Indicated by Ground-Water Temperatures

Temperature ranges of 19.5-21.5°C and of 23.5-25°C are observed in the wells of groups JM1 and JM2, respectively. Bartov and Bein (1977) reported an average local thermal gradient of 1.8°C/100 m. The local average rainy season temperture is 10°C, and the annual average temperature is 18°C. Ein Karem 17 has been selected to represent the JM1 group of wells, and Eshtaol 7 to represent the JM2 group of wells.

At the E. Karem 17 well (well depth 520 m, depth of water table 170 m, that is, average depth of exploited aquifer 350 m), a temperature of 1.8°Cx3.5+18°C=24.3°C would be expected for the case of full temperature equilibration, for slow intake in porous media. However, a temperature of only 19.5°C has been obtained for the water pumped from this well, reflecting a memory of the winter season temperature. This indicates rapid karstic conduit recharge allowing for only partial temperature equilibration. Esthaol 7, the deepest well of group JM2, was drilled to a depth of 1,226 m. The pumped water system was encountered at a depth of 600 m, that is, the average depth of the exploited aquifer was 900 m. For full temperature equilibration the pumped water would be expected to have a temperature of 1.8°Cx9+18°C=34.2°C. In fact, a temperature of only 25°C is observed for the water pumped in the Eshtaol 7 well. This indicates that the rapid karstic flow exists also in the confined zone of the Lower Judean Group aquifer.

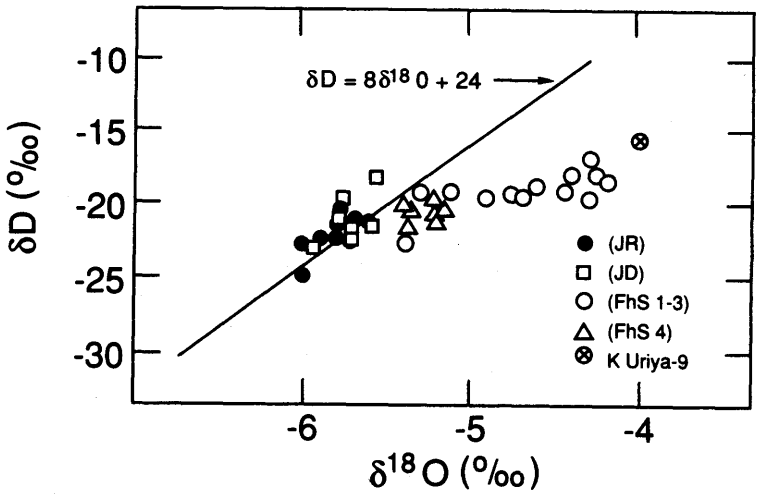

Figure 9. Stable isotope composition of the Judean Group ground-water system.

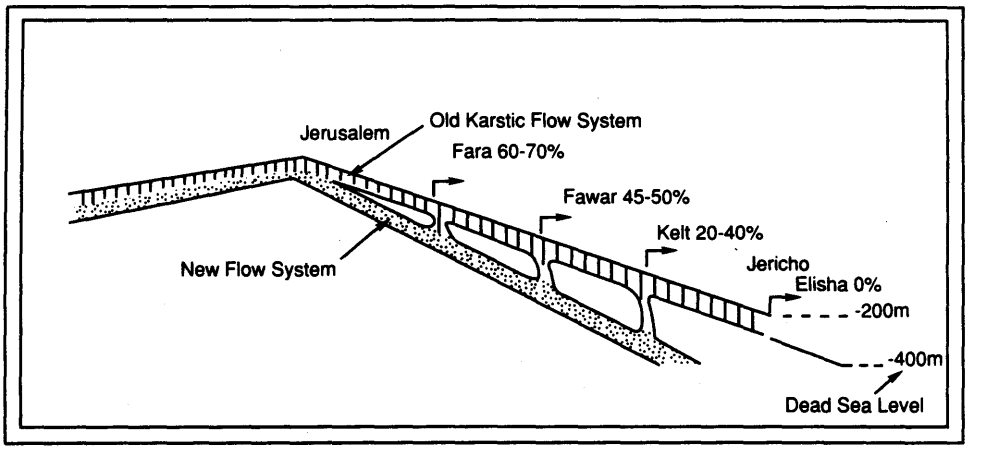

Figure 10. Schematic presentation of the ground-water flow systems in the Judean Desert. Mixing percentages in the sampled springs are calculated from the ^{14}C data of the wells and the springs in the area.

Karstic Flow as Indicated by Noble Gases, Excess Air, and Intake Temperature

Noble gas data include equilibrium concentrations of recharge water at 10°C and 18°C (average rainy season temperature and the average ambient annual temperature, respectively) at 650 m (average altitude at the recharge area). A general trend of excess atmospheric noble gases is observable with a pattern of excess He> excess Ne> excess Ar> excess Kr> excess Xe. Excess air has been observed for karstic systems (Herzberg and Mazor, 1979) and in some soils in South Africa (Heaton and Voegel, 1981). The present observation of excess air supports the conclusion of a karstic nature of the study area. The noble gas data were used to compute intake temperatures. The noble gas-deduced temperatures range from 7°C to 18°C, between the average annual surface temperature and the winter rainy season temperature. The average depth of the aerated zone is about 200 m. Hence, the increase in temperature for 200 m should be about 3.6°C. Temperature equilibration at the base of the aerated zone should lead to a temperature of 21.6°C (annual average temperature + 3.6°C). The calculated intake temperatures (7-18°C) indicate that temperature equilibration in the aerated zone is only partial. Thus, the comparison of noble gas-deduced intake temperatures and the ambient surface temperatures indicates a rapid recharge into the local aquifer, in spite of the relatively large depth of the aerated zone. Hence, both the excess noble gases and the calculated noble gas intake temperatures indicate short karstic flow recharge. Recharge through homogeneous porous media in the aerated zone seems to be of minor importance. Independent indication for a short transit time in the unsaturated zone is provided by the tritium data. Carmi and Gat (1973) noted that flooding events are reflected immediately (on the same or the following day) in the wells' tritium data.

Foothills and Shefela

The sampled wells can be divided into four groups (Fig. 2) by geographical distribution: Group FhS1, four wells in the foothills area; Group FhS2, four wells in the Kefar Uriya area; Group FhS3, four wells in the Nahshon area; and Group FhS4, four wells in the Rosh Ha'ayn-Lod area.

Chemical and Isotopic Composition

Based on the chemical and isotopic composition of the ground water the Judean Group is subdivided into two subsystems: 1) the Upper Judean Group system (Upper Cenomanian, Turonian, and Lower Senonian), with relatively high TDS (up to 40 meq/L) and low in ^{14}C (as low as 18 pmc), indicating the existence of a slow ground-water flow system, and 2) the Lower Judean Group system (Lower Cenomanian, Albian), significantly lower in TDS (about 12 meq/L) and high ^{14}C values (as high as 75 pmc), indicating the existence of a fast karstic flow system. Thus, in the FhS area, two types of flow systems have been defined, a slow flowing system underlain by a fast flowing one.

The chemical-isotopic evolution in the Upper System is controlled by: 1) water-rock interactions that occur along the FhS area where the Senonian rocks overlie the Judean Group, and 2) contribution of ground water from local Senonian aquifers to the Judean Group ground-water system in areas where the Senonian strata are thinning, changing facies, or missing (mainly in the Nahshon area, FhS3). The water-rock interactions are explained by two geochemical processes: 1) organic carbon oxidation by nitrate and sulfate reduction, resulting in a P_{CO2} increase, decrease of DO and NO_3^- to zero, and redox potential to -290 mV, and the appearance of H_2S (Fig. 7). The source for the dissolved organic carbon is the solid-phase organic matter from the Senonian rocks; and 2) incongruent dissolution of dolomite, driven by irreversible dissolution of sulfate. The gypsum contained in the Senonian rocks is flushed by ground water resulting in an influx of calcium ions. As a result, the water becomes supersaturated with respect to calcite which starts to precipitate, causing the water to become undersaturated with respect to dolomite. Dolomite continues to dissolve as calcite precipitates. These stages are evident from the gradual increase in the SO_4^{2-} in ground water from the recharge area through FhS1, FhS2, to FhS3.

In the Nahshon area (FhS3), young water from the overlying local Senonian aquifer enters into the Judean Group system as indicated by the observed increase in salinity, tritium, and ^{14}C, relative to the FhS2 group (Fig. 7). Mixture with Senonian waters is also evidenced by the ^{18}O and deuterium data, since the FhS wells are located on a mixing line with the Senonian waters, represented by K. Uriya 9 (Fig. 9). Geochemical-isotopic mass transfer calculations along selected flow paths in the FhS area (Kroitoru 1987) reveal a decrease of about 10 pmc in the ground-water ^{14}C due to water-rock interactions at the Foothills (FhS1) and a further drop of 6 pmc at the Shefela (FhS2) wells. The corrected ^{14}C values point to an age of recent to 1600 years at the Foothills (FhS1) and 5500 to 7500 years at the Shefela (FhS2) area.

In contrast to the Upper Judean Group system, no further water-rock interactions occur in the Lower Judean Group waters, as indicated by the similarity between the JM1 and JM2 groups which are 15 km apart, the latter located at the foothills area. No accessible wells from this system are available further downgradient in the Shefela area. However, it is suggested that the Lower Judean Group system continues to act as a separate unit, containing fresh and probably young water, as compared to the overlying Upper Judean system. A separate recharge area for the lower system is indicated by: 1) the $\delta^{18}O$ and deuterium data (Fig. 9), since these values were found to be heavier in the upper system, indicating recharge at lower altitudes, and 2) the ground-water temperatures in the upper system are higher (by about 4°C) than those of the lower system, in spite of the fact that they are pumped from 400 to 800 m shallower depths.

The contribution of low ^{14}C and high tritium observed at the Rosh Ha'ayn-Lod area, has been shown to indicate mixing of the JM2, FhS2, and FhS3 ground-water systems. The local absence of the Senonian aquitard in this area (Fig. 5) may also allow direct local recharge. The mixed water was discharging at the Rosh Ha'ayn springs until pumping dried them up in the beginning of the 1960's.

Judean Desert

Seven wells and four springs were sampled from the Judean Desert. The wells can be divided into three groups (Fig. 2) based on their geographic location and their water chemistry: Group JD1, three wells in the Jerusalem area; Group JD2, two wells northwest of Jericho; and Group JD3, two wells west of Jericho. The springs sampled are the Wadi Kelt springs (Fara, Fawar, Kelt) and Elisha (Fig. 4).

Chemical Composition

The chemical data reveal that the JD1 wells are similar in composition to the water in phreatic JM1 waters (Fig. 7). Further east, the JD2 waters reveal an increase of about 5 meq/L in cation concentration, led by Mg^{2+} and Na^{+}, and similar increases in anion concentrations, mainly Cl^{-} and small amounts of SO_4^{2-} and HCO_3^{-}. The JD3 wells, bordering upon the Rift Valley, reveal a more distinct increase in Na^{+}, Ca^{2+}, and Mg^{2+}, along with Cl^{-}, SO_4^{2-} and HCO_3^{-}, reaching a TDS concentration of 40 meq/L. These trends can be explained by intermixing of ground water originating from the Rift Valley Fill, and interaction with the aquifer rocks, which change in composition from limestone in the west to dolomite in the east. The Wadi Kelt and Elisha springs are nearly uniform in their chemical composition (Kroitoru et al., 1985). The composition of the water (by equivalents) is $Ca^{2+} > Mg^{2+} > Na^{+}$ and $HCO_3^{-} > Cl^{-} > SO_4^{2-}$ and the water is fresh, containing an average of 12 meq/L TDS, with only slight seasonal variations.

Isotopic Composition

Both tritium and ^{14}C reveal a sharp and remarkable decrease at the transition zone from the phreatic section of the studied water system (Group JM1) to the eastern confined system (Group JD1). This discontinuity seems to indicate that the flow from the phreatic section to the confined one is restricted, a phenomenon that seems to be more common than so far noticed (Mazor and Kroitoru, 1987). Approaching the Rift Valley, the JD3 wells reveal a slight increase in ^{14}C and tritium (Fig. 7), indicating intermixing with a recent, post-bomb water component. Thus, the saline water that intermixes in the JD3 wells, is of a post-bomb age. The deuterium and $\delta^{18}O$ data of the Judean Desert wells are undistinguishable from values in the Judean Mountains phreatic aquifer (Fig. 9). This is an important observation as it establishes that recharge in the Judean Mountains is the sole source of water in the Judean Desert ground-water system that is tapped by the studied wells (JD1, JD2, and JD3 groups). There is no trace of paleowater, namely, water recharged under a different climatic regime.

The Judean Desert springs reveal a distinct pattern as compared to the wells. The tritium concentrations are 7-22 TU and the ^{14}C values are 57-91 pmc (Fig. 7). Thus, a post-bomb component is dominant and fast flow from the phreatic aquifer of the recharge zone is established. The ^{14}C values warrant closer examination. They are 57-62 pmc for the Fara spring, 68-70 pmc for the Fawar spring, 72-80 pmc for the Kelt spring, and 84-91 pmc for the Elisha spring. Thus, the ^{14}C concentration increases with the distance from the recharge zone. This unexpected trend invokes the following model. In the Fara spring, recent, post-bomb, and old water (from the confined part, represented by the wells group JD1) intermix. The contribution of old water is smaller in the downgradient Fawar and Kelt springs and nil at the Elisha spring that issues on the western border of the Rift Valley. Mixing ratios have been calculated assuming the recent end-member is of the Elisha type water (~90 pmc) and the old end-member is represented by the well water (~40 pmc). The results are presented in Figure 10.

The average ground-water flow velocity from the Judean Mountains to the Elisha spring is about 1.5 km/a (Kroitoru et al., 1987). This calculation is based on the observation that the bomb tritium signal was first observed in 1968 at the Elisha spring. Thus the Elisha spring seems to be fed by fast underground flow, which in turn, indicates the presence of karstic conduits in the upper part of the Judean Desert ground-water system. The karstic conduits must be fossil since, at present, evolution of karst is arrested in the desert regime.

The Judean Desert ground-water system thus seems to host old ground water of 1800 to 4000 years old in its deeper part, the "Wells System," and recent water in its upper part, the "Springs System." The two systems seem to be partially interconnected, providing an old water component to the springs, most significantly in the western part (close to the recharge area) and less farther eastward. The model is depicted in Figure 10.

Measurements of the "Springs System" indicate the same trend as in the JM group. Both excess noble gases and calculated noble gas temperature (Kroitoru, 1987) provide an additional indication for fast karstic recharge in this system.

GENESIS OF THE SYSTEMS

The western drainage area of the Judean Group ground-water system has an upper slow-flow system and a deeper fast-flow system. The degree of karstification seems to be controlled by the extent of the recharge areas and the distribution of their facies. The upper system being fed by a narrow band of karstiferous Cenomanian-Turonian outcrops passing laterally to chalky, shelf basinal units leading to little karstification. In contrast, the lower system is fed by extensive outcrops at the Judean anticline providing water for intensive karstic development.

The eastern drainage area of the Judean Group ground-water system has a flow pattern that is a reverse picture of the western region: an upper fast-flow karstic system emerging in the springs and a lower slow-flow system encountered by the wells. The existence of well-developed karstic conduits in the upper system

indicates a high former base level. This must have been the high level of the Lisan Lake (up to 180 m below mean sea level) (Begin et al., 1987), which correlates with the Elisha spring altitude (180 m below mean sea level). As the Lisan lake receded and the drainage basin was lowered, a new system started to develop (Fig. 10), most probably under drier and less favorable climatic conditions.

REFERENCES

Bartov, Y., and Bein, A., 1977, Mediterranean-Dead Sea hydroelectric project. The existence of oil, gas and thermal water: GSI report 77/8/MM (in Hebrew).

Begin, Z., Brooker, W., Buchbinder, B., Druckman, Y., Kaufman, A., Magaritz, M., and Neev, D., 1987, Dead Sea and Lake Lisan levels in the last 300 years: GSI/29/85.

Bein, A., 1974, The development of reefs in the Judean Group, in the Carmel and Coastal Plain, Israel: GSI report.

Carmi, I., and Gat, J. R., 1973, Tritium in precipitation and freshwater sources in Israel: Israel Journal of Earth Sciences, v.. 22, p. 71-92.

Gat, J. R., and Dansgard, W., 1972, Stable isotope survey of the fresh water occurrences in Israel and the Jordan Rift Valley: J. Hydrol., 16 p. 177-211.

Greitzer, Y., 1963, Groundwater salinity in the Cenomanian-Turonian aquifer of central Israel, TAHAL report P.N. 293.

Guttman, Y., 1980, Ghitit-Kane and Samar area. Calibration of a numerical model for the reconstruction of the ground-water movement of the Lower Judean Group Aquifer: TAHAL report 01:80/96 (in Hebrew).

Guttman, Y., and Kronfeld, J., 1982, Tracing interaquifer connections in the Kefar Uriya-Agur region (Israel), using natural uranium isotopes: J. Hydrol. 55, p. 145-150.

Heaton, T. H. E., and Vogel, J. C., 1981, 'Excess air' in ground water: J. Hydrol. 50, p. 201-216.

Herzberg, O., and Mazor, E., 1979, Hydrological applications of noble gases and temperature measurements in underground water systems: examples from Israel: J. Hydrol. 41, p. 217-231.

Kroitoru, L., Gilad, D., and Mazor, E., 1985, Hydrological characteristics of the Wadi Kelt and Elisha springs. Scientific basis for water resources management: IAHS Publ. no. 153, p. 207-218.

Kroitoru, L., 1980, Nubian Sandstone Aquifer; geological hydrological and geochemical aspects: M.Sc. Thesis, Tel Aviv University (Hebrew, English Abstract).

Kroitoru, L., 1987, The characterization of flow systems in carbonatic rocks defined by the ground-water parameters: central Israel: PhD Thesis, submitted to the Feinberg Graduate School of the Weizmann Institute of Science, Rehovot, Israel.

Kronfeld, J., and Rosenthal, A., 1984, Isotope hydrology of the Judea Group aquifer in the Judean Desert: Annual IGS Meeting Program and Abstracts, p. 59.

Mandel, S., 1961, Properties and genesis of the Turonian-Cenomanian aquifer in western Israel as example of a large limestone aquifer: PhD Thesis, submitted to the Senate of the Technion-Israel Institute of Technology, Haifa, Israel, (in Hebrew).

Mazor, E., and Molcho, M., 1972, Geochemical studies on the Feshcha springs, Dead Sea basin: J. Hydrol., 15, p. 37-47.

Mazor, E., and Kroitoru, L., 1987, Phreatic-confined discontinuities and restricted flow in confined groundwater systems: IAEA-SM-299/80, p. 427-437.

Mero, D., 1978, Possible pollution of the Turonian-Cenomanian aquifer in Mesilat-Zion area by oil storage spill: TAHAL report 04/78/87 (in Hebrew).

Mercado, A., 1980, The ground-water salinity in the Yarkon Taninim-Beer Sheva Basin. A conceptual model on the salinity regime and its source: TAHAL report 01/80/60 (in Hebrew).

Rosenthal, A., and Kronfeld, J., 1982, $^{234}U/^{238}U$ disequilibria as an aid to the hydrological study of the Judea Group aquifer in eastern Judea and Samaria, Israel: J. Hydrol., 58, p. 149-158.

Shachnai, E., 1980, Yarkon Taninim-Beer Sheva Basin, an updated hydrological model: TAHAL report 0°/oo1/80/12 (in Hebrew).

Shachnai, E., 1981, Ma'ale Adummim 2 well, summary and findings: TAHAL report (in Hebrew).

THE HYDROGEOLOGY OF DOLOMITIC FORMATIONS IN THE SOUTHERN AND WESTERN TRANSVAAL

J.R. VEGTER[1]
and
M.B.J. FOSTER[2]
Department of Water Affairs
Private Bag X313
Pretoria 0001
Republic of South Africa

INTRODUCTION

The most significant occurrence of carbonate rocks in the Republic of South Africa is the dolomitic strata of early Proterozoic age. The chronostratigraphically equivalent Chuniespoort and Ghaap Groups outcrop over an area of about 29,000 km^2 in the Transvaal and Northern Cape (Fig. 1) and attain maximum thicknesses of 1,880 and 1,600 m respectively. From isotopic dating of intrusive rocks in units above and below the Chuniespoort Group, the age of these sediments has been put at about 2,300 Ma. In this paper, attention will be focused only on the south-central and western Transvaal.

This region contains the highly populated and industrialized Pretoria-Witwatersrand-Vereeniging (PWV) area, the important gold mines of the Far West Rand, and the extensive agricultural plains of the Western Transvaal. Its general geology is well known largely as a result of the exploration for gold. Hydrogeology and engineering geology have also received more attention here than elsewhere, as a result of the problems associated with human interference in the hydrologic environment of this carbonate region.

Considerable problems have been encountered in the gold mines of the Far West Rand as a result of very large ground-water inflows where the dolomitic formations overlie the gold-bearing strata of the Witwatersrand Supergroup. Dewatering of dolomite aquifers by the mines resulted in unprecedented ground subsidence and sinkhole formation. Associated with this, considerable effort has been spent conducting gravity surveys and drilling programs in order to delineate potentially unstable ground (Kleywegt and Pike, 1982). Rapid urbanization similarly requires investigations into ground stability, liquid and solid waste disposal, and pollution control.

Recent detailed hydrogeological investigations, including geophysical surveys and exploratory drilling, have contributed much to knowledge of this terrain. They were conducted in order to assess and develop the dolomitic ground-water resources for emergency supplies to the metropolitan PWV area in a period of prolonged drought and critically low reservoir levels.

---

[1]*Present address*: Private Box 59739, KARENPARK, 0118 Republic of South Africa
[2]Dept. of Geology and Geophysics, University of Minnesota, Minneapolis, MN 55455 USA

International Contributions to Hydrogeology, Vol. 13 (1992)
© Verlag Heinz Heise, Hannover, FRG

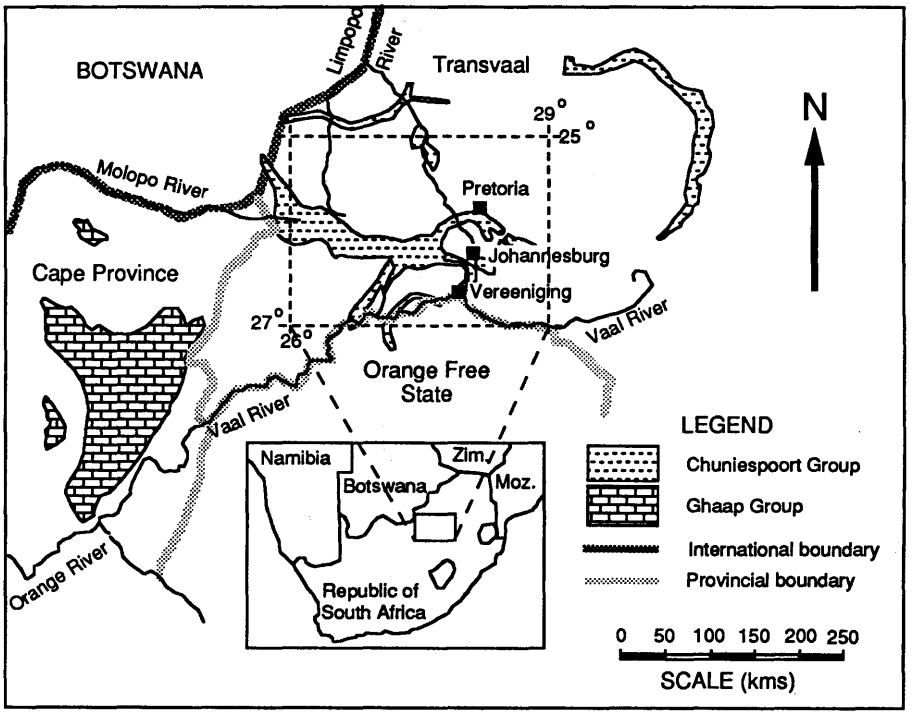

Figure 1. Distribution of Proterozoic dolomitic strata in the Northern Cape and Transvaal.

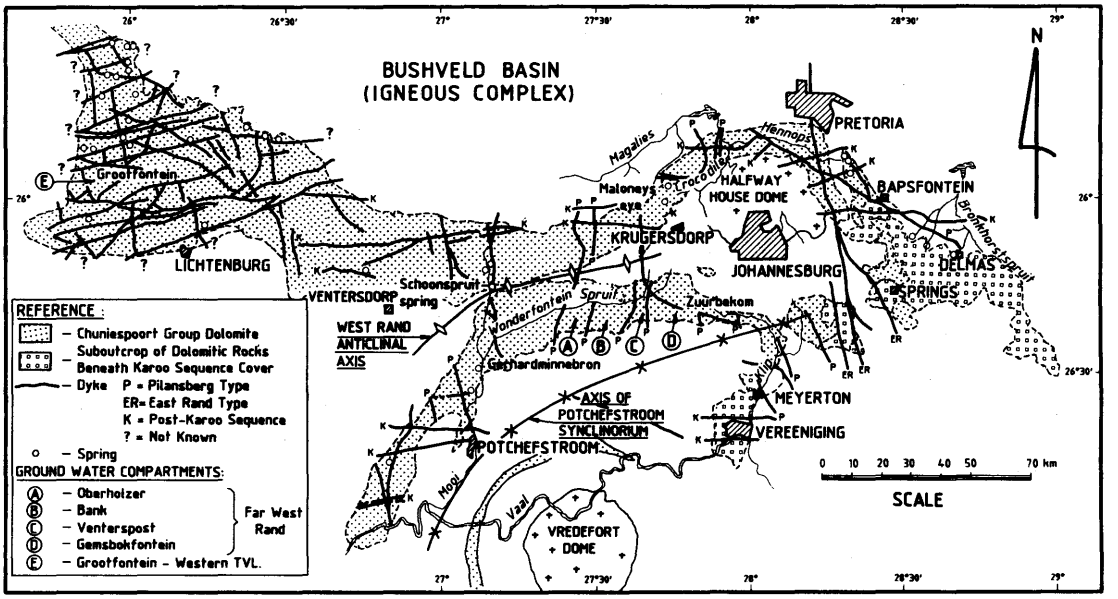

Figure 2. Dikes and ground-water compartments in south-central and western Transvaal.

The area under description (Figs. 1 and 2) is situated on the Highveld which forms part of the country's interior plateau. It extends over the watershed between the northward draining tributaries of the Limpopo River and the southward flowing tributaries of the Vaal River. Headwaters of the Molopo flow to the west. The surface elevation varies from 1,750 m at Johannesburg and 1,400 m at Potchefstroom to 1,460 m at Lichtenburg. The climate is warm temperate with summer convectional rainfall varying across the area between a mean of 640 mm in the west to 730 mm in the east. Annual potential evaporation varies between 1,400 mm and 1,800 mm.

GEOLOGY

The dolomitic formations of the Chuniespoort Group were deposited in a vast epeiric basin on the Kaap-Vaal craton, one of the oldest blocks on the African plate. They form part of a 12,000 m thick succession of clastic and chemical sediments and volcanic rocks of the Transvaal Sequence. The Chuniespoort Group attains a thickness of 1,200 m on the Far West Rand, and near Bapsfontein a thickness of 1,000 m has been recorded.

Lithostratigraphy

Excluding the extreme far west where ironstones make their appearance at the top of the succession, the Chuniespoort Group in south-central and western Transvaal comprises four lithostratigraphic formations (Fig. 3). The formations are distinguished on the basis of their chert content. Owing to poor exposure, the recognition and mapping of the different formations presents considerable difficulties in places.

Two main types of lithology are present: 1) chert-free micritic or recrystallized dolomite and 2) chert-rich dolomite composed of alternating beds, bands, and laminae of chert and dolomite.

Geochemistry

Samples of drill cuttings taken at one-meter intervals from five boreholes penetrating different stratigraphic horizons in the Bapsfontein area have been analyzed using X-ray fluorescence. The CaO content of the rock was found to vary from about 10 to 35% and the MgO content from about 8 to 21%. SiO_2 content ranged from less than 1 to over 60% in chert-rich zones. In 84.5% of the samples, the Ca:Mg ratio exceeds the theoretical value for pure dolomite (molar Ca:Mg ratio of 1:1 equivalent to a 1:0.72 ratio by weight of CaO:MgO).

Samples taken south of Pretoria show that the FeO content varies from less than 0.1 to 6.1% and MnO ranges from about 0.2 to 3.7%. The FeO:MnO ratio of 44 samples averages 0.9; the range in values is 0.2 to 1.85. Small amounts of Ba, Co, Sr, V, and Sn in the order of tens of parts per million are also present. It is believed that these chemical data are representative of the whole area under discussion.

System / Erathem	SEQUENCE	GROUP	FORMATION		LITHOLOGY AND MEMBER	Thickness (m)
PERMO-CARBONIFEROUS	KAROO	ECCA	Dwyka		Sandstone Mudstone Carbonaceous shale, coal Diamictite	
PROTEROZOIC	TRANSVAAL	PRETORIA	Timeball Hill		Shale Diamictite Klapperkop Quartzite Mb wacke and ferruginous quartzite.	270-660
			Rooihoogte		Graphitic and silty shale Quartzite Shale Bevets Conglomerate Member Breccia	10-150
		CHUNIESPOORT	Eccles		Chert-rich dolomite with large and small stromatolites	380
			Lyttelton		Dark chert-free dolomite with large elongated stromatolitic mounds	150
			Monte Christo		Light coloured recrystallised dolomite with abundant chert; stromatolitic; basal part oolitic	700
			Oaktree		Dolomite becoming darker upwards. Chocolate-coloured weathering	200
			Black Reef Quartzite		Shale Quartzite Arkosic grit	25-30

Figure 3. Partial stratigraphic column showing only strata directly underlying or overlying the Chuniespoort Group (after SACS, 1980).

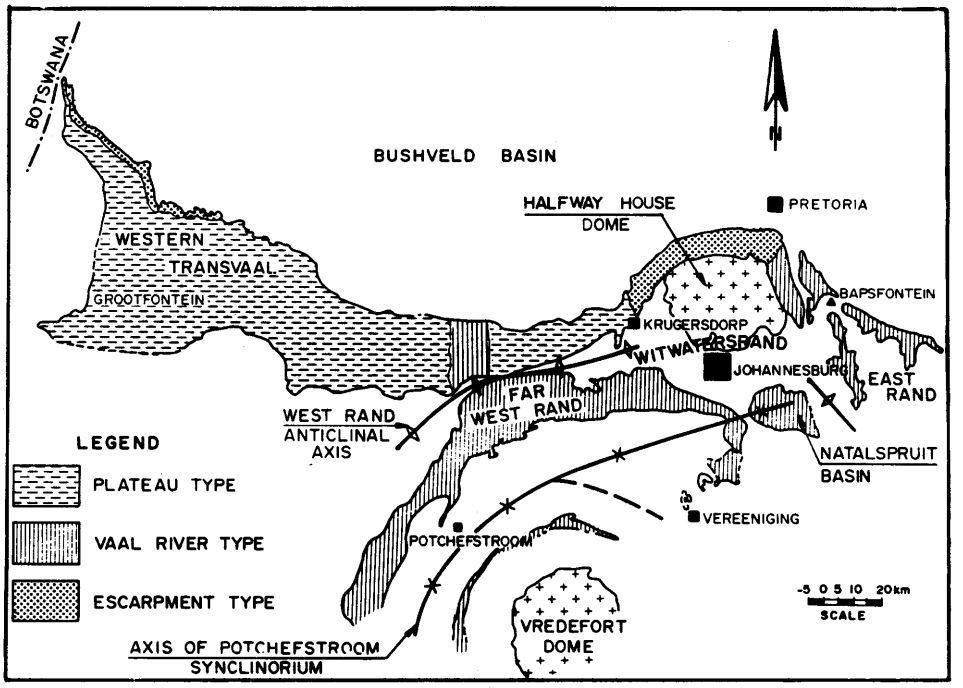

Figure 4. Distribution of karst morphological types (after Martini and Kavalieris, 1976).

Sedimentology and Diagenesis

Algal sedimentary features are widely developed in all the formations. Detailed studies of the stromatolite morphology have indicated that lithological variation is a response to different depositional environments. The chert-rich Monte Christo and Eccles Formations are characterized by oolites, lamination, and ripple marks as well as columnar and domal stromatolites with a maximum relief of 1 m. These features are diagnostic of an intertidal to supratidal environment comparable to the modern examples of Shark Bay, Western Australia, and the tidal and freshwater marshes of the Everglades, Florida. Large elongate domal stromatolites of the chert-poor Oaktree and Lyttelton Formations are up to 16 m long and 3 m in relief. The only known stromatolite forms growing today comparable in size occur in the subtidal environment of the Eastern Bahama Bank.

There has been no extensive petrological or isotopic studies of the Chuniespoort Group dolomites to aid our understanding of the diagenetic history of these carbonates. Both the dolomite and the chert are probably replacement minerals but they are present in widely differing proportions in the different lithostratigraphic units of the Chuniespoort Group. It is therefore likely that the results of diagenesis are linked to either the depositional environment or compositional differences in the original carbonate sediments. Seawater-freshwater mixing zones have been considered to provide suitable geochemical conditions for the processes of both dolomitization and silicification (Hanshaw et al., 1971; Badiozamani, 1973; Knauth, 1979). Using a seawater-freshwater mixing zone model the presence or absence of chert may be explained by mixing zone migration history. The subtidal chert-poor dolomites were deposited in a gradually subsiding basin where the mixing zone would have undergone a one way migration. The stromatolite morphology of the chert-rich units record a series of minor transgressions and regressions which would have been accompanied by similar back and forth movement of the mixing zone. This interpretation is difficult to apply however to the units of the Chuniespoort Group where fine interlamination of dolomite and chert would require rapid oscillation of the mixing zone position. This very small scale variation has been interpreted as a reflection of depositional or geochemical/diagenetic conditions varying on a seasonal or annual time scale (Foster, 1988). In view of the continuing debate on the processes of dolomitization and the lack of field data, this interpretation must be considered speculative. None of the other dolomitization models, recently reviewed by Tucker (1990) can presently be ruled out.

Three unconformities marked by angular chert fragments in a shale matrix and overlain by thin shale beds have been identified in the carbonate succession. A regional angular unconformity also marked by a chert-shale breccia separates the Chuniespoort and overlying Pretoria Groups. The chert breccias represent insoluble residues of carbonate dissolution on subaerial erosion surfaces.

Structural Geology

The major structural features in the southern and western Transvaal originate from the period of upheaval and igneous intrusion (between approximately 2,100 and 1,700 Ma) which followed the deposition of the Transvaal Sequence. A full description of this complex period of tectonism and igneous intrusion is beyond the scope of this paper, but the main features are the Transvaal Basin intruded by the Bushveld Complex, the West Rand anticline, the Halfway House and Vredefort granitic domes, and the Potchefstroom synclinorium (Fig. 2). Except for the narrow band of steeply dipping and overturned dolomitic strata which encircle the Vredefort dome and which have not been studied hydrogeologically, rocks of the Chuniespoort Group have in general not undergone intense deformation. Dips are for the most part low to moderate and folding is generally gentle. Owing to the poor exposure of the Chuniespoort Group, faulting is best observed in the immediately overlying and underlying units. Normal, wrench, reverse, and thrust faults have been mapped in various parts and are evident in the published 1:250,000 geological sheets (Geological Survey of South Africa, 1986, nos. 2526, 2528, 2626, 2628).

Igneous Intrusions

One of the most characteristic features of the regional geology is its network of intersecting dikes (Fig. 2). There were at least three main episodes of dike emplacement (Day, 1980): Pilanesberg (1,310 ± 60 Ma), East Rand (1,120 ± 65 Ma) and post-Karoo Sequence age (150 to 190 Ma). In addition, the Chuniespoort Group strata have been intruded by sills possibly associated with intrusion of the mafic layered suite of the Bushveld Complex (2,096 Ma) as well as sills of post-Karoo age.

Post-Transvaal Sediments

After the early Proterozoic, the area was subjected to an extended period of erosion, including Carboniferous glaciation on a continental scale, and no evidence of sedimentation between the Transvaal and Karoo Sequences remains in this area. Only lower basin-margin Karoo sediments are present. These consist of diamictite, found only in deeply eroded channels, followed by glaciolacustrine and glaciofluvial deposits of the Dwyka Formation of late Carboniferous-early Permian age, in turn followed by shales, mudstones, sandstones, and coal beds of the Vryheid Formation of the Ecca Group.

The extensive tracts of transported soils from the Tertiary to Recent times are largely hillwash deposits derived from the chert and quartzite ridges of the Rooihoogte and Timeball Hill Formations. They comprise coarse chert debris and red sands, the latter being widespread and possibly redistributed by wind during an arid climatic period (Brink, 1985).

KARST

Dissolution Process of Dolomitic Rock

Martini and Kavalieris (1976) recognize three distinct successive stages of dissolution of dolomite corresponding to three zones of rotten rock with a total thickness of about 10 cm. The incipient stage is evident as intergranular staining of carbonate crystals by oxides of iron and manganese and depletion of Ca and Mg at crystal boundaries. Although dissolution is strongly selective along crystal boundaries, microprobe analysis of fresh dolomite shows no primary variation in composition across crystal boundaries. In a later stage of dissolution, the dolomite is characteristically granular and is easily crushed. Carbonate crystals show a heavy oxide coating. Quantitative analysis for Ca and Mg of fresh and weathered dolomite reveal that the Ca/Mg ratio remains unchanged during dissolution. In the final stage of dissolution, which is only preserved in protected environments, all the carbonate is removed and a cellular fabric composed of iron and manganese oxides and hydroxides and silica, pseudomorphous after the original crystal structure remains. This is a highly erodible and compressible soil locally termed 'wad'.

History of Karst Development

Although erosion during successive periods has progressively removed traces over the greater part of the dolomitic strata, there is evidence of at least four periods of karstification according to Martini and Kavalieris (1976):

1. Pre-Pretoria period (about 2,250 Ma) - Evidence for a period of karstification before the deposition of the Pretoria Group is widely represented by a chert breccia with dark siliceous matrix developed on top of the carbonate sequence. In the far western Transvaal, Martini (1975) has described karst features that developed in this period. These features consist of paleosinkholes and cave passages filled with residuals now represented by black siliceous shale, rich in carbon inherited from the dolomite, collapsed chambers, and breccia bodies. In places, mineralization with fluorspar, lead, and zinc has taken place. The unconformities within the Chuniespoort Group may also be considered palaeokarst horizons.

2. Pre-Waterberg period (about 1,700 Ma) - Outside the area under consideration, red sandstone correlated with Waterberg Group rocks has been observed infilling dissolution cavities.

3. Pre-Karoo period - This erosion period lasted about 1,300 Ma and includes Carboniferous continental glaciation. Drilling for geotechnical purposes, coal mining, and exploration for refractory clay deposits (e.g., Wilkins et al., 1987) have repeatedly demonstrated that Karoo strata were deposited on an undulating karst palaeotopography. Although it has been suggested by certain workers (e.g., Marker, 1974) that outliers of Karoo sediments owe their existence to collapse into karst depressions when the Karoo cover was being eroded, evidence

provided by Wilkins et al. (1987) demonstrates that primary sedimentation processes formed the succession in the Karoo outliers. Localized dips and small-scale folds along the edges of outliers and a thickening of higher-lying beds over filled-up floor depressions point to continued subsidence during sedimentation. Subsidence may have been caused either by karstic collapse or by dewatering and compaction.

4. Post-Karoo period (Tertiary to Recent) - Episodic uplift of much of South Africa commenced during fragmentation of Gondwanaland in the late Mesozoic and was followed by further uplift in late Tertiary. This led to renewed exposure of the Chuniespoort Group and evolution of a karst landscape. Evidence for post-Karoo karst formation is provided by sinkholes and dolines near Pretoria in which clayey and sandy silt have been deposited on top of Karoo infilling. On the Far West Rand, paleosinkholes have been infilled by red eolian sand and fluvial gravel, sand, and clay. The red sand is considered to be representative of Tertiary eolian sand deposits which cover extensive areas of southern Africa.

Geomorphology

With the exception of the dissected northwestern flank of the Halfway House Dome, the dolomitic strata typically occupy flat featureless terrain or wide shallow valleys. The strata are largely obscured by patches of Karoo Sequence (only partially shown in Fig. 2) or the more extensive Tertiary to Recent deposits. Higher ground is normally occupied by chert ridges. The lowest quartzite of the overlying Pretoria Group commonly forms an escarpment rising up to 100 m above the Chuniespoort Group outcrop (Fig. 9).

Three karst morphological types have been identified in south-central and western Transvaal by Martini and Kavalieris (1976). The distribution of the types is shown in Figure 4.

1. The Plateau type is the most extensive morphological type and occupies the flat plateau between Krugersdorp and the Botswana border. The Plateau type has few surface streams and those flowing from bounding formations disappear upon entering the dolomitic terrain. From these points of disappearance dry stream courses may extend several kilometers further on the dolomite. Spring flows rising from the dolomite likewise disappear underground. In the western Transvaal, several large polje-like depressions occur. They are not generally associated with water caves as in the classic poljes of Yugoslavia but drain into sediment-choked dissolution features at their margins. The existence of sinuous ridge-like diamondiferous gravel deposits in the western Transvaal, which are the remains of palaeo-river courses, indicates that the present-day morphology has developed probably since the late Tertiary or Pleistocene. Partridge and Maud (1987), on the other hand, regard the surface as a lowered African erosion surface which dates back to early Cretaceous. The Plateau type morphology has evidently undergone little change over a long period.

2. The Vaal River type consists of wide, weakly-incised valleys developed on the flanks of the Potchefstroom synclinorium as well as southeast of Pretoria and

carries perennial streams where the aquifers have not been dewatered by the gold mines. The karst topography is generally less obvious than the Plateau type. In contrast, accessible caves are more numerous, including some of the larger systems found in South Africa.

3. The Escarpment type occurs between Pretoria and Krugersdorp. The name is derived from the type area which lies along the edge of the interior plateau in the eastern Transvaal. The topography is rugged and highly dissected and similar in most respects to that developed on the adjoining rock types. Greater downcutting has occurred in this area. Valley floors are 150-200 m lower than in the adjacent dolomitic areas to the east and west. Caves are abundant and situated well above valley bottom level, perched on valley sides.

Marker and Moon (1969) found that cave levels in the Chuniespoort Group throughout the Transvaal occur on three preferred altitudes. These they relate to the African (Early Cretaceous), Post African (Early Miocene), and proto-Quaternary erosion surfaces. Detailed surveys on the Far West Rand by Martini et al. (1977) suggest, however, that cave levels are governed by the elevation of springs which emerge where dikes cut the thalweg (Fig. 5).

Although caves are expected to develop more readily just below the water table, and this appears to be the case on the Far West Rand, Kleywegt and Enslin (1973) report that in this region leaching along tensional faults and fractures extends to depths of between 50 m and 200 m below the water table. Similarly, drilling in the Klip River Valley and elsewhere has shown that, although the most intense dissolution occurs within a short distance below the water table, voids and cavities also occur considerably deeper.

Speleology

Martini and Kavalieris (1976), Martini et al. (1977), and Moon (1972) provide descriptions of caves in this region. Fissure caves are probably the most common type. The largest known cave system has a combined passage length of 12.3 km. Most caves have a phreatic origin. Where the dolomite is intensely interbedded with chert layers, the carbonate component may be dissolved on both sides of the original joint without development of a cave passage - the chert and very porous "wad" remaining undisturbed and occupying the same volume as the unaltered dolomite. Irregular cavities develop by collapse and compaction of this residue.

A large number of caves owe their pattern to upward migrating collapse of the roof of the original dissolution passage. The large water-filled holes occurring in the Western Transvaal are due to collapse taking place below the water table and are comparable with the cenotes of Yucatan. The upward progression of a collapsed chamber leads eventually to the development of a body of dislocated dolomite surrounded by a "ring cave." Most cave entrances are pit-like, being formed either by roof collapse of chambers or by the development of a sinkhole through a residual filling.

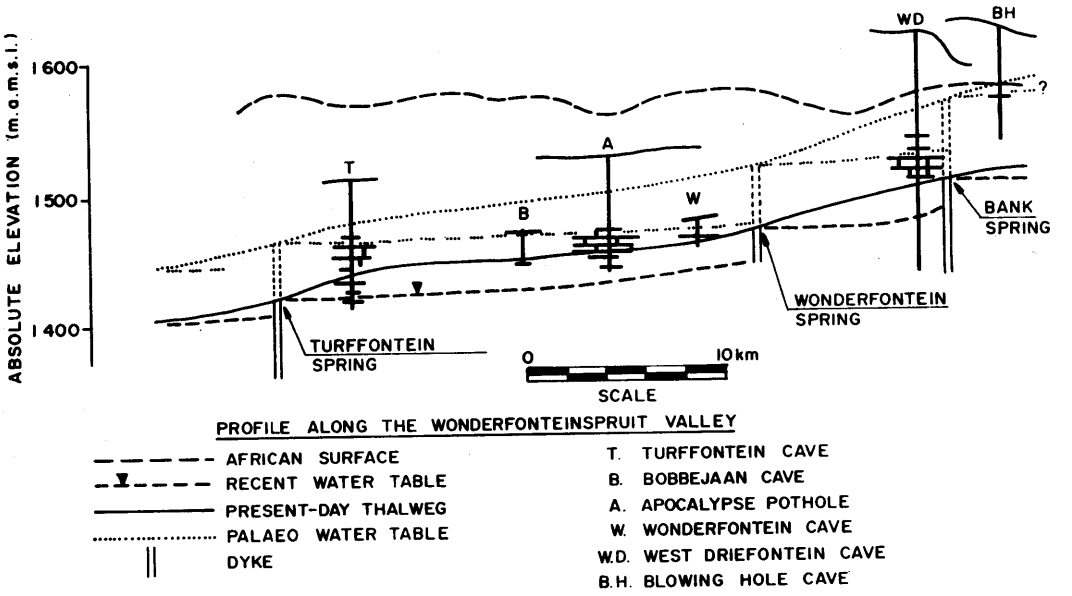

Figure 5. The effect of dikes on cave levels (after Martini et al., 1977).

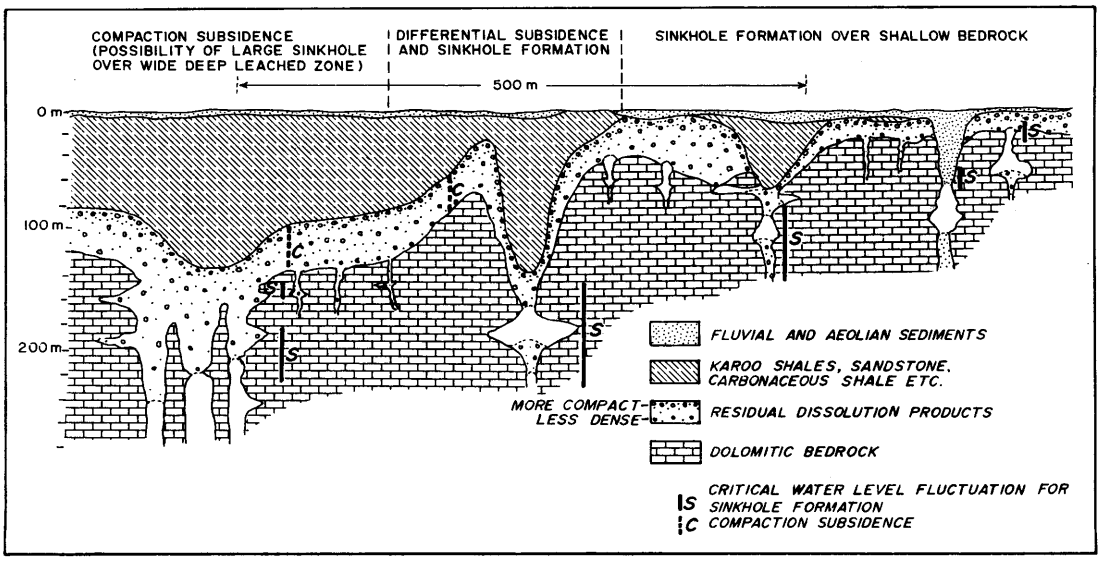

Figure 6. Semi-diagrammatic depiction of karst conditions on the Far West Rand illustrating presumed critical water-table fluctuation for compaction and sinkhole formation (after Kleywegt and Pike, 1982).

Present-day Sinkhole Formation and Subsidence

Over the past 30 to 40 years, human activities have led to a much accelerated rate of sinkhole formation and subsidence. These activities, principally urbanization and mining, are responsible for the local disruption and concentration of surface runoff, for increased infiltration due to leakages from water and sewage mains, and for the dramatic lowering of the piezometric surface in four groundwater compartments in the Far West Rand. These processes adversely affect the stability of the blanket of superficial deposits and the residual products of dissolution. Much has been written on this subject (e.g., Kleywegt and Enslin, 1973), and only the most important aspects are mentioned here.

Kleywegt and Pike (1982) draw attention to the fact that, in contrast to the properties of normal sedimentary sequences, the age and degree of compaction of the in situ dolomitic residuum increases from the dolomitic bedrock upwards. This is the consequence of the continuing process of dissolution and formation of residual material. The residuum changes from the very low-bearing capacity, easily erodible wad and residual chert, directly above bedrock, through a mixture of chert and manganese oxides grading upwards into a compact chert breccia cemented by Mn and Fe oxides. This character of the residual deposits has an important bearing on sinkhole formation and subsidence.

It is generally accepted that sinkholes occur through the progressive collapse of arches or domes which span air-filled voids in the residuum. The conditions for the formation of sinkholes have been detailed by Jennings et al., (1965) as follows:

1. Abutments for the roof of a void provided by dolomite pinnacles or the sides of grikes.
2. Development of arching conditions in the residuum.
3. Development of a void below the arch.
4. A reservoir to accept material which is removed to enlarge the void and a means of transportation such as water.
5. A disturbance to cause roof collapse. Water in the arched material in the vadose zone leads to loss of strength, erosion, and removal of binding material. In the phreatic zone, dewatering leads to a loss of buoyant support.

Subsidence is generally ascribed to a lowering of the water table through unconsolidated residuum which results in compaction and the formation of depressions which often have small scarps at the margins. Kleywegt and Pike (1982) contend that apart from compaction, collapse also plays a role. Figure 6 illustrates the different conditions for the formation of sinkholes and compaction. The sinkhole and subsidence hazard caused by dewatering places a serious constraint on the utilization of the large volume of ground water held in dolomitic strata for an emergency supply to the metropolitan PWV area (Vegter, 1987).

GEOLOGICAL CONTROL OF KARST DEVELOPMENT

The present level of knowledge about the karst development in the Chuniespoort dolomitic strata is the result of field observations and the examination of caves, extensive detailed gravity surveys and drilling undertaken for

geotechnical reasons, and the assessment of ground-water resources. The gravity method has been found to be the geophysical method best suited for determining the configuration of dolomitic bedrock as a result of the density contrasts between fresh dolomite and the various types of cover material (Table 1).

Lithostratigraphy

At the surface, the chert-free dolomite units weather forming karren or dolomite pavements (lapiez) where the normally roundly weathered blocks are separated by soil-filled grikes. Despite a high density of incipient joints, major dissolution occurs only on well spaced discontinuities. The cherty units have rugged outcrops; the resistant chert supporting large voids resulting from the dissolution of the carbonate rock. Where observed at outcrop, dissolution occurs on many more joints and bedding planes in the alternating chert and dolomite sequences than in the chert-poor units.

Table 1. Average density values for bedrock and overburden occurring in areas underlain by the Chuniespoort Group (after Enslin et al., 1976).

Lithology	Average density value (kg/m^3)
Fresh dolomite	2,850
Incompletely leached dolomite bedrock	2,600
Overburden material (surface deposits, wad, and incompletely leached dolomitic bedrock)	2,350
Karoo Sequence sediments	2,000-2,400
Surface deposits	1,600
In situ completely leached zone with inverse density variation with depth: compact cemented chert breccia with density of 2600 kg/m^3 over horizon of porous wad of 1000 to 1200 kg/m^3	2,100

These different weathering characteristics continue below the surface (Fig. 7). Ground-water exploration drilling south of Johannesburg showed that in the chert-rich formations water-bearing zones attained thicknesses up to 60 m. The considerable widening of the passages below chert ceilings, as depicted in Figure 7, have been described by Kent et al. (1975). The aquifer material in such zones has been described as very fractured and weathered chert, often with little evidence of any dolomite. Near the Pretoria Group outcrop, some chert may be chert breccia of the Rooihoogte Formation and not weathered Chuniespoort Group. Within the chert-poor Oaktree and Lyttelton Formations, all water strikes occur in discrete dissolution features in fresh dolomite. The dimensions of these features below water level are not known because air percussion drilling has failed to advance against conditions of air loss and high water pressure. Water strikes are commonly associated with thin bands of shale or chert.

Gravity anomaly maps in the Klip River Valley reveal zones of preferential weathering of the chert-rich Monte Christo and Eccles Formations and indicate that extensive zones of porous and permeable material form only where the weathering of closely spaced geological structures coalesce in these units. Because of the small volume of coarse residual weathering products resulting from the dissolution of the chert-poor units of the Oaktree and Lyttelton Formations, extensive gravity lows tend to be infilled with wad and semi-permeable Karoo Sequence deposits (Fig. 7).

Palaeokarst

Throughout the south-central and western Transvaal, extensive dissolution is commonly found at the pre-Karoo palaeokarst surface, especially where gravity anomaly maps indicate deeper weathering of the dolomitic formations. The occurrence of good aquifer conditions in these weathered zones is dependent upon the presence of coarse porous material (generally chert) preventing the ingress of the clayey residue (weathered Karoo or wad) into boreholes. Differentiating between in-situ weathered chert and transported chert debris from drill cuttings is problematic and leads to uncertain interpretation of the detailed hydrogeology.

Intraformational episodes of karstification are now represented by unconformities. Several ground-water exploration boreholes obtained good water supplies after penetrating these horizons in excess of 200 m below ground surface, beneath extensive thicknesses of unweathered dolomitic strata. This effect could also be attributed to bedding-parallel structural features.

Tectonism and Igneous Intrusions

The control exerted by jointing and faulting upon karstification processes is evident from cave surveys (Fig. 8) as well as residual gravity maps. Kavalieris and Martini (1976) and Moon (1972) have shown the most important direction of cave passages west of the Halfway House dome to be east-west with another approximately perpendicular to it. Kavalieris and Martini (1976) relate the orthogonal pattern to post-Karoo crustal arching along a NNE-SSW axis. The major east-west joint set is comparable to the dominant strike trend of the post-Karoo dikes. Others have associated the joint-controlled cave development to both older and more localized structural features (Partridge and Brink, 1965; Moon, 1972).

The dissolution pattern which emerges from residual gravity maps is more complicated than is evident from the cave surveys. Easterly and northerly trending linear zones of deep leaching run parallel with both the post-Karoo as well as the Pilanesberg and East Rand dike systems (Fig. 2). The dikes were intruded along lines of weakness caused by crustal tension. The strike-parallel system of joints and fissures has been extensively weathered forming linear zones of dissolution. The continuity of these linear zones of dissolution is often unaffected by lithostratigraphy. Exploratory drilling on the Far West Rand has confirmed dissolution channels in excess of 50 m wide. The hydrogeological characteristics of these zones are dependent upon the nature of the residual and transported material filling them. Some northwesterly and northeasterly trending features have been

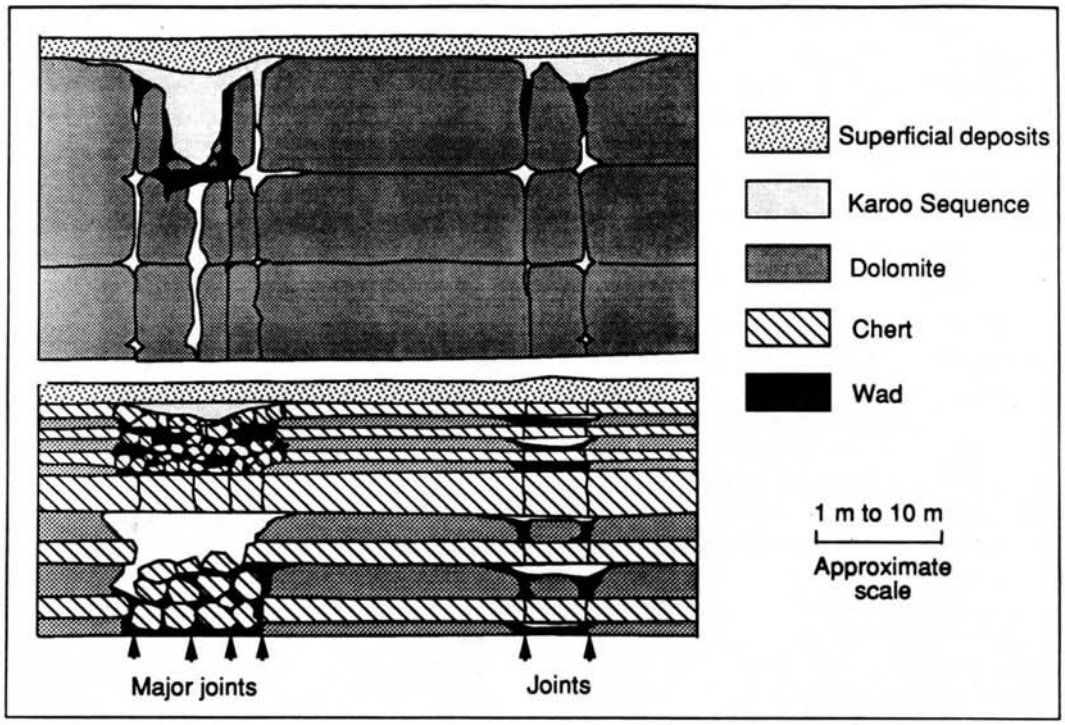

Figure 7. Sketch representation of weathering patterns in chert-poor and chert-rich dolomite (from Foster, 1988).

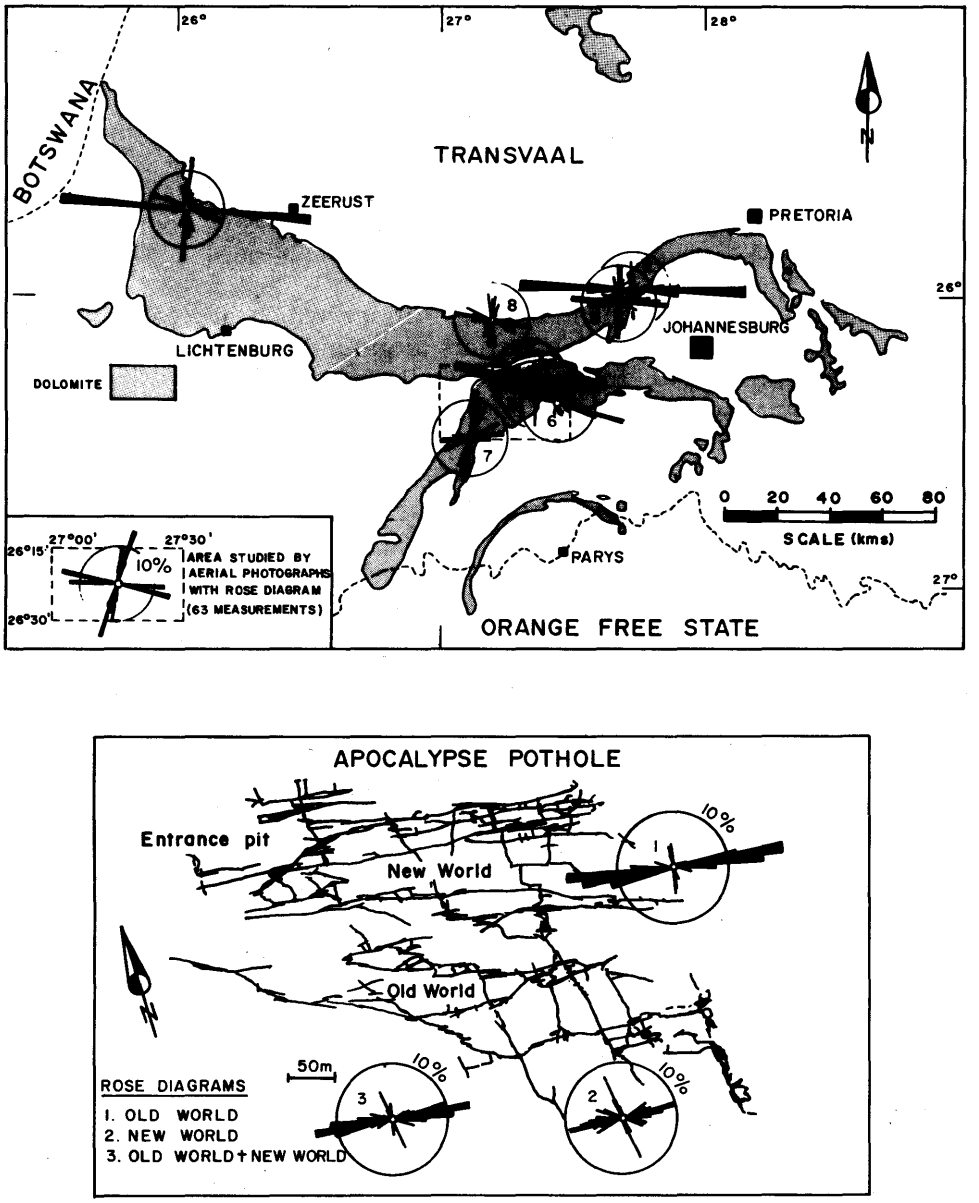

Figure 8. a) Strike of cave passages in south-central and western Transvaal (from Kavalieris and Martini, 1976); b) Strike of fissures in largest known cave in south-central and western Transvaal (from Kavalieris and Martini, 1976).

connected with faults encountered in gold mining. The complex pattern of crossing linear zones is evident on the gravity anomaly maps.

On the Far West Rand, a number of post-Transvaal tension faults of relatively small vertical displacement trend roughly parallel to the N-S Pilanesberg dike system and feed dolomitic ground water into the mine workings. The inrush of dolomitic ground water into West Driefontein Gold Mine, at a rate of more than 360,000 m^3/day in 1968, is a powerful example of transmissive zones occurring to great depths. A low-angle normal fault was found to be the cause.

Discontinuities in the potentiometric surface which are usually observed across dikes indicate that they act as barriers to ground-water flow and divide the dolomitic strata into separate ground-water units or compartments (Figs. 2 and 5). Residual gravity data indicate that, in places, dike contact zones are favorable loci for dissolution of the dolomitic strata. Sills also act as barriers to ground-water movement. On the East Rand, water is commonly encountered in boreholes on or near the upper and lower contacts of three sills. On the other hand, in the Natalspruit basin, between Vereeniging and the East Rand, the contacts of a 80-m thick post-Karoo dolerite sill have not yielded any water. In general, folding appears to play only a minor role in karst development. At one location north of Vereeniging, however, karst development is associated with a NW-SE striking anticline and a coincident zone of faulting.

AQUIFER CHARACTERISTICS

The mantle of transported material and residual dissolution products, together with the underlying zone of cavernous to fractured bedrock, constitute aquifers capable of holding and transmitting large volumes of water. Fractures, some of which extend through the whole dolomitic succession, connect the upper water-bearing zone to deeper-lying aquifers in the dolomitic bedrock. Where present, Karoo strata act as semi-confining beds and give rise, in places, to temporarily perched ground-water bodies. Figure 9 is a semi-diagrammatic representation of hydrogeologic conditions in the Wonderfontein Valley.

As has already been mentioned, dikes have a profound influence on the hydrologic regime, by acting as barriers to ground-water movement and, thus, dividing the dolomitic strata into separate hydraulic units or compartments. Mine dewatering on the Far West Rand has produced head differences of several hundred meters between adjacent compartments as a result. Surface or subsurface flow may occur between compartments. On the surface, water crosses the dikes after issuing as springs on the upstream side. Subsurface flow may occur at gaps in the dikes, where faults displace dikes, and where weathered and fractured dike rock extends to below the ground-water level.

Various methods have been used to determine aquifer storativity and transmissivity which vary widely depending on the degree of karstification and the nature and thickness of the saturated mantle. Analyses of pumping test data and of the catastrophic flooding of the West Driefontein Gold Mine in 1968 have produced storativity values varying between 0.0005 and 0.069 (Fleisher, 1981; Schwartz and

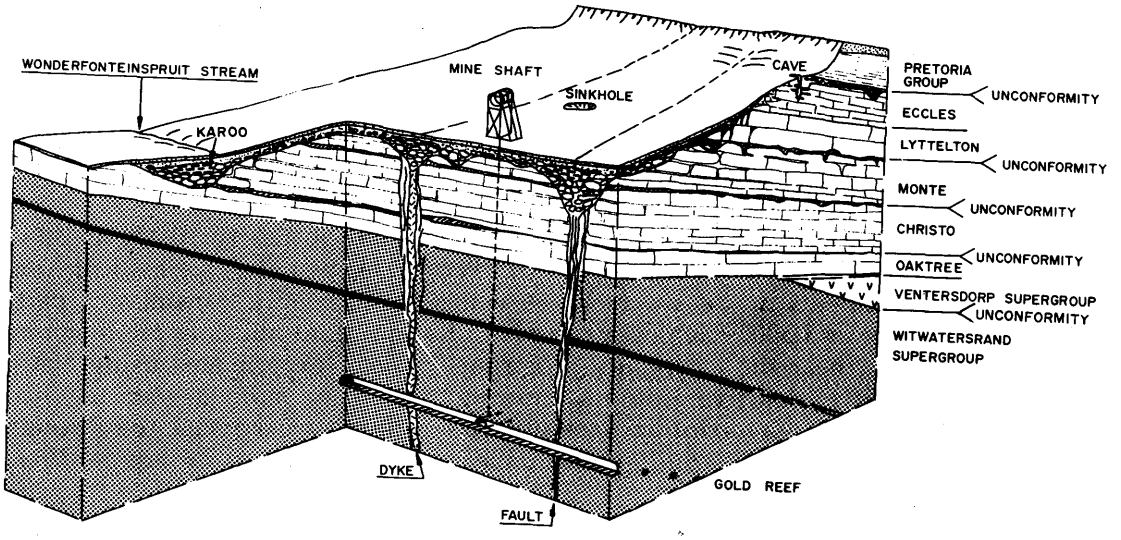

Figure 9. Schematic representation of aquifer conditions along the valley of the Wonderfonteinspruit Stream.

Midgley, 1975). Ground-water and chemical mass balances for individual ground-water compartments have yielded effective porosity values of between 1.0 and 3.4%. Detailed analyses of the dewatering of several ground-water compartments by gold mines, as well as shaft and borehole logs, have shown that in good aquifer zones effective porosity may range from as high as 14% at the water table to less than 2% at 150 m below the surface (Foster, 1987).

Transmissivities range from less than 10 m^2/day to nearly 30,000 m^2/day (Schwartz and Midgley, 1975; Fleisher, 1981). Poor transmissivities are evident from piezometric gradients in the order of 1:50 whilst in the highly transmissive parts gradients as low as 1:5000 have been recorded. Natural flow velocities are therefore very low except near the emergence of springs. Tracer experiments using NaCl, fluorescein, and radioactive isotopes showed that where mine dewatering had produced a cone of depression in excess of 100 m deep, water recharged through boreholes at the surface could enter mine workings within 24 hours (West Driefontein Mine, pers. comm.).

HYDROLOGY

Most springs issue on or near the contacts with dikes, the underlying quartzitic Black Reef Formation, or the overlying clastic rocks of the Pretoria Group. The positions of some springs in the Western Transvaal are governed by chert beds and others by extensive quartz veins. Flows range from less than 0.001 to about 3 m^3/s (greatest flow at Schoonspruit Spring). The more important springs have fairly constant flows which do not deviate by more than 40 to 65% from the mean. No proper study has been made of daily fluctuations and of the early responses of springs to rainfall events. It would appear that the responses, in general, are relatively small compared to total flow.

Fleisher (1981) states that, in contrast to springs rising from karstic terrains in many parts of the world, most springs here show no annual recession. The lack of an annual recession under a regime of summer-season rainfall is ascribed by Fleisher to a two-phase system of recharge whereby each rainfall episode would affect the aquifer twice: firstly, by rapid downward conduit-type flow via fissures and fractures beneath areas with a thin or absent cover of permeable superficial deposits, and, later, by slower diffuse percolation through a thick cover of soil and lesser permeable materials. The simultaneous response of spring flow to changes in piezometric level supports this contention. With delayed recharge continuing through the dry winter season, recession of flow does not occur (Fig. 10a).

Most of the spring hydrographs show that exceptionally high rainfall seasons are followed for a period of three to four years by above-average spring discharge. This is well illustrated by the hydrographs of Maloney's Eye (Fig. 10b). Similar fluctuations of the piezometric level have been observed in the Wondergat sinkhole in the western Transvaal and elsewhere (Fig. 10c). This phenomenon can be ascribed to the delayed recharge as well as limited outflow at the springs.

Ground-water replenishment by rainfall in compartments lacking surface streams has been estimated by means of water balances and other methods. Mean

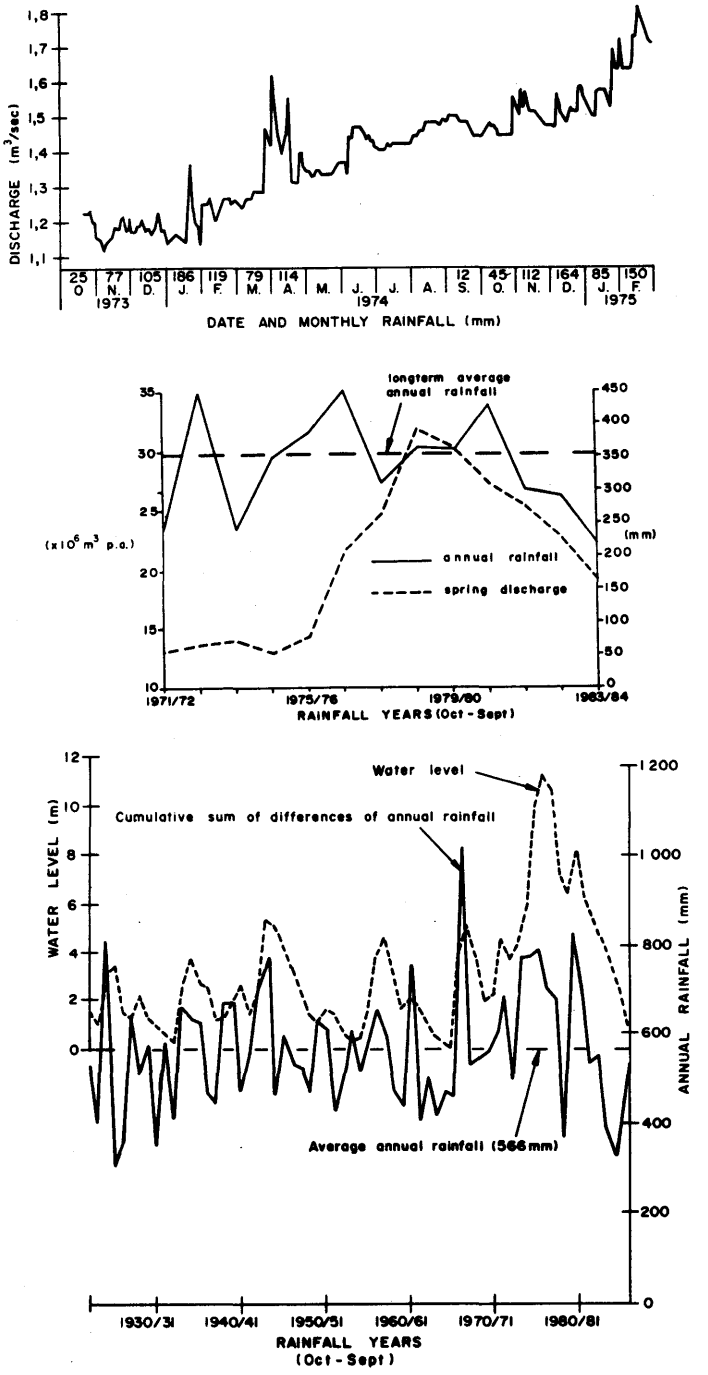

Figure 10. a) Schoonspruit Spring discharge hydrograph showing immediate summer rainfall recharge and continued recharge in winter months (after Fleisher, 1981); b) Maloney's Eye discharge hydrograph showing long-term response to exceptionally high rainfall years; c) Wondergat water-level fluctuations in response to high rainfall years.

annual recharge has been found to range from 60 mm in the west to about 110 mm in the east. The ratios of storage to mean annual recharge (Table 2) reveal that total aquifer storage is generally much greater than the annual recharge and also indicate that maximum aquifer through-flow time should be in the order of 100 years.

Table 2. Ground-water storage and recharge for selected dolomitic ground-water compartments.

Compartment	Surface area (km^2) (A)	Original volume storage ($10^6 m^3$) (B)	Effective water-column height (m) (C=B/A)	Mean annual recharge (mm) (D)	Storage/ Mean annual recharge (C/D)
Grootfontein (Western Transvaal)	128	220	1.7	70	25
Venterspost (Far West Rand)	54	460	8.5	85	100
Oberholzer (Far West Rand)	150	1,050	7.0	85	82

CONCLUSIONS

Varying depositional and diagenetic environments in the Precambrian resulted in dolomitic formations with fundamentally different weathering characteristics. Unimpeded downward percolation of aggressive ground water in vertical joints, faults, and fissures has caused the chert-poor Oaktree and Lyttelton Formations to develop karstic solutional porosity along well spaced solution channels. Ubiquitous chert beds and laminations in the Eccles and Monte Christo Formations encourage horizonal development of carbonate dissolution. The transmissive zones in the chert-rich units thereby comprise a much thicker and more extensive chert-supported porous permeable zone.

The effects of a palaeokarstic episode may be evident from gravity anomaly maps and drilling (as in the case of the pre-Karoo surface), indeterminate due to subsequent erosion (as in the case of the pre-Waterberg period), or they may be obscure due to their occurrence at depth within the dolomitic bedrock. All the erosional episodes, however, during Chuniespoort sedimentation as well as in subsequent periods, have affected the whole of the Transvaal Basin.

Although extensive erosion surfaces form major elements of today's southern African landscape, karst erosion levels are locally determined by the level of erosion of the dikes which form ground-water barriers. The retardation of the ground-water flow by the dikes has presumably reduced the rate of carbonate dissolution but may have allowed more complete dissolution at certain horizons by maintaining the height of ground-water levels for greater periods than would otherwise have been the case.

Tectonism is responsible for the creation of the joints and fissures essential for karst erosion to take place in ancient carbonate rocks. Throughout the south-central and western Transvaal, folds, faults, major joints, dikes, and sills have all been found to be associated with zones of greater dissolution and, hence, greater transmissivities and storativities. Not one of these tectonic features dominates karst development. In any given area, there is normally one dominant structural or intrusive feature associated with the greatest development of karst.

Lithostratigraphy, palaeokarst history, tectonics, and the network of intersecting dikes are the major controls on the development of the karst aquifer in the Chuniespoort Group. Knowledge of these subjects is therefore crucial for an understanding of the hydrogeology of this karst region.

Acknowledgements-This paper is published with permission of the Director-General of the Department of Water Affairs, and the use of official records is gratefully acknowledged. We thank PPC Cement Company Limited for permission to use X-ray fluorescence results from their laboratories, Dr. R.J. Kleywegt and Dr. J. Martini of the Geological Survey of South Africa and Mr. A.G. Reynders of the Water Research Commission for constructive criticism and editorial assistance, and colleagues of the Directorate of Geohydrology who have assisted us in many ways.

REFERENCES

Badiozamani, K., 1973, The Dorag dolomitization model--application to the Middle Ordovician of Wisconsin: J. Sed. Pet. v. 43, no. 4, p. 965-984.

Brink, A.B.A., 1985, Engineering Geology of Southern Africa: vol. 4. Building Publications, Pretoria.

Day, R.W., 1980, Prominent dike systems in the Southern Transvaal: Annals Geol. Surv. S. Afr. v 14:1, p. 85-91.

Enslin, J.F., Kleywegt, R.J., Beukes, J.H.T., and Gordon-Welsh, J.F., 1976, Artificial recharge of dolomitic ground-water compartments in the Far West Rand Goldfield of South Africa, in Land Subsidence: Proc. 2nd Int. Symp. Anaheim, Publ. 121 I.A.H.S. p. 495-506.

Fleisher, J.N.E., 1981, The geohydrology of the dolomite aquifers of the Malmani Subgroup in the Southwestern Transvaal, Republic of South Africa: Internal report Gh 3169, Directorate of Geohydrology, Dept. Water Affairs, Pretoria.

Foster, M.B.J., 1987, First revision of the geohydrology of the Zuurbekom and Gemsbokfontein compartments: Internal report GH 3542, Directorate of Geohydrology, Dept. Water Affairs, Pretoria.

Foster, M.B.J., 1988, Geological control of aquifer properties of the Chuniespoort Group in the Klip River Valley and Natalspruit Basin, Transvaal: Unpubl. MSc Thesis, Dept. Geography, Rhodes Univ., 135 p.

Hanshaw, B.B., Back, W., and Dieke, R.G., 1971, A geochemical hypotheses for dolomitization by groundwater: Econ Geol. 66(5), 710-724.

Jennings, J.E., Brink, A.B.A., Louw, A., and Gowan, G.D., 1965, Sinkholes and subsidences in the Transvaal dolomite of South Africa: Proc. 6th Int. Conf. Soil Mechanics and Foundation Engineering Montreal.

Kavalieris, I. and Martini, J.E.J., 1976, Structural control of some Western Transvaal caves: S. Afr. J.Sci. v. 72, p. 308-313.

Kent, L.E., Kavalieris, I., Martini, J.E.J., and Hugo, P.L.V., 1975, Wonderfontein Cave: Ann. Geol. Surv. S.Afr. 11, p 289-296.

Kleywegt, R.J., and Enslin, J.F., 1973, The application of the gravity method to the problem of ground settlement and sinkhole formations in dolomite on the Far West Rand, South Africa: Proc. IAEG Symposium on sinkholes related to soluble rocks, Hannover, Deutsche Geselschaft fur Erd - und Grundbau, Essen.

Kleywegt, R.J., and Pike, D.R., 1982, Surface subsidence and sinkholes caused by lowering of the dolomitic water table on the Far West Rand gold field of South Africa: Ann. Geol. Surv. S.Afr. 16, p. 77-108.

Knauth, L.P., 1979, A model for the origin of chert in limestone: Geology v. 7, p. 274-277.
Marker, M.E., and Moon, B.P., 1969, Cave levels and erosion surfaces in the Transvaal, South Africa: S.Afr. Geogr. J. 51. p. 106-113.
Marker, M.E., 1974, A note on the occurrence of Karoo sediments near Pretoria and its relevance to the dating of karst weathering: Trans. geol. Soc. S. Afr. 77, p. 69-70.
Martini, J.E.J., 1975, Palaeokarst diagenetic porosity and palaeogeography as major mineralization control in Transvaal dolomite south of Zeerust: S. Afr. J. Sci. v. 71.
Martini, J.E.J., and Kavalieris, I., 1976, The karst of the Transvaal (South Africa): Int. J. Speleol. v. 8. p. 229-251.
Martini, J.E.J., Kavalieris, I., and Stuart, F.F., 1977, The West Driefontein cave and its significance in the palaeohydrology of the Far West Rand, Transvaal: Seventh Int. Congress Speleology, Sheffield.
Moon, B.P., 1972, Factors controlling the development of caves in the Sterkfontein area: S.Afr. geogr. J. 54, p. 145-151.
Partridge, T.C., and Brink, A.B.A., 1965, Transvaal Karst: Some considerations of development and morphology, with special reference to sinkholes and subsidences on the Far West Rand: S.Afr. Geogr. J. 47, p. 11-34.
Partridge, T.C., and Maud, R.R., 1987, Geomorphic evolution of Southern Africa since the Mesozoic: S.Afr. J. Geol. 90:2. p. 179-208.
Schwartz, H.I., and Midgley, D.C., 1975, Evaluation of geohydrologic constants for the Far West Rand dolomitic formations: Civil Eng. in S.Afr. v. 17, no. 2.
South African Committee for Stratigraphy (SACS), 1980, Stratigraphy of South Africa, Part 1 (Comp. L.E. Kent): Lithostratigraphy of the Republic of South Africa, South West-Africa/Namibia, and the Republics of Bophuthatswana, Transkei and Venda. Handbook geol. Surv. S.Afr., 8.
Tucker, M. E., and Wright, V. P., 1990, Carbonate Sedimentology: Blackwell, London, 482 p.
Vegter, J.R., 1987, Constraints on the utilization of groundwater resources in dolomitic strata, South Africa: Second Multidisciplinary Conf. Sinkholes and Environmental Impacts of Karst, Orlando, Florida, p. 343-347.
Wilkins, C.B., Eriksson, P.G., and Van Schalkwyk, A., 1987, Two generations of karst-filled sedimentary rocks within Chuniespoort Group dolomites south of Pretoria: S.Afr. J.Geol. 90:2. p. 155-167.

KARST HYDROGEOLOGY IN TASMANIA

KEVIN KIERNAN
Forestry Commission
30 Patrick Street
Hobart, Tasmania, 7000
Australia

INTRODUCTION

The total extent of karst aquifers in Australia is considerable (Smith, 1988) but exposed karst is less abundant than in any other continent (Jennings, 1975). Although the island of Tasmania has an area of only 68,000 km^2, and therefore, comprises barely more than 1% of Australia, it contains a disproportionate share of the country's exposed karst. The extent of exposed karst in Tasmania has not yet been determined accurately (Fig. 1), but initial approximations suggest that the most karstic of Tasmania's carbonate rock formations occur at the surface over ~277,000 ha or ~4.4% of the area of the island. These figures do not take into account interstratal karst aquifers that are likely to be present in various parts of Tasmania and which have occasionally been encountered during mining and tunnelling operations (Hughes, 1957).

Tasmania lies at ~41-43°S latitude in the westerly wind regime of the Roaring Forties. Rainfall ranges from over 3,300 mm/a on the western mountains to ~500 mm in the rainshadow areas further east, with a winter maximum. These maximum precipitation totals are exceeded in Australia only in parts of tropical Queensland, but the rainfall events in Tasmania are less intense and of longer duration. Western Tasmania is one of only three areas in Australia where the mean annual runoff exceeds 1,250 mm, the continental average being only 45 mm with less than 5% of Australia exceeding 250 mm (Watson, 1976). Western Tasmania receives only ~1,500 sunshine hours annually, less than any other part of Australia, but the total rises to ~2,500 hours in the northern midlands. Air temperatures are moderated by the close proximity of the Southern Ocean, no part of the island lying more than 115 km from the sea. Sea surface temperatures around the coast are 11-15°C. The mean annual temperature at sea level in the west is ~9-10°C.

Western Tasmania consists of a fold-structure province formed of pre-Carboniferous rocks and characterized by north-south trending ridges of resistant conglomerates and quartzites that rise above valleys cut in phyllites and carbonate rocks. Eastern Tasmania consists of a fault-structure province formed on flat-lying post-Carboniferous sedimentary rocks and Jurassic dolerite, and is characterized by tabular interfluves and a rectangular drainage pattern. Tasmania has been relatively stable tectonically since the early Tertiary although there is some evidence of minor Pleistocene movement in the southwest and minor ongoing seismic activity is well documented (Richardson, 1988).

International Contributions to Hydrogeology, Vol. 13 (1992)
© Verlag Heinz Heise, Hannover, FRG

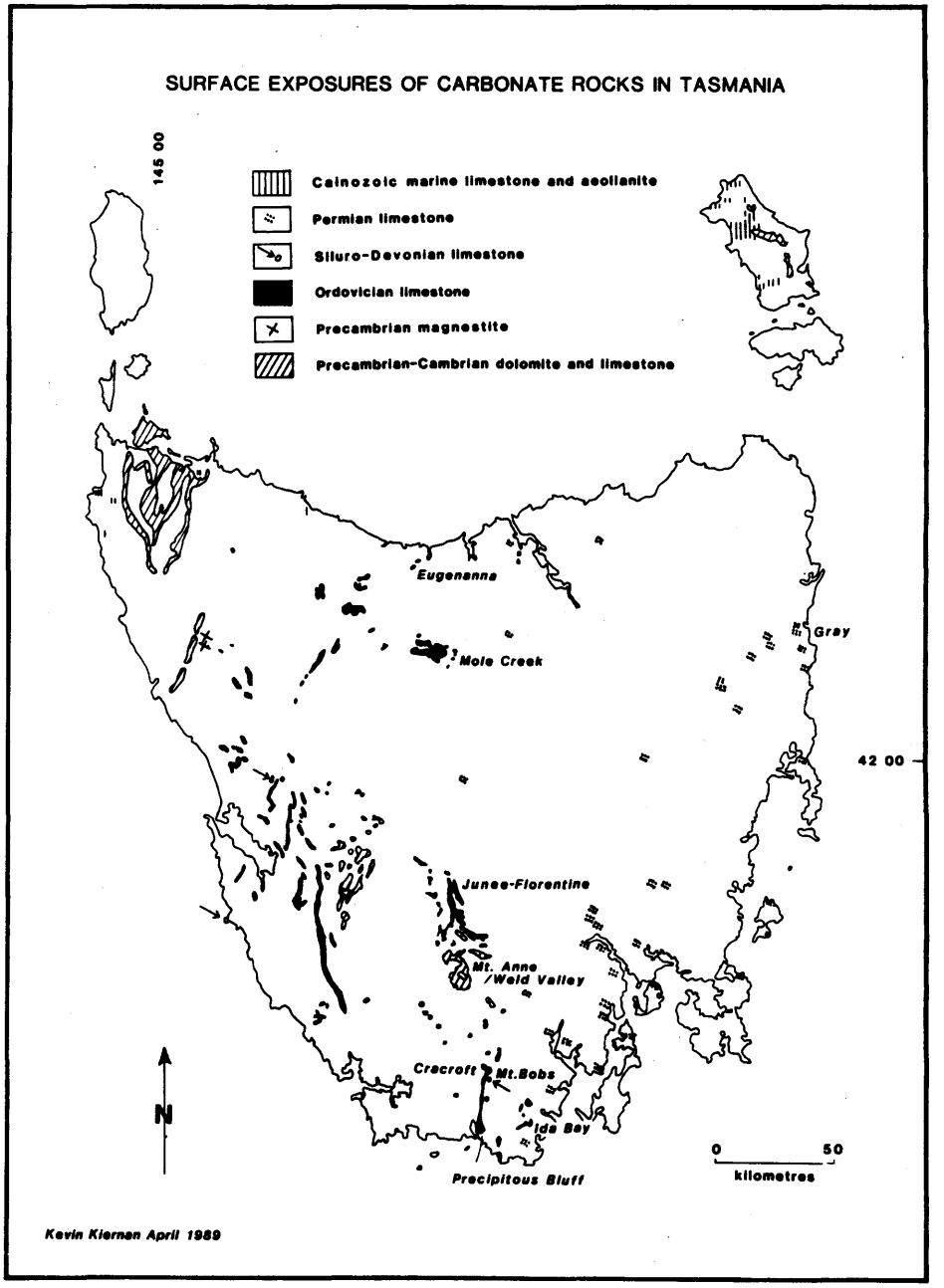

Figure 1. Extent of exposed carbonate formations recorded to date in Tasmania. Geological mapping is far from complete, and it is anticipated that further outcrops will be found and that the boundaries of some of those depicted will be refined. The extent of the smaller occurrences, and in particular the Permian limestone outcrops, is exaggerated on this map due to difficulties of representation at this scale.

Although Tasmania is now totally deglaciated, ice caps, valley and cirque glaciers developed on at least four and possibly six or more occasions during the late Cenozoic and had a significant effect upon the evolution of some of the karst (Kiernan, 1982, 1989a). At these times periglacial conditions extended to low altitudes outside the glacial limits. Many of the carbonate rock localities are mantled by unconsolidated allogenic surface sediments that were deposited in response to slope instability that resulted from reductions in the forest biomass that occurred during the episodes of cold climate. In some caves, cave streams were displaced by sediment influxes that caused a temporary reversion to surface drainage. At Precipitous Bluff and in a few other locations, carbonate rocks occur on the coast and Quaternary sea-level change appears to have influenced evolution of some of the underground drainage systems.

TASMANIAN KARST AREAS

Much of the karst is essentially unexplored, particularly in the west where there is very dense natural vegetation, including temperate rainforest, eucalypt forests, and some scrublands and sedglands, and there are few roads or walking tracks. The principle karst has developed in dolomites and limestones of upper Precambrian-lower Cambrian age (total extent ~140,000 ha) and in the limestones of the Gordon Group, which consists of ~1,500 m of warm marine carbonate formations of predominantly Ordovician age (~136,000 ha). These rocks occur along valley floors in the fold province but attain their highest topographic relief further east where overlying post-Carboniferous rocks have protected them from weathering and erosion. Karst has also been developed on Precambrian magnesite (~227 ha) and Siluro-Devonian limestones (~140 ha). The rocks of the fault province include some thin and generally impure limestones of Permian age where only minor karst features have been reported to date (Eberhard and Eberhard, 1989) but some karstic aquifers are likely to occur. Some karst phenomena also occur in Cenozoic marine limestones and eolianites that occur in northwestern Tasmania and on some of the islands in Bass Strait, which separates Tasmania from continental Australia. The oldest evidence of karstification comes from Eugenana in northern Tasmania where a cave fill exposed by quarrying contains fossil spores of middle Devonian age (Burns, 1964). However, no research has been undertaken on other potential phases of paleokarst development prior to the evolution of the present karst terrains, although paleokarst sediments are known from other sites such as Ida Bay in southern Tasmania.

The greatest topographic relief attained by any of the carbonate rocks is in the Weld Valley/Mt. Anne area where the dolomite rises 600 m above the valley floor and contains the deepest cave yet explored in Australia, Anne-a-Kanada (-373 m). The longest underground drainage system in the Precambrian rocks is probably the Lake Timk system in the same area. Watersinks occur around the lake margin and one of these gives access to a cave that is not water-filled and which has been followed in under the lake bed to a depth of at least 20 m below the lake surface. Exploration remains incomplete, but it is clear from the fact that the sub-lacustrine cave is not water-filled that the lake surface does not represent the base level of vadose circulation in the dolomite in this part of the Timk Valley. The water is

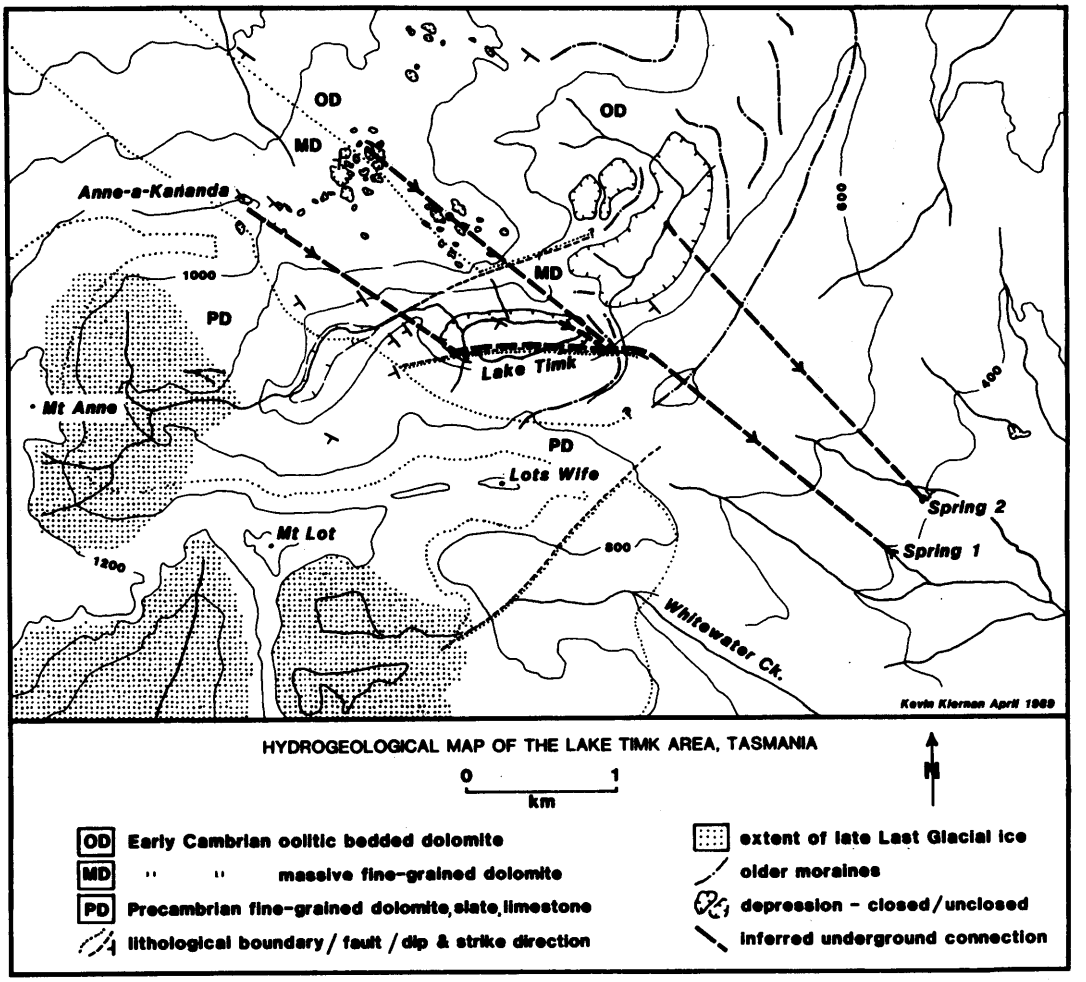

Figure 2. Hydrogeological interpretation of the Lake Timk area in the Weld Valley-Mt. Anne karst (from Kiernan, 1989b). At the close of the late Last Glacial (Wisconsin) Stage the 25 m deep rockbasin was drained via a surface meltwater channel 15 m above the present water level. Geological information based in part on Turner et al. (1985). A major karst watersink subsequently developed at the eastern end of the lake, but this is now only seasonally active following the development of new lower level sinks around the lake shore and possibly beneath the lake bed. It is conceivable that earlier karst outlets were blocked by glacial and/or proglacial sedimentation during the middle-late Pleistocene.

believed to emerge ~2.4 km away on the opposite side of a major surface drainage divide but this has not yet been proven by dye tracing (Kiernan, 1989b, 1990a). Drainage from the Anne-a-Kanada area may join the Lake Timk drainage by following the strike of the dolomite southward until it is deflected along a fault that raises relatively impermeable rocks to the surface along the southern shore of the lake. If this is the case, the linear distance between the presumed resurgence and its most distant sources may be ~4.8 km (Fig. 2). Karst development in this area is most pronounced in oolitic bedded dolomite and massive fine-grained dolomite facies of Early Cambrian (?) age, and apparently negligible in late Precambrian fine-grained dolomite and limestone that lies immediately adjacent to it (Turner et al., 1985). In far northwestern Tasmania, karstification in the Precambrian/Cambrian carbonates is most pronounced in oolitic limestone that has resisted dolomitization (Longman and Mathews, 1961; Kiernan, 1980).

The three longest caves recorded from Tasmania, Exit Cave at Ida Bay (≥ 20 km), Growling Swallet in the Florentine Valley (≥ 12 km), and Herberts Pot at Mole Creek (≥ 5.3 km), are all developed in Ordovician limestone. The two deepest caves in this rock are the Ice Tube/Growling Swallet system (~354 m) and Khazad-Dum (~323 m) in the adjacent Tyenna River Valley. Both the latter are major streamsinks and their waters follow the strike of the limestone beds to resurge from Junee Cave (Fig. 3), an outflow located in the Tyenna Valley 9.4 km from Growling Swallet (Gleeson, 1976). This is the greatest linear distance between any streamsink and its resurgence yet proven in Tasmania. However, the drainage from more distant streamsinks as far as 5-6 km north of Growling Swallet may also flow to Junee Cave (Kiernan, 1971; Gleeson, 1976). Junee Cave is the largest spring in Tasmania, with measured discharges from April 1971-March 1972 ranging from 202-3,616 L/s (Goede, 1973). Six underground drainage systems at Mole Creek span linear distances of 2.2-3.6 km, another in the Cracroft Valley reaches 2.5 km, and the linear distance between Exit Cave and its furthest streamsink is 2.3 km. The thickly bedded Cashions Creek Limestone, which is readily identified by the presence of the fossil gastropod *Maclurites,* hosts some of the most prominent caves and karst formed in the Gordon Group limestones (Kiernan, 1988a). The Cashions Creek limestone consists of spherical to subspherical oncolites supported by intraclastic calcarenite, and it is characterized by fragmented fossil shells and erosional contacts between beds (Banks and Burret, 1988). Karst is also well developed in the Benjamin Limestone, which in the Florentine Valley consists of ~1,200 m of predominantly micritic limestone.

The glaciokarstic Lake Sydney in the Mt. Bobs area drains into a streamsink formed in Siluro-Devonian limestone and bypasses the 1-km long Pine Lake further down the same valley to emerge in the upper reaches of Farmhouse Creek (Kiernan, 1989c). The geology of the area is not completely known but it is likely that Lake Sydney water follows the strike of the limestone beds to pass west of Pine Lake. However, given the evidence of active vadose circulation beneath the bed of Lake Timk, the possibility of a similar situation in this valley cannot be discounted totally.

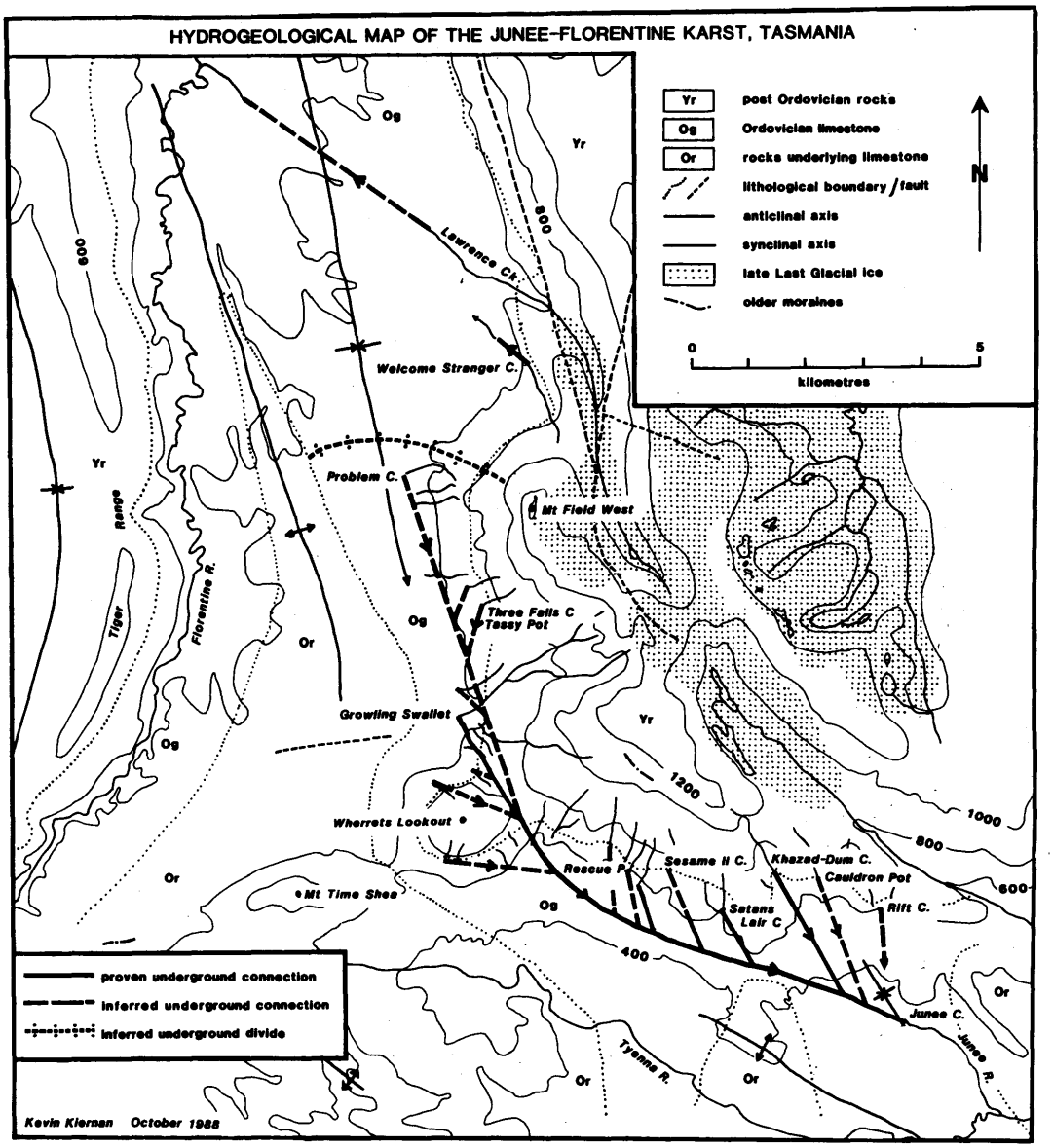

Figure 3. Hydrogeological interpretation of the Junee-Florentine karst, south-central Tasmania. Structural and drainage information based in part on Hughes (1957), Corbett (1964), Kiernan (1971, and unpublished data), Goede (1973), and Gleeson (1976). Meltwater from glaciers and snowfields that existed during the Pleistocene reached much of the karst. Past glacial limits in the area have not been researched in detail and the map depicts an estimate only of the comparatively small glaciers that existed during the late Last Glacial (Wisconsin) Stage; the ice cover earlier during the Pleistocene was probably much more extensive.

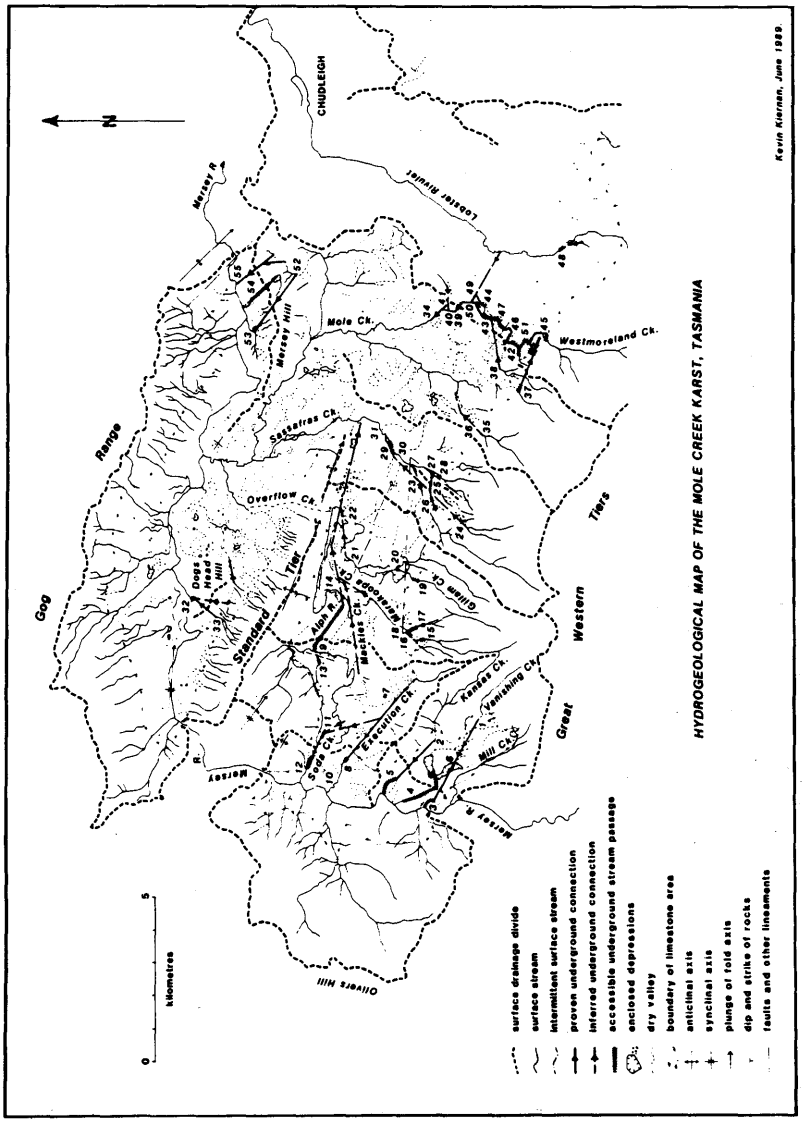

Figure 4. Hydrogeological map of the Mole Creek karst (from Kiernan, 1989e). Drainage in the Mole-Lobster divide mostly after Jennings and James (1967) and Gleeson (1976), elsewhere after Kiernan (1984, and unpublished data). Cave locations indicated on map: 1. Hidden Cave, 2. Rubbish Heap Cave, 3. Tailender and Mill Caves, 4. Croesus Cave, 5. Lynds Cave, 6. Rat Hole, 7. Little Trimmer Cave, 8. Lime Pit, 9. Kubla Khan Cave, 10. Ploughmans Spring, 11. Maze Puzzle and Kohinoor Caves, 12. Soda Creek Cave, 13. Howes Cave, 14. Alph Cave, 15. Devils Pot, 16. Marakoopa I Cave, 17. Marakoopa II Cave, 18. Snailspace, 19. Gillam Cave, 20. MC 81-82, 21. Gurrs Cave, 22. Varve Cave, 23. Baldocks Cave, 24. Prohibition Cave, 25. My Cave, 26. Nut Bath Cave, 27. Cyclops Cave, 28. Glow-worm Cave, 29. Sassafras Cave, 30. Sassafras II Cave, 31. Caterpillar Cave, 32. Union Cave, 33. Harry Creek Cave, 34. Scotts Rising, 35. Waterworks Cave, 36. Scotts Cave, 37. Kelly Pot, 38. Old farmhouse streamsink, 39. Roaring Hole, 40. Mouse Cave, 41. Cow Cave, 42. Herberts Pot, 43. Wet Cave, 44. Honeycomb I Cave, 45. Westmoreland Cave, 46. Dangerous Hole, 47. Georgies Hall Cave, 48. Lobster Rising, 49. Honeycomb II Cave, 50. Blackberry Hole, 51. Leech Pot, 52. Redwater Pot, 53. Den Cave, 54. Mersey Hill Cave, 55. Fault Creek Spring.

THE MOLE CREEK KARST

The most detailed information yet available on the geological controls on karst and the nature of the aquifers comes from the Mole Creek area in central northern Tasmania. The Mole Creek karst comprises a belt of Ordovician limestone ~1000 m thick bounded to the south by the margin of Tasmania's Central Plateau, known locally as the Great Western Tiers (1,200 m), to the west and north by the Mersey River (280-180 m), and to the east by broad plains formed on post-Carboniferous rocks. The mean annual temperature is ~12°C on the lower slopes where rainfall totals ~1,000 mm compared to perhaps 1,800 mm on the crest of the Tiers. The limestone crops out over ~250 km^2 at ~200-600 m altitude with a maximum topographic relief of 320 m. It has been folded during the Middle Devonian into a series of anticlines and synclines the axes of which strike from NW-SE or E-W. This folding locally raises to the present landsurface the impermeable underlying sandstones of the Moina Formation which form an elongate ridge known as Standard Tier and which bound the limestone to the north. The limestone is locally overlain by Siluro-Devonian metasediments and more widely by marine and freshwater sediments of Permian and Triassic age. The crest of the Tiers is capped by Jurassic dolerite. Tertiary basalt overlies the limestone to the west and also caps Mersey Hill. Some faulting has occurred in association with Jurassic and Tertiary epeirogeny. A hydrogeological map of the Mole Creek karst is presented as Figure 4 and forms the basis for the following discussion.

Controls on the Evolution of the Karst Hydrogeology

Acidic runoff is delivered to the karst from the forest and scrublands that have developed on the surrounding rock formations. The impermeable and coherent Permo-Triassic rocks have focused infiltration into the limestone along the unconformity at the upslope margin of the limestone outcrop, leading to the development of many large open intake conduits. In contrast, the structure of the Moina Formation facilitates the production of thick slope deposits that consist of angular clasts and a sandy matrix and which have spilled over the limestone margin. These slope deposits dissipate infiltration and no large intake conduits are known in this terrain. Similarly, vertical jointing in the basalt also permits diffuse infiltration. On Mersey Hill this vertical jointing has facilitated collapse of the basalt into cavities in the limestone to form a large subjacent karst uvala and several smaller sinkholes in some of which streamsinks occur.

Streams that sink at the foot of the Tiers carry a substantial load of very coarse, up to boulder size, dolerite clasts. These affect considerable mechanical erosion in the parts of the cave systems where the hydraulic gradient is steep, but clays derived from weathering of the dolerite accumulate and impede underground circulation where the hydraulic gradient is low, a situation that also applies in the caves beneath the basalt cap on Mersey Hill. These streamsinks are the most significant sources of aquifer recharge. Discharge is affected primarily by a series of prominent springs. The largest of these are Scotts Rising, the source of the Mole Creek itself; Sassafras Creek Cave, the source of Sassafras Creek; a large spring

northwest of Sassafras Creek Cave that is presumed to be the resurgence of the Mayberry water; the Marakoopa Cave and River Alph springs at Mayberry; Union Cave and Den Cave at the northern edge of the karst; and Lime Pit, Lynds Cave, and the Tailender spring at the western extremity of the limestone. North of Standard Tier lies a broad limestone strath that is veneered by glaciofluvial sediments deposited by the Mersey River. A number of deep rock-walled sinkholes in this area that are permanently waterfilled discharge substantial volumes of water during the winter. Some may be minor estavelles.

Broad-scale geological structures exert the most conspicuous controls on the karst hydrogeology. Most of the underground streams are deflected along the strike of the limestone beds, in many cases flowing eastwards parallel to the plunge of the fold axes. Hence, some streams pass beneath prominent surface drainage divides. For example, the River Alph sinks in the Loatta polje at the western end of the limestone belt and emerges into the Mayberry polje further to the east where it sinks again (Kiernan, 1984, 1989d, 1989e). Although stream tracing has not yet been conducted, the emergence of the long strike ridge of Standard Tier on the southern side of the Mayberry polje cuts off subterranean drainage northward and leaves little option but for the underground water to continue its eastward course beneath another major surface divide to emerge from a large spring in the Sassafras Creek Valley (Jennings, 1967, 1985). Similarly, the stream that sinks into Kelly Pot at the head of the Mole Creek Valley is deflected along the strike to breach another major surface drainage divide and emerge in the Lobster Rivulet Valley (Jennings and James, 1967). At least one other stream follows a parallel course.

A second major influence on the direction of underground drainage is the hydraulic gradient. Comparatively rapid incision by the Mersey River relative to its smaller tributaries has been a major factor. The steep gradient of tributaries that descend from the Great Western Tiers enables them initially to cut across the strike of the limestone until the gradient lessens. At the far western end of the limestone belt the gradient has favored underground drainage westward to the Mersey River rather than eastward along the plunge of the folded rocks. The large size and configuration of the Kubla Khan system suggests it was initially the principal underground outlet for the drainage eastward from the Loatta polje. However, incision by the Mersey River appears to have progressively steepened the hydraulic gradient westward, pirating much of the Loatta water to the Kohinoor-Soda Creek drainage system and, more recently, facilitating the development of an outflow from Lime Pit.

Another geological control on the formation of karst has been the relative resistance to erosion of the various rock units. Sensation Gorge, which extends northward from the Mayberry polje through the relatively impermeable Moina Formation rocks that form Standard Tier, was probably cut by a watercourse that was superimposed from the former cover rocks and/or by a glacial meltwater stream. Today this gorge serves only as an overflow when the stage is too high for the karstic channels to evacuate all the water from the Mayberry polje. While the Moina rocks have impeded downcutting by the streams, incision has progressed headward up the Sassafras Creek Valley, steepening the hydraulic gradient towards

the east and providing a lower base level to which the Mayberry water has been able to flow underground (Jennings, 1967).

A history of climatic change and cold climate geomorphic processes has also been important to the evolution of the karst, primarily through its control on the deposition and character of the landforms and surface sediments and on the evolution of surface drainage patterns that have been established above the carbonate rocks. The floor of the Lobster Rivulet Valley at the eastern end of the limestone belt is buried beneath glaciofluvial gravels that are probably of Middle Pleistocene age. These fans have displaced surface drainage into peripheral channels that have developed against the foot of the limestone ridges that trend northwards from the foot of the Tiers. This has facilitated the development of vadose caves along the periphery of the ridges. This process probably accounts for the deflection westward of Westmoreland Falls Creek, originally a tributary of the Lobster Rivulet, to join the drainage from Kelly Pot which flows in roughly the opposite (eastward) direction. This combined water then passes through a series of vadose invasion caves back beneath the Mole-Lobster divide into Mole Creek Valley (Jennings and Sweeting, 1959). The Kelly Pot water therefore completes a double underground crossing of the surface drainage divide. Similarly, in the Sassafras Creek Valley the principal underground drainage conduit has developed just inside the margin of a limestone divide, parallel to a peripheral surface drainage channel, and only a few meters below the level of its thalweg (Kiernan, 1984, 1989c).

However, some of the caves contain clastic deposits similar to those that form the glaciofluvial fans, which suggests that initial speleogenesis may have predated the present fans and peripheral channels on the surface. Earlier episodes of glaciation are known to have occurred on the Tiers. Indeed, the presence of tills of early Pleistocene age in the Croesus Cave area and on Mersey Hill (Kiernan, 1982, 1984, 1989d; Hannan and Colhoun, 1987) and further east in the Chudleigh area (Colhoun, 1976) indicates that most, if not all, of this karst area was once inundated by glacial ice. Subglacial and submarginal meltwater drainage would also have favored speleogenesis in those positions where the caves occur. If decanting of meltwater from the present glaciofluvial fans compounded, rather than initiated, cave development it might explain the presence of some fan gravels in some caves (Kiernan, 1982). Alternatively, the caves may have been initiated along unloading joints formed after the early Pleistocene ice was removed. Ongoing research is being directed toward resolving some of these questions.

Variations in Groundwater Distribution with Stage

Hydrogeological research in the Mole Creek karst has not yet seriously pursued the question of drainage changes with variations in stage. While many of the streamsinks are permanent, a number of the most prominent springs are only intermittent. For instance, the Cyclops Cave spring dries up in summer despite continued recharge of the aquifer from the My Cave and Cobbler Cooler/Nut Bath streams. This water is believed to flow to Sassafras Cave, normally the source of Sassafras Creek, but in very dry summers the stream in the latter cave also vanishes with the water emerging instead from the surface streambed several hundred meters further downstream or from a series of streambank springs that occur in the

same general area. It is highly likely that the baseflow from My Cave contributes to this discharge.

Similarly, discharges from some other caves are intermittent with the baseflow emerging from inaccessible springs. For instance, the baseflow from Mersey Hill Cave emerges from a spring in the bed of the Mersey River (A. Goede, pers. comm.). The Lime Pit spring presumably now carries the baseflow that previously discharged from Soda Creek Cave. The discharge from Tailender Cave is also intermittent, but there is a permanent spring in the Mersey riverbed near the cave mouth (Kiernan, 1984, 1989e).

Complex ananbranching of low-gradient baseflow streams is evident in the Honeycomb Cave area (Jennings, 1967), and equally complex drainage probably exists in many less-studied parts of this karst. For instance, flood flows from a streamsink near Baldocks Cave occupy a surface channel, but when the stage is lower the water is accommodated by an accessible stream passage in Baldocks Cave. At least some of the Baldocks Cave water probably emerges from a spring that empties into the surface stream from Cyclops Cave. At still lower stage both the Baldocks Cave stream and the surface stream from Cyclops Cave vanish, the spring near Baldocks remaining active, but the water disappearing underground again after only a short distance. At very low stage, the spring ceases to flow altogether despite continued recharge of the aquifer from the streamsink near Baldocks Cave and probably from the baseflow leakage out of My Cave, this water presumably flowing directly to Sassafras Cave or one of the baseflow springs further downstream.

No accurate discharge figures are available, but Jennings (1967) has estimated that the flow from the largest spring, Scotts Rising, reached 10 m^3/s after heavy rain in August 1961. However, the mean discharge is probably less than 1 m^3/s. Lynds Cave has a mean discharge of <50 L/s, but the main channel has been estimated to discharge up to 480 L/s in flood with at least a similar volume discharging from associated springs at and below river level. Such limited attenuation of flood discharges suggests that open conduit systems are present. Travel times during dye tests confirm this impression, although they have varied widely between different cave systems. On the one hand, fluorescein injected into Honeycomb Cave at low stage took 55 hours and 33 minutes to reach Scotts Rising, 1.65 km away and 30 m lower (J. N. Jennings and M.M. Sweeting, pers. comm.). On the other hand, fluorescein injected into Kansas Creek at Rubbish Heap Cave under flood conditions reached the Lynds Cave outflow 2.4 km away and 120 m lower in only 70 minutes, implying a velocity of 2.06 km/hr. Similarly, a rapid velocity of 1.13 km/hr has been recorded at high stage between the My Cave inflow and the Cyclops Cave outflow. These velocities are very rapid indeed by world terms. In part they reflect the steep gradients of many of the systems (Table 1), but the formerly greater volumes of meltwater that enlarged the conduits probably also played a role.

Table 1. Dimensional parameters and gradients of some underground drainage systems in the Mole Creek karst.

System	Linear distance (km)	Approx. vertical range (m)	Approx. mean gradient (m/km)
Hidden-Tailender	3.0	280	93
Rubbish Heap-Lynds	2.4	120	50
Execution-Lime	3.3	205	62
Kohinoor-Soda	1.2	80	67
Howes-Kubla Exit	1.8	30	17
Devils-Marakoopa	0.7	140	200
Mayberry-Sassafras	2.75	60	22
Prohibition-Sassafras	3.6	290	81
Baldocks-Sassafras	1.85	60	32
Harry Creek-Union	0.9	40	44
Redwater-Den	2.2	35	16
Kelly-Wet	2.65	220	83
Westmoreland-Wet	2.0	90	45
Honeycomb-Scotts Rising	1.65	30	18

Some springs appear to behave out of phase with others in the same general vicinity or otherwise anomalously due to microclimatic differences in the recharge areas. This is exemplified by the Lynds Cave, Croesus Cave, and Tailender springs that lie within 2 km of one another at the western end of the karst area. The catchment of Kansas Creek, which flows to Lynds Cave, extends to the top of the Tiers, an area subject to very heavy rainfall. The catchment of Vanishing Creek, which flows via Rat Hole to Tailender Spring, lies on the middle and lower slopes. An estimated discharge of 480 L/s was observed at Lynds Cave on March 24, 1984, following 65 mm of rain on the crest of the Tiers during the preceeding 24 hours, but the level of Tailender spring and the stream in Rat Hole Cave rose only slightly. The following day Vanishing Creek rose appreciably in response to heavier rain on the slopes, but Kansas Creek dropped dramatically. On neither day did the Croesus Cave stream vary greatly from its usual discharge of ~10 L/s, which is generally maintained within a range of 2-4 L/s irrespective of the weather, suggesting its source is primarily diffuse rather than conduit interception. However, Croesus is by far the largest of the three caves and may previously have been the course of Kansas Creek, Vanishing Creek, or both. Rare major floods have occurred in Croesus Cave, suggesting the reactivation of a fossil channel at very high stage or, more probably, overland flow from Kansas Creek into an uvala above upstream Croesus Cave.

KARST RESOURCES, EXPLOITATION, AND MANAGEMENT

Little information is available regarding the character of the underground karst waters. In the far northwest, most of the water from the karst aquifers is satisfactory for domestic, agricultural, and irrigation use, but the iron content can be moderately high (Gulline, 1959). The temperature of resurging waters varies from 6.0-8.8°C at Junee Cave (Goede, 1973) to 9.2-10.8°C at Mole Creek (Kiernan, 1984). Field pH during 11 months of monitoring at Junee Cave varied from 7.40-8.65, $CaCO_3$ from 44.0-94.5 mg/L, and $CaCO_3$+$MgCO_3$ from 51.0-108.0 mg/L with a tendency towards maxima in these values during autumn and minima during spring (Goede, 1973). In the Mole Creek area, pH values measured from underground streams range from 6.6-8.5 with filterable residue ranging from 15-190 units (Kiernan, 1984). These figures relate to primarily allogenic waters. Less is known of autogenic karst water, but a total Ca and Mg value of 295 mg/L has been obtained from a cave stream at Ida Bay that is believed to be fed solely by seepage water, which contrasts with a value of 67.5 mg/L obtained from an allogenic cave stream in the same area (A. Clarke, pers. comm.). Cave dripwaters sampled from Scotts Cave at Mole Creek had a pH of 8.1-8.3 and $CaCO_3$ hardness of 103-153 mg/L (Kiernan, 1984). Goede (1981) found that over a period of thirteen months the mean total hardness of drips from Little Trimmer Cave at Mole Creek and Frankcombe Cave in the Florentine Valley was 268 ppm and 204 mg/L respectively. More recently, weekly sampling from Little Trimmer Cave between July and October 1990 revealed a mean total hardness value of 252 ppm for the cave stream, which is believed to be fed primarily by percolation. Dripwater flows recorded from a variety of sites in the cave varied from 146 to 320 ppm over the same period (Eberhard and Kiernan, 1990).

Human occupation and modification of Tasmania's karst dates back to at least 30 ka BP when Prehistoric Aborigines took advantage of a more open vegetation that existed in the western and southern karst regions during the late Last Glacial Stage. The distribution of archaeological sites shows that access along grassland areas in gentle limestone valleys, shelter in caves, and the availability or otherwise of water on the surface played a major role in shaping the patterns of occupation of the karst regions. Extensive middens were deposited in some caves. The Aborigines' use of fire to keep the vegetation open and to promote fresh growth that would encourage game species is likely to have led to erosion in parts of the landscape and there is evidence of associated sediment influxes into caves that have locally modified the karst drainage (Kiernan et al., 1983; Cosgrove, 1989).

Since European settlement in 1804, there has been increasing development of some karst areas for agriculture and timber (Kiernan, 1984). However, most of Tasmania's karst remains uninhabited and some of it has been protected in national parks that have been placed on the List of the World's Cultural and Natural Heritage established by UNESCO. Some of the karst aquifers elsewhere have become locally significant as water supplies (Gulline, 1959). However, practices such as rubbish dumping in sinkholes, poor stock management around watercourses, and possibly some leakage of human fecal material from septic tank systems has led

to contamination of groundwater at Mole Creek and at Ida Bay. The most heavily polluted spring is at Mole Creek where maximum recorded values of coliform, fecal coliform, and fecal streptococci content per 100 mL total 30,000, 2,800, and 2,800, respectively. Problems of ground surface instability and resulting engineering difficulties have arisen in several karst areas (Kiernan, 1990b, 1988b), in at least one case due to dewatering operations at a limestone quarry and elsewhere to drainage changes associated with road construction and the clearing of native forests for pasture or by the timber industry. The development of hydro-electric projects has been complicated by karstic foundations (Roberts and Andric, 1974). Hence, a range of karst management issues is emerging.

CONCLUSIONS

In this tectonically stable environment the predominant controls upon the formation of karst and the distribution of groundwater are the broad structure of the limestones coupled with the impact of previous episodes of cold climate that have given rise to abundant meltwaters and widespread slope instability. The deposition of coarse clastic sediments during these times has deranged the surface drainage and superimposed structurally anomalous drainage patterns upon the carbonate rocks. The most prominent underground drainage systems have been generated by vigorous allogenic streams that carry a substantial load of hard lithic tools that facilitate mechanical erosion. These streamsinks remain important sources of aquifer recharge since many of these streams originate in localities that receive much higher rainfall than do the karst areas themselves. Nevertheless, diffuse recharge from autogenic seepage waters is probably of greater relative significance to aquifer recharge today than it was at times when glaciers and snowfields were present in the highlands. Discharge of the aquifers is via small surface springs and presumably also via submerged springs in the beds of the principal rivers that form the effective vadose base level in the impounded karst areas. Submarine discharge is possible from some coastal karst aquifers. Only in a few cases is it likely that significant volumes of underground water from the karst aquifers discharge into aquifers in other rocks since the principal carbonate formations that host karst are often surrounded by relatively impermeable rocks.

The karst hydrogeology has important management implications in terms of land-use, engineering, water supply, and groundwater pollution problems. The limited familiarity of Tasmanian land managers with the implications of karst increases the likelihood of problems arising in future due to inadvertent errors. However, to date only a few problems have become evident due to the limited economic activity in the karst areas. Hence, if awareness can be raised, the opportunity exists for management of a high standard to be applied to karst where there is no legacy of past neglect to inhibit success.

Acknowledgements--I am grateful to Phil Jackson, Andrew McNeil, Attila Brana, Henry Shannon, Ron Mann, Brendan Diacono, and Rolan Eberhard for assistance with some of the water tracing experiments, and to Dr. Humphrey Elliot for comments on a draft of this paper.

REFERENCES

Banks, M. R., and Burrett, C. F., 1988, The Gordon Group (Early Ordovician to Early Silurian) - mainly platform carbonates, pp. 201-224 in Burrett, C. F., and Martin, E. L., eds., Geology and Mineral Resources of Tasmania: Geological Society of Australia Special Publication 15, 574 p.

Burns, K. L., 1964, Devonport: Geological Survey Explanatory Report K'55-6-29, Tasmanian Department of Mines, Hobart.

Colhoun, E. A., 1976, The glaciation of the lower Forth Valley, northwestern Tasmania: Australian Geographical Studies 14: 83-102.

Corbett, K. D., 1964, Geology of the Florentine Valley Area: BSc. (Hons.) thesis, University of Tasmania.

Cosgrove, R., 1989, Thirty thousand years of human colonisation in Tasmania: New Pleistocene dates: Science 243: 1706-1708.

Eberhard, R., and Kiernan, K., 1990, Little Trimmer Project: instrumented monitoring of the underground environment: in Brooks, S., ed., Cave Leeuwin 1991, Proceedings of the 18th Biennial Conference of the Australian Speleological Federation, p. 66-69.

Eberhard, S., and Eberhard, R., 1989, Caves on Tasmania's east coast: the Gray-Mt. Elephant karst area, Speleo Spiel 246: 1-15.

Gleeson, L., 1976, Hydrology projects at Mole Creek and Junee: Southern Caver 8(2): 11-13.

Goede, A., 1973, Hydrological observations at the Junee resurgence and a brief regional description of the Junee area, Tasmania: Helictite 11(1): 3-24.

Goede A., 1981, Variation in hardness of cave drips at two Tasmanian sites: Helictite 19(2): 57-67.

Gulline, A. B., 1959, The Underground Water Resources of the Smithton District: Underground Water Supply Paper 5, Tasmanian Department of Mines.

Hannan, D. G., and Colhoun, E. A., 1987, glacial stratigraphy of the upper Mersey Valley, Tasmania: Australian Geographical Studies 25(2):36-46.

Hughes,. T. D., 1957, Limestones in Tasmania: Geological Survey Mineral Resources 10, Hobart, Tasmanian Department of Mines.

Jennings, J. N., 1967, Some karst areas of Australia, pp. 256-292, in Jennings, J. N., and Mabbutt, J. A., eds., Landform Studies from Australia and New Guinea: ANU Pres, Canberra and Cambridge University Press, Cambridge.

Jennings, J. N., 1975, How well off is Australia for caves and karst? A brief geomorphic estimate, Proceedings, 10th Biennial Conference, Australian Speleological Federation: 82-90, ASF, Sydney.

Jennings, J. N., 1985, Karst Geomorphology: Blackwell, Oxford and New York, 292 pp.

Jennings, J. N., and James, B. N., 1967, Underground water movements in the Mole Creek-Lobster Rivulet divide, Tasmania: Australian Journal of Science 30(3): 108-109.

Jennings, J. N., and Sweeting, M. M., 1959, Underground breach of a divide at Mole Creek, Tasmania: Australian Journal of Science 21 (8): 261-262.

Kiernan, K., 1971, Caves and karst of Junee-Florentine, Tasmania: Australian Speleological Federal Newsletter, 53: 4-10.

Kiernan, K., 1980, More north-west Tasmanian karst: the Julius River-Lake Chisholm area: Southern Caver, 11(4): 3-8.

Kiernan, K., 1982, Glaciation and karst in Tasmania: Review and speculations: Helictite 20 (1): 11-16.

Kiernan, K., 1983, Relationship of cave fills to glaciation in the Nelson River Valley, central western Tasmania: Australian Geographer 15: 267-375.

Kiernan, K., 1984, Landuse in Karst Areas: Forestry Operations and the Mole Creek Caves: Australian Heritage Commission Library, Canberra, 320 pp.

Kiernan, K., 1988a, Caves and karst areas of Tasmania; A brief survey: Journal of the Sydney Speleological Society 32(6): 107-121.

Kiernan, K., 1988b, The Management of Soluble Rock Landscapes: An Australian Perspective, Speleological Research Council Ltd., Sydney, 61 pp.

Kiernan, K., 1989a, Multiple glaciation of the upper Franklin Valley, Western Tasmania Wilderness World Heritage Area: Australian Geographical Studies 27, 2, 208-233.

Kiernan, K., 1989b, Bathymetry and origin of Lake Timk, South-West Tasmania: Helictite, 28, 1:18-21.
Kiernan, K., 1989c, Drainage evolution in a Tasmanian glaciokarst, Helictite 27, 1, 2-12.
Kiernan, K., 1989d, Caves, Karst and Management at Mole Creek, Tasmania: Dept. of Parks, Wildlife and Heritage Occasional Paper 22, 130 p.
Kiernan, K., 1989e, Underground drainage at Mole Creek, Tasmania: Australian Geographical Studies 28, 2: 224-239.
Kiernan, K., Jones, R., and Ranson, D., 1983, New evidence from Fraser Cave from glacial age man in southwest Tasmania: Nature 301(5895): 28-32.
Kiernan, K., 1990a, The alpine geomorphology of the Mt. Anne massif, southwestern Tasmania: Australian Geographer 21, 2: 113-125.
Kiernan, K., 1990b, Soil and water degradation in carbonate rock terranes: Australian Journal of Soil and Water Conservation, 3,4: 26-33.
Longman, M. J., and Mathews, W. L., 1961, Limestone at Redpa: Mines Dept. Tas. Tech. Rep. 6.
Richardson, R. G., 1988, Geophysics, Chapter 13 in Burrett, C. F., and Martin, E. L., eds., Geology and Mineral Resources of Tasmania: Geological Society of Australia Special Publication 15, 574 p.
Roberts, G. T., and Andric, M., 1974, Investigations into the watertightness of the proposed Gordon-above-Olga hydro-electric storage, southwest Tasmania: Quarterly Journal of Engineering Geology, 7(2): 121-136.
Smith, D. I., 1988, Carbonate aquifers in Australia-A review. Paper presented to 4th meeting of International Geographical Union Study Group S7, Human Impacts in Karst, 14-20 August, 1988, Canberra, Australia.
Turner, N. J., Calver, C. R., McClenaghan, M.P., McClenaghan, J., Brown, A. V., and Lennox, P. G., 1985, Pedder, Geological Atlas 1: 50,000 Sheet 8112S, Tasmanian Department of Mines, Hobart.
Watson, B., 1976, Climate and Hydrology of the West Coast of Tasmania: Hydro Electric Commission, Hobart.

HYDROGEOLOGY OF REGIONAL CARBONATE AQUIFERS IN EASTERN NEVADA

JOHN W. HESS
Water Resources Center
Desert Research Institute
2505 Chandler Ave., Suite 1
Las Vegas, Nevada 89120
USA

INTRODUCTION

Carbonate rocks underlie approximately 130,000 km^2 of the eastern one-third of the state of Nevada (Fig. 1). These fractured and solutionally modified rocks also extend beneath western Utah, southeastern Idaho, and eastern California. Large warm-water springs are associated with these carbonate rocks, and wells drilled into fractured zones in the rocks have been pumped at high rates with little water-level decline. In the large area underlain by carbonate rock, ground-water flow paths are not always concordant with the hydrographic and structural basins. Hydrologic evidence suggests extensive regional-scale circulation of ground water between some hydrographic and structural basins within the carbonate rock province (Fig. 2) (Mifflin and Hess, 1979; Mifflin, 1988). Recharge to the aquifer system occurs mostly from winter snow-pack melt water in the mountain ranges of north-central and east-central Nevada and the high mountain ranges in southern Nevada.

Interest in the carbonate aquifers of eastern Nevada developed more than 30 years ago as evidenced by work of the U.S. Geological Survey conducted in cooperation with the Nevada Department of Conservation and Natural Resources. This paper is a summary of the research efforts conducted by many individuals and organizations over that period of time with support from numerous federal, state, and local sources. Current research interest in the hydrogeology of the area has been driven by the water-supply needs of a rapidly expanding population in southern Nevada, a state with limited surface water that has been extensively developed. Recent studies of the ground-water resources of the carbonate rock aquifers in Nevada have been undertaken by the Desert Research Institute, U.S. Geological Survey, and U.S. Bureau of Reclamation. These studies have focused on three questions: 1) Where is water potentially available in the aquifer, 2) How much water potentially can be withdrawn from the aquifers, and 3) What effects might result from development of the aquifers?

BACKGROUND

The Great Basin is characterized by internal drainage and general aridity. There are few major rivers and streams, thus, ground water has been a key element in water supply. This reliance on ground water naturally led to major concern about its origin, occurrence, and sustained developable volume. Over the years the general physiography, geologic structure, and lithology have exercised considerable influence on where and how ground water has been developed, on estimates of

International Contributions to Hydrogeology, Vol. 13 (1992)
© Verlag Heinz Heise, Hannover, FRG

Figure 1. Location of carbonate-rock province.

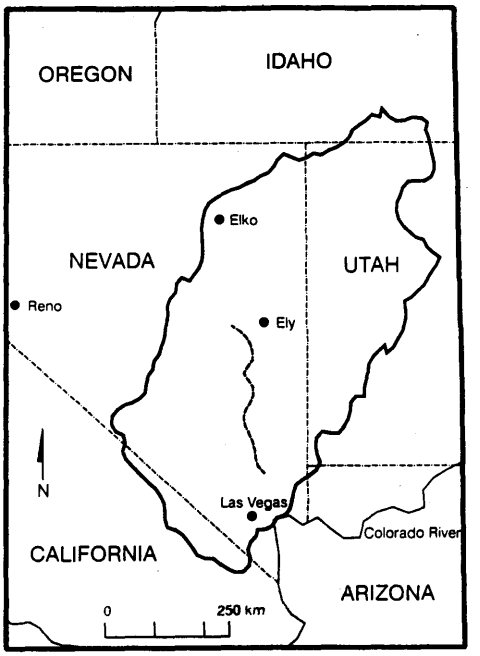

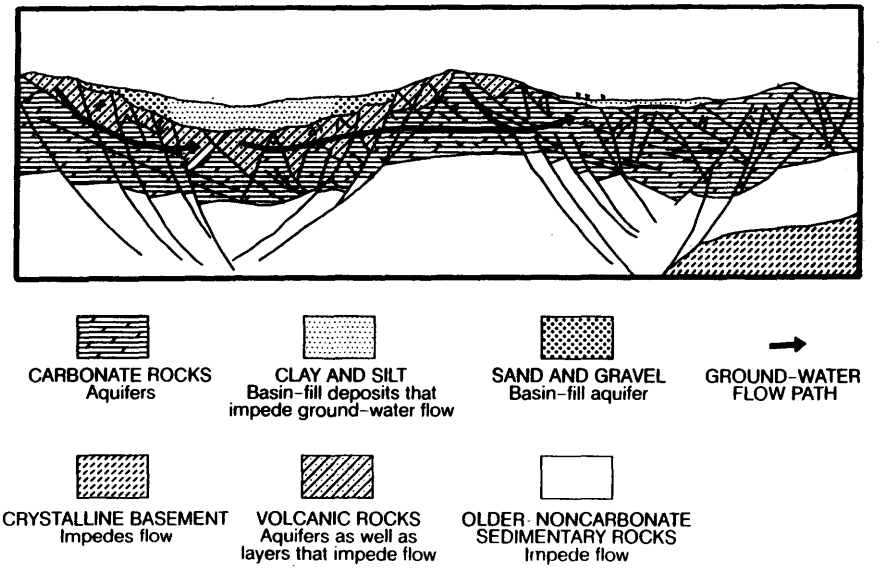

Figure 2. Schematic hydrogeologic section across mountain ranges and intervening basins, showing configuration at depth of aquifers and rocks that impede flow. Approximate width and depth of schematic section, 50 km by 12 km (modified from Anderson et al., 1983).

how much ground water is available, and on how ground water flows within the system. It is this interest in water supply that has influenced investigations of the hydrogeology of the carbonate rocks in Nevada.

There is abundant evidence in Nevada that ground water does indeed occur within the carbonate rock province, at least locally (Maxey and Mifflin, 1966; Mifflin, 1968; Winograd and Pearson, 1976; Mifflin and Hess, 1979; Dettinger, 1989). The many wells drilled into the carbonate rocks at the Nevada Test Site 100 km northwest of Las Vegas (Winograd and Thordarson, 1975) and in the southern end of the White River Flow System 80 km north of Las Vegas (Berger et al., 1988) amply demonstrate local occurrence of carbonate aquifers (Fig. 3). Other evidence is the occurrence of many large warm-water springs associated with these rocks.

Unbalanced water budgets in large areas of Nevada indicate substantial ground-water flow through carbonate rocks (Nevada Hydrologic Atlas, 1972; Mifflin, 1968). Geochemical and isotopic evidence of regional carbonate rock aquifers include work in the Spring Mountains, Las Vegas Valley, the Ash Meadows area, and the Muddy River Springs area of southern Nevada by Emme (1986), Hershey et al. (1987), Kirk and Campana (1988), Lyles and Hess (1988), Noack (1988), and Thomas (1988). Large interbasin ground-water flow systems exist in much of the region within the carbonate rocks (Eakin, 1966; Mifflin, 1968; Naff et al., 1974; Kirk and Campana, 1988; Roth and Campana, 1989). Many of the intermountain basin alluvial aquifers may also be related to these larger carbonate flow systems (Bateman et al., 1972, 1974; Noack; 1988, Lyles and Hess, 1988).

The thick sequence of carbonate rock layers (Fig. 3) is continuous enough to transmit water at regional scales only beneath a north-south corridor 90-150 km wide that extends southward from east-central Nevada to beyond the Spring Mountains area west of Las Vegas (Dettinger, 1989). There are two major regional flow systems within this corridor in southern Nevada: the Ash Meadows-Death Valley system and the White River-Muddy River Springs system. Flow in these systems probably is concentrated along highly transmissive zones associated with recently active faults and confluences of flow near major warm-water springs. Carbonate rocks outside of the corridor primarily occur as isolated blocks that form limited aquifers recharged by local precipitation.

PHYSIOGRAPHY AND CLIMATE

The carbonate rock province encompassing approximately 130,000 km^2 in Nevada generally lies in eastern and southern Nevada, east of longitude 117°. This area is mostly within the central Great Basin section of the Basin and Range physiographic province. The area is characterized by isolated, elongate, subparallel block-faulted mountain ranges and broad intervening, nearly flat-floored alluvial valleys or basins. The mountains tend to run north or northeast with many regularly spaced between 25 and 40 km apart. They are 30 - 160 km long, 8 - 25 km wide, and many have elevations between 2,400 and 3,000 m above mean sea level. Basin sediment, derived from the surrounding mountains, ranges in thickness from a few hundred meters to greater than 3,000 m. Valley floor elevations range

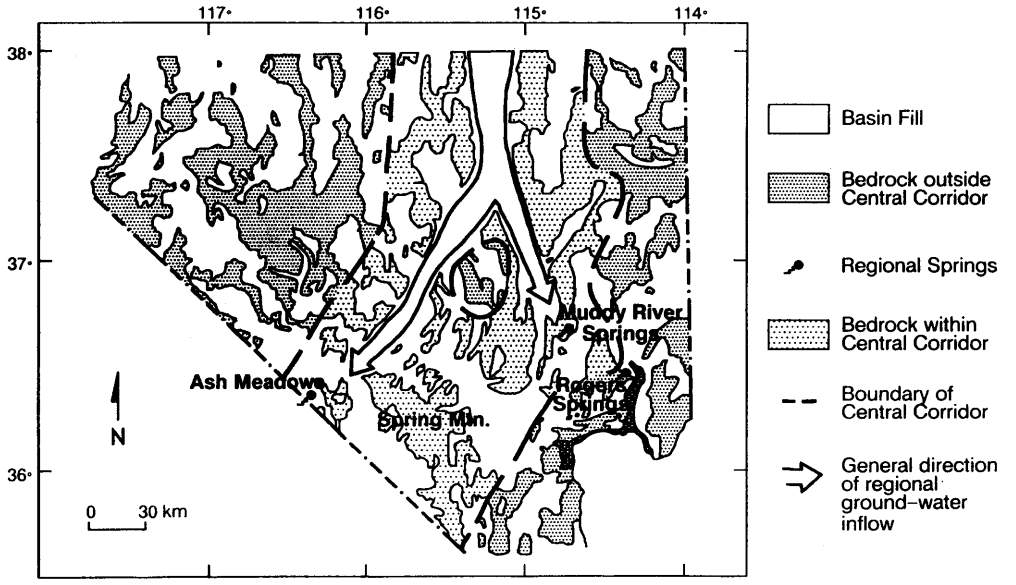

Figure 3. Central corridor of carbonate rock that forms the regional ground-water flow system (modified from Dettinger, 1989).

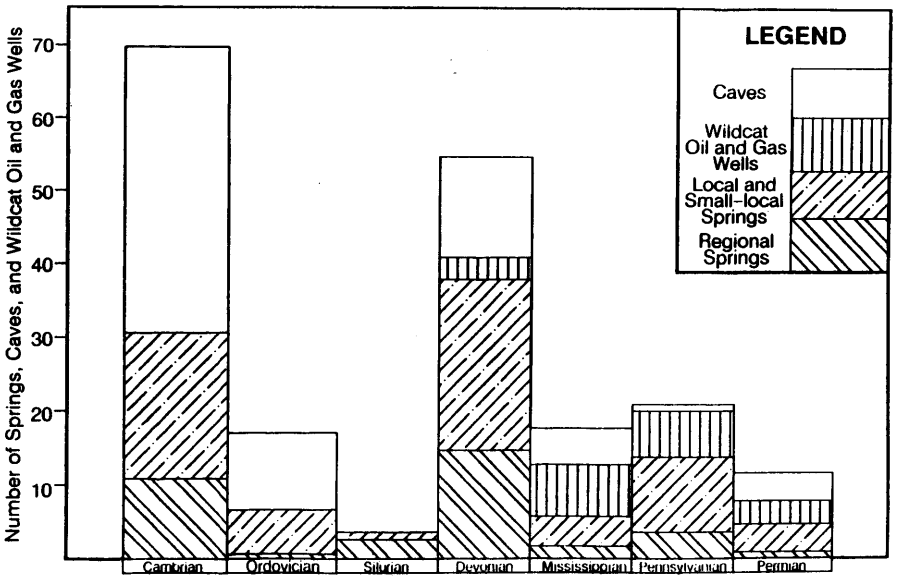

Figure 4. Permeability data sources by geologic age for eastern Nevada (from Mifflin and Hess, 1979).

from approximately 600 m in Las Vegas Valley to about 2,100 m in the central part of the area.

Local climatic conditions in the region are extremely variable, depending primarily on altitude. Valleys are arid to semiarid, characterized by low precipitation and humidity and extreme diurnal temperature variations. Mountains are semiarid to subhumid, receiving about one half of their precipitation as snow during the winter. Thunderstorms account for much of the summer precipitation. Annual precipitation is quite variable, with mean annual precipitation ranging from as little as 80 mm in some of the southern valleys to more than 760 mm in the highest mountain ranges. The majority of the basin and foothill areas receives 130 - 300 mm.

GEOLOGIC CONTROLS

The geological structure of the region is characterized by a series of north-south trending mountain ranges. These ranges are composed of rocks having general lithologies ranging from carbonate to volcanic and granitic. These same rock types also underlie the valleys at depths ranging from several hundreds to several thousands of meters. The valleys are filled with unconsolidated alluvium and lake sediments of Pleistocene or younger age and, in some basins, with semi-consolidated Tertiary sediments.

Eastern Nevada is stratigraphically complex. It lies within the miogeosynclinal belt of the Cordilleran geosyncline, in which 9,000 - 12,000 m of marine sediments accumulated during Precambrian and Paleozoic eras (Roberts, 1964; Stewart, 1964). Precambrian and lower Paleozoic carbonate and transitional assemblages consist of limestone, dolomite, and minor amounts of shale, siltstone, and quartzite. Upper Paleozoic carbonate and siliceous detrital rocks include thin sequences of conglomerate, siltstone, and limestone within the Antler Orogenic Belt, relatively thick sequences of shale, siltstone, sandstone conglomerate, sandy limestone, and limestone along the eastern margin of the Antler Orogenic Belt or in the foreland basin to the east, and moderately thin to thick sequences of carbonate rock in the foreland basin or on the shelf.

Probably three periods of deformation have affected the carbonate rock sequences within the region of interest. In some areas Permian-Triassic deformation seems probable, with attendant metamorphic and igneous activity. Folding and thrust faulting of the Upper Precambrian and Paleozoic rocks occurred during the Late Mesozoic-Early Tertiary Laramide orogeny. Normal block faulting, which produced the present-day basin and range topography, began during the Oligocene and reached a maximum in the Miocene with some activity extending to the present time. Strike-slip faults and shear zones have been active during the Laramide and block faulting tectonic periods. Movement along the Roberts Mountain Thrust was as much as 140 km (Wallace, 1964). Displacements of 40 - 65 km have been mapped along the Las Vegas Valley Shear Zone, in Death Valley, the Amargosa Desert, the Nevada Test Site, and in the Las Vegas Valley.

Geologic history influences at least four important areas of consideration in the understanding of regional carbonate aquifers. First and most fundamental is the distribution of the carbonate rocks in the subsurface. The history of faulting, folding, and erosion controls the basic distribution of the rock types of interest. In much of the region, knowledge of this distribution is more or less restricted to bedrock exposures due to the extremely complicated history of deformation and lack of subsurface data. Further, presence of many low- and high-angle thrust faults, associated folding, and superimposed normal faulting greatly complicates the prediction of distribution of formations in the subsurface, particularly in the basin areas.

Secondly, structural development has rearranged rocks to the extent that permeable and impermeable lithologies are often juxtaposed. This can in turn create corridors of permeability in any given direction and generate relatively impermeable boundaries on a localized and, perhaps, regional scale.

The third aspect of geologic history of considerable importance is the direct impact of structure on permeability. Most carbonate rocks deform at shallow depths within the crust in a brittle manner, and thus shear and fracture during deformation. Concentration and extent of fractures in carbonate rocks is important in determining the degree of development of secondary permeability.

The fourth aspect of structural history perhaps controlling permeability in the carbonate rocks relates to present and past patterns of ground-water flow due to position in past circulation systems of ground water. From at least Miocene time, and perhaps early Tertiary, the relative positions of carbonate rocks in the Basin and Range Province have been changing with respect to recharge areas, discharge areas, and normal flow paths of ground water. This type of structural history may have important influences over the distribution of permeability in the subsurface.

HYDROGEOLOGY

Hydraulic Properties

There is limited direct information on hydraulic properties such as permeability, hydraulic conductivity, and transmissivity for deep-lying carbonate rocks. To identify permeable zones and estimate hydraulic properties in the carbonate rocks, four different types of data were used (Mifflin and Hess, 1979): 1) number and mapped length of solution caves, 2) carbonate springs, 3) petroleum wildcat wells, and 4) aquifer tests. This information has been compiled by geologic age, and is discussed below.

Solution caves are an extreme example of secondary permeability in carbonate rocks. They are useful as indicators of carbonate rock solubility under various geologic settings and in defining the paleohydrology of an area. Lithology, structure, stratigraphy, and geologic history play major roles in development of caves. The number of caves and total mapped length (Mifflin and Hess, 1979) are summarized by geologic age in Table 1. Cambrian carbonate units contain the most caves (39) and the greatest total mapped cave length (7,000 m). Devonian

carbonates follow with 14 caves and 1,500 m. These two groups of carbonate strata contain 68% of the caves and 74% of the cave length. Thus the cave data suggest that Cambrian and Devonian strata have high potential for solutional permeability.

Table 1. Cave summary for Nevada.

Age	Number of Caves	Approximate Total Length (m)	Comments
Cenozoic	2	200	
Cretaceous	0	0	
Jurassic	0	0	
Triassic	3	600	
Permian	4	550	
Pennsylvanian	1	300	
Mississippian	5	500	Monte Cristo Group in Clark County
Devonian	14	1500	Devil's Gate Limestone in Elko County
Silurian	0	0	
Ordovician	10	750	Pogonip Group in Nye County
Cambrian	39	7000	Pole Canyon Limestone in White Pine County

Available lithologic data for carbonate springs is summarized in Table 2. Rock units at the point of spring discharge do not necessarily indicate the strata in which the water is flowing at depth. They do, however, indicate permeability in that particular unit, at least at the land surface. Other geologic controls, as in the case of the caves, are also important factors in controlling the stratigraphic location of spring discharge (Mifflin and Hess, 1979). Table 2 indicates that the largest number of springs are associated with the Devonian carbonates, including 15 regional springs and 23 local springs. Both spring and cave data suggest that these two geologic rock units have the highest permeability. They represent 70% of the regional springs and 66% of the total number of springs.

Table 2. Geologic age of rock units associated with carbonate springs in eastern Nevada.

Age	Regional Springs	Local Springs	Total
Permian	1	4	5
Pennsylvanian	4	10	14
Mississippian	2	4	6
Devonian	15	23	38
Silurian	3	1	4
Ordovician	1	6	7
Cambrian	11	20	31

Records of petroleum wildcat wells in eastern Nevada available at the Nevada Bureau of Mines and Geology were searched for information about zones

of lost circulation, water production, and fractures in the carbonate rock. Data included geophysical logs, lithologic logs, and drill-stem tests (DST's). To date, over 480 wildcat wells have been drilled in Nevada, and some type of record exists for each one.

Table 3 summarizes the geologic age for indicators of high permeability in wildcat wells. The lack of permeability indicators in the Silurian, Ordovician, or Cambrian probably reflects a lack of data (Mifflin and Hess, 1979).

Table 3. Number of petroleum wildcat wells with permeability indications in eastern Nevada.

Age	Number of Wells
Permian	3
Pennsylvanian	6
Mississippian	7
Devonian	3
Silurian	0
Ordovician	0
Cambrian	0

Analysis of DST's from over 100 wildcat wells indicate a wide range of hydraulic conductivities (K) and transmissivities (T) for the carbonate rocks (McKay and Kepper, 1988). K values range from 2.8×10^{-6} m/day to 5.7 m/day. T values range from 4.9×10^{-5} m^2/day to 46 m^2/day. Comparison of T's and K's derived from DST's with those obtained from aquifer tests suggest that DST methods may underestimate these parameters by several orders of magnitude. Devonian rocks had the highest hydraulic conductivities and transmissivities.

Hydraulic properties of the carbonate aquifer are also available from the limited number of aquifer tests on wells drilled into carbonate rock (Lyles, 1987; Berger et al., 1988; Morin et al., 1988). Average transmissivities fall between 460 and 1,020 m^2/day. The MX wells in Coyote Springs Valley are extremely productive. Tests conducted at 215 L/s with 3.7 m of drawdown indicated a transmissivity of about 18,500 m^2/day (Ertec Western, Inc., 1981). Most other wells in the carbonate rocks are much less productive.

Cave, spring, and wildcat well permeability data are summarized in Figure 4 where a number of permeability indicators have been plotted against geologic age in a bar graph. The Cambrian and Devonian carbonate units are most frequently associated with permeability indicators based on the data available. This is compatible with the hydrostratigraphic classification for southern Nevada developed from Nevada Test Site studies (Winograd and Thordarson, 1975) in which the lower carbonate aquifer includes the rocks between the Cambrian and Devonian. It is described as a complexly fractured aquifer with transmissibilities ranging from approximately 4 to 4,000 m^2/day.

Flow Systems

Understanding the regional carbonate flow systems requires knowledge of where the carbonate rocks are present and where they are continuous enough to form regional aquifers. A regional ground-water flow system is defined as a large ground-water flow system which encompasses one or more topographic basins. It may include within its boundaries several ground-water basins; interbasin flow is common and important with respect to total volume of water transferred within the system boundaries; lengths of flow paths are relatively great when compared to lengths of flow paths of local ground-water flow systems. A local ground-water flow system is generally confined to one topographic or ground-water basin; interbasin flow is not important with respect to total volume of water transferred within the system; the majority of water within the system discharges within the associated ground-water basin; flow paths are relatively short when compared to regional systems.

In southern Nevada, there is a continuous central corridor within the carbonate rock province with potential aquifer thickness of 1,000 to 6,000 m. This thick corridor probably contains the principal conduits for regional flow from east-central Nevada into southern Nevada, with flow ultimately discharging at Ash Meadows and Death Valley and at the Muddy River Springs (Fig. 3) (Dettinger, 1987). Highly transmissive zones, indicated by large spring discharges may act as large-scale drains, collecting water from adjacent, less transmissive rock that underlies most of the area. The drains would ultimately conduct much of the flow that discharges at the large regional springs.

Geochemical and isotopic balances and models were used to update flow system configurations, water budgets, and mixing rates in east-central and southern Nevada. Results altered previous concepts of regional flow beneath southern Nevada and flow paths of water recharged in the northern part of the flow system. Thomas (1988) found that recharge from the Sheep Range flows towards the Muddy River Springs rather than radially toward other adjacent valleys. Lyles and Hess (1988) used ion and isotope geochemistry to delineate the hydrologic character of the Las Vegas Shear Zone (a right-lateral strike-slip fault in northwestern Las Vegas Valley). They suggest that ground-water mixing is taking place along the Shear Zone. Ground water from the Spring Mountains (recent to about 3,000 years old) is mixing with regional carbonate ground water along the Shear Zone, forming a mixture that is approximately 18,000 years old. Parts of the Las Vegas Shear Zone appear to be a barrier to ground-water flow, and parts act as a conduit for regional flow and mixing. The studies of Emme (1986), Schroth (1987), Kirk and Campana (1988), and Thomas (1988) generally verify the overall budgets and flow system configurations developed by previous investigators (Rush, 1964; Eakin, 1966; Winograd and Friedman, 1972) for regional flow beneath the White River drainage in east-central Nevada (Fig. 3).

Ground-Water Volumes

The ground-water resources in the carbonate rock aquifers are the sum of the perennial yield of the aquifers and the water in storage. There are approximately 197 x 10^6 m^3 from mountain recharge and 25 x 10^6 m^3 by inflow from east-central Nevada (Dettinger, 1989). Of this volume, 160 x 10^6 m^3 of water are entering the central corridor and thus are part of the regional flow system.

Water in storage is by far the largest part of the water resource of the carbonate rock aquifers. In southern Nevada, the volume of carbonate rock is estimated to be 83,000 km^3. Using a 1% porosity, the total volume of stored water would be on the order of 10^{11} m^3. The estimated volume of water stored in the upper 30 m of the central corridor of the carbonate rock aquifer in southern Nevada is on the order of 7 x 10^9 m^3 (Dettinger, 1989).

Development Impacts

Possible effects of developing the carbonate aquifers include declining water levels, decreasing stream flows, drying up of springs and meadows, and changing water chemistries. These effects are direct or indirect responses to water level changes in the carbonate aquifer due to development. The major concern is the potential impact on adjacent aquifers resulting from development of the carbonate aquifers.

To date there has been little sustained development of the carbonate aquifers. Thus there is limited experience regarding the possible effects of their development. There is, however, historical experience in two areas in southern Nevada where ground-water development has occurred in basin-fill aquifers adjacent to carbonate aquifers: Ash Meadows and Muddy River Springs. Observations in these areas provide information concerning the potential for interaction of aquifers near pumped wells. They are, however, the reverse case of the type of development of concern here. The direct connection between a basin-fill aquifer and the carbonate aquifers has been demonstrated at Ash Meadows. Withdrawls from irrigation wells in the basin-fill near Devils Hole drew down water levels by more then a third of a meter in the carbonate rock aquifers between 1969-72 (Bateman et al., 1974; Dudley and Larson, 1976). Water levels recovered slowly over a period of 15 years after pumping ceased. In contrast, development of the basin-fill aquifers over the past 20 years around the Muddy River Springs has resulted in minimal changes in water levels in the carbonate aquifers (Pohlmann et al., 1988). Thus, experience with aquifer development at Ash Meadows and Muddy River Springs areas indicates that the potential for adverse effects from development of the carbonate aquifer exists. The differences between these two historical responses indicate that different hydrogeologic settings can be expected to respond differently to carbonate aquifer development.

SUMMARY

More than 30 years of research has gone into the understanding of the hydrogeology of the regional carbonate aquifers in Nevada. The carbonate rock aquifers of eastern and southern Nevada are widely distributed, fractured, and solutionally developed rocks that allow circulation of ground water on a regional scale between structural basins. Recharge to the aquifer system occurs mostly from winter snow-pack runoff in the mountain ranges. Large warm-water springs are associated with the carbonate rocks. Cave, springs, wildcat petroleum wells, and aquifer tests have been used to identify permeable zones and to estimate aquifer hydraulic properties. The lower carbonate aquifer, including rocks between the Cambrian and Devonian, appears to be the most permeable. In southern Nevada, a thick central corridor of carbonate rock contains the principal conduits for regional flow from east-central Nevada into southern Nevada, with flow ultimately discharging at Ash Meadows and Death Valley and at the Muddy River Springs. Ion and isotope geochemistry were used to delineate flow system configurations, determine water budgets, and determine mixing rates. Annual recharge to the carbonate aquifer system in southern Nevada is approximately 197 x 10^6 m^3. Impacts from development of the carbonate aquifers will be site specific depending on the local hydrogeologic setting.

REFERENCES

Anderson, R. E., Zoback, M. L. and Thompson, G. A., 1983, Implications of selected subsurface data on the structural form and evolution of some basins in the Northern Basin and Range Province, Nevada and Utah: Geological Society of America Bulletin, v. 94, p. 1055-1072.

Bateman, R.L., Mindling, A.L., Naff, R.L. , and Joung, J.M., 1972, Development and management of ground-water and related environmental factors in arid alluvial and carbonate basins in southern Nevada: Desert Research Institute, Water Resources Center, Project Report 18, 43 p.

Bateman, R.L., Mindling, A. L., and Naff, R. L., 1974, Development and management of ground water in relation to preservation of desert pupfish in Ash Meadows, southern Nevada: Desert Research Institute, Water Resources Center, Publication 17, 39 p.

Berger, D.L., Kilroy, K. C., and Schaefer, D. H., 1988, Geophysical logs and hydrologic data for eight wells in the Coyote Spring Valley area, Clark and Lincoln Counties, Nevada: U.S. Geological Survey Open-File Report 87-679, 59 p.

Dettinger, M.D., 1987, Influence of Tertiary-age extensional tectonics on present-day regional groundwater flow and discharge in southern Nevada and vicinity (abs.): Geological Society of America Abstracts with Programs, v. 19, no. 6, p. 371-372.

Dettinger, M.D., 1989, Distribution of carbonate-rock aquifers in Southern Nevada and the potential for their development--summary of findings, 1985-88: U.S. Geological Survey, Carson City, Nevada, 37 p.

Dudley, W.W., Jr. and Larson, J. D., 1976, Effect of irrigation pumping on desert pupfish habitats in Ash Meadows, Nye County, Nevada: U.S. Geological Survey Professional Paper 927, 52 p.

Eakin, T.E., 1966, A regional interbasin ground-water system in the White River area, southeastern Nevada: Water Resources Research, v. 2, p. 251-271.

Emme, D.H., 1986, Delineation of subsurface flow in the Upper Meadow Valley Wash area, southeastern Nevada: University of Nevada, Reno, unpublished M.S. thesis, 89 p.

Ertec Western, Inc., 1981, MX siting investigation, water resources program, results of regional carbonate aquifer testing, Coyote Spring Valley, Nevada: Long Beach, Calif., Ertec Western, Inc., report, 190 p.

Hershey, R.L., Lyles, B. F., and Hess, J. W., 1987, Hydrologic and hydrogeochemical investigation of the Spring Mountains, Clark County, Nevada (abs.): Geological Society of America Abstracts with Programs, v. 19, no. 7, p. 701.

Kirk, S.T., and Campana, M. E., 1988, Simulation of groundwater flow in a regional carbonate-alluvial system with sparse data--The White River flow system, southeastern Nevada: Desert Research Institute, Water Resources Center, Publication 41115, 76 p.

Lyles, B.F., 1987, Data report--Water level data from northern Las Vegas Valley: Desert Research Institute, Water Resources Center, Publication 41106, 26 p.

Lyles, B.F., and Hess, J. W., 1988, Isotope and ion geochemistry in the vicinity of the Las Vegas shear zone: Desert Research Institute, Water Resources Center, Publication 41111, 78 p.

Maxey, G.B., and Mifflin, M. D., 1966, Occurrence and movement of ground water in carbonate rocks of Nevada: National Speleological Society Bulletin, v. 28, p. 141-157.

McKay, W.A., and Kepper, Jack, 1988, Estimating hydraulic parameters using wildcat oil and gas data-a feasibility study in east-central Nevada: Desert Research Institute, Water Resources Center, Publication 41116, 48 p.

Mifflin, M.D., 1968, Delineation of ground-water flow systems in Nevada: Desert Research Institute, Water Resources Center, Report H-W4, 111 p.

Mifflin, M.D., and Hess, J. W., 1979, Regional carbonate flow systems in Nevada: Journal of Hydrology, v. 43, no. 2, p. 217-237.

Mifflin, M.D., 1988, Region 5, Great Basin, in W. Back, J.S. Rosenshein, and P.R. Seaber, eds., Hydrogeology: Boulder, Colorado, Geological Society of America, The Geology of North America, v. 0-2, p. 69-78.

Morin, R.E., Hess, A. E., and Paillet, F. P., 1988, Determining the distribution of hydraulic conductivity in a fractured limestone aquifer by simultaneous injection and geophysical logging: Ground Water, v. 26, no. 5, p. 587-595.

Naff, R.L., Maxey, G. B., and Kaufmann, R. F., 1974, Interbasin groundwater flow in southern Nevada: Nevada Bureau of Mines Report 20, 28 p.

Nevada Hydrological Atlas, 1972, State of Nevada, Carson City, Nevada, 22 maps.

Noack, R.E., 1988, Sources of ground water recharging the principal alluvial aquifers in Las Vegas Valley, Nevada: University of Nevada, Las Vegas, unpublished M.S. thesis, 167 p.

Pohlmann, K.F., Morris, T. M., and Patterson, P. A., 1988, Nevada Power Company Reid-Gardner groundwater level monitoring program--1987 annual report: Desert Research Institute, Water Resources Center report, 54 p.

Roberts, R.J., 1964, Paleozoic rocks, in: Mineral and Water Resources of Nevada: Nevada Bureau of Mines Bulletin 65, p. 22-25.

Roth, J.G., and Campana, M. E., 1989, A mixing-cell model of the railroad valley regional groundwater flow system, central Nevada: Desert Research Institute, Water Resources Center, Publication 41123, 175 p.

Rush, F.E., 1964, Ground-water appraisal of the Meadow Valley area, Lincoln and Clark Counties, Nevada: Nevada Department of Conservation and Natural Resources, Ground-Water Resources - Reconnaissance Report 27, 43 p.

Schroth, B.K., 1987, Water chemistry reconnaissance and geochemical modeling in the Meadow Valley Wash area, southern Nevada: University of Nevada, Reno, Unpublished M.S. thesis, 97 p.

Stewart, J.H., 1964, Precambrian and lower Cambrian rocks, in Mineral and Water Resources of Nevada: Nevada Bureau of Mines Bulletin, 65, 21 p.

Thomas, J.M., 1988, Delineation of regional ground-water flow systems in southern Nevada using isotopic and chemical data (abs.): Geological Society of America Abstracts with Programs, v. 20, no. 7, p. A363.

Wallace, R.E., 1964, Topography, in Mineral and Water Resources of Nevada: Nevada Bureau of Mines Bulletin 65, p. 11-12.

Winograd, I. J., and Friedman, Irving, 1972, Deuterium as a tracer of regional ground-water flow, southern Great Basin, Nevada and California, Geological Society of America Bulletin, v. 83, p. 3691-3708.

Winograd, I.J., and Thordarson, W., 1975, Hydrogeologic and hydrochemical framework, south-central Great Basin, Nevada-California, with special reference to the Nevada Test Site: U.S. Geological Survey, Professional Paper 7612-C, 126 p.

EVAPORITE KARST IN THE PERMIAN BLAINE FORMATION AND ASSOCIATED STRATA IN WESTERN OKLAHOMA, USA

KENNETH S. JOHNSON
Oklahoma Geological Survey
University of Oklahoma
Norman, Oklahoma 73019
USA

ABSTRACT

Bedded evaporites (gypsum and salt) of Permian age have been dissolved naturally by ground water to form a major evaporite-karst region in western Oklahoma. The Blaine Formation and associated evaporites comprise 30-250 m of strata that dip gently into broad, structural basins. Outcropping gypsum, dolomite, and red-bed shales of the Blaine display typical karstic features, such as sinkholes, caves, disappearing streams, and springs. Large caves are developed in gypsum beds 3-8 m thick at several places, and a major gypsum-dolomite karst aquifer provides irrigation water to a large region in southwestern Oklahoma. Salt karst is present beneath much of western Oklahoma, where salt layers above and below the Blaine Formation have been partly dissolved at depths of 10-250 m below the land surface. Salt dissolution causes development of brine-filled cavities, into which overlying strata collapse, and the brine eventually is emitted at the land surface in large salt plains.

INTRODUCTION

Evaporites, including gypsum (or anhydrite) and salt, underlie about 35 to 40% of the land area of the contiguous 48 states of the United States. In areas where the evaporites crop out, or are less than 250 m deep, they may be partly or wholly dissolved by unsaturated water to form karst features identical to those formed in carbonates. The present report summarizes the processes, geologic setting, and characteristics of a major evaporite-karst region in western Oklahoma, in the southwestern part of the United States. The study region consists mainly of rural grasslands currently being used for agriculture or ranching; it has a subhumid (nearly semiarid) climate, with precipitation averaging 55-70 cm/a.

An overview of evaporite karst in the United States is given by Quinlan et al. (1986), and studies dealing with evaporite-karst features in western Oklahoma and adjacent Texas include those of Jordan and Vosburg (1963), McGregor et al. (1963), Myers et al. (1969), Johnson (1972, 1981, 1986, 1990a, 1990b), Gustavson et al. (1982), Bozeman et al. (1987), Runkle and Johnson (1988), and Hovorka and Granger (1988). Also, White (1988) provides a good overview of karst processes in evaporite rocks.

International Contributions to Hydrogeology, Vol. 13 (1992)
© Verlag Heinz Heise, Hannover, FRG

DEVELOPMENT OF EVAPORITE KARST

Whereas most karst features in the world are developed in carbonate rocks, evaporite rocks are much more soluble than carbonates and they can be sculptured into similar karst features. Karst features develop at a much faster rate in evaporites than in carbonates, and evaporite karst persists at and near the land surface mainly in arid to semiarid areas of the world where rock-dissolving precipitation and seepage from streams are minimal. The southwestern United States, including western Oklahoma, western Texas, and southeastern New Mexico, constitutes the major area of evaporite karst in the United States. Principal among the karstic units in western Oklahoma is the Permian Blaine Formation, which consists of 30-75 m of interbedded gypsum (or anhydrite), dolomite, and shale. In the subsurface, overlying and underlying formations contain interbedded salt and shale, and thus the entire bedded-evaporite sequence locally is as much as 250 m thick.

Evaporite-karst features in western Oklahoma are mostly covered by a mantle of overlying soil, sediment, or rocks, but in some areas the gypsum karst is exposed. The term "interstratal karst" (Quinlan et al., 1986; White, 1988) is used for dissolution beneath a covering layer of younger, nonkarstic rocks. This term applies to all the salt karst and much of the gypsum karst in western Oklahoma. Fresh water percolates down through overlying rocks and dissolves the salt or gypsum, forming a system of cavities (Fig. 1). As a cavity enlarges, and the roof can no longer be supported, overlying rocks settle or collapse; this disruption of the overlying rocks increases their permeability and allows more fresh water to percolate down to the evaporite rocks.

Gypsum karst is exposed at many places along the outcrop belt of the Blaine Formation. Although gypsum is much more soluble than carbonate rocks, the low rainfall in western Oklahoma prevents the complete dissolution or erosion of gypsum in outcrops, and thus it stands as a resistant and conspicuous caprock on escarpments, buttes, and hills throughout the area. In such areas, the dissolution of gypsum has created a series of sinkholes, caves, and other karst features that are well exposed.

GEOLOGIC SETTING OF WESTERN OKLAHOMA

Permian Paleogeography

Rock units involved in evaporite-karst studies in western Oklahoma and nearby areas are mainly of early Guadalupian (Permian) age. These strata make up a thick sequence of red beds and evaporites deposited in and near a broad, shallow, inland sea that extended north and northeast of the marine-carbonate platform that bordered the Midland Basin (Fig. 2) (Johnson, 1981, 1990b). Evaporites, mainly gypsum (or anhydrite) and salt (halite), were precipitated from evaporating seawater as layers on the sea floor, or grew as coalescing crystals and nodules within the mud just below the depositional surface. Thick red-bed shales, siltstones, and sandstones were deposited around the perimeter of

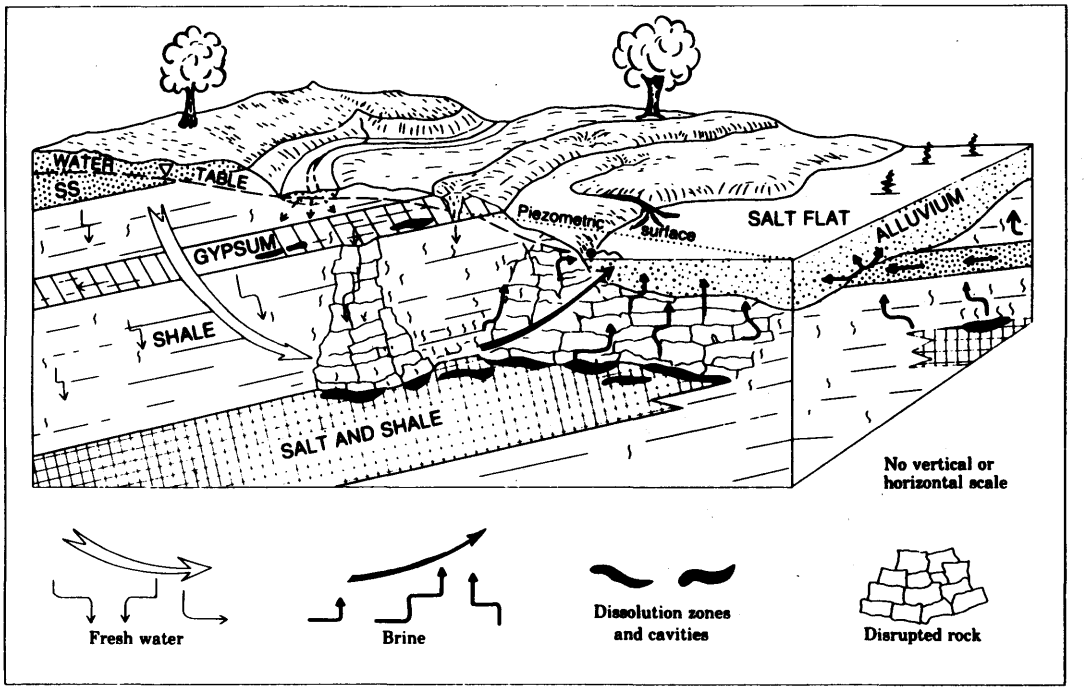

Figure 1. Schematic block diagram of interstratal karst, showing circulation of fresh water and brine in areas of salt dissolution in western Oklahoma. No scale for diagram, but length may be 1-15 km, and height 30-300 m (from Johnson, 1981).

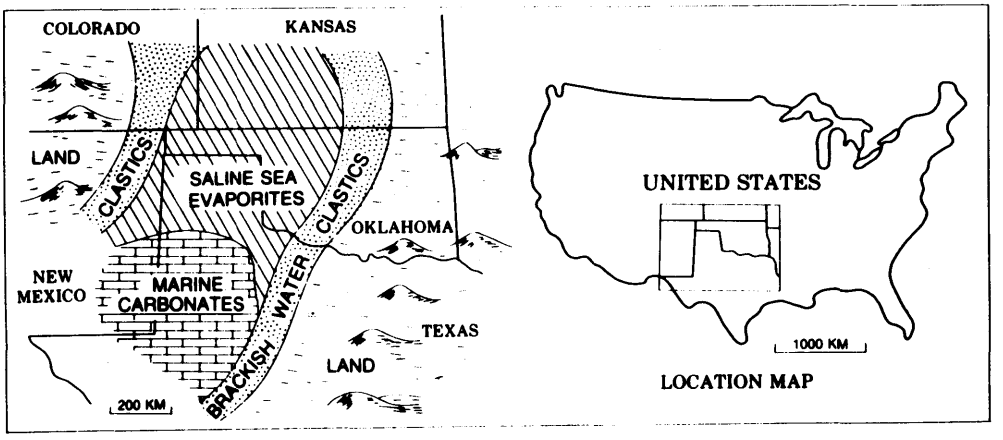

Figure 2. Permian paleogeography and principal facies in southwestern USA during deposition of evaporites in the Blaine Formation (from Johnson, 1981).

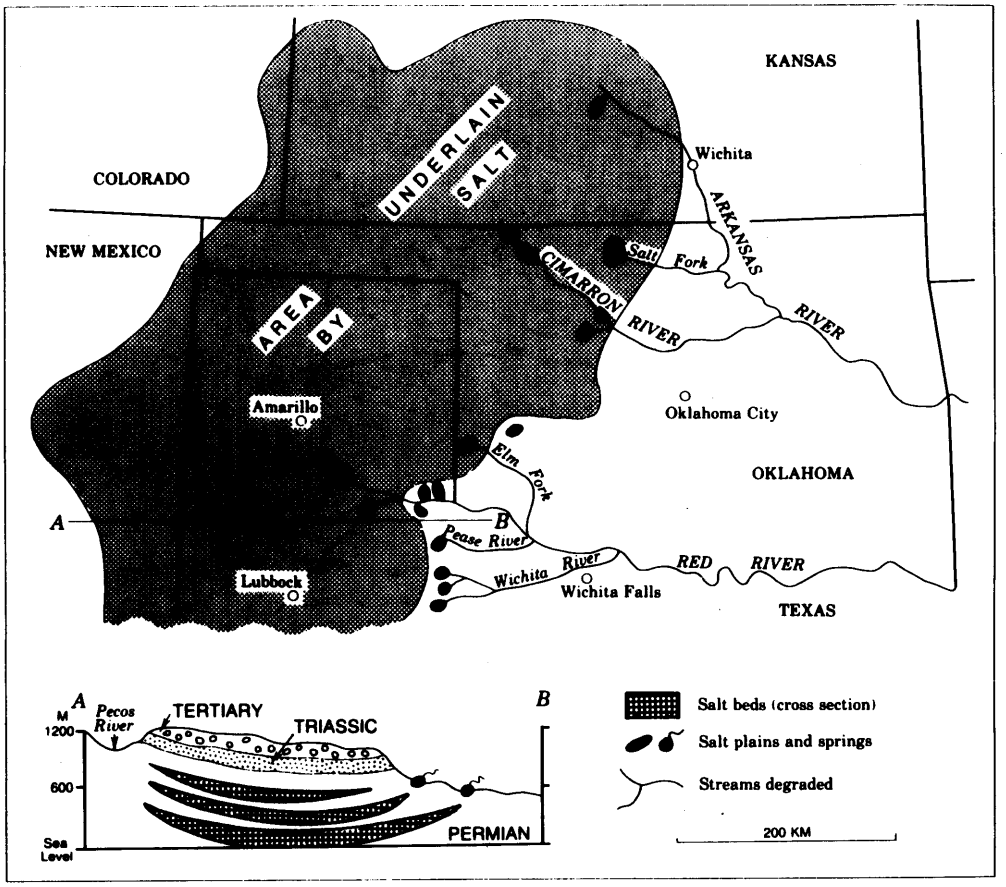

Figure 3. Map and schematic cross section showing distribution of Permian salt and salt plains in western Oklahoma and adjacent areas (from Johnson, 1981).

the evaporite basin, and some of these also extended as blanket deposits across the basin. Many thin, red-bed clastic units are interbedded with the evaporites.

Evaporites deposited in the inland sea during Permian time now occur in several thick rock units that underlie a vast area extending across western Oklahoma and adjacent states (Fig. 3). Principal stratigraphic units studied for this report are (in ascending order) the Flowerpot Shale, Blaine Formation, and Dog Creek Shale (Fig. 4).

In outcrops, the Flowerpot typically is 60-100 m thick and consists mainly of reddish-brown shale with thin layers of greenish-gray shale, gypsum, and dolomite. Salt is present in the upper and middle parts of the Flowerpot at shallow to moderate depths, just back from the outcrop in many areas of western Oklahoma and adjacent states (Fig. 4). The total thickness of the Flowerpot salt (the sequence of salt-bearing strata in the Flowerpot formation) generally is 30-90 m (Jordan and Vosburg, 1963). The salt unit consists of reddish-brown shale containing layers, crystals, and veins of transparent to translucent salt. Commonly the salt is reddish, owing to shale impurities, and in many layers it is intimately intermixed with shale. Individual salt beds typically are 0.5-3.0 m thick, and halite appears to make up about half of the entire Flowerpot salt unit.

Outcrops of the Blaine Formation consist of gypsum beds, typically 2-10 m thick, separated by red-brown shales 2-8 m thick; each gypsum bed is underlain by a dolomite bed that commonly is 0.05-2.0 m thick. Anhydrite, instead of gypsum, normally is present in the Blaine where the unit is more than 10-60 m below the land surface, and anhydrite is present in some outcrops. The total thickness of the Blaine ranges from ~30 m in northwestern Oklahoma to 60-75 m in southwestern Oklahoma and nearby parts of Texas. In the deep subsurface of the Anadarko Basin, and farther west in the Texas Panhandle, the Blaine Formation contains several salt interbeds that are 2-6 m thick.

The Dog Creek Shale consists of 15-60 m of red-bed shales in outcrops, although gypsum and dolomite beds 0.1-5.0 m thick are present in the lower half of the formation in southwestern Oklahoma and in Texas. The formation also contains 50-100 m of salt interbeds (called the Yelton salt) in the deep Anadarko Basin and in parts of the Texas Panhandle (Fig. 4). The Yelton salt is lithologically similar to the Flowerpot salt.

Post-Permian History

Post-Permian rocks of western Oklahoma and the Texas Panhandle include remnants of Triassic, Jurassic, Cretaceous, Tertiary, and Quaternary strata. There was no significant tectonic activity in the region during this long period of time, and the sediments accumulated in terrestrial and shallow-marine environments. Few remnants of Triassic, Jurassic, and Cretaceous rocks remain in the region. Up to several hundred meters of Triassic and Jurassic fluvial, deltaic, and lacustrine red beds remain in the western part of the Texas Panhandle, and up to several tens of meters of Cretaceous marine shales and

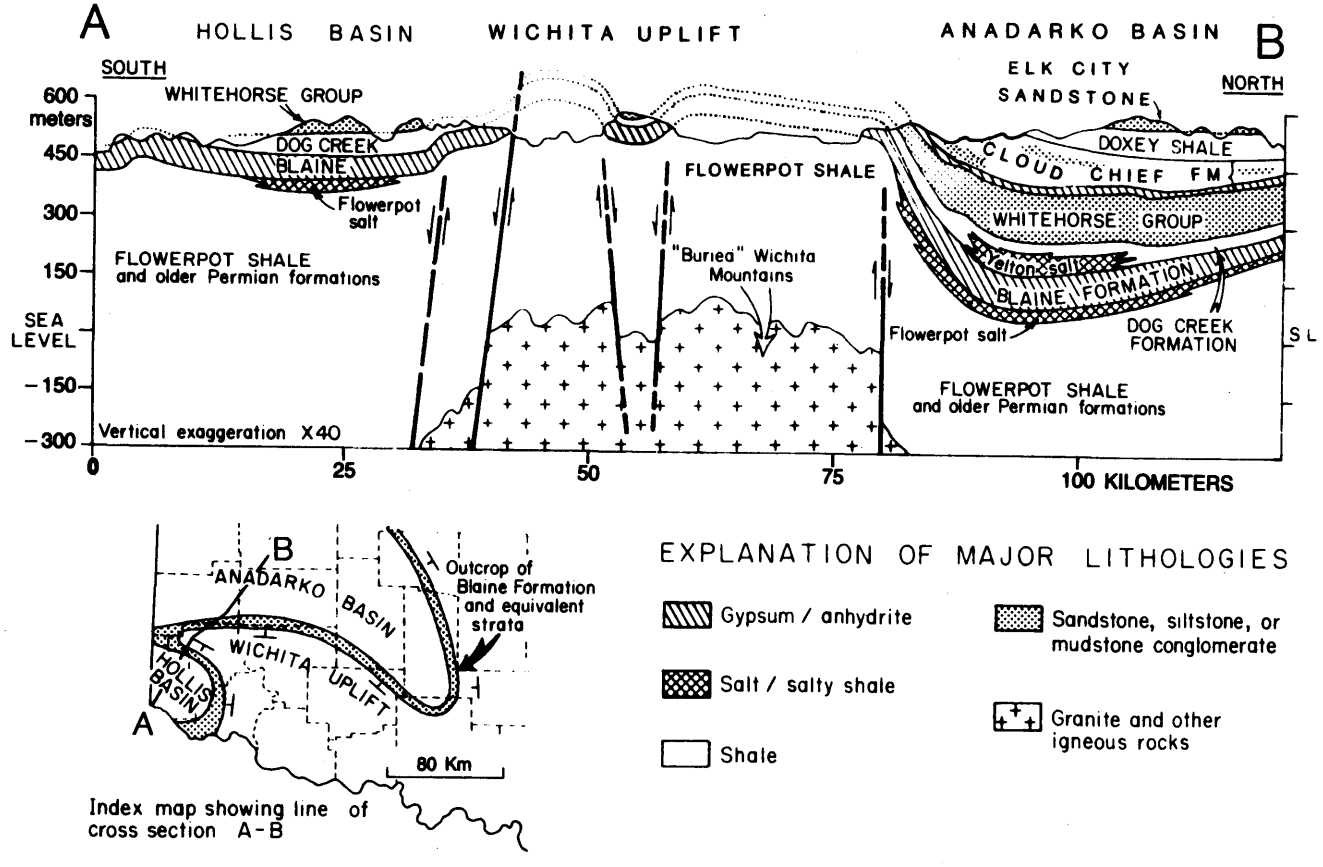

Figure 4. North-south cross section showing stratigraphy and structure of Permian evaporites and other rocks in southwestern Oklahoma (modified from Johnson and Denison, 1973).

limestones occur as outliers in scattered chaotic blocks that have collapsed some 30-100 m due to dissolution of underlying Permian salts in western Oklahoma.

Tertiary strata (the Ogallala Formation of Miocene-Pliocene age) are widespread in the study region. They are a sequence of interbedded fluvial and windblown sediments deposited upon an east-sloping erosional surface cut into Permian red beds (and locally into Triassic, Jurassic, or Cretaceous strata). The Ogallala comprises 30-200 m of sand, silt, clay, and gravel, and it is an excellent fresh-water aquifer.

Quaternary sediments are alluvial, eolian, and lacustrine deposits derived from rivers and streams flowing to the east and southeast across the region. Mainly they occur as terrace deposits and alluvium; they typically are 3-15 m thick, and locally they reach 30 m thick along major rivers; they are porous and permeable, and commonly are excellent aquifers.

Fresh ground water has circulated down to the evaporites in the Blaine Formation and associated strata at various times in the past, thus creating the karstic features seen in the evaporites. Ground-water circulation and karst development are ongoing processes in the region, inasmuch as both gypsum and salt deposits are currently being dissolved.

GYPSUM KARST

Gypsum and dolomite beds of the Blaine Formation make up a major karstic unit that crops out and is at shallow depths in southwestern and northwestern Oklahoma. The formation is 30-75 m thick and consists of a sequence of laterally persistent gypsum, dolomite, and shale interbeds. Surface and near-surface Permian strata are essentially structurally undisturbed in western Oklahoma: strata typically dip gently towards the central part of either the Hollis Basin or Anadarko Basin (Fig. 4) at rates of 2-6 m/km (0.1-0.3 degree).

Outcropping and near-surface gypsum and dolomite beds of the Blaine have been partly dissolved by circulating ground water, thus locally creating a cavernous and karstic system. Karst features include sinkholes, caves, disappearing streams, springs, and underground water courses, and in some areas the Blaine is a major aquifer. These features are most common in areas where the Blaine consists predominantly of thick gypsum beds and thin shale interbeds.

Development of porosity, and eventually of the open conduits through which water flows, occurs most commonly in the dolomite layers and the lower part of each of the overlying gypsum beds. Dolomite porosity locally is due to early dissolution of fossils (mainly pelecypod shells), of cement around oolites and pellets, or of small nodules of gypsum; in other places it is intercrystalline porosity. In many places the development of porosity is so advanced that the dolomite beds have a honeycombed appearance, with only a skeletal framework of rock supporting a system of voids.

Early flow of water through the dolomite beds causes concentration of gypsum dissolution at the base of the gypsum beds. Thus, the cavern system most commonly encountered is at and near the contact between gypsum and dolomite layers. Locally, the caverns have been developed along joints and bedding planes in the gypsum, but no preferential orientation of the dissolution features is known yet.

Caverns generally have a height and width that range from a few cm to about 3 m, although locally they are up to 18 m wide. Enlargement of individual cavities and caverns occurs due to dissolution and also due to abrasion by gravel, sand, and silt carried by through-flowing waters. The sediment carried by ground water is deposited locally in the underground caverns, and it partly or totally fills some of the openings.

In some areas the caverns have become so wide that their roofs have collapsed to partly close the caverns. The collapse structures and fractures thus enable vertical movement of water in many parts of the karst system. Such enhancement of vertical flow of water through fractures and collapse structures accelerates dissolution of all affected strata, thus increasing the amount of karst features in those areas. Dissolution and resultant collapse also create many problems in the local correlation of strata making up the Blaine: in some boreholes, one or more of the individual gypsum beds has been completely removed by dissolution, and overlying strata have collapsed, apparently occupying the stratigraphic position of the dissolved strata.

Karst features are generally sparse to nonexistent in those areas where the Blaine is buried at depths in excess of 20-60 m below the surface. In these areas there has been little or no hydration of massive beds of anhydrite to gypsum, and the pathways for ground-water movement appear to be limited to the dolomite beds.

Southwestern Oklahoma

Two major karstic aspects of the Blaine Formation have been examined in southwestern Oklahoma: the Blaine aquifer, which provides large quantities of irrigation water in the Hollis Basin area, and the J. C. Jester Cave system, the longest known cave system in Oklahoma and, reportedly, the longest gypsum cave in the western world.

Blaine Aquifer

The Blaine aquifer is a major karst aquifer that is providing irrigation water in the 2,500 km^2 of the Hollis Basin (Fig. 4) in southwestern Oklahoma (Johnson, 1986, 1990a; Runkle and Johnson, 1988). The aquifer typically is 50-65 m thick in the basin and consists of 9 thick gypsum units (each 3-8 m thick) interbedded with thin dolomite beds (0.1-1.5 thick) and shale beds (0.3-8.0 m thick) (Fig. 5A).

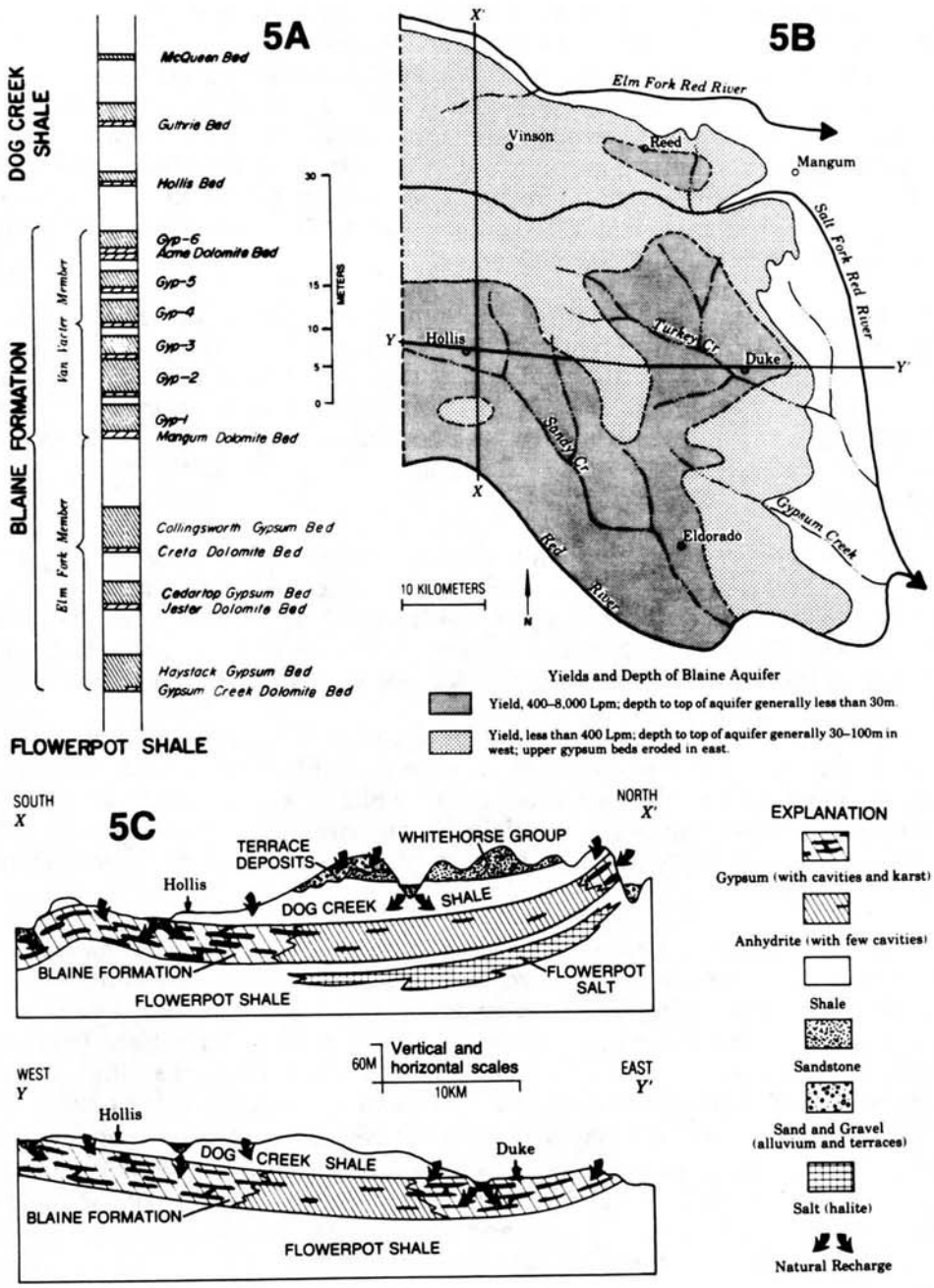

Figure 5. Hydrogeology of the Blaine aquifer in the Hollis Basin of southwestern Oklahoma (from Johnson, 1986): 5A is standard stratigraphic column; 5B is map showing ground-water yields; 5C shows two cross sections through irrigation district.

The Blaine Formation is divided into an upper member, the Van Vacter Member, and a lower member, the Elm Fork Member (Fig. 5A). The Van Vacter is about 30 m thick and is made up of six evaporite-clastic sequences. In some areas, water moving through the Van Vacter Member has dissolved and removed the gypsum and eroded the thin shales, thus developing a good hydraulic connection among gypsum beds. The Elm Fork Member is about 35 m thick and consists of three evaporite-clastic sequences. Shale beds, which tend to impede the vertical movement of water, are two to five times thicker in the Elm Fork Member than the Van Vacter Member.

In areas where depths to the top of the Blaine aquifer are greater than 30 m, anhydrite or a combination of anhydrite and gypsum is present (Fig. 5C). The presence of anhydrite indicates that only small quantities of slow-moving water have infiltrated the aquifer. Because of the relatively limited exposures to fresh, fast-moving water, anhydrite has not been converted to gypsum, and the gypsum has not been dissolved away. In these areas the permeability of the Blaine aquifer is low (Fig. 5B).

In the western part of the study area, the Blaine aquifer is overlain by 15-60 m of Dog Creek Shale (Fig. 5C), consisting of reddish-brown shale with three notable gypsum and dolomite beds in the lower 20 m. Where more than 30 m thick, the Dog Creek Shale acts as a confining unit; where it has been eroded to a thickness of less than 30 m, the Dog Creek Shale is a leaky confining unit.

The Blaine aquifer is recharged naturally (Fig. 5C): 1) mostly where karstic gypsum beds of the Blaine crop out; 2) where the Blaine aquifer is overlain by less than about 30 m of the Dog Creek Shale, which is a leaky confining unit; and 3) where the Blaine aquifer is overlain by alluvium or terrace deposits. The Blaine aquifer is an unconfined aquifer, except where overlain by at least 30 m of Dog Creek Shale.

Surface-water recharge to the ground-water system enhances the conversion of anhydrite to gypsum and the dissolution of gypsum, thereby increasing the permeability of the Blaine aquifer (Figs. 5B, 5C). In many areas less than 5 km from the streams, gypsum and dolomite beds have been largely or totally dissolved, thus creating large conduits that allow large quantities of water to move rapidly through the aquifer. Estimated transmissivity of the Blaine aquifer ranges from about 1,500 to about 5,700 m^2/day, with an average of about 3,250 m^2/day. The estimated storage coefficient ranges from about 0.0004 to about 0.03, with an average of about 0.016 (Steele and Barclay, 1965). Average annual runoff is estimated at 1.3-3.1 cm, and average annual evapotranspiration is estimated to be 60 cm in the study area (Pettyjohn, 1983).

Irrigation wells completed in the Blaine aquifer are typically 15-100 m deep and commonly yield 1,000-8,000 L/min. Depth to water in the Blaine is about 1.5-25 m below land surface. The water is a calcium sulfate type; the average dissolved-solids concentration is about 3,100 mg/L, which is suitable for irrigation but generally is unsuitable for drinking. At a few localities, sodium

and chloride concentrations are large enough to kill irrigated crops, but in general there has been no harmful buildup of salts in soils that have been irrigated for more than 40 years.

D. C. Jester Cave

The D.C. Jester Cave system was surveyed between 1983 and 1987 (Bozeman et al., 1987). The surveyed length of the main passage is 2,413 m, but along with the side passages the total length is 10,065 m, making Jester Cave the longest cave in Oklahoma and the longest gypsum cave reported in the western world (Bozeman et al., 1987). The cave follows a sinuous course, the passageways generally 1-3 m in diameter. It is a dry cave, except during and after periods of moderate rainfall.

Most parts of the Jester Cave system are developed in a 5-m thick bed of white gypsum (gypsum bed 1) near the middle of the Blaine Formation (Fig. 6A). This gypsum immediately overlies 0.5 m of resistant dolomite that forms the floor of the main cave in many areas. In addition to the main cave, many tributary branches are present in the cave system. There are also many sinkholes and other entrances to the cave system from the land surface (Fig. 6A).

The local structure of the Jester Cave area consists of Blaine strata dipping towards the west and southwest at about 10 m/km (about 0.5 degree). A cursory examination of the alignment of various segments of the Jester Cave system suggests that they may be controlled by several sets of joints or fractures in the rock. If subtle joint patterns do control the cave system, then ground water has dissolved the rock and moved along the principal joint system until it intersected a cross-cutting joint; the water then followed that cross-cutting joint for a short distance until again encountering another solutionally enlarged fracture in the principal joint system.

Northwestern Oklahoma

Northwestern Oklahoma contains a number of gypsum-karst regions, but none is as well known or has been visited as much as the Alabaster Cavern area of Woodward County.

Alabaster Cavern was discovered by settlers in the late 1800's and was first explored in 1898, but tourism at the cave was not seriously encouraged until the mid-1950's (Myers et al., 1969). The main cave, as well as four other known smaller caves, are now included in the Alabaster Caverns State Park, one of the finest tourist attractions in northwestern Oklahoma. The following description is based mainly upon the study by Myers et al. (1969).

Alabaster Cavern is almost wholly developed within the Medicine Lodge Gypsum Bed (Fig. 6B). The accessible part of the cave is about 700 m long and has a maximum width of 18 m and a maximum height of 15 m. Although there are many branches from the main chamber, most lateral openings are small and have not been explored. A second, smaller cave, called the Upper Room, has developed in the Nescatunga Gypsum and an underlying shale (Fig. 6B). The

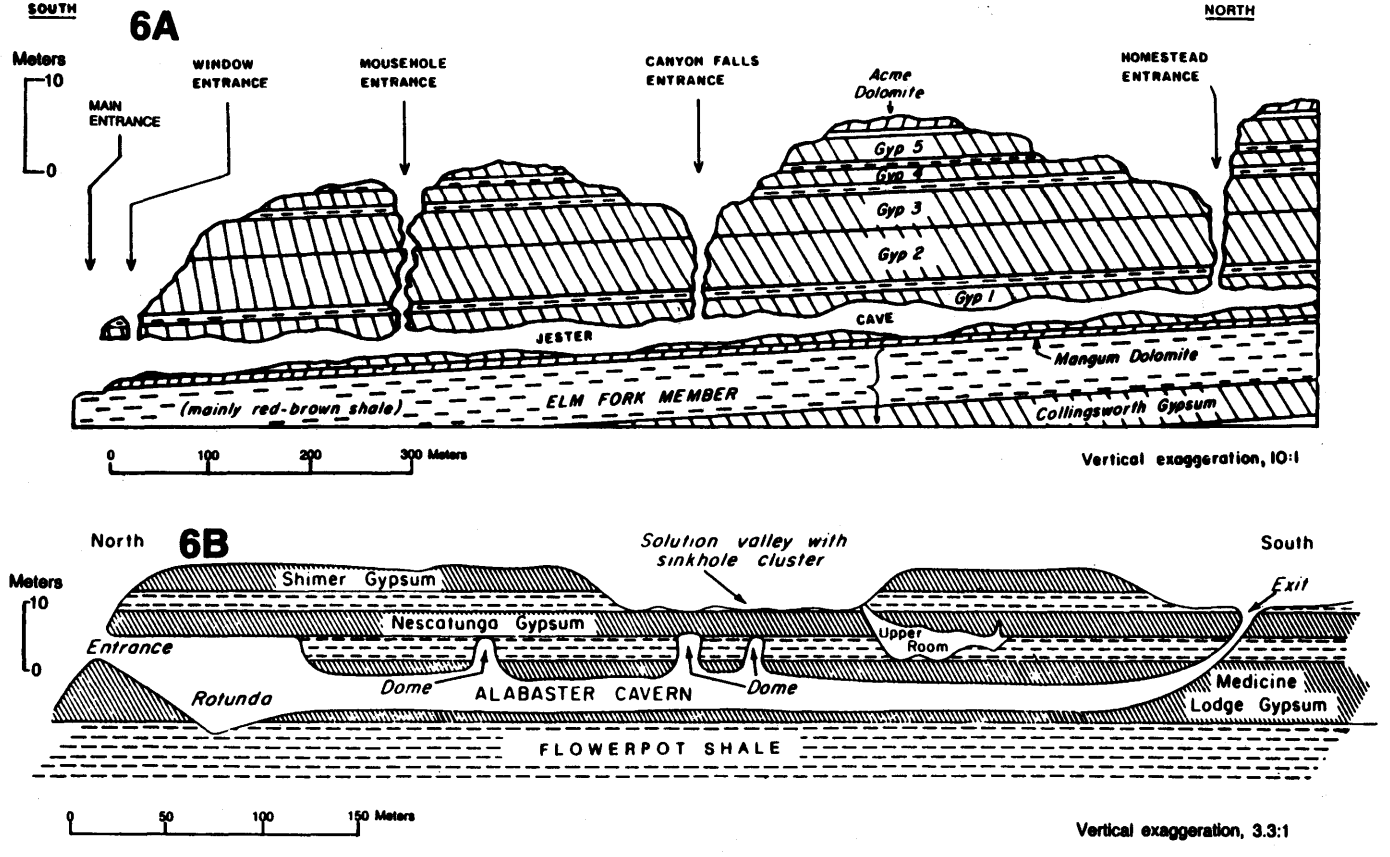

Figure 6. Schematic cross sections through major gypsum caves in the Blaine Formation of western Oklahoma: 6A shows Jester Cave, developed in gypsum bed 1 near the base of the Van Vacter Member in southwest Oklahoma (from Bozeman et al., 1987); 6B shows Alabaster Cavern, developed mainly in the Medicine Lodge Gypsum in northwest Oklahoma (from Myers et al., 1969).

Upper Room has a single known opening through a sinkhole. Although no large opening has been found connecting the Upper Room to Alabaster Cavern, there are probably small, open crevices or tubular connections.

Alabaster Cavern consists of three main sections, each of nearly equal length: a collapse section near the entrance, a middle section with domes in the roof, and a channel section at the end. In the collapse section, the cavern floor is a mass of gypsum, shale, and selenite boulders that have fallen from the roof. In the Rotunda, the first and largest room, the roof is the base of the Nescatunga Gypsum and the floor is part of the Flowerpot Shale: thus, the entire Medicine Lodge Gypsum has been dissolved, and parts of the underlying and overlying shales are also eroded.

The ceiling of the middle section is characterized by many domes. The land surface above the dome section is a dissolution valley with a cluster of sinkholes that recharge the perennial stream flowing through the cave. The abrasive action of the underground stream that helped form the cavern is best seen in the channel section, where the gypsum roof, walls, and floor are smooth and polished.

Rock layers at Alabaster Cavern are essentially flat-lying: they dip no more than 1-2 m/km (less than 0.1 degree). The strata are not faulted or noticeably jointed, and there is no conspicuous alignment to various segments of the cave system or drainage features. Control on development of the cave system is not clear, but most likely it is the result of faint and irregular fractures in the rock that have established slightly preferential zones of ground-water dissolution, and these fissures then were widened by through-flowing waters once the underground stream system was developed. Myers et al. (1969) believe that Alabaster Cavern probably began to develop in the latter part of the Pleistocene Epoch, when the nearby major river and its tributaries cut down to elevations below the Blaine gypsums.

SALT KARST

Salt (halite) beds in the Flowerpot, Blaine, and Dog Creek formations (Fig. 4) are being dissolved at shallow to moderate depths in western Oklahoma, and these strata constitute a significant interstratal karstic unit in the region. The most conspicuous surface manifestations of this process are the large and barren, salt-encrusted salt plains that have formed in a number of stream and river courses where the high-salinity brines are being emitted (Figs. 1, 3). Data on salt karst in this region are mainly from Johnson (1981).

Fresh ground water is recharged generally to the west of the salt plains, in upland areas where unconsolidated sands (Ogallala Formation) or sandstone, gypsum, dolomite, alluvium, or terrace deposits are at the surface (Fig. 1). This water migrates downward and laterally (eastward) to salt beds which are 10-250 m below the surface, and dissolves the salt to form brine. The resulting brine is then forced laterally and upward by hydrostatic pressure through aquifers or through fractures in aquitards until it is discharged at the surface (Fig. 1).

Subsurface flow of fresh water and the brines is laterally through aquifers, such as sandstone or cavernous gypsum, dolomite, or salt, and the water also moves vertically through fractures, sinkholes, and collapse features.

A total of seven significant salt plains are present in western Oklahoma (Fig. 3). Several of the salt plains are only 2-10 hectares in size, whereas the two largest are 16 and 64 km^2. Individual salt plains release brines with concentrations of 20-340 g NaCl/L, and they each contribute 100-3,000 metric tons of NaCl per day that degrades the quality of water flowing in the Arkansas and Red River systems.

Salt is highly soluble, more soluble than any other rock in the Permian sequence of western Oklahoma and nearby areas. Ground water in contact with salt will dissolve some of the salt, providing the water is not already saturated with NaCl. For extensive dissolution to occur, it is necessary for the brine thus formed to be removed from the salt deposit; otherwise the brine becomes saturated, and the process of dissolution stops.

Four basic requirements are necessary for salt dissolution to occur here, or in other evaporite basins (Johnson, 1981):

1) A deposit of salt against which or through which water can flow.
2) A supply of water unsaturated with NaCl.
3) An outlet whereby the resulting brine can escape.
4) Energy (such as a hydrostatic head or density gradient) to cause the flow of water through the system.

When all four of these requirements are met, salt dissolution and brine transport can be quite rapid, in terms of geologic time.

There are four principal ways whereby fresh ground water is recharged in the region (Fig. 1):

1) Water seeps into the ground through permeable rocks and soils, such as in areas where sandstone is at the surface.
2) Water enters the bedrock through highly permeable alluvium and terrace deposits along and near the major streams and rivers.
3) Water enters the ground through sinkholes, caverns, and other karstic features, in areas where gypsum, dolomite, or limestone is at the surface.
4) Water enters the ground through joints and fractures in the rocks, particularly where underlying salt beds are partly dissolved and the rock is more fractured owing to collapse.

After the water has dissolved some of the salt and has become brine, there are six principal ways whereby the brine moves underground and is eventually discharged (Fig. 1):

1) Brine moves through dissolution cavities in the salt or other soluble rocks.
2) Brine moves vertically and/or laterally through joints and fractures, particularly where the rock is disrupted over dissolution cavities.
3) Brine moves laterally through aquifers consisting of sandstone, siltstone, or other permeable rocks.
4) Brine may be discharged at a point source as a saline spring.

5) Brine may be discharged along the course of a stream bed and become part of the surface flow.
6) Brine may enter the base of an alluvial deposit, where it can be forced upward under hydrostatic pressure and then drawn upward by capillary action as the brine is evaporated. A thin crust of salt then is precipitated on the land surface as water is evaporated from the brine.

In all cases cited above, the energy needed to cause flow of the water is the hydrostatic head created in the recharge areas. The brine moves laterally and upward toward the piezometric surface.

The process of salt dissolution produces cavities, normally at the undip limit or at the top of the salt unit, into which overlying rocks can settle or collapse chaotically (Fig. 1). Disrupted rock helps to make salt dissolution a somewhat self-perpetuating process, inasmuch as cavern development followed by collapse and fracturing of the rock will cause a greater vertical permeability, and this allows further access of fresh water to the salt. In most areas, strata overlying a salt-dissolution zone are mildly to intensely folded, faulted, jointed, or fractured where they have collapsed and subsided into the dissolution cavities.

Boreholes drilled in and around the salt plains commonly encounter artesian flows. Solution cavities or zones of lost circulation 0.1-1.0 m thick are also common at the top of the salt unit, but these features generally are absent within the salt unit (Fig. 1). Such features represent the zones at which dissolution is most actively taking place and the pathways whereby high-salinity brine is escaping from the salt beds. The thin, somewhat cavernous zone at the top of the salt is an artesian aquifer wherein the piezometric surface locally rises approximately to, or just above, the elevation of the surface of the salt plains (Fig. 1).

CONCLUSIONS

The Blaine Formation and associated strata constitute a major evaporite karst unit in western Oklahoma and adjacent areas. Gypsum, dolomite, and shale interbeds with an aggregate thickness of 30-75 m in outcrops contain a well developed suite of karstic features, such as caves, sinkholes, and disappearing streams; where these same strata are in the shallow subsurface, they locally are a major karst aquifer used as a source of irrigation water. Where salt is interbedded with red-bed shale, gypsum (or anhydrite), and dolomite in the deeper subsurface, the evaporite unit is typically 100-250 m thick. Salt at depths of 10-250 m below the surface locally is being dissolved by ground water to form a karst system typified by brine-filled cavities, collapse structures (in overlying strata), and salt plains.

Acknowledgements--Publication of this report is authorized by the Director of the Oklahoma Geological Survey.

REFERENCES

Bozeman, S., and 9 others, 1987, The D.C. Jester Cave system: Central Oklahoma Grotto, Oklahoma Underground, v. 14, 56 p.

Gustavson, T. C., Simpkins, W. W., Alhades, A., and Hoadley, A., 1982, Evaporite dissolution and development of karst features in the Rolling Plains of the Texas Panhandle: Earth Surface Process and Landforms, v. 7, p. 545-563.

Hovorka, S. D., and Granger, P. A., 1988, Subsurface to surface correlation of Permian evaporites--San Andres-Blaine-Flowerpot relationships, Texas Panhandle, in Morgan, W. A., and Babcock, J. A., eds., Permian rocks of the Midcontinent: Midcontinent SEPM Special Publication No. 1, p. 137-159.

Johnson, K. S., 1972, Guidebook for geologic field trips in Oklahoma, Book II, Northwest Oklahoma: Oklahoma Geological Survey Educational Publication 3, 42 p.

Johnson, K. S., 1981, Dissolution of salt on the east flank of the Permian Basin in the southwestern USA: Journal of Hydrology, v. 54, p. 75-93.

Johnson, K. S., 1986, Hydrogeology and recharge of a gypsum-dolomite karst aquifer in southwestern Oklahoma, USA, in Gunay, G., and Johnson, I. V., eds., Karst Water Resources, Proceedings of the International Symposium on Karst Water Resources, Ankara, Turkey, July 7-19, 1985: International Association of Hydrological Sciences Publication No. 161, p. 343-357.

Johnson, K. S., 1990a, Hydrogeology and karst of the Blaine gypsum-dolomite aquifer, southwestern Oklahoma: Oklahoma Geological Survey Special Publication 90-5, Guidebook for Field Trip No. 15, Geological Society of America (Annual Meeting, 1990), 31 p.

Johnson, K. S., 1990b, Standard outcrop section of the Blaine Formation and associated strata in southwestern Oklahoma: Oklahoma Geology Notes, v. 50, p. 144-168.

Johnson, K. S., and Denison, R. E., 1973, Igneous geology of the Wichita Mountains and economic geology of Permian rocks in southwest Oklahoma: Oklahoma Geological Survey Special Publication 73-2, Guidebook for Field Trip No. 6, Geological Society of America (Annual Meeting, 1973), 33 p.

Jordan, L., and Vosburg, D. L., 1963, Permian salt and associated evaporites in the Anadarko Basin of the western Oklahoma-Texas Panhandle region: Oklahoma Geological Survey Bulletin 102, 76 p.

McGregor, D. R., Pendry, E. C., and McGregor, D. L., 1963, Solution caves in gypsum, north-central Texas: Journal of Geology, v. 71, p. 108-115.

Myers, A. J., Gibson, A. M., Glass, B. P., and Patrick, C. R., 1969, Guide to Alabaster Cavern and Woodward County, Oklahoma: Oklahoma Geological Survey-Guidebook 15, 38 p.

Pettyjohn, W. A., 1983, Water atlas of Oklahoma: Stillwater, Oklahoma, University Center for Water Research, Oklahoma State University, 72 p.

Quinlan, J. F., Smith, R. A., and Johnson, K. S., 1986, Gypsum karst and salt karst of the United States of America, in Atti symposio internationale sul carsismo nelle evaporiti (Proceedings, International Symposium on Karst in Evaporites): Palermo, Italy, October 27-30, 1985: Le Grotte d'Italia, Series 4, v. 13, p. 73-92.

Runkle, D. L., and Johnson, K. S., 1988, Hydrogeologic study of a gypsum-dolomite karst aquifer in southwestern Oklahoma and adjacent parts of Texas, USA, in Karst hydrogeology and karst environment protection: Geological Publishing House, Beijing, China, Proceedings of the IAH 21st Congress, held in Guilin, China, October 10-15, 1988, v. 21, part 1, p. 400-405.

Steele, C. E., and Barclay, J. E., 1965, Ground-water resources of Harmon County and adjacent parts of Greer and Jackson Counties, Oklahoma: Oklahoma Water Resources Board Bulletin 29, 96 p.

White, W. B., 1988, Geomorphology and hydrology of karst terrains: Oxford University Press, New York, 464 p.

THE ROLE OF GROUND WATER IN THE DEPOSITION OF TRAVERTINE-MARL

JANET S. HERMAN
Department of Environmental Sciences
University of Virginia
Charlottesville, VA 22903
USA

and

DAVID A. HUBBARD, JR.
Virginia Division of Mineral Resources
P. O. Box 3667
Charlottesville, VA 22903
USA

ABSTRACT

A hydrochemical survey of 12 travertine-depositing streams in the folded and faulted rocks of the Valley and Ridge physiographic province of the Appalachian Mountains in Virginia established the chemical evolution of stream water. The waters are primarily Ca-HCO_3-type and evolve in a downstream direction by CO_2 outgassing, concomitant increases in pH, and calcite precipitation. The greatest calcite precipitation, resulting in the travertine buildups, occurs just downstream from the greatest CO_2 losses. Chemical and hydrological processes can adequately explain the precipitation of calcite from the streams in this study. Input of carbonate-rich water from discrete springs or tributaries or from diffuse ground-water flow through stream beds is determined structurally by the location of fractures or faults. This input of carbonate-rich ground water to the stream is a critical control on the ultimate formation of travertine and marl.

INTRODUCTION

Karst features can be identified as positive or negative features of the landscape. In a karstified limestone terrain, familiar negative features that result from the dissolution of calcium carbonate include caves and sinkholes. Positive karst features resulting from the deposition of calcium carbonate include cave formations in the subsurface and travertine-marl along surficial streams. The focus of this research is on the deposits of travertine-marl. Our goal in this study is to achieve an integrated understanding of hydrogeological and geochemical processes that lead to the formation of travertine-marl.

Travertine-marl is a general term referring to surficial freshwater carbonate materials deposited by spring and stream water (Hubbard and Herman, 1990). More specifically (Gary et al., 1972), travertine is hard, dense, finely crystalline, compact or massive but commonly concretionary limestone, white, light gray, or very pale to pale brown in color, often having a fibrous or concentric structure and splintery

International Contributions to Hydrogeology, Vol. 13 (1992)
© Verlag Heinz Heise, Hannover, FRG

fracture, formed by rapid chemical precipitation of $CaCO_3$ from solution by agitation of the water or other means of outgassing of CO_2 around a spring or along a stream. It may also be precipitated by or on bacteria or algae and on other plants and organic or inorganic substrate. The spongy, cellular, or less compact variety is commonly termed tufa. Marl is soft, loose, earthy, and semifriable or crumbling unconsolidated material consisting chiefly of a mixture of clay and $CaCO_3$ in varying proportions; $CaCO_3$ content can vary from a minimum of 35% to almost 100%.

Deposits of these surficial freshwater carbonate materials are predominantly found in the Valley and Ridge physiographic province of the Appalachians. A considerable range in morphology is exhibited by the travertine-marl deposits. Extensive low-relief deposits dominated by marl are typical of sites in the northern portion of the Valley and Ridge province of Virginia. Travertine buildups, forming bluffs and falls in active stream channels, are notable components in most deposits throughout Virginia (Fig. 1). Some deposits contain extensive broad accumulations of marl upstream from travertine buildups. Most travertine-marl deposits are recognized only by the waterfalls created by the travertine buildups in the stream channel. The marl accumulations upstream from these depositional structures are typically obscured by vegetation and soil development, but they may be exposed in entrenched stream banks.

Depositional Model

A generalized depositional model describes the development of many of these deposits in Virginia (Hubbard et al., 1985; Hubbard and Herman, 1990). Travertine-marl deposits are found downstream from locations of ground-water discharge from carbonate bedrock. This ground-water discharge may take the form of discrete springs that fully or partially feed the stream flow or it may be in the form of diffuse input to the stream bed. The point or diffuse emergence of ground water is controlled structurally by faults and fractures that provide permeable and soluble pathways for the upward migration of ground water to the surface.

The ground water that has circulated through Cambrian and Ordovician limestone and dolomite at depth issues onto the surface near equilibrium with respect to calcite and with a partial pressure of CO_2 that is elevated relative to the open atmosphere. Carbon dioxide outgasses from the water; the outgassing is enhanced by the hydrological agitation. The continuing loss of CO_2 as the water flows downstream causes the solution to become increasingly supersaturated with respect to calcite.

Calcite precipitation occurs at some distance downstream from the emergence, either as a discrete spring or as diffuse flow through the stream bed, of carbonate-rich ground water. A combination of factors influence the deposition of travertine. Primarily, the water must reach a high degree of supersaturation before significant calcite precipitation occurs. This condition is typically met at a waterfall or cascade where increased turbulence of the stream causes the highest rates of CO_2 outgassing. Additionally, an appropriate substrate is a factor in localizing calcite

Figure 1. A complex travertine buildup on Sweet Springs Creek, Allehgany County, Virginia, USA, and its 8-m-high waterfall. This system, not part of the present geochemical study, is illustrative of the morphology of a travertine buildup.

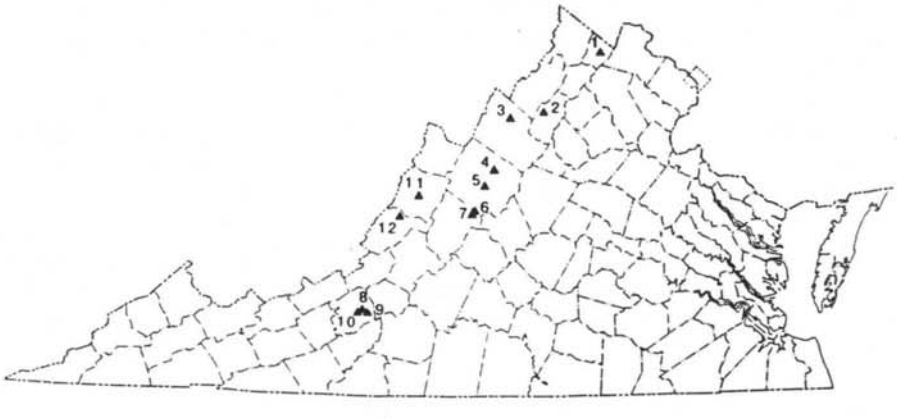

Figure 2. Locations of the Virginian travertine-depositing streams sampled in the course of this study (triangles). 1. James, 2. Hamburg, 3. Arbagast, 4. Quicks Mill, 5. Folly Mills, 6. Glenn Falls, 7. Moores Creek, 8. Falls Hollow, 9. Shawsville, 10. Mound, 11. Warm Springs, 12. Falling Spring.

precipitation. Substrates can be previously precipitated calcite, mosses or algae, or other inorganic or organic surfaces occurring in the stream bed.

Travertine initially forms on some obstruction in the stream bed, such as a bedrock ledge or a fallen tree, that increases the turbulence of stream flow. Travertine accumulation on the obstruction causes even more turbulence and further enhances travertine deposition. Thus, travertine buildups are formed in a self-perpetuating process. Buildups may form at multiple sites along a stream as long as CO_2 outgassing and calcite precipitation are chemically possible. Deposition of travertine on a buildup reduces the stream gradient. The decreased gradient allows fine-grained carbonate-rich sediments (marl) to accumulate immediately upstream from the buildup. Eventually, the travertine-marl deposition reduces the stream gradient sufficiently to allow the lateral migration of the stream during a high-flow event. Thus, the migrating stream forms a series of valley-wide transverse travertine buildups with associated upstream marl accumulations.

This paper summarizes what we have learned about the hydrological and geochemical controls on the chemical evolution of travertine-depositing streams and the formation of travertine in our studies of 12 streams in Virginia (Herman and Hubbard, 1990). Sampling of water was designed to test our hypothesis that the input of carbonate-rich ground water, whether from a discrete spring or from diffuse flow, has a critical effect on the formation of travertine and that the location of the input is determined by faults or fractures. Thus, the hydrogeological controls on travertine deposition are elucidated.

METHODS

A total of 12 sites were sampled (Fig. 2; Table 1). The nature of the travertine-depositing systems sampled for this study included streams fed by discrete cold springs, streams fed by diffuse input of ground water where the stream crosses a known fault, streams fed by discrete warm springs, and a travertine-mound-depositing spring. The sites were selected from more than 60 known travertine-marl locations in Virginia (Hubbard, 1985; Hubbard et al., 1985) in order to examine a range of hydrogeologic settings.

The water samples were collected from springs, whenever discrete springs could be identified, and from major tributary inputs immediately upstream from travertine deposits (Table 1). Sampling was conducted upstream and downstream from fault traces where diffuse input of ground water to the stream was hypothesized to be influencing travertine formation. Additionally, samples were collected above and below waterfalls formed by the travertine. In several streams, additional samples were collected further downstream from the travertine buildup. The length of sampled flow path varied from 0 km at the site of a spring-deposited travertine mound to 5.2 km at Falling Spring Creek, a site that was the focus of a comprehensive study (Lorah and Herman, 1988). More typically, the sampled flow path was on the order of 0.5 km long. Because similar hydrological and seasonal conditions were sought for the comparisons among streams, the water samples were collected within an eight-week period of September through November 1986.

Table 1. Summary of location and type of water samples. Asterisked sites were sampled twice for chemical analysis.

Site Name	County	Number and location of samples
1) James	Clarke	2: spring; base of falls
2) Hamburg	Page	3: upstream; crest of falls; base of falls
3) Arbagast	Rockingham	2: spring; base of falls
4) Quicks Mill	Augusta	4: upstream; spring input*; crest of falls*; base of falls*
5) Folly Mills	Augusta	5: upstream from fault; overlying fault breccia; tributary; crest of falls; base of falls
6) Glenn Falls	Augusta/ Rockbridge	3: upstream from fault; downstream from fault; base of falls
7) Moores Creek	Rockbridge	4: tributary; upstream; crest of falls; base of falls
8) Falls Hollow	Montgomery	3: overlying fault breccia; crest of falls*; base of falls*
9) Shawsville	Montgomery	3: overlying fault breccia; crest of falls; base of falls
10) Mound	Montgomery	1: spring
11) Warm Springs	Bath	3: spring; downstream from tributary input; stream
12) Falling Spring	Alleghany	3: spring; crest of falls; base of falls

RESULTS

Complete chemical data for all the streams are reported in Herman and Hubbard (1990); a brief summary of those data is given in Table 2 below. The temperatures of the travertine-depositing waters range from the high value of 33°C for one of the two thermal springs studied to a range of 9° - 21°C for stream water (Table 2). Temperature change along a stream segment was never more than 4°C on a single collection date.

The spring and stream waters all have pH values between 7.09 and 8.43 (Table 2). The lowest values are observed at springs (7.09-7.62). The non-thermal streams had higher pH values (>8.04) than the thermal streams (~7.80). The general trend in samples from the same site is an increase in pH in the downstream direction. For instance, at the Quicks Mill site, the pH of the stream which is fed by multiple springs is 7.55; the pH of one of the major springs feeding the stream is 7.56; the pH at the crest of a travertine cascade 1.6 km downstream from the spring is 8.14; the pH at the base of the cascade is 8.41 (Table 3; Figs. 3 and 6A; see also Hoffer-French and Herman, 1989).

Figure 3. Small travertine structure (approximately 1 m high) within the cascade series that was sampled along Falling Spring Run at the Quicks Mill site.

Figure 4. Three-meter-high travertine buildup at Folly Mills site.

Table 2. Chemical composition of travertine-depositing stream and spring water samples. A total of 35 samples were collected from 10 non-thermal streams. A total of 6 samples were collected from 2 thermal streams. All concentrations are reported in mg/L.

	Non-thermal Water		Thermal water	
	Average	Range	Average	Range
T (°C)	15.4	9.0 - 21.0	28.5	22.0 - 33.0
Cond. (μS/cm)	351	258 - 412	848	780 - 975
pH	8.07	7.09 - 8.43	7.89	7.45 - 8.37
HCO_3	323	233 - 442	257	189 - 339
Ca	73	58 - 91	133	107 - 160
Mg	28	16 - 43	28	24 - 32
Na	3.9	0.5 - 8.4	4.0	3.3 - 4.6
K	2.8	0.9 - 4.7	14	11 - 17
SO_4	13	2.2 - 49	286	254 - 317
Cl	6.4	1.3 - 16	2.8	1.8 - 3.6
NO_3	5.6	0.5 - 21	<0.5	<0.5
Molar Ca/Mg	1.69	1.02 - 3.03	2.87	2.74 - 3.01
Molar Na/K	2.35	0.882 - 4.30	0.510	0.407 - 0.616
TDS	464	346 - 628	724	595 - 870
log P_{CO2}	-2.64	-3.11 - -1.55	-2.52	-2.97 - -1.95
SI_c	+0.80	-0.03 - +1.14	+0.83	+0.34 - +1.35

All the non-thermal waters sampled in this study are calcium-bicarbonate type (Table 2). Typical calcium concentration is 73 mg/L (range 58 - 91 mg/L). The highest concentrations were observed for the thermal waters (160 mg/L). Magnesium is the second most abundant cation (16-43 mg/L). Bicarbonate is the dominant anion in all samples except those from the two thermal streams. Typical bicarbonate concentrations is about 323 mg/L (range 233 - 442 mg/L). In one thermal stream, bicarbonate and sulfate concentrations are comparable; in another, sulfate dominates. Sulfate concentrations range widely in the non-thermal streams (2.2 - 49 mg/L). In the thermal streams, sulfate is as high as 317 mg/L. The nitrate concentration varies widely (<0.5 - 21 mg/L) probably reflecting the varying degree of contamination by human and animal wastes. The molar Ca/Mg ratios of all the waters are between 1.02 and 3.03. The molar Na/K ratios were greater than 1.0 for the non-thermal waters and less than 1.0 for the thermal water.

All the waters sampled are supersaturated with respect to the CO_2 content of the open atmosphere ($10^{-3.5}$ atm). The calculated values span a range of nearly two orders of magnitude from $10^{-1.55}$ to $10^{-3.11}$ atm. The largest values are observed for the non-thermal springs ($10^{-1.55}$ - $10^{-2.09}$ atm). The smallest values are observed for the samples collected below the waterfalls ($10^{-2.66}$ - $10^{-3.09}$ atm). In general, within a set of samples collected at one site, the P_{CO2} decreases for downstream samples. For example, at the Quicks Mill site the P_{CO2} of the major spring feeding the stream is

Table 3. Partial chemical composition and calculated parameters of individual water samples for several of the studied streams. (Complete data for all streams are reported in Herman and Hubbard (1990).) Within each site group, the samples are ordered upstream to downstream. More information on sample locations is listed in Table 1. All ion concentrations are reported in units of mg/L. Saturation index is reported for calcite (SI_c).

Sample name	T (°C)	pH	HCO_3	Ca	Mg	Na	K	SO_4	Cl	log P_{CO2}	SI_c
Discrete spring input:											
Quick Mills strm	15.0	7.55	350.7	61.1	30.7	3.39	2.42	2.19	1.88	-2.88	+0.26
Quicks Mills spr	14.0	7.56	354.9	70.7	29.2	3.08	1.80	2.47	1.46	-2.09	+0.32
Quicks Mills afall	14.7	8.14	350.7	79.2	28.2	2.60	1.92	3.18	2.21	-2.69	+0.94
Quicks Mills bfall	16.0	8.41	325.8	67.7	28.3	2.39	2.14	3.33	2.55	-2.99	+1.12
Diffuse ground-water input:											
Folly Mills aflt	19.5	8.40	303.6	62.9	29.2	4.49	3.51	8.58	6.76	-2.99	+1.09
Folly Mills trib	15.5	7.87	309.7	67.4	26.8	1.55	2.99	6.02	3.23	-2.46	+0.58
Folly Mills brec	17.0	8.26	314.6	69.8	27.4	3.42	2.96	7.16	4.91	-2.85	+0.99
Folly Mills afall	16.5	8.38	316.7	68.9	26.8	2.88	2.96	7.30	4.82	-2.97	+1.09
Folly Mills bfall	16.0	8.42	315.1	64.8	28.7	4.54	3.97	7.16	4.91	-3.02	+1.09
Falls Hollow brec	9.0	8.09	401.2	78.9	30.1	2.47	2.36	10.28	1.96	-2.61	+0.85
Falls Hollow afall	11.0	8.05	441.7	86.5	43.3	3.06	1.94	49.29	1.46	-2.52	+0.89
Falls Hollow bfall	10.0	8.18	400.4	71.1	42.3	2.05	1.58	48.58	1.37	-2.70	+0.89

$10^{-2.09}$ atm; the P_{CO2} at the crest of a travertine cascade 1.6 km downstream from the spring is $10^{-2.69}$ atm; the P_{CO2} at the base of the cascade is $10^{-2.99}$ atm (Table 3; Figs. 3 and 6A).

Nearly all of the waters collected for this study are supersaturated with respect to calcite. Two spring samples are in equilibrium with respect to calcite (SI_c =0± 0.05). Saturation indices (SI_c) for the supersaturated samples range from +0.08 to +1.35, or from 1.2 to 22.4 times supersaturated. For most sets of samples collected from a single site, the waters become more supersaturated in the downstream direction. At Quicks Mill, for example, the saturation state of the major spring feeding the stream with respect to calcite is SI_c = +0.32; at the crest of the travertine cascade SI_c = +0.94; at the base of the cascade SI_c = +1.12 (Table 3; Figs. 3 and 6A). At three of the study sites, the stream composition has shifted back toward equilibrium in the sample collected furthest downstream.

DISCUSSION

The chemical compositions of the 12 travertine-depositing streams studied are similar. The 10 non-thermal streams are Ca-HCO_3-type water, the thermal stream at Flling Spring Creek is a Ca-HCO_3, SO_4-type water, and the thermal stream at Warm Springs is a Ca-SO_4-type water. All the water samples have a large dissolved solids content (TDS, Table 2) for fresh surface waters, especially rich in Ca^{2+} and Mg^{2+}, reflecting the input of ground waters from carbonate rocks. The Ca/Mg molar ratios show that most of the waters have come in contact with dolomite as well as limestone at some point in their flow path (White, 1988). The thermal water is chemically distinguished from the non-thermal water by its high SO_4^{2-} concentration and small Na/K molar ratio.

The springs are supersaturated by as much as two orders of magnitude with respect to the CO_2 levels of the open atmosphere. This elevated P_{CO2} causes the spring-water pH values to be relatively low. The stream water has lower P_{CO2} than the springs because the CO_2 progressively outgasses from the streams along their flow paths. The streams still remain supersaturated with respect to CO_2, however, for a significant distance downstream from the major spring inputs. The higher values of pH for the stream water relative to the springs can be attributed to the CO_2 outgassing.

Two springs in this study are near equilibrium with respect to calcite, but all the streams are supersaturated. In previous studies that spanned several seasons, stream water undersaturated with respect to calcite was only observed during very wet conditions such as in late winter or early spring (Hoffer-French and Herman, 1989; Lorah and Herman, 1988). The calcite saturation indices become increasingly positive in the downstream direction as outgassing occurs.

Eight of the 12 sites sampled exhibit decreasing Ca^{2+} concentrations in the segment of flow path from above the travertine waterfall to below it; thus, the Ca^{2+} loss is localized at the waterfalls. At two other sites no loss of Ca^{2+} is observed although they are morphologically similar to the other waterfall sites. At one other

site, one of the thermal streams, no active accumulation of travertine is observed. At the mound site, only the spring was sampled; thus, there is no flow segment.

Two types of processes could cause the decreased Ca^{2+} concentrations: 1) dilution by input of water with lower Ca^{2+} concentration or 2) loss of Ca^{2+} from solution through formation of or reaction with a solid. The concentrations of unreactive species such as Cl^- do not decrease in the same stream segments as the Ca^{2+} concentrations do, however, as would be expected if dilution were important (Herman and Lorah, 1987). Among the studied streams, four show a small decrease in Mg^{2+} over the same flow segments showing loss of Ca^{2+} The Na^+ and K^+ concentrations do not show any consistent change. Calcium is the only cation being removed significantly from solution.

The presence of active travertine and the supersaturation of stream water with respect to calcite both indicate that the most likely removal mechanism for Ca^{2+} is calcite precipitation. Samples were not collected along a long enough length of the flow path for most streams in this study to show downstream adjustment toward equilibrium. Typically, saturation indices continue to increase for some distance downstream from the waterfalls although maximum calcite precipitation is localized at the falls. This increase in SI_c is driven by CO_2 outgassing and increase in pH; calcite precipitation rates lag behind. In Falling Spring Creek, decreased saturation indices are finally observed 4 km downstream from the waterfalls (Lorah and Herman, 1988), which is a greater distance than sampled in most of the streams of this study.

Critical Ground-water Input

Samples were collected to provide a general description of the nature of travertine-depositing streams in the Valley and Ridge province of Virginia and to examine the effect of discrete or diffuse input of carbonate-rich water to these streams. Ground water is the hypothesized input, although no direct observation of ground water (i.e., as collected from wells) is part of this study. The chemical composition of spring water is taken as an indication of the ground-water composition. The discrete input of carbonate-rich water may occur as springs or as tributary streams. In either case, these inputs can be directly sampled as discrete water sources. The contrasting condition is diffuse input of carbonate-rich water, which, in our hypothesized scenario, occurs as diffuse flow of ground water through a stream bed and cannot be sampled.

Several of the study sites appeared to be hydrologically simple: discrete springs are contributing significant volumes of water to the stream not far above the site of travertine deposition (Table 1 - James, Arbagast, Quicks Mill (Table 3; Figs. 3 and 6A), Warm Springs, Falling Spring). Our model of CO_2 outgassing and $CaCO_3$ deposition at the waterfalls explains the increase in pH and the decrease in Ca^{2+} and HCO_3^- concentrations between samples collected upstream and downstream from the waterfalls. The other major ions typically show some minor changes in concentrations, but there is no consistent pattern. A pattern of the loss of dissolved CO_2 occurring slightly upstream from the loss of Ca^{2+} is common. The

HCO_3^- concentration begins to decrease upstream from the crest of the cascade, and Ca^{2+} concentration drops at the cascade (See more detailed studies of two of the streams in Lorah and Herman, 1988 (Falling Spring Creek); Hoffer-French and Herman, 1989 (Quicks Mills)).

Several of our study sites were selected to examine the effects of suspected diffuse inputs of Ca-HCO_3-rich ground water to the stream (Table 1 - Folly Mills (Table 3; Figs. 4 and 6B), Moores Creek, Hamburg, Shawsville, Glenn Falls, Falls Hollow, Table 3; Figs. 5 and 6C). Folly Mills, with five samples (Table 3; Figs. 4 and 6B), is a good site to test our model. A tributary stream (trib) flows along a fault upstream from the sampling point. This tributary contributes water that is higher in Ca^{2+} and HCO_3^-, lower in pH, and cooler than the main stream as sampled upstream from where it crosses a mapped fault (aflt). The mixed-stream composition overlying the fault breccia (brec) is even higher in Ca^{2+} and HCO_3^- concentrations, although there is no obvious gain of water from a discrete source. We infer diffuse input of carbonate-rich ground water to the stream bed in the vicinity of the fault. By the crest of the falls (afall), where there is minor travertine, Ca^{2+} concentration decreases slightly. The small increase in HCO_3^- in the same sample is not consistent with the common pattern of loss of dissolved CO_2 preceding measurable loss of Ca^{2+}. Below the falls (bfall), the Ca^{2+} concentration is significantly lower and is lower than any upstream sample except the original main stream; HCO_3^- is only slightly lower. None of the other chemical constituents give clear or consistent evidence for the input, either discrete or diffuse, of water of different composition. We believe all these water sources to be very similar in their major ion chemistry and that they differ only slightly in the parameters that most directly affect calcite precipitation: Ca^{2+} and HCO_3^- concentrations, pH, and temperature.

Stream samples from well above (brec), above (afall), and below (bfall) the waterfalls were collected at Falls Hollow (Table 3; Figs. 5 and 6C). The stream flows over a fault breccia between the two sample locations upstream from the waterfalls. There is no obvious input of surface or ground water along that reach of stream. The Falls Hollow stream composition is remarkable in the large increases of Ca^{2+}, HCO_3^-, Mg^{2+}, and SO_4^{2-} concentrations with little change in pH between the two upstream samples. These samples provide the clearest chemical evidence of diffuse input of ground water to the stream of those collected in this study. In their more comprehensive study, Kirby and Rimstidt (1990) also argue for the input of carbonate-rich ground water via diffuse flow through the stream bed above the falls. Large drops in HCO_3^- (from 441.7 to 400.4 mg/L; Table 3) and Ca^{2+} (from 86.5 to 71.1 mg/L; Table 3) concentrations and increased pH are observed between the samples from above and below the falls without other significant changes in chemical composition, indicating significant travertine deposition.

CONCLUSIONS

Similarities in water composition and stream morphology are typical among the travertine-depositing streams of Virginia. Observations of the chemical composition of stream waters show that they are usually Ca-HCO_3-type waters. The

Figure 5. Final 6-m plunge at the base of a 15-m-high cascade along the stream in Falls Hollow.

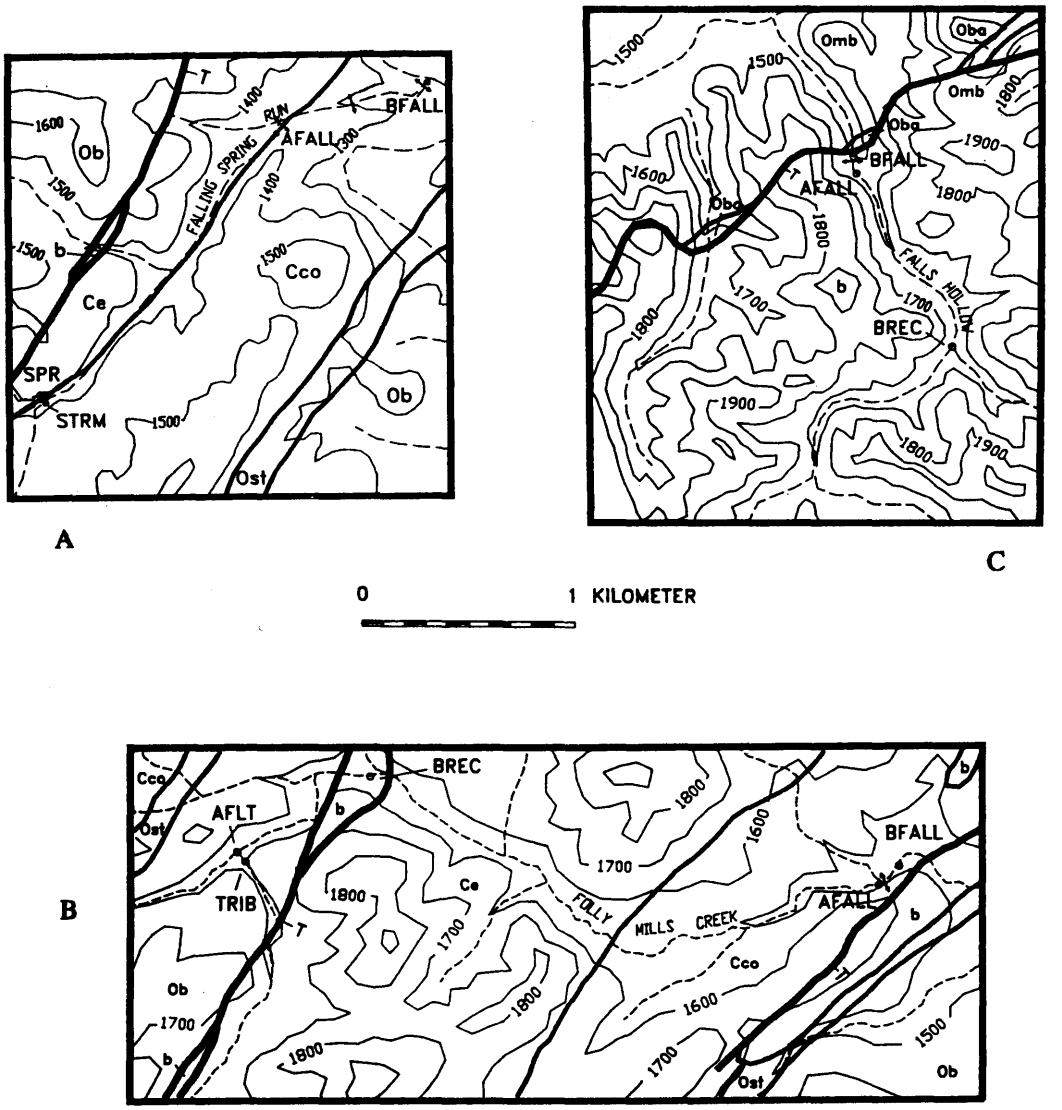

Figure 6. Maps of sample collection sites along travertine-depositing streams at (A) Quicks Mills, (B) Folly Mills, and (C) Falls Hollow. Water sample locations are indicated by dots and are named AFALL and BFALL for upstream and downstream from a waterfall, AFLT for upstream from a fault, BREC for a location on fault breccia, TRIB for tributary, SPR for spring, and STRM for stream (see Tables 1 and 3). Travertine buildups are indicated by double-pointed arrows. The geology is labeled: Omb Martinsburg Formation; Oba Bays Formation; Ob Beekmantown Formation; Ost Stonehenge Limestone; €co Conococheague Formation; €e Elbrook Formation; b Max-Meadows-type breccia. Dark lines are fault traces with T indicating hanging-wall rocks; light lines are contour intervals in feet; dashed lines are streams.

processes of CO_2 outgassing and calcite precipitation account for most of the chemical changes seen along the short segments of flow path that were sampled. Greatest CO_2 losses most often are measured immediately upstream from or at a travertine buildup. The greatest losses of Ca^{2+}, indicating calcite precipitation, are observed at the buildup. Dilution is not a significant factor in determining Ca^{2+} concentration.

The studied streams were selected to examine the hypothesis that input of carbonate-rich water is a critical control on travertine deposition. Some stream compositions are influenced by discrete inputs from springs or tributaries. In other streams, chemical evidence indicates there is diffuse ground-water input through the stream bed. Structural control on the localization of this input is apparent in streams that cross known faults. From our examination of the chemical evolution of the water of these streams, we conclude that the input of carbonate-rich water is essential to the formation of travertine.

Our resulting genetic model for travertine deposits requires input of carbonate-rich ground water to the stream. Faults and fractures control the upward migration of that ground water. Outgassing of CO_2 is driven by chemical gradients and hydrological agitation. The greatest loss of CO_2 from solution precedes the greatest Ca^{2+} mass transfer. Calcite precipitation is localized at the waterfalls. Travertine buildups grow by a self-perpetuating process. Although our field experience is restricted to Virginia, we suspect that the hypothesis proposed here could be adapted to other areas of extensive travertine-marl deposition.

REFERENCES

Gary, M., McAfee, R., Jr., and Wolf, C. L., eds., 1972, Glossary of geology: Washington, D.C., American Geological Institute, 805 p.

Herman, J. S., and Hubbard, D. A., Jr., 1990, A comparative study of travertine-marl depositing streams in Virginia, in Herman, J. S., and Hubbard, D. A.,Jr., eds., Travertine-Marl: Stream Deposits in Virginia. Virginia Division of Mineral Resources Publication 101, p. 43-64.

Herman, J. S., and Lorah, M. M., 1987, CO_2 outgassing and calcite precipitation in Falling Spring Creek, Virginia, U.S.A.: Chemical Geology, v. 62, p. 251-262.

Hoffer-French, K. J., and Herman, J. S., 1989, Evaluation of hydrological and biological influences on CO_2 fluxes from a karst stream: Journal of Hydrology, v. 108, p. 189-212.

Hubbard, D. A., Jr., 1985, Annotated bibliography of the Valley and Ridge travertine-marl deposits of Virginia: Virginia Division of Mineral Resources, Virginia Minerals, v. 31, n. 1, p. 9-12.

Hubbard, D. A., Jr., Giannini, W. F., and Lorah, M. M., 1985, Travertine-marl deposits of the Valley and Ridge province of Virginia-a preliminary report: Virginia Division of Mineral Resources, Virginia Minerals, v. 31, n. 1, p. 1-8.

Hubbard, D. A., Jr., and Herman, J. S., 1990, Overview of travertine-marl volume, in Herman, J. S., and Hubbard, D. A., Jr., eds., Travertine-Marl: Stream Deposits in Virginia. Virginia Division of Mineral Resources Publication 101, p. 1-4.

Kirby, C. S., and Rimstidt, J. D., 1990, The geology and geochemistry of the Falls Hollow travertine deposit, in Herman, J. S., and Hubbard, D. A., Jr., eds., Travertine-Marl: Stream Deposits in Virginia. Virginia Division of Mineral Resources Publication 101, p. 33-42.

Lorah, M. M., and Herman, J. S., 1988, The chemical evolution of a travertine-depositing stream: geochemical processes and mass transfer reactions: Water Resources Research, v. 24, p. 1541-1552.

White, W. B., 1988, Geomorphology and hydrology of karst terrains: New York, New York, Oxford University Press, 464 p.

KARST REGIONS OF THE SOUTHEASTERN UNITED STATES

P. E. LAMOREAUX
P.E. LaMoreaux & Associates
P.O. Box 2310
Tuscaloosa, AL 35403
USA

and

H. E. LEGRAND
Consulting Hydrogeologist
331 Yadkin Drive
Raleigh, NC 27609
USA

ABSTRACT

The Coastal Plain that characterizes much of the eastern and southern margins of the United States contains limestones of Tertiary and Cretaceous ages that have karst features. These limestone are interbedded between gently coastward dipping beds of sands and clays. The outcropping parts of the limestone formations are exposed to many conventional karst processes; yet, the low-lying topographic feature of the total region provides somewhat subdued karst topographic features. The Tertiary limestone formations that underlie Florida and parts of Georgia, South Carolina, North Carolina, and Alabama represent significant and productive aquifers. In these outcrop areas a thin layer of sand or clay covers the limestone; coastward, or down dip, the limestones are more deeply covered and contain artesian water. Deeper coastward parts of the limestone commonly contain brackish water. Relatively soft impermeable chalk and marl characterize the Cooper Marl in South Carolina. The Selma Chalk in Alabama is a massive compact chalk that has a thin zone of karstification at its exposed upper surface. Outcrop areas of these formations are commonly flat or gently rolling without typical karst features. The Edwards Limestone in Texas crops out in a broad plateau and represents a productive aquifer. It is a bare rock plateau that is elevated above the true Coastal Plain. The downdip movement of water is blocked by a fault zone, resulting in large springs discharging along the fault. A wide range of environmental problems have developed in the karst formations of the region. However, except for the vulnerability of the Edwards Limestone to be contaminated, most of the other karst areas are at least partly protected from surface contamination by a cover of less permeable sands and clays. In comparison to many complex structural karst regions of the world, the karst setting of the Atlantic and Gulf Coastal Plains represents a low-lying and gently dipping homoclinal Coastward-dipping plain. The general karst processes prevail, but many of the conventional karst land features are subdued or uncommon in much of the region.

International Contributions to Hydrogeology, Vol. 13 (1992)
© Verlag Heinz Heise, Hannover, FRG

INTRODUCTION

The Atlantic and Gulf Coastal Plain contains carbonate rocks that are interbedded with sand and clay formations in a general coastward-dipping monoclinal system. The carbonate rocks and their more predominant sand and clay units are of Cretaceous Age and younger. Altitudes range from about 200 meters near the inner margin of the Coastal Plain to sea level near the coasts. The topography is generally that of a rolling plain with low hills and subdued escarpments. The major streams flow coastward. Some small streams flowing on the limestone formations have gaining or losing characteristics according to the degree of karstification. In most of the region the climate is temperate and humid, although the Edwards Limestone in southcentral Texas is exposed to semiarid conditions.

For descriptive purposes the carbonate rocks and their karstification are divided into the following categories:

Cretaceous Limestone
- Permeable rocks--Edwards Limestone
- Relatively impermeable rocks--Selma Chalk

Tertiary Limestone
- Permeable rocks--Floridian Aquifer and equivalent in Georgia, Alabama, South Carolina, and North Carolina
- Relatively impermeable rocks--Cooper Marl

Quaternary Limestone
- Permeable rocks--Biscayne Aquifer

A description of each limestone unit and region is included in this report. Also included is a discussion of the degree of karstification and comparative karst features.

Edwards Plateau Karst

In central west Texas a large expanse of the Edwards Limestone, of Cretaceous age, forms a broad plateau. Reaching as much as 800 meters above sea level and not a part of the predominant lower-lying Coastal Plain, the Edwards Limestone lies within the monoclinal coastward-dipping rock system. Bare limestone is broadly exposed to moderate amounts of precipitation in its eastward outcrop area, but the western part is chiefly an arid grassland. The high permeability results from abundant fractures and from assorted shallow dolines, and collapse sinks.

The Edwards is a highly productive aquifer, providing water to numerous cities, including the total supply for San Antonio. Large springs also occur, especially along the Balcones Fault Zone. The Balcones Fault is represented by a downfaulted coastward block that places relatively impermeable beds in the path or coastward-moving Edwards water. Downdip and coastward of the Balcones Fault the water in the Edwards Limestone is essentially stagnant and saline.

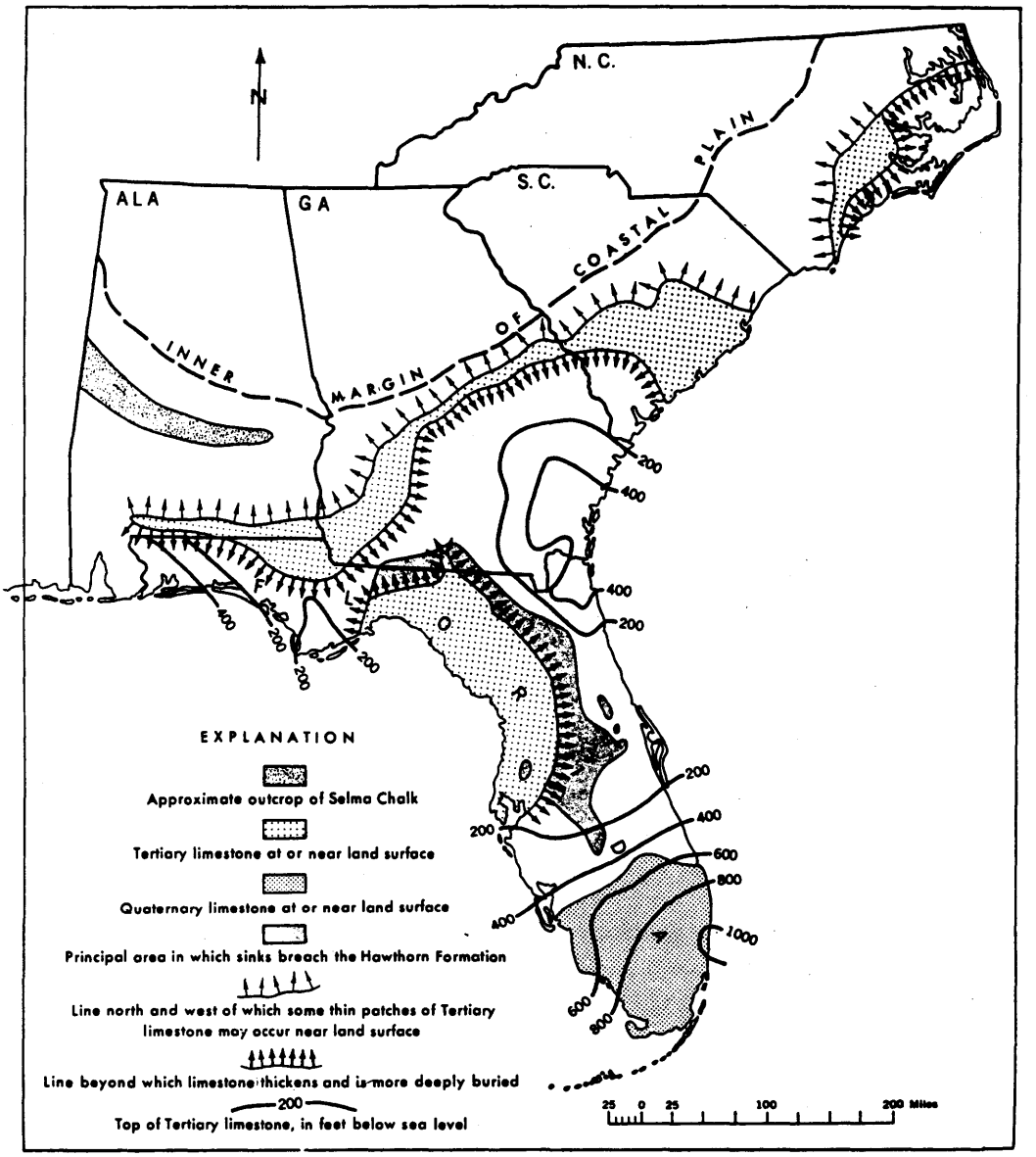

Figure 1. Map showing outcrop areas of Quaternary, Tertiary, and Cretaceous limestone. Contours show top of Tertiary limestone in the subsurface (Stringfield and LeGrand, 1966, p. 4).

The Edwards Limestone outcrop region may be characterized as a type of plateau karst, having sinks and caverns. However, parts of the plateau are deeply dissected with locally rolling or mountainous areas. Some of the deep dissected areas are sources of springs yielding perennial streams. The high permeability of the limestone and its broad exposure result in a potential for contamination of water supplies if protective measures are not taken. The U.S. Environmental Protection Agency has designated the Edwards as a "Sole Source Aquifer," requiring a high level of protection against water contamination.

The Selma Chalk

Forming a crescent-shaped outcrop belt in central Alabama and extending into northeastern Mississippi is chalk of the Selma Group. The Selma is composed chiefly of relatively impervious chalk and marl. The area is represented mostly by a low, nearly flat plain with residual soils being very thin. In some areas the soil is eroded away and the white chalk is exposed (Monroe, 1941, p. 32). Most streams that originate in the chalk belt are intermittent as a result of high evapotranspiration on the impervious chalk. Springs are absent and wells are not common or productive.

Sinkholes and pronounced karst features are present only in the upper few feet of the exposed chalk. In a sense, however, the remainder of the chalk is relatively impervious and may be considered as an impervious karst surface plain.

Permeable Limestone of Tertiary Age (Floridan Aquifer)

Cropping out in a broad belt extending from western Florida across southeastern Alabama and Georgia and northward into South Carolina and North Carolina is a belt of low-lying limestone of Tertiary Age (Figure 1). The limestone and overlying beds dip gently under the Atlantic and Gulf Coastal Plain, where they form a part of the subsea Coastal Plain. The limestone tends to thicken downdip.

On the nearly flat interstream areas the limestone is generally concealed by thin sand and clay deposits of younger material or by residuum from dissolution of the impure carbonates. Surface streams are scarce only in north and central Florida. Shallow sinks (some of which contain lakes) are common over large areas where the cover of overlying material is less than 25 meters. Positive karst elements, such as mogotes, are absent or concealed below overlying materials. A few escarpments having moderate topographic relief occur along lines where overlying insoluble materials are too thick for karst circulation to have optimum potential (Figure 2) (Herrick and LeGrand, 1964).

The permeability of the limestones range from poor in some marls to extremely good in some formations. Despite the wide range in permeability, water moves en masse throughout most of the limestones; to a great extent some dissolution has occurred almost throughout the rocks so that the permeability tends to be more evenly distributed than in many limestones of the world.

The generally subdued topography and the nearly even distribution of more than 100 cm of rain each year keep the water table and other ground-water levels

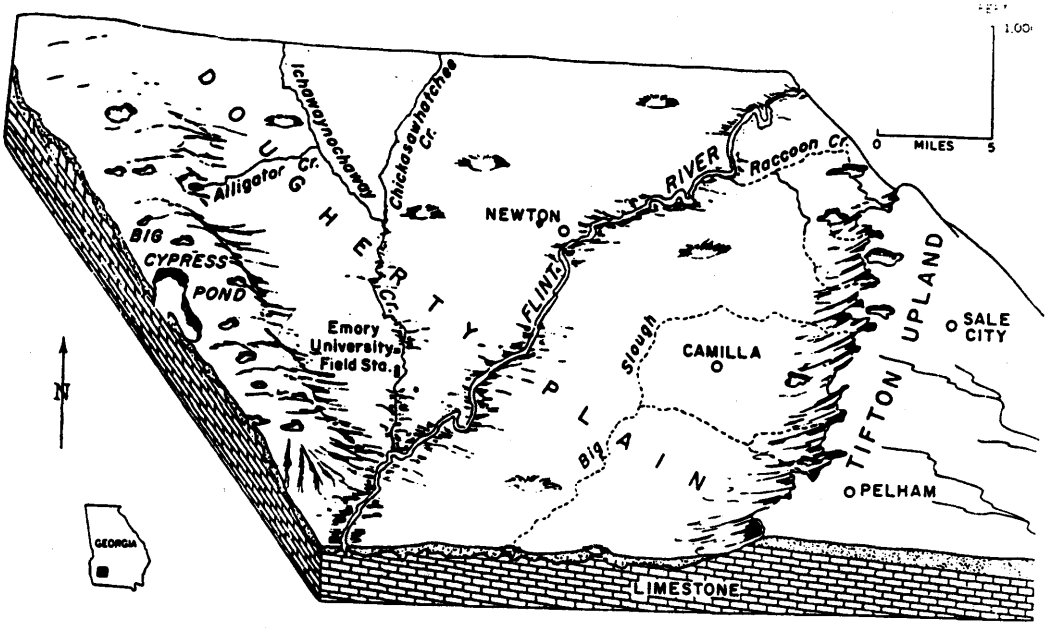

Figure 2. Diagrammatic sketch of Flint River valley, Baker, and Mitchell Counties, GA. Clay beneath the Tifton Upland belongs to the Hawthorn Formation and that beneath the Dougherty Plain represents downslumped masses of the Hawthorn as well as insoluble residue of former limestone beds (Herrick and LeGrand, 1964).

near land surface in most of the region. Where confined, water in the homoclinal artesian system has an overall coastward movement; however, local circuitous flow paths are directed to specific discharge areas. A limit to downdip and coastward movement of water beneath overlying clays and sands is caused by deeper burial and dense saltier water in the deeper and coastward parts. Considerable discharge of limestone water is by diffuse seepage into and through overlying beds. The discharge of springs ranges from a few liters per minute to more than 28 m^3/s (Stringfield, 1966). Many of the large springs are in the outcrop area in central Florida. Almost all of the springs yield clear water continuously, chiefly because of the prevalent sandy cover that allows filtering of water into the limestone.

The aquifer system, commonly referred to as the Floridan Aquifer, is one of the most productive sources of ground water in the United States. It is the main source of water supply in southern Georgia and north and central Florida; to a lesser extent, the aquifer is productive in South Carolina, North Carolina, and Alabama. In spite of the large pumpage of water from municipal and industrial wells, flowing artesian wells are still common in some coastal parts of Georgia and Florida. The aquifer system contains a typical calcium bicarbonate water in both the outcrop areas in the upper parts of the confined regions. Deep parts of the limestone contain salty water, as well as shallow parts in some coastal areas. The confined (artesian) parts of the aquifer are protected from surface contamination. Problems of contamination from surface sources occur where the limestone is exposed.

The Cooper Marl

A part of the Tertiary Limestone outcrop area in South Carolina is represented by the Cooper Marl. It is a granular, soft, impermeable marl on and in which no karst features occur. The permeability is so small that an unlined tunnel in the marl has been used to conduct the water supply of Charleston many miles from a surface reservoir to the city (Stringfield, 1966, p. 53). The absence of karstification is partly due to the absence of fractures in the granular marl and to the low topographic relief.

The Biscayne Aquifer

A Quaternary limestone system in southern Florida, referred to as the Biscayne Aquifer, is represented by a low flat plain slightly above sea level. The limestone has a coquina texture and is mantled in most places by a thin layer of quartz sand. It has pervasively a very high permeability because of the original character and also because of extensive dissolution.

Since the Biscayne Aquifer is very permeable and very vulnerable to contamination and is the sole source of drinking water for more than 3 million people in southeast Florida, the U.S. Environmental Protection Agency has designated it as a "sole-source aquifer," requiring special protection. The water table is near land surface. In spite of the high permeability, the limestone area is not characterized as a mature karst setting. Large pronounced sinks and other surface karst features are absent.

PALEOHYDROLOGY

Several erosional unconformities within the limestone rocks indicate that the rocks were elevated above sea level at several times and were subjected to karstification and to the development of permeability by circulation of water and solution within the system. Thus much of the solutional network was developed prior to middle Miocene time when a blanket of relatively impermeable clays covered the limestone and has since preserved it in an artesian system. The groundwater circulation system has been reactivated since the withdrawal of the middle Miocene sea but more particularly since the withdrawal of the highest stage of the Pleistocene sea. Some solution is occurring in the freshwater part of the artesian system now, but its contribution to the development of permeability is less than that before middle Eocene time (LeGrand and Stringfield, 1971, p. 1292).

KEY DISTINCTIVE KARST CHARACTERISTICS OF THE REGION

Some key karst principles apply almost universally in carbonate rock terrains. Yet, variations in karst processes and ranges in hydrogeologic settings result in a great range of characteristics that invite comparison of some karst conditions (LeGrand and LaMoreaux, 1975, p. 17). Listed below are certain key features of the Coastal Plain karst, especially as applied to human habitat. The main discussion is solely on the true low lying Coastal Plain, but a few additional comments are directed to the Edwards Plateau, which is elevated above the Coastal Plain.

1. The prevailing cover of residual soils and younger deposits of sand and clay causes some karst processes to be less obvious than in bare karst regions.

2. Local land subsidence as sinks commonly is slow and progressive because of gradual movement of sands and clays into solutional openings near the top of the underlying limestone. However, sudden collapse sinks often occur, especially in central Florida, where plumping of wells alters the natural karst water-level fluctuations.

3. In contrast to many karst regions, there is very little undesirable or uninhabitable land because topographic relief is low, generally the sinks are subdued and have gentle slopes, and ample water supplies are available almost everywhere.

4. The water table or artesian water level is near land surface in much of the region. Lakes are locally common. Caverns, to the extent that they occur, almost everywhere are below the water table.

5. In typical karst regions where dissolution has increased the permeability, some of the surface streams go underground. This condition exists in parts of central Florida; the scarcity of surface streams causes some problems for waste disposal in the region.

6. A wide range in permeability occurs overall, but in each limestone formation the permeability is more evenly distributed than that in many karst areas. The Cooper Marl and Selma Chalk are relatively impermeable, not having had any

significant solutional development of permeability. The Quaternary Biscayne Aquifer has had its moderate degree of primary permeability further increased through circulation and solution of near-surface water. Most of the Tertiary limestones have moderately high permeability caused by pervasive circulation and dissolution throughout the limestone in the outcrop areas and in the shallow confined areas.

7. In many karst regions of the world the permeability is so great that recharge water passes through the system so readily that ground-water storage for human use is not at an optimum level. In contrast, the Tertiary limestone region has moderately high and overall excellent storage capacity; the overlying sand and clay blanket tends to moderate the recharge and circulation of water, as well as to prevent serious contamination in most areas. As a result of these factors, the Tertiary limestones of the Coastal Plain represent some of the best karst aquifers of the world.

Being an inland and more elevated extension of a part of the Coastal Plain in Texas, the Edwards has some characteristics of both the true Coastal Plain karst and of the European karsts. The thin or scarce soils are due to low precipitation or erratic distribution of precipitation, which retards weathering and aids erosion. The elevated plateau has exposed beds of rather even distribution of permeability, resulting in a general even distribution of dissolution, so that rugged topography due to differential solution erosion has not been extensive. Mature and even late youthful stages of karst topography have not yet fully developed.

REFERENCES

Herrick, S.M. and LeGrand, H.E., 1964, Solution subsidence of a limestone terrain in southwest Georgia: Internat. Assoc. Sci. Hydrogeology Bull. v.9, no. 2, p. 25-36.

LeGrand, H.E. and LaMoreaux, P.W., 1975, Hydrogeology and Hydrology of karst, in Hydrogeology of Karstic Terrains: Internat. Assoc. Hydrogeologists, Paris, France, p. 9-19.

LeGrand, H.E. and Stringfield, V.T., 1971, Development and distribution of permeability in carbonate aquifers: Water Resources Research, v. 7, no. 5, p. 1284-1294.

Monroe, W.H., 1941, Notes on deposits of Selma and Ripley age in Alabama: Geol. Survey Ala., Bull. 49, 44 p.

Stringfield, V.T., 1966, Artesian water in the Tertiary limestone in the southeastern states: U.S. Geological Survey Prof. Paper 517, 226 p.

Stringfield, V.T. and LeGrand, H.E., 1966, Hydrology of limestone terrains in the Coastal Plain of the southeastern states: Geol: Soc. America Special Paper 96, 46 p.

LOCALIZATION AND SEASONAL VARIATION OF RECHARGE IN A COVERED KARST AQUIFER SYSTEM, FLORIDA, USA

MARK STEWART
Geology Department
University of South Florida
Tampa, Florida 33620-5200
USA

and

JOHN PARKER
Southwest Florida Water Management District
2379 Broad Street
Brooksville, Florida 34609-6899
USA

ABSTRACT

West-central Florida is a covered karst terrane. Early Tertiary limestones are overlain by 5-30 m of unconsolidated sands, silts, and clays. There is little or no surface drainage, and 0.15-0.60 m/a of recharge annually moves from the unconfined water-table aquifer in the unconsolidated sediments to the underlying, semi-confined, karstic Floridan Aquifer. Downward movement of recharge waters is highly localized and seasonally variable as a result of the effects of karst processes on the stratigraphy of the sediments overlying the limestones.

The limestone has significant insoluble residue and weathers to sandy clay and clayey sand, forming a semi-confining layer above the limestone. Poorly-sorted marine sediments and well-sorted eolian sands overlie the semi-confining clays. Downward movement of these unconsolidated sediments into karst cavities in the limestone leads to a "raveled" stratigraphy. The result is a complex, dimpled topography for the surface of the clay layer. Raveling removes the clay layer above active cavities and creates columns of clean dune sands which often extend downward into the limestone. The location of most of the columns is not apparent from surface topography. The sand columns form preferential flow paths for vertical ground-water flow. They are often a few meters or less in diameter and constitute only a few percent of the total surface area, but conduct most of the recharge from the surficial aquifer to the Floridan Aquifer. Recharging ground-water moves laterally in the surficial aquifer to sand columns then vertically downward to the limestone. The result is highly localized recharge. Rates of recharge are dependent principally on the size, frequency, and hydraulic conductivity of the sand columns and water-table elevations. When water-table levels are high, lateral flow is in the higher permeability sands. When water-table levels fall below the clean sand/silty, clayey sand contact, lateral flow to the columns is impeded, and recharge rates decrease.

In west-central Florida, ground-penetrating radar has been used successfully to map the top of the semi-confining clay layer. Low areas on the clay surface represent potential sites for localized recharge. During times of high

International Contributions to Hydrogeology, Vol. 13 (1992)
© Verlag Heinz Heise, Hannover, FRG

recharge, electrical streaming potentials are generated, creating strong self-potential (SP) anomalies. Mapping SP anomalies allows rapid determination of sites of localized recharge for ground-water contamination assessments. Sand columns are also potential sites of cover-collapse sinkholes.

INTRODUCTION

Hydrogeologic Setting

West-central Florida (Fig. 1) is a covered- or mantled-karst terrane. In covered-karst terranes, a mantle or cover of unconsolidated sediments overlies the limestone, partially obscuring the underlying karst features (Sweeting, 1973). In west-central Florida, an average of 5-30 m of clayey, silty, sandy sediments of Miocene to Recent age cover the Eocene to Miocene limestone and dolostone of the Floridan Aquifer (Sinclair et al., 1985). Surface drainage in the region has low densities and is poorly integrated. Topographic relief is low, and the surficial eolian sands have high infiltration capacities. The result is high ground-water recharge rates to the Floridan Aquifer of 0.15-0.60 m/a (Ryder, 1984). Because of the low surface drainage densities, most recharge to the surficial aquifer system moves downward into the Floridan Aquifer.

Karst features such as vertical shafts and caves are known in the Tertiary limestone, but are not well-expressed at the surface. Based on drillers' reports, the highly weathered surface of the Tertiary limestone can have local relief of as much as 100 m. However, this bedrock relief is greatly subdued and masked by the karst cover. Karst processes have affected the stratigraphy and lateral variability of the unconsolidated sediments overlying the limestone. The lower-most unconsolidated unit is a sandy clay, which is a weathering residuum of the limestone. Karst processes have perforated this clay layer, allowing the more permeable surficial sands to come in contact with the limestones of the Floridan Aquifer. This lateral variability of vertical stratigraphy creates highly localized recharge to the Floridan Aquifer. The lateral variability is on a scale of 1-10 m. Therefore, this phenomenon of localized recharge, resulting from covered-karst processes, is important to site-scale ground-water contamination assessments. In this study, a 2-ha site near Tampa, Florida, is used as an example. However, similar geologic conditions occur over an area of about 30,000 km^2 in west-central Florida.

General Geology of West-Central Florida

The upper few hundred meters of the carbonate Florida Platform contains a major regional aquifer system, the Floridan Aquifer, comprised of Eocene to Miocene limestone and dolostone. The maximum fresh-water-saturated thickness of the Floridan is about 700 m, and the average thickness in west-central Florida is about 300-400 m (Miller, 1984). The Eocene and Oligocene carbonate rocks are relatively pure. However, the Miocene carbonates of the Tampa member of the Hawthorn Group (Scott, 1988) are more sandy and clayey. The weathering residuum of these Miocene carbonate units and the clayey unconsolidated units of the Miocene Hawthorn Group form an upper semiconfining unit for the Floridan Aquifer. Plio-Pleistocene, marine, silty, clayey sands and Pleistocene and Recent eolian sands overlie the Miocene units. The very well sorted, fine to very fine

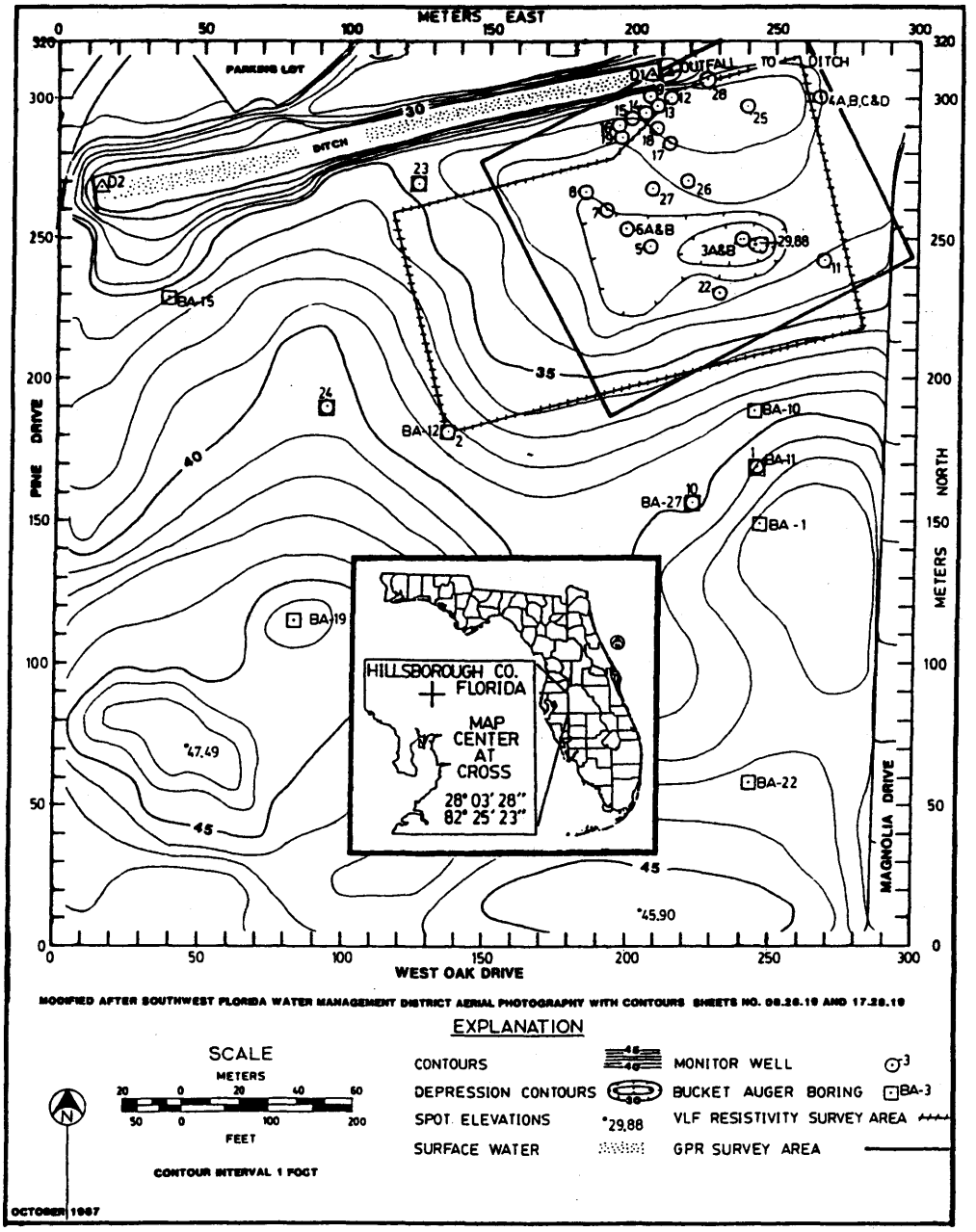

Figure 1. Study site.

eolian sands are the surficial geologic unit over nearly all of west-central Florida. In general, the mean grain size and degree of sorting of the unconsolidated units both decrease with depth.

The land surface of west-central Florida has low local relief (1-10 m). Surface drainage is poorly integrated, and broad, shallow, closed depressions are common features of the landscape. Several allochthonous streams which originate in a region of low recharge in central Florida cross west-central Florida, but most drainage is internal. Because of the low relief, poorly-integrated surface drainage, and the surficial blanket of eolian sands, ground-water recharge rates are high, 0.15-0.60 m/a (Ryder, 1984). The large hydraulic conductivity contrast between the surficial aquifer system and the Floridan creates a "prairie profile" flow system (Meyboom, 1966), where most of the land surface is a recharge area for the Floridan. Water-table elevations are higher than the potentiometric surface of the Floridan over most of west-central Florida, except near the coast and along the lower valleys of the allochthonous streams.

The karst cover obscures most major karst features. West-central Florida does exhibit classical fluvio-karst features (Sweeting, 1973) such as steep-walled closed depressions, sinking streams, large springs, and caves. However, the karst cover, especially the dune sands, has smoothed the landscape and subdued all but the largest features. Most wells encounter cavities during the drilling, not uncommonly several meters in height. The depth to the top of the limestone can vary 30-50 m over horizontal distances of 1-10 m, indicating the highly weathered, karstic nature of the upper surface of the Tertiary limestone.

The insoluble residues in principally the Miocene limestone form a stiff clay cap over the rock (Carr and Alverson, 1959). As observed in excavations and quarries, the clay cap bridges and fills many smaller cavities in the limestone, but collapse of the clay into underlying cavities in the limestone is common (Sinclair et al., 1985). Where the clay layer has been breached by subsidence or collapse, the overlying sandy materials can move downward into cavities in the limestone. Large cavities can form in the unconsolidated materials and create cover-collapse sinkholes when they ravel their way to the surface. This process can be gradual, episodic, or even catastrophic (Sinclair et al., 1985). The results of this subsidence/raveling process are a discontinuous semi-confining layer over the Floridan Aquifer and the vertical sand columns connecting the surficial and Floridan aquifer systems.

METHODS

In order to study the effects of karst processes on local recharge to the Floridan Aquifer, a 2-ha study site was selected near Tampa, Florida (Fig. 1). The site is within an active cover-collapse sinkhole region. The 260-ha University of South Florida campus, within which the site lies, has experienced over 20 small cover-collapse sinkholes since 1960. The largest was induced during the drilling of a water supply well, and it was about 3 m across and 5 m deep with vertical walls. Three small sinkhole collapses have occurred on the study site since 1982, two natural and one induced by drilling a test well.

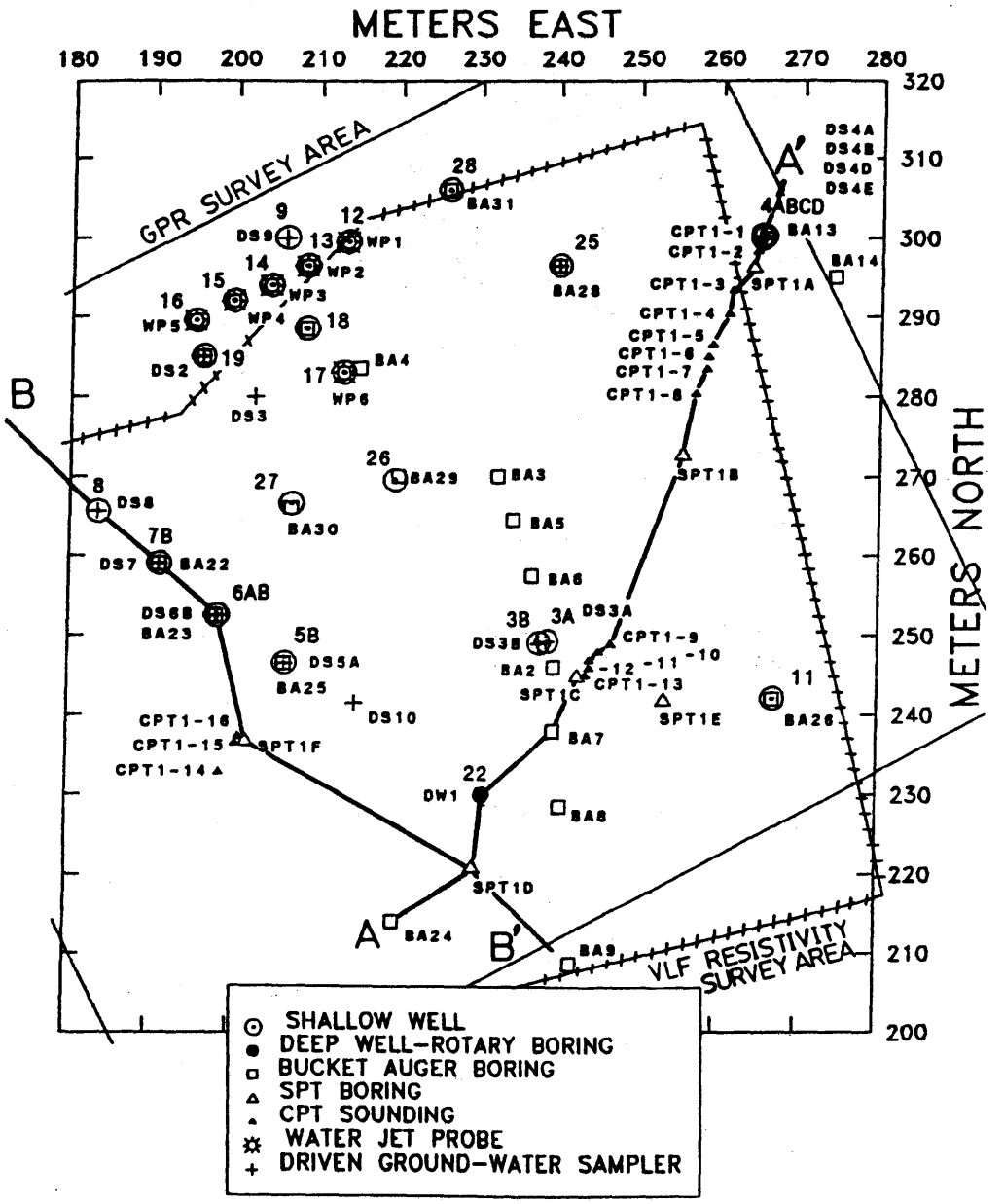

Figure 2. Locations of sampling sites and geologic sections A-A′ and B-B′.

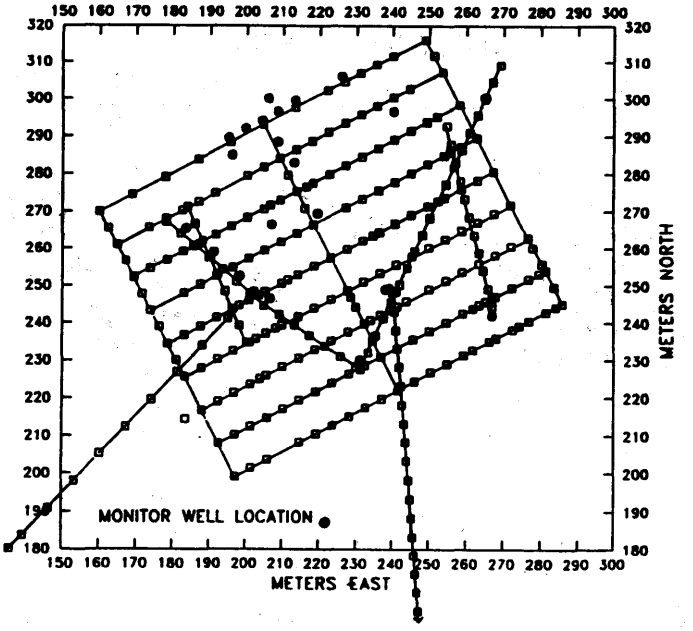

Figure 3. Locations of GPR survey lines. Elevations of principal reflectors were obtained at sites indicated by open squares.

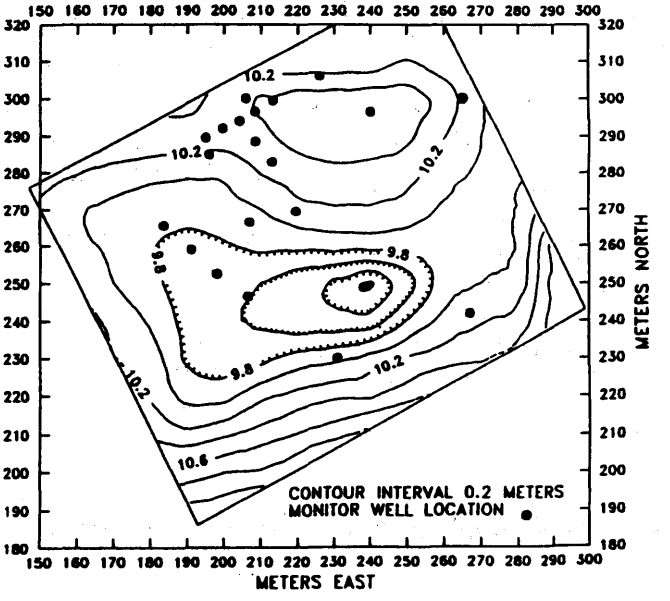

Figure 4. Contour map of surface elevations within GPR survey area. Contour interval is 0.2 m.

An existing topographic map of the USF campus, including the site, with a one-foot (0.31 m) contour interval was used for basic elevation control. Local elevations were surveyed for water levels and other spot elevations to an accuracy of 0.003 m. A 3-inch (7.62 cm) hand auger was used to sample the unconsolidated materials to a depth of 8 m. Sediment samples were obtained from all major units of the karst cover. Grain-size analysis was completed on 11 representative samples. A concurrent study of the use of cone-penetrometer testing (CPT) to evaluate potential cover-collapse sinkholes (Bloomberg et al., 1986) provided both CPT data and information from standard penetration tests (SPT), split-spoon sampling, and rotary borings. The depth to the top of the cohesive clay overlying the limestone was determined by jetting a 0.75-inch (1.91 cm) pipe to refusal and noting the depth (Fig. 2).

Ground-penetrating radar (GPR) surveys were used to map the shallow stratigraphy of the unconsolidated units (Fig 3). Reflectors noted on the radar records were identified and calibrated using soil auger, rotary boring, CPT, SPT, and elevation survey data. Self-potential (SP) surveys were used to detect significant vertical flows of ground water (Ogilvy, 1967).

Ground-water levels were measured in small-diameter (0.5 inch, 1.3 cm), PVC piezometers (Fig. 2). These were installed by driving a small-diameter water sampler with a weight, then placing the piezometers in the open hole after the samplers were removed. The piezometers are slotted at the bottom. Hydraulic conductivities of the sandier unconsolidated units were estimated from grain-size analyses (Powers, 1981).

RESULTS

The detailed surface topography of the site (Fig. 4) shows only one closed surface depression, approximately 80 by 40 m in size, with local relief of about 1 m. In contrast, the surface of the top of the clay semiconfining unit shows a very convoluted surface (Fig. 4). There are eighteen closed depressions within the 12,000 m^2 of the radar survey, or one depression for every 26-by-26-m block. About half of the depressions are contained within larger depressions. The local relief on the clay surface is about 5 m. Most of the smaller depressions are not reflected in the surface topography. This is apparent in the perspective diagrams of land surface and clay topography (Fig. 6).

Cross sections A-A′ and B-B′ (Figs. 2, 7, and 8) show the vertical and horizontal variations in lithology. Unit I is a well sorted, very fine to fine sand. Unit IIA is a silty, very fine to fine sand. Unit IIB is a silty, organic, very fine to fine sand. Unit III is a sandy clay. Unit IV is a soft, chalky, weathered limestone with granules and cobbles of chert and silicified limestone. Unit V is unweathered Miocene Tampa limestone. The sections have been constructed using information from auger borings (BA), rotary drilling (DW), cone-penetrometer tests (CPT), water-jet probes, split-spoon sampling (SPT), and the radar surveys. Note that for the five subsidence/collapse sinkholes shown on sections A-A′ and B-B′ Units III and IV are missing and are replaced by Units I and IIB. The cover-collapse structure at well 4

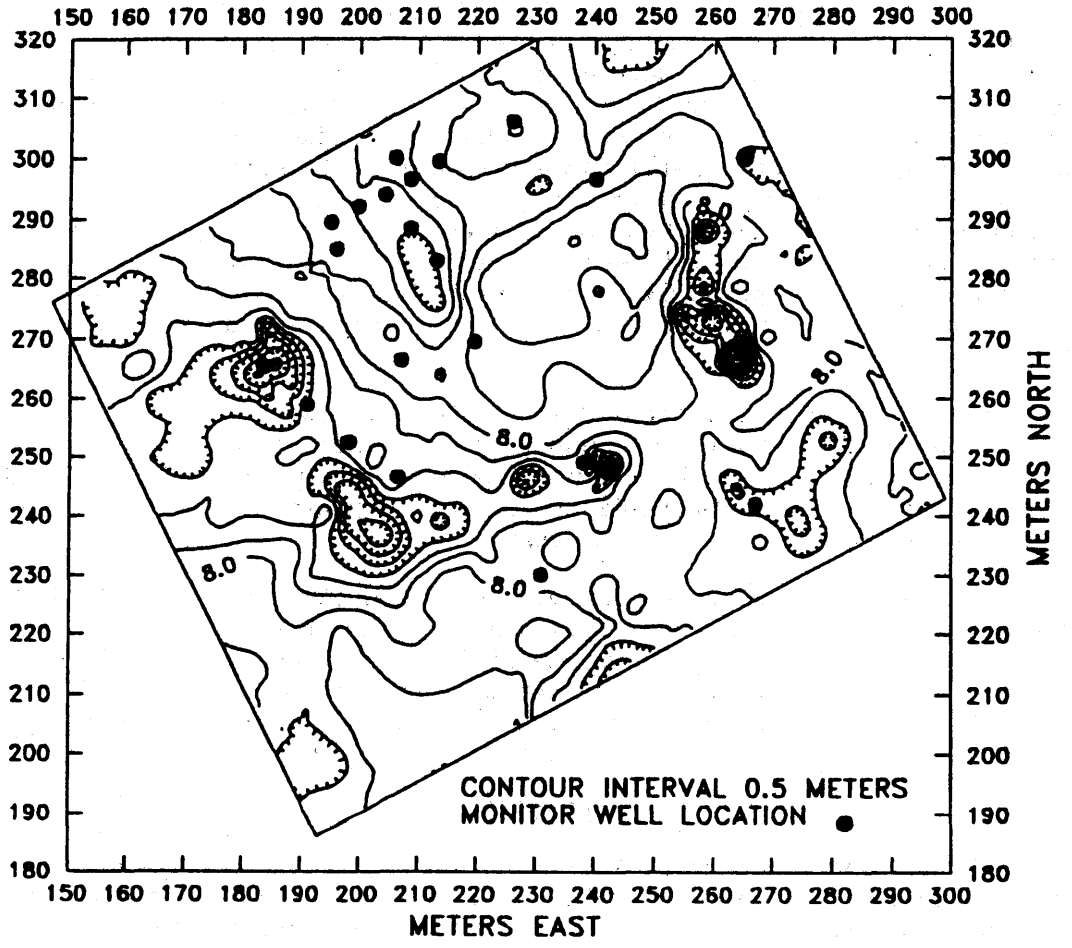

Figure 5. Contour map of the elevation of the top of the sandy clay semiconfining unit. Data are from GPR surveys. Contour interval is 0.5 m.

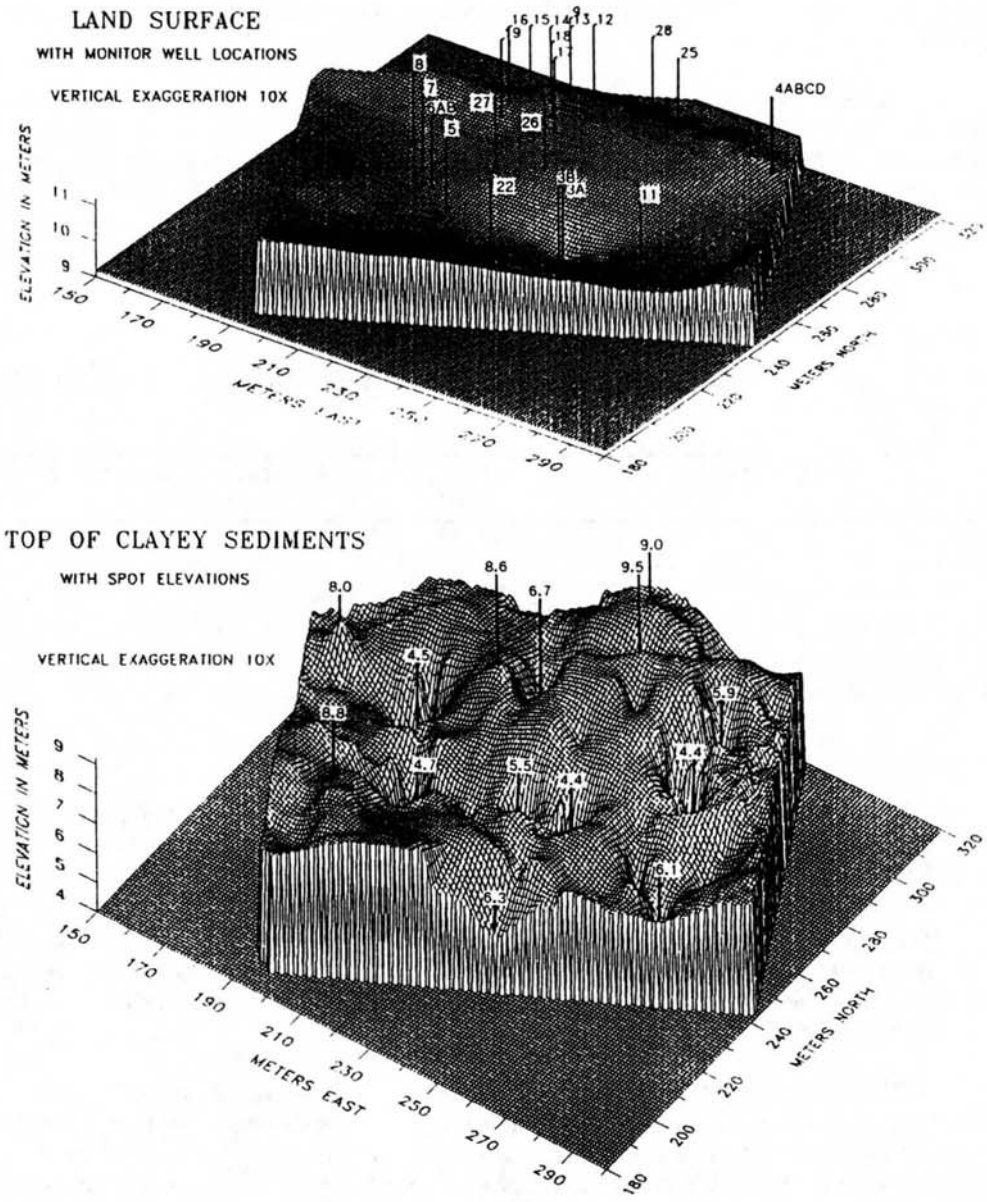

Figure 6. Perspective diagrams of surface topography and elevation of the top of the sandy clay semiconfining unit.

on section A-A' (Fig. 7) has recently been active. The well 4 feature collapsed in 1982 and 1984.

Grain-size analysis was completed for 8 representative samples of the sandy units (I, IIA, IIB). The lowest sand percentage is 94%. The estimated hydraulic conductivity of the samples was determined by Alamri (1985), using the procedure and nomograph from Powers (1981). The results are listed in Table 1. Analysis of three samples of Unit III, the sandy clay, averaged 57% clay, 34% sand, and 9% silt. Sinclair (1974) provides an estimate of 0.002 m/day for the hydraulic conductivity of the same unit from an earlier study in the Tampa area.

Table 1. Hydraulic conductivities of representative samples of the karst cover (from Alamri, 1985)

Lithology	Unit	Hydraulic conductivity (m/day)
Fine sand	I	35
V. fine sand	I/II	10-15
Silty fine sand	IIA	15-20
Silty, clayey sand	IIB	8-10
Sandy clay (from Sinclair, 1974)	III	0.002

Figure 10 is a contour map of water-table elevation for April. April is normally the month with the lowest rainfall, and Figure 10 represents dry-season conditions. As shown by the arrows, there are at least three regions of converging ground-water flow, near wells 6B, 3B, and 4A. At this time of year, water levels in the ditch on the north side of the site (Fig. 1) are higher than the water table, and the ditch recharges the water-table aquifer. Note that the steep gradient created by recharge from the ditch flattens along a SW-NE zone passing through the regions of converging flow.

Well 4 contains four piezometers open to different depths (Fig. 7). Well 4A is open to a column of clean sand (Unit I) filling a cover-collapse feature. Well 4D is in sandy sediments filling a void in the limestone. During periods of high water-table elevations, there is a head difference of about 0.20 m between 4A and 4D, with well 4A having the higher head. In late May and early June, the end of the dry season, the head difference is about 0.05 m. These head differences represent downward (recharge) hydraulic gradients of 0.025 and 0.006, respectively.

A reconnaissance self-potential (SP) survey was completed to detect streaming potentials created by concentrations of vertical ground-water flow (Clasen, 1989). Figure 12 is a contour map of SP anomalies from a 10-by-10-m survey grid. Two large negative anomalies occur at (80,0) and (60,-60). These are the approximate locations of the collapse/subsidence features at well 4A and CPT-12 (Figs. 2 and 7), respectively.

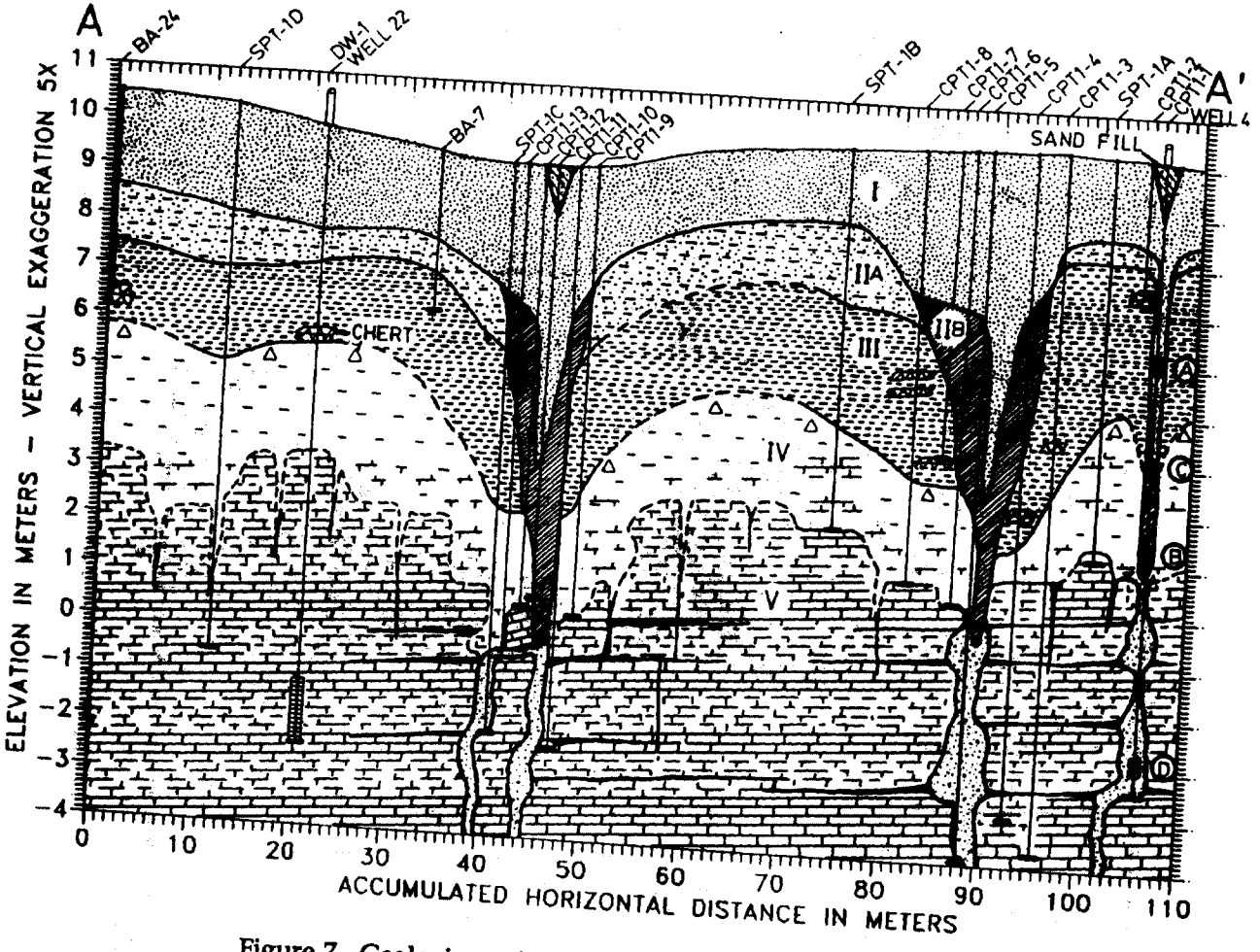

Figure 7. Geologic section A-A'. See Figure 2 for location of section.

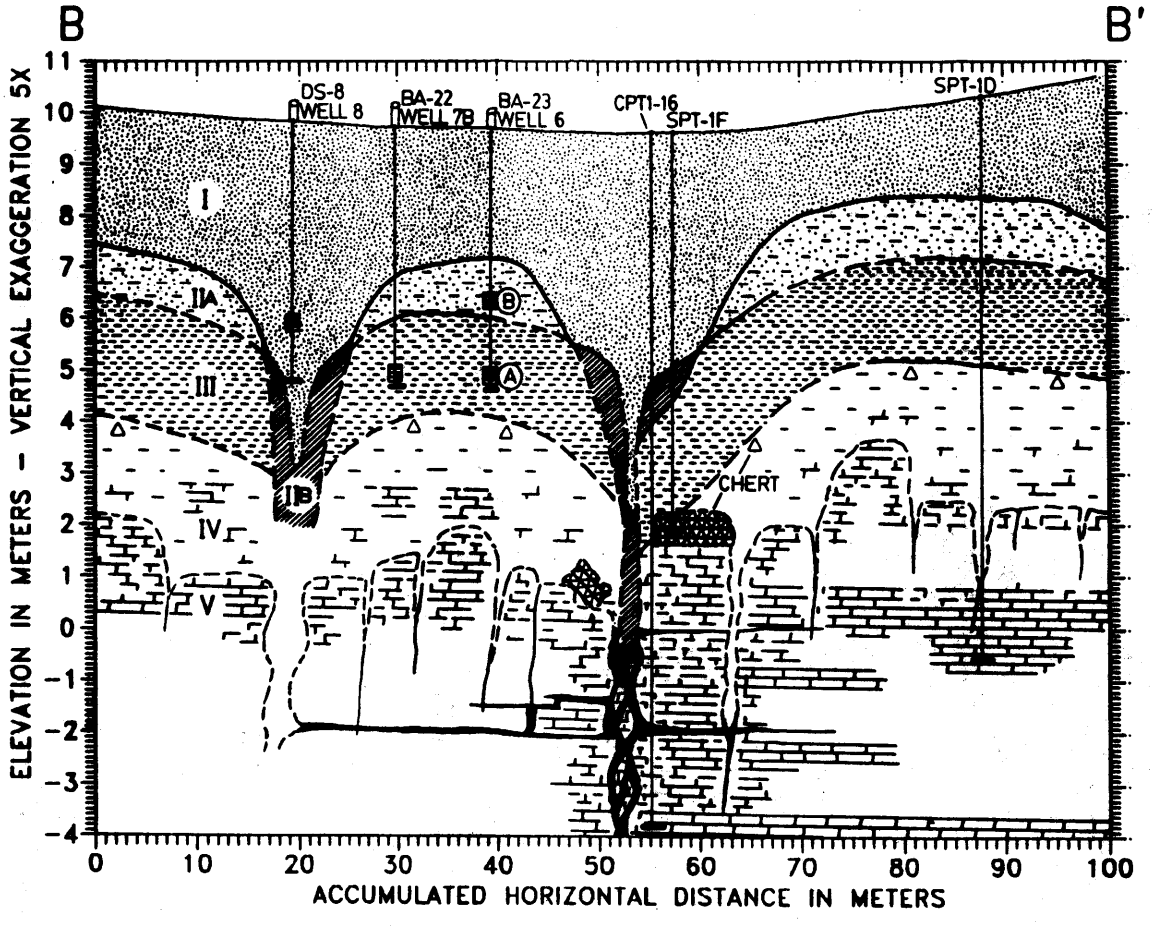

Figure 8. Geologic section B-B'. See Figure 2 for location of section.

DISCUSSION

Karst processes have created numerous cavities within the Tertiary limestone, and a weathered, irregular bedrock surface with a discontinuous clay cap. The clay weathering residuum forms a semiconfining layer for the Floridan Aquifer. However, cover subsidence and collapse have perforated the clay and provided pathways for the overlying sandy materials to move downward into cavities in the limestone. This has created vertical sand columns and a highly convoluted clay surface. In west-central Florida, eolian processes have smoothed the surface topography, so that the locations of the sand columns are often not apparent at the surface.

The sand columns connect the sandy surficial aquifer to the underlying Floridan Aquifer and are very significant hydrologically. For example, the wet-season head difference between the water-table and the potentiometric surface of the Floridan Aquifer on-site is about 0.2 m. If an average hydraulic conductivity of 10 m/day is used for the sand columns (Table 1) and 2×10^{-3} m/day for the clay semiconfining unit (Sinclair, 1974), the rate of vertical flow per square meter is 0.3 m/day for the sand columns and 1×10^{-4} m/day for the clay layer. Clearly, much more water can recharge through the sand columns than through the clay. If an average cross-sectional area of 6 m^2 is assigned to each sand column, each column recharges 1.8 m^3/day to the Floridan during the wet season. If only half of the 18 depressions on Figure 5 are active sand columns, these 9 columns would contribute about 16 m^3/day of recharge to the Floridan, while only about 1 m^3/day would be contributed by leakance through the clay over the 12,000 m^2 site. Clearly karst processes have created very localized recharge to the Floridan.

Evidence that the sand columns are preferential sites for downward movement of ground water is provided by the water-table map (Fig. 10) and the SP anomaly map (Fig. 12). The water-table map shows three areas of converging flow near wells 6B, 3B, and 4A. Flow is converging on the cover subsidence/collapse features at CPT-16 (section B-B', Fig. 8), CPT-12 (section A-A', Fig. 7), and CPT-1 (section A-A', Fig. 7). Since there is no surface discharge at these points, the converging ground water must be moving downward. In covered karst terranes, regions of converging flow lines in the water-table aquifer are areas of localized ground-water recharge.

Flowing ground-water can create streaming potentials if the flow is of sufficient volume (Ogilvy et al., 1969; Bogoslovsky and Ogilvy, 1972). Downward-flowing ground water creates negative SP anomalies (Ogilvy, 1967). SP anomalies are largest in sand-filled columns, and decrease as aperture size increases (Bogoslovsky, 1972), as in karst solutional openings. Two of the three regions of converging ground-water flow (Fig. 10) produce strong, negative, SP anomalies (Fig. 12). This suggests that SP-anomaly surveys may be a suitable method for determining which clay-surface depressions represent active drains.

As noted earlier, the steep water-table gradient created by recharge from a surface-water body on the north side of the site decreases markedly along a NE-SW

zone passing through wells 4A and 3B (Fig. 10). Examination of the clay-surface topography (Fig. 5) shows that this decrease in hydraulic gradient occurs along a NE-SW trend of depressions in the clay surface. As there is no evidence for greatly increased hydraulic conductivity in the SE corner of the site, the reduced gradient must be due to interception of ground-water flowing southeastward from the ditch by vertical drains (sand columns). This suggests that sudden changes in water-table gradients may reveal the locations of cover-collapse features that are acting as drains for the shallow aquifer.

In a non-karstic semiconfined aquifer, recharge to the semiconfined system is a function of the head difference between the water table and the potentiometric surface and the leakance coefficient (K'/m') of the semiconfining layer. However, in the covered-karst system of west-central Florida, two characteristics of the shallow stratigraphy create a pronounced seasonal variation in recharge. First, the average K'/m' value of the cover-collapse features is four orders of magnitude greater than that of the clay semiconfining unit (1.3 and 5 x 10^{-4} per day, respectively). This results in most of the recharge moving through the karst-induced sand columns. Second, the hydraulic conductivity decreases with depth in the water-table aquifer (Fig. 7; Table 1). When water-table elevations are high, lateral flow in the shallow aquifer to the drains includes the higher-permeability sands (Sept. 4, Fig. 13). However, when water-table elevations are below the boundary between Units I and II, the average hydraulic conductivity of the saturated shallow aquifer decreases (July 27, Fig. 13). At the end of the dry season (June 3, Fig. 13), the water-table elevations are below the average elevation of the Unit II/III contact, and lateral flow to the drains is greatly impeded. Examination of Figure 6 shows that flow to the drains becomes increasingly tortuous as water-table elevations fall and shallow ground-water flow follows the thicker sections of Units I and II overlying depressions in the clay layer. This combination of decreasing average hydraulic conductivity and increasingly tortuous flow paths as water-table levels fall in the dry season leads to a more pronounced seasonality of recharge to the semi-confined aquifer than would be expected in a non-karstic system with laterally uniform K'/m' values.

Two pieces of field evidence support the existence of exaggerated seasonal variation in recharge. First, Figure 11 illustrates that a significant downward vertical gradient exists between wells 4A and 4D when water levels are above 6.5 m. When water levels fall below 6.5 m the vertical gradient decreases from about 0.025 to 0.013. This means the volume of water per unit time moving through the sand column is halved. Also, SP measurements during an extended drought in the spring of 1990 indicated that the negative SP anomaly at well 4 had nearly disappeared, again indicating a strong reduction in flow to and down the drain.

The significance of this karst-dominated recharge system to site-scale, ground-water contamination studies is obvious. First, contaminants introduced into the shallow aquifer may follow tortuous flow paths as the greatest ground-water flow volumes will be toward active drains and will follow the thicker sands overlying the depressions and troughs in the clay surface. This complicates the process of locating monitor wells to detect and characterize the contamination. Second, the perforation of the clay layer by sand columns provides a direct hydraulic connection between the water-table and Floridan aquifers. As these sand columns constitute

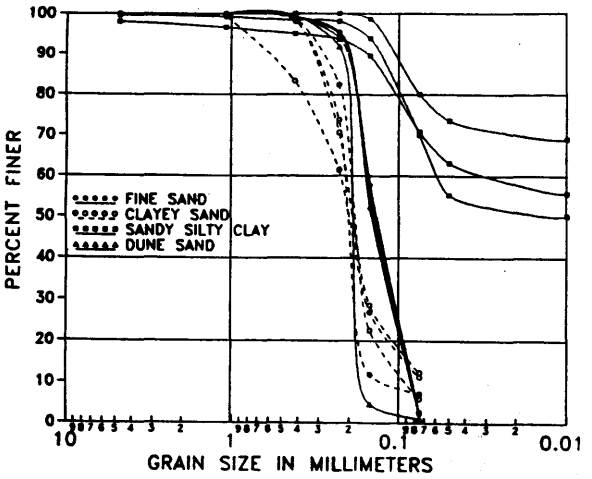

Figure 9. Cumulative percent-finer-than grain size for eleven representative samples of the unconsolidated karst cover.

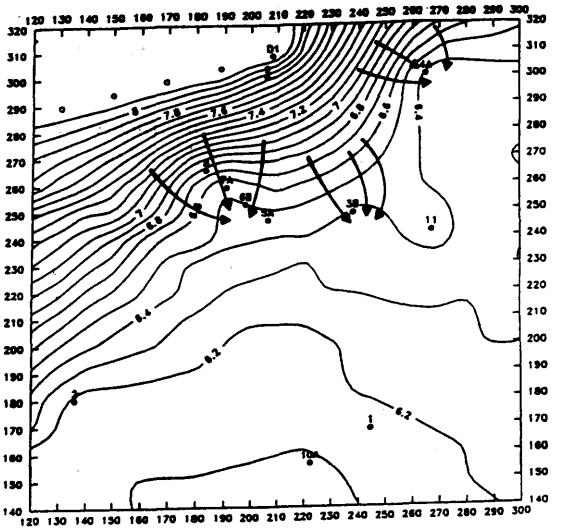

Figure 10. Contour map of the water-table elevation on April 29, 1985. Contour interval is 0.2 m.

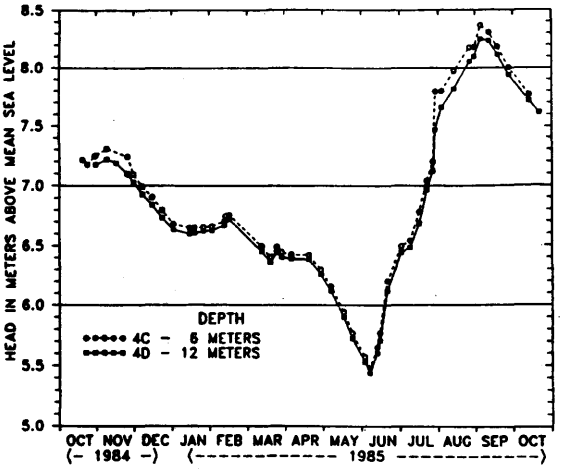

Figure 11. Weekly water-level measurements for monitor wells 4A and 4D. See Figure 7 for location of screened intervals.

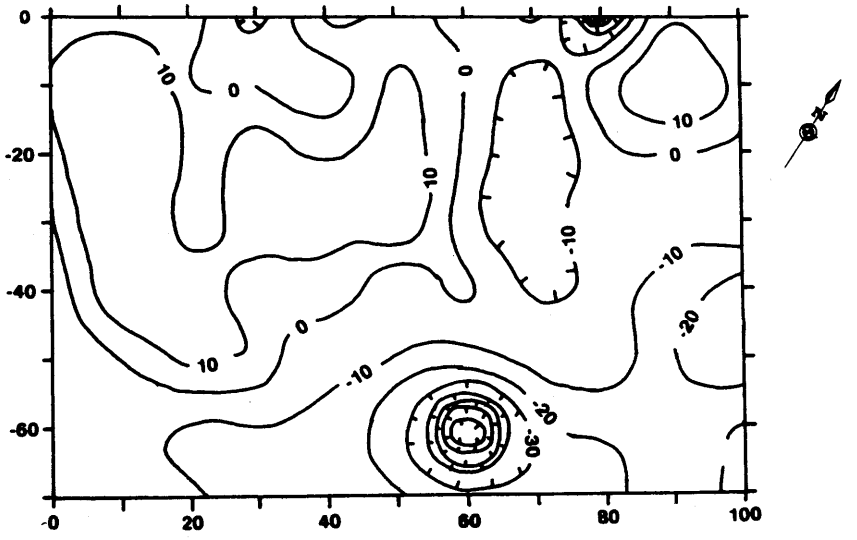

Figure 12. Contour map of SP anomalies. Data were collected on a 10-by-10-m grid. Contour interval is 10 millivolts. (After Clasen, 1989.)

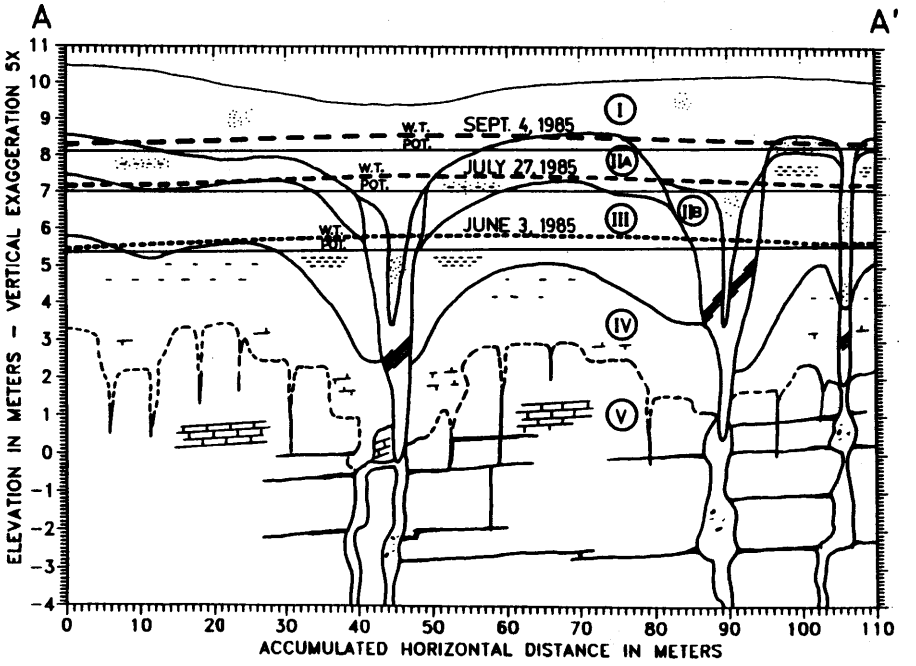

Figure 13. Superposition of water-table and Floridan Aquifer potentiometric surface elevations on geologic section A-A'. See Figure 2 for location of section.

only a small percentage of the total site area (about 1% at the test site), they are unlikely to be discovered by random test borings unless a large number are drilled. Third, the strong seasonal variation in recharge means that monitor wells in the Floridan Aquifer will see contaminant pulses during periods of high water-table elevations and a decrease in contaminants in the dry season, even if the shallow contaminant source is continuous.

CONCLUSIONS

Recharge to the karstic, semiconfined Floridan Aquifer is strongly controlled, both in volume and location, by lateral variations in the lithology and hydraulic conductivity of the unconsolidated karst cover. This lateral variability is the result of the perforation of the clay semiconfining layer and the creation of vertical sand columns as a result of cover subsidence/collapse karst processes. Seasonal variations in recharge are exaggerated as lateral flow to the karst drains is impeded as water-table levels decline.

The karst-induced drains are very significant to assessments of ground-water contamination. The sand columns form direct hydraulic connections between the shallow water-table system and the Floridan Aquifer. Flow to the drains in the shallow aquifer can be tortuous as flow follows the thicker sands over clay-surface depressions. The drains occur with sufficient spatial frequency to influence even small sites (26 by 26 m). The sand columns are not well expressed by surface topography and represent only a very small percentage of total surface area (about 1%).

Ground-penetrating radar (GPR) surveys are very useful for mapping the topography of the clay surface and locating potential karst drains. During periods of higher water-table elevations, strong, negative self-potential (SP) anomalies are created over active drains. This combination of GPR and SP surface geophysical surveys provides a method for mapping subsidence features and determining which are hydraulically active prior to locating and installing monitor wells.

Acknowledgements--Part of this study was funded by a grant from the Southwest Florida Water Management District. The CPT and SPT data were collected by Diane Bloomberg as part of a geochemical study funded in part by Williams and Associates, Clearwater, Florida. Martin Clasen provided the GPR and SP field data. The GPR surveys were completed with an instrument loaned to USF by Detection Sciences of Carlisle, Massachusetts. Abdullah Alamri performed the grain-size analysis.

REFERENCES

Alamri, A., 1985, Geophysical and hydrogeological study of the effects of a storm-water retention pond on the Floridan aquifer: unpublished M.S. thesis, Univ. South Florida, Tampa, 248 p.

Bloomberg, D., Upchurch, S. B., Hayden, M. L., and Williams, R. C., 1986, Cone-penetrometer exploration of sinkholes: Stratigraphy and soil properties, in Beck, B., Wilson, W., and Balkema, A. A., eds., "Karst Hydrology: Engineering and Environmental Applications:" Boston, p. 145-152.

Bogoslovsky, V. A., 1972, The study of streaming potentials on fissured media models: Geophysical Prospecting, v. 20, p. 109-117.

Bogoslovsky, V. A., and Ogilvy, A. A., 1972, Deformations of natural electrical fields near drainage structures: Geophysical Prospecting, v. 21, p. 716-723.

Carr, W. J., and Alverson, D. C., 1959, Stratigraphy of middle Tertiary rocks in part of west-central Florida: U.S. Geol. Surv. Bull. 1092, p. 1-111.
Clasen, Martin J., 1989, Application of alternative surface geophysical techniques to hydrogeologic surveys: unpubl. M.S. thesis, Univ. South Florida, Tampa, 104 p.
Meyboom, P., 1966, Groundwater studies in the Assiniboine River drainage basin, Part I: the evaluation of a flow system in south-central Saskatchewan: Can. Dept. Mines, Tech. Surv., Geol. Surv. Can. Bull. 139.
Miller, J. A., 1984, Hydrogeologic framework of the Florida aquifer system in Florida and parts of Georgia, South Carolina, and Alabama: U.S. Geol. Surv. Prof. Paper 1403-B.
Ogilvy, A. A., 1967, Studies of underground water movement: Geol. Surv. Can. Rept. 26, p. 540-543.
Ogilvy, A. A., Ayed, M. A., and Bogoslovsky, V. A., 1969, Geophysical studies of water leakage from reservoirs: Geophysical Prospecting, v. 27, no. 1, p. 36-62.
Powers, J. P., 1981, Construction dewatering: A guide to theory and practice: John Wiley and Sons, Canada, 484 p.
Ryder, P. D., 1984, Hydrology of the Floridan aquifer system in west-central Florida: U.S. Geol. Surv. OFR 84-611.
Scott, T. M., 1988, the lithostratigraphy of the Hawthorn Group (Miocene) of Florida: Florida Geol. Surv. Bull. 59, 148 p.
Sinclair, W. C., 1974, Hydrogeologic characteristics of the surficial aquifer in northwest Hillsborough County, Florida: U.S. Geol. Surv. Water Res. Inves. 81-50, 19 p.
Sinclair, W. C., Stewart, J. W., Knutilla, R. L., Gilboy, A. E., and Miller R. L., 1985, Types, features, and occurrence of sinkholes in the karst of west-central Florida: U.S. Geol. Surv. Water Res. Inves. 85-4126, 81 p.
Sweeting, M. M., 1973, Karst Landforms: Columbia Univ. Press, New York, 862 p.

COASTAL KARST FORMED BY GROUND-WATER DISCHARGE, YUCATAN, MEXICO

WILLIAM BACK
U.S. Geological Survey
Water Resources Division
431 National Center
Reston, Virginia 22902
USA

In association with the 21st International Geologic Congress that met in Washington, D.C., July 1989, the Karst Commission sponsored a field trip to the Yucatan Peninsula of Mexico, (Fig. 1) led by William C. Ward, University of New Orleans, and me. The guide book* (Ward et al., 1985) for that trip and the references contained therein, especially (Back et al., 1984) along with a later article (Back et al., 1986) on the coastal geomorphology of the region provide the basis for this chapter. An additional resource in compiling the present paper is a brief summary of the environmental history of the Yucatan as discussed in Back and Lesser (1981). The purpose of the field trip was to provide an opportunity for the participants to 1) observe the environment and resources that the Mayan people had available to develop their civilization; 2) understand their water-management practices; 3) understand the process of carbonate deposition and diagenesis; and 4) observe coastal features that are dramatically being formed at the present time by encroachment of ocean water and the discharge of fresh and brackish water.

Beginning with the Mayans and continuing to the present time, the civilization of northern Yucatan has sustained itself largely on ground water. This has been a necessity, rather than a matter of convenience, because the abundant rainfall evaporates quickly or infiltrates rapidly. There are no rivers, or even morphologic expressions of them, on the northern Yucatan Peninsula. This is a flat, low-lying, semi-arid, limestone platform, which has a tropical savannah climate and is continuously swept by warm, moisture-laden breezes. However, because of the lack of any large-scale relief on the northern part of the peninsula, little or no rainfall occurs through most of the year. Whereas the region has up to 1500 mm of rainfall annually, most of it is restricted to the rainy period of May to September.

The environmental history of the Yucatan is in large part influenced by the properties of karst. The northern third of the peninsula, which is about 150 km wide, is an almost level karst plain underlain by horizontal Tertiary formations consisting mainly of limestone, marl, and gypsum. The formations range in elevation from sea level along the coast to slightly more than 30 m above sea level in the interior. There, fluted limestone is exposed over large areas and generally is pitted and scarred by solution depressions and small ridges. The limestone has extremely high permeability that causes rapid infiltration of rainfall with nearly

* Copies of "Geology and Hydrogeology of the Yucatan and Quaternary Geology of Northeastern Yucatan Peninsula" may be ordered from NOGS, c/o Department of Earth Sciences, University of New Orleans, Lakefront, New Orleans, Louisiana 70148 ($20).

International Contributions to Hydrogeology, Vol. 13 (1992)
© Verlag Heinz Heise, Hannover, FRG

Figure 1. Map showing the location of Yucatan Peninsula of southeastern Mexico. The study area is the coastal area of the state of Quintana Roo along the Caribbean Sea.

Figure 2. Aerial photograph of the east coast of the Yucatan showing two of the many crescent-shaped beaches formed by ground-water discharge.

simultaneous discharge of ground water to the ocean. The limestone is so permeable and movement through the system so rapid that not enough head is developed in the ground-water body to provide adequate storage in the aquifer for human needs. Indeed, the potentiometric surface of the northern Yucatan Peninsula is only a few meters above sea level throughout the region. Not only does the high permeability decrease the amount of freshwater available, it also makes the aquifer particularly susceptible to contamination by domestic and municipal sewage and waste, barnyard waste, and the natural decomposition of the abundant vegetation in the warm, humid environment. If the limestone were overlain by less permeable sediments, the sediments could serve as a filtering medium. This would tend to purify the water by decreasing the flow rate and providing longer residence time, thus permitting the decomposition of organic contaminants. In addition, the warm climate is particularly conducive to the growth of bacteria in polluted water. Widespread pollution has generated a host of endemic water-borne diseases.

Presently, one environmental problem in the Yucatan is the encroachment of saltwater from the ocean that surrounds the peninsula on three sides (Fig. 1). The large hydraulic conductivity along with the lack of high freshwater head permit an extensive body of saltwater to underlie the entire northern third of the peninsula. It is the existence of this saltwater body within the carbonate aquifer and its geochemical and geomorphological consequences that are the emphasis of this chapter.

The encroachment of saltwater into this coastal karst provides a dramatic example of how physical processes can combine with chemical reactions and biological activity to alter a carbonate coastline significantly. This coastline extends for about 150 km and is characterized by many crescent-shaped lagoons and beaches. The primary control is ground-water discharge that sets up the sequence of reactions that cause the dissolution. A secondary control is the network of fractures in the bedrock near the shoreline. The extensive dissolution that is occurring at the present time makes it easy to observe and evaluate the results of these physical, chemical, and biological processes.

Many years ago we hypothesized and others have now clearly demonstrated that the contact between the encroaching saltwater and the discharging freshwater is a highly reactive geochemical zone with significant hydrogeological consequences. The primary consequences are the increase in permeability and porosity caused by the resultant dissolution, which, in turn, lead to the development of many inlets, coves, lagoons, and crescent bays particularly along the east coast of Quintana Roo (Fig. 2). Based on an application of chemical thermodynamic principles, we and others have shown that simple physical mixing of two chemical types of water, both of which are at equilibrium or supersaturated with respect to particular carbonate minerals, can result in a mixed water that is undersaturated with respect to those minerals and, therefore, capable of dissolution. In a coastal environment, discharging freshwater mixes with the saline water that intrudes into the aquifer to form brackish water, part of which discharges as sub-marine or coastal springs and seeps (Fig. 3). A dynamic mixing zone occurs along the Yucatan coast because of

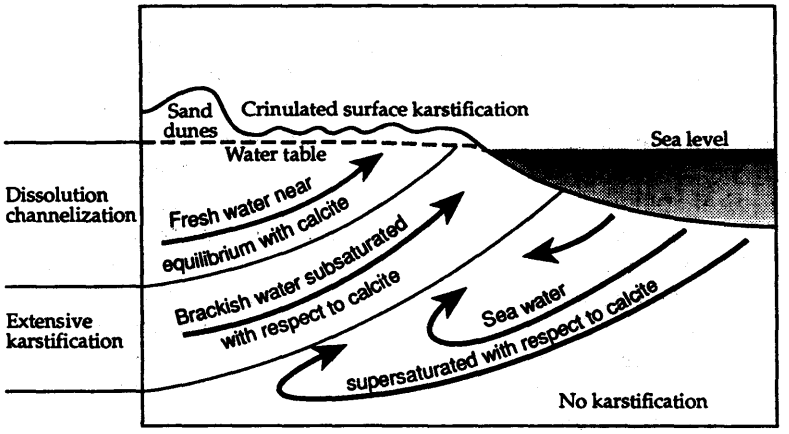

Figure 3. A schematic cross section showing the delineation of zones of karstification generated by ground-water flow patterns.

heavy rainfall that rapidly infiltrates the extremely permeable limestone and flows toward to the ocean where it discharges from the aquifer. Replenishment of the discharged brackish water generates flow from the ocean through the aquifer to form a subsurface zone of mixing. Although the land surface is karstified with micro-relief features and the shallow aquifer has undergone significant dissolution along the fractures in the bedrock, the most extensive karstification is in the zone of mixing. In this zone, the rock has lost all evidence of dissolution along the fractures and has the general appearance of "swiss cheese." No dissolution of limestone can occur in the fully saline portion of the aquifer because the seawater is supersaturated with respect to calcite. However, because of past fluctuations of sea level and the concomitant migration of the interface, dissolution has occurred earlier even where it cannot under the present hydrologic regime.

Based on geochemical and hydrogeologic principles, along with the theoretical calculations and field observations, we have demonstrated that the evolutionary development of this karstified coastline is as follows. After fracturing of the limestone, ground water flowing from the inland part of the peninsula was channeled along the dominant fractures in its effort to discharge along the coast. This flowing water mixed with the seawater that had encroached into the aquifer. The mixing formed a zone of mixing from which brackish water was discharged. The major flow, and, therefore, the major dissolution, occurred along fractures with the widest openings; this led to the establishment of major discharge points where dominant fractures intercepted the coast. These discharge points are the locations of incipient coves. The area of discharge and ground-water flow pattern became a self-perpetuating mechanism that expanded the area of dissolution to form a branching network of subsurface solution channels that coalesced to form a cave system, whose orientation was controlled by the original fracture pattern. As the dissolution continued, it removed the structural support for the one- to two-meter thick slab of limestone, the bottom of which is the cave roof and the top of which is land surface. Eventually there remained no support for the roof of the cave and it collapsed. This process is occurring at the present time. The roof blocks submerge into the brackish water where they are dissolved and the lagoon is enlarged. This enlargement opens the lagoon to wave action, permits physical erosion, and provides a habitat for marine organisms that cause further erosion by biological activity. These processes continue until the lagoon is an open body of water, separated from the adjacent lagoons by headlands that are gradually eroded by wave action until the coastline develops a serrated configuration, resulting in the coalescence of many crescent-shaped beaches (Fig. 2).

Because of the fluctuation of sea level and the migration of the mixing zone, we believe that throughout geologic time mixing zone dissolution has played a major role in the development of porosity. Mixing zone dissolution provides an alternative hypothesis for many of the features that have been referred to as "paleo-karst," generally attributed to sub-areal erosion as a function of sea-level change. We further expect that the dissolution phenomena occur in many other coastal limestone areas and that they will be recognized as a major geomorphic agent when other investigators study the development of porosity and chemistry of discharging ground water in coastal caves and lagoons.

REFERENCES

Back, W., Hanshaw, B.B. and Van Driel, J. N., 1984, Role of groundwater in shaping the eastern coastline of the Yucatan Peninsula, Mexico, in LaFleur, R.G., ed., Groundwater as a Geomorphic Agent: Boston, Massachusetts, Allen & Unwin, p. 281-293.

Back, W., Hanshaw, B.B., Herman, J.S., and Van Driel, J.N., 1986, Differential dissolution of a Pleistocene reef in the ground-water mixing zone in coastal Yucatan, Mexico: Geology, v. 14, no. 2, p. 97-192.

Back, W. and Lesser, J. M., 1981, Chemical constraints of groundwater management in the Yucatan Peninsula, Mexico, in Beard, L. R., guest ed., Water for Survival: J. Hydrol., v. 51, p. 119-130.

Ward, W.C., Weidie, A.E., and Back, W., 1985, Geology and Hydrogeology of the Yucatan and quaternary geology of Northeastern Yucatan Peninsula: NOGS, c/o Dept. of Earth Sciences, University of New Orleans, Lakefront, New Orleans, Louisiana, 160 p.

CONTROLS ON KARST IN COSTA RICA

SERGIO MORA
Department of Geology
Instituto Costarricense de Electricidad
Escuela de Geología
Univ. de Costa Rica, INGEOSA
Costa Rica

ABSTRACT

At least sixteen karst areas developed in limestone, ranging from Cretaceous to Pleistocene, exist in Costa Rica. Whereas their geologic background is known as a result of regional stratigraphic reconnaissance, with few exceptions, detailed explorations have not been accomplished. Information on basic geologic conditions, geomorphology, speleology, ecology, and hydrogeology is available from only the Barra Honda karst. General development of karst systems in Costa Rica has reached a young to moderately mature maximum stage with the occurrence of classic features.

INTRODUCTION

Geologically, Costa Rica is a relatively young country. The oldest rocks found are the Late Mesozoic Nicoya Complex, an ancient sea floor/mantle-derived suite of rocks. Since the Late Mesozoic, strong tectonic events have accreted, faulted, and uplifted this rock and allowed deposition of oceanic and neritic sediments. Climatic and bathymetric conditions allowed the development of broad carbonate platforms in which the karst terrains later formed.

In Costa Rica, most geologic processes are determined by the interaction of Cocos, Caribbean, and Nazca plates; interactions among these plates provide the energy source for all geotectonic activity. The entire continental region of Costa Rica is on the Caribbean plate, and several physiographic regions are associated with tectonic activity (Mora, 1983). Several peninsulas are interpreted as forming an outer arc along the Pacific coast. While recent interpretations of the D.S.D.P. results, however, suggest that this outer arc region does not represent an accretionary prism, new seismic reflection profiles show instead a slight accretion in front of the Nicoya shore (Seyfried, 1986, pers. comm.). The Pacific Margin has been affected by various periods of uplift, thus creating good bathymetric conditions for the development of carbonate platforms and reefs throughout the Tertiary and the Quaternary. The inner arc is composed of three major subdivisions:

1. The plutonic-volcanic axis, built by Miocene intrusives, intermediate-to-basic in composition and Neogene-Holocene volcanic rocks (Tournon, 1984).
2. A tilted sedimentary cordillera composed of folded and thrusted Tertiary turbiditic units (Eocene to Pliocene) (Mora, 1979; Mora and Valdés, 1983).
3. The inner-arc basins, consisting of northwest-trending depressions, mostly tectonic in origin and partially filled by continental and, in some cases, marine sediments.

International Contributions to Hydrogeology, Vol. 13 (1992)
© Verlag Heinz Heise, Hannover, FRG

In the case of Costa Rica, the back-arc basin extends throughout a large sedimentary basin, located on the Caribbean side, on which Tertiary sediments have been folded and subsequently covered by Quaternary sediments (Rivier, 1973).

Sediments and ophiolitic basalts originating from an oceanic rift formed a primitive island arc. This oceanic crust was strongly deformed during the Santonian by north-south compression, under which large "nappes" were generated (Baumgardner, 1984). These units represent the underlying basement for karst-generating limestones in some areas. By late Santonian, the Middle America Trench was established as an extensional-convergent margin (Auboin, 1979). During the Paleocene-Eocene, andesitic arc volcanism began to develop as a result of subduction processes. Post-Oligocene uplifting continued during the Pliocene and through the Quaternary, constructing the inner arc.

GEOLOGICAL ENVIRONMENTS OF KARSTIC LIMESTONE

All the limestone showing evidence of karst features was deposited in shallow marine environments. Episodic and intensive tectonic-orogenic activity, accompanied by rapid rate of uplift, occurred mainly during the Eocene through Miocene. Some areas with proper environmental conditions were hosts to reefs and other types of carbonate platforms which subsequently were uplifted. Sedimentologic, stratigraphic, and age data about most of the limestones of Costa Rica are already available. However, the absolute age of karst landscapes and their dissolutional events, are still poorly known. Karst regions in Costa Rica have been ranked from "a" representing the ones with the most well-developed features to "e" the least developed, depending upon the occurrence and degree of development of caves, aven, aquifers, sinkholes, and karren (lapiez), etc.

Upper Eocene Rocks

Reef limestone of Upper Eocene age is widespread throughout Costa Rica (Fig. 1). Most facies of this kind are composed of orbitoid foraminifers, algal nodulae (oncoids), and their synsedimentary erosional products. Boundstones, wackestones, grainstones, oosparite, and intrasparite are very common lithologies (Mora, 1979; Schprechman, 1984). The best known karst localities are Corredor (1 in Fig. 1), Cajón (3 in Fig. 1), and Damas (8 in Fig. 1), in which preliminary exploration has been conducted (Mora, 1979; Mora and Valdés, 1983; Asociación de Espeleólogos Costarricenses, 1986).

At Corredor (Asociación de Espeleólogos Costarricenses, 1986; Mora and Alvarado, 1986) a blind valley drains into a cave which sumps. Springs resurging at nearby Ciudad Neilly are intensively exploited for irrigation and domestic water use. At the Cajón site, several sinkholes, karren areas, cave entrances, and springs have been found, but no speleological exploration has yet been attempted. This site has been proposed to hold a major dam for hydroelectric power, and detailed geologic investigations have been carried out to determine the technical feasibility of that project (Mora, 1979; Grant, 1973; SNC-ACRES-TIL, 1979). The Damas karst is well known among local people who associate the cave with traditions and legends of lost people, appearances of ghosts, and volcanicism. However, scientific exploration

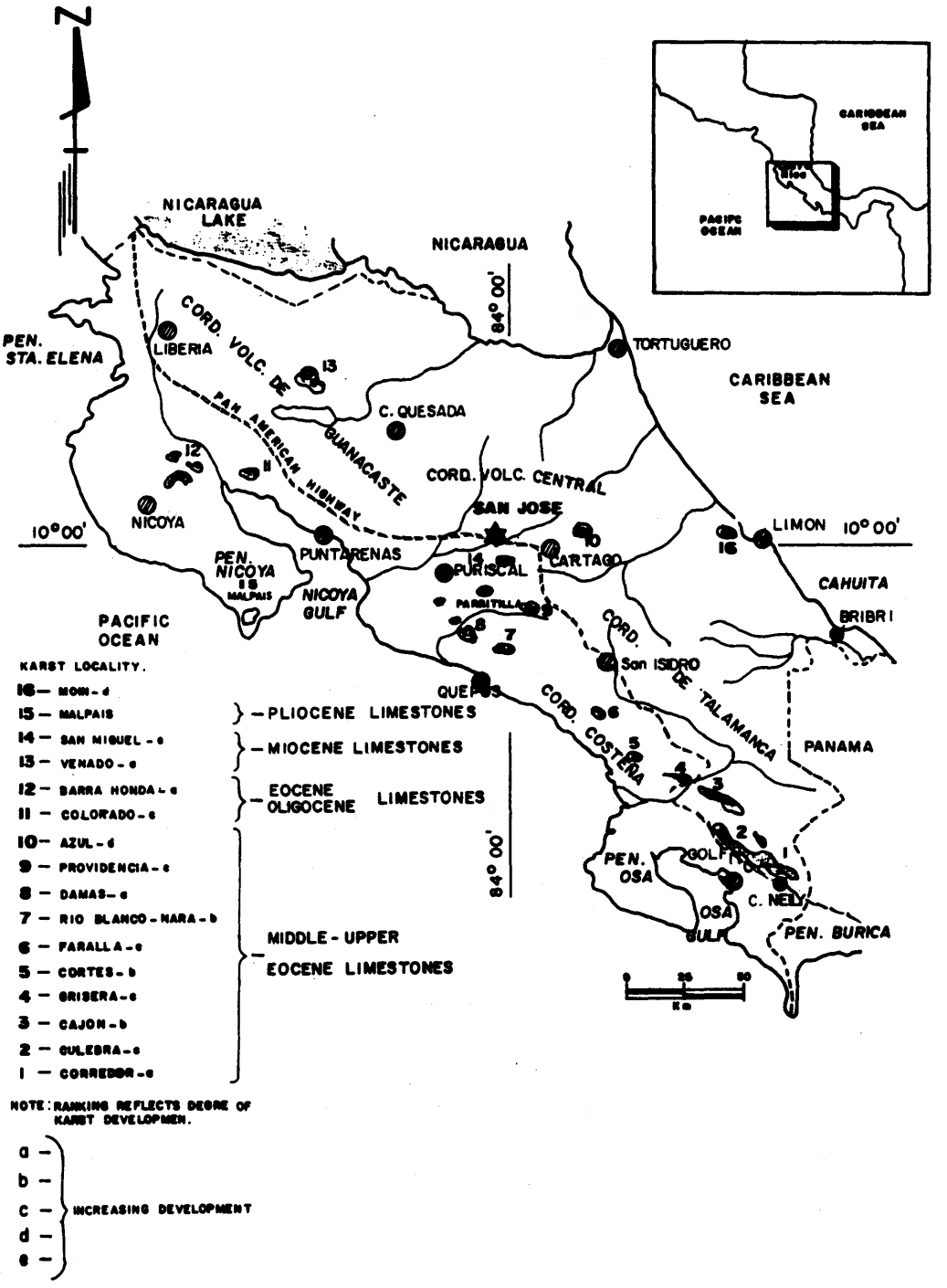

Figure 1. Karst localities in Costa Rica.

has not been done. It has an intricate system of galleries, halls, and several peripheral springs yielding considerable volumes of water (Mora and Valdés, 1983). Other karst localities in Eocene limestone have similar geologic conditions but little or no specific information is available.

Eocene-Oligocene Rocks

Two known outcrops of Eocene-Oligocene limestone occur in Costa Rica, of which the Barra Honda karst (12 in Fig. 1) is certainly the best known and best developed. It was designated a National Park in 1974. The other area of karst developed on Eocene-Oligocene limestone is Colorado (11 in Fig. 1). Both karst localities are developed in the Barra Honda Formation, composed of algal limestone, with biostroms and locally well developed bioherms as well as back-reef deposits. The age of this limestone is still the subject of controversy. Only a few guide fossils are known, and they suggest, as well as correlations with underlying clastic units, that the limestone is Eocene-Oligocene age (Mora 1978; Mora, 1981; Rivier, 1983). However, new tectonic and sedimentologic interpretations suggest that a more ancient Campanian-Maastrichtian age is possible (Calvo, 1987, pers. comm.). The arguments are not convincing yet, and the original interpretation of the age is accepted here.

The maximum thickness for the Barra Honda Formation is 250 m and it forms a resistant layer which typically caps the tops of hills (Fig. 2). The cap rocks represent remnents of the once continuous carbonate platform. These limestone caprocks have exposures no thicker than 90 m around the flanks of the hill. However, caves as deep as 200 m are known from the interior of Barra Honda cap hill. Apparently, the limestone is thicker within the interior of the hill than along the flanks (Fig. 3). This suggests the development of synsedimentary "cuvettes," where continuous deposition caused subsequent weight-subsidence in the center of the hills. The Barra Honda Formation is not overlain by any other unit, suggesting a rather continuous uplift of this area since deposition of the unit or a late development of the dissolution history and mechanisms.

Peripheral springs yield important volumes of water even during long dry seasons. Many of the springs are extensively exploited as a water supply by surrounding communities. Although the cave networks have been widely explored, and several springs occur at the base of the hills, no extensive groundwater reservoir nor conduit flow system has yet been discovered in the Barra Honda area. This karst area is also important from archaeological and anthropological viewpoints, since human remains and artifacts have been found inside and outside of the Barra Honda caves (Mora, 1979; Pereira, 1980; Mora, 1981).

Very little is known about the Colorado karst, even though its geologic context is already well understood (Rivier, 1983). However, behind its appearance as a moderately developed karst, important thickness of limestone layers could allow the development of more important features other than conspicuous karren, small caves, and sinkholes. No big springs have been reported from this site, which is mainly exploited as source of calcium carbonate for a cement factory and ornamental stone for architectural purposes.

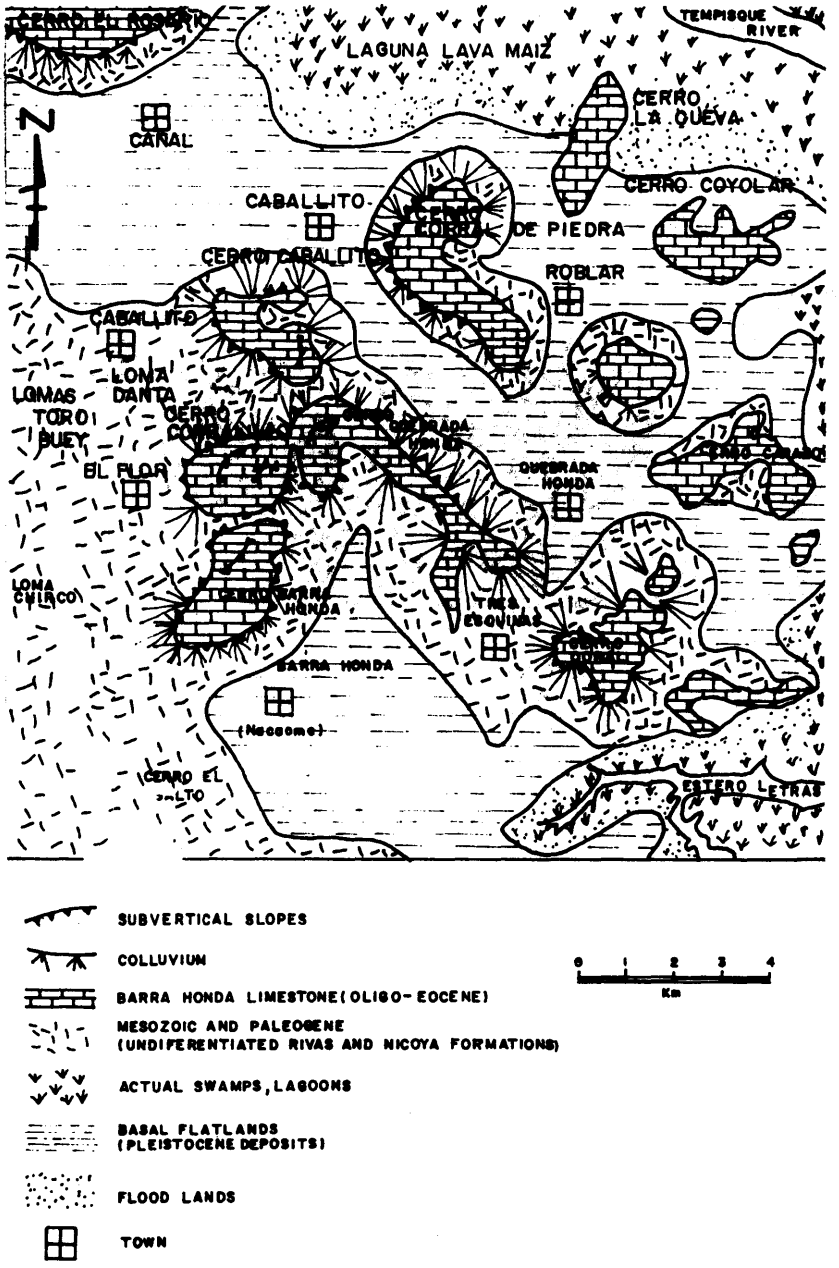

Figure 2. Geomorphologic map of Barra Honda and surroundings.

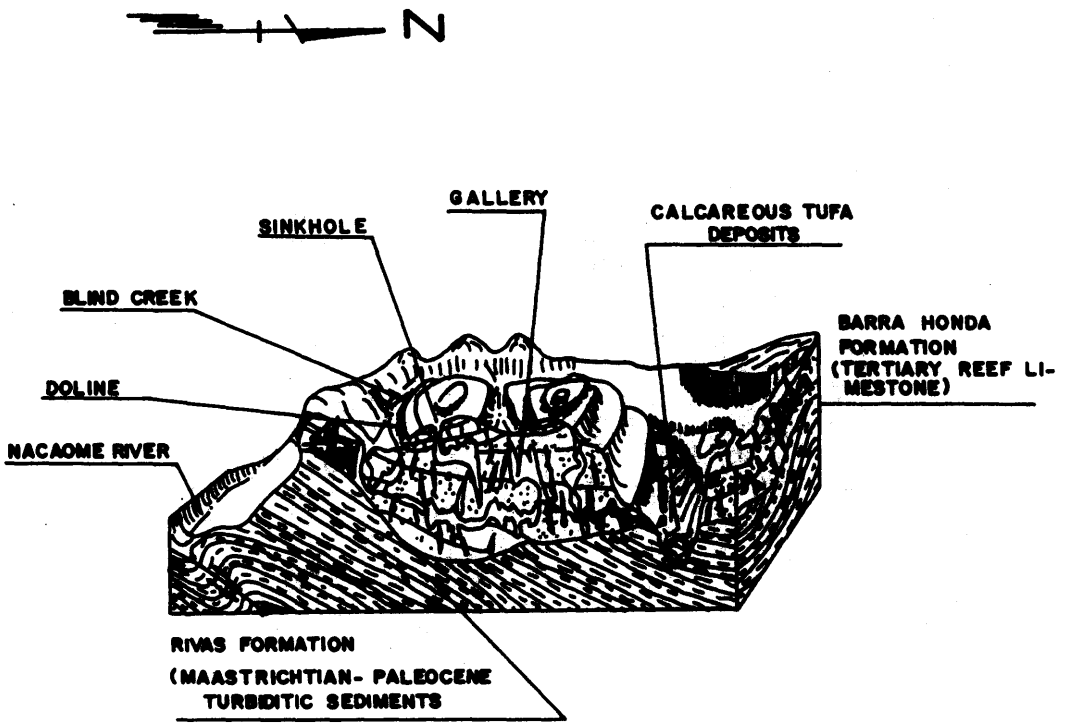

Figure 3. Barra Honda karst system (modified from Wells, 1973).

Miocene Rocks

Miocene limestone and calcareous clastic units, as well as other carbonate facies, developed on both Pacific and Caribbean shores (Fig. 1). Deltaic, transitional, and beach deposits were very widespread (Mora, 1979; Fischer, 1980, 1981). Miocene limestone is mostly composed of calcareous sandstone, conglomerate, and shale in beds ranging from a few centimeters to a few meters thick. Three main karst localities are developed in Miocene limestone: Venado (13 in Fig. 1), San Miguel (14 in Fig. 1), and Malpaís (15 in Fig. 1). The most important site among these is Venado, which has large caverns, sinkholes, and blind creeks. No deep underground scientific exploration has yet been undertaken.

Plio-Pleistocene Rocks

Due to the general climatic setting, shore configuration, and local bathymetry, coral reefs began to develop during the late Pliocene and exist locally along the Caribbean coast. The biggest and best known karst locality in Plio-Pleistocene coral limestone is Moin (16 in Fig. 1), which also contains abundant gastropods and other mollusc fossils. The thickness of this unit is about 40 m and shows microkarst features. Some hydrogeological studies have been carried out due to its exploitation as an aquifer (Losilla, 1979, pers. comm; Mora et al., 1980), since this aquifer feeds almost all needs for potable water of the port of Limón. Peripheral springs yield an average 100 L/s during low rainfall periods and more than 120 L/s after rainfall of considerable intensity. However, some pollution has been recently detected from salt intrusion, quarry activities, and old nearby trash deposits.

CONCLUSIONS

There are several important karst sites in Costa Rica, most of them developed on Tertiary reef, platform, and shore limestones, exposed mainly in the southern and western areas near the Pacific coast. Some of the karst areas are very well developed, displaying classic features such as karren, sinkholes, dolines, and caves. Present and future exploitation of springs for community water supply make these karstic limestones very important. However, exploration and detailed studies have been carried out only on very preliminary reconnaissances. Data are sparce and relatively inaccessible. Barra Honda is the only partial exception to this situation due to its designation as a National Park. Increasing economic interest, archaeological, economical, and recreational importance require urgent attention be given to the karst localities in order to better understand their geologic conditions, hydrogeology, and the development of these tropical karst landscapes.

Acknowledgements--I thank Dr. Stephen T. Wells from the University of New Mexico who made suggestions on how to improve the structure and content of this paper and Mrs. Rosibel de Jiménez, who reviewed the original manuscript.

REFERENCES

Asociación de Espeleólogica Costarricense, 1986, Descubren primer lago subterráneo del país. La República, 27/1/86, p. 3.

Auboin, J., 1979, Prémiers résultats des forages profonds dans le Pacifique au niveau de la Fosse du Guatemala. Leg. 67, Deep Sea Drilling Project. C. R. Académie des Sciences de Paris, v. 289, p. 1215-1220.

Baumgardner, P., 1984, Sedimentación y paleogeografía del Cretácico y Cenozoico del litoral pacífico de Costa Rica: Revista Geológica de América Central, Escuela Centroamericana de Geología, Universidad de Costa Rica, v. 2, p. 17-35.

Fischer, R., 1980, Recent tectonic movements in the Costa Rica Pacific coast. Tectonophysics 70, T25-T33.

Fischer, R., 1981, El desarrollo geográfico del Mioceno en Costa Rica. Ann. 2o. Congreso Latinoamericano de Paleontología; Proto Alegre, Brasil. p. 565-579.

Grant, L., 1973, Dye tests for Boruca limestone. Internal unpublished report. Alcoa-Hensley-Schmidt. Instituto Costarricense de Electricidad. 9 p.

Mora, D., Lucke, O., y Ramírez, O., 1980, Delimitación de la unidad hidrogeológica y zona de recarga de las fuentes de Moín. Informe interno, Instituto Costarricense de Acueductos y Alcantarillados, 12 p.

Mora, S., 1978, Estudio geológico de los Cerros Barra Honda y alrededores. Tesis de Bachillerato en Geología, Escuela Centroamericana de Geología, Universidad de Costa Rica, 188 p.

Mora, S., 1979, Estudios geológicos y geotécnicos para el Proyecto Hidroeléctrico Boruca. Departamento de Geología, Instituto Costarricense de Electricidad. Informe interno inédito. 2 vols. 275 p.

Mora, S., 1981, Barra Honda. Editorial EUNED, San José, Costa Rica, 92 p.

Mora, S., 1983, Una revisión y actualización de la clasificación morfotectónica de Costa Rica. Boletín de Vulcanología, v. 12, p. 18-36. Universidad Nacional Autónoma, Heredia, Costa Rica.

Mora, S., y Valdés, R., 1983, Estudio geológico-geotécnico para el Proyecto Hidroeléctrico Savegre. Departamento de Geología, Instituto Costarricense del Electricidad. 3 Vols. 375 p.

Mora, S., y Alvarado, G., 1986, Análisis geológico premilinar de la Fila de la Cal, en los alrededores de Ciudad Neilly, Costa Rica. Escuela de Geografía, Universidad Costa Rica. Informe interno inedito. 32 p.

Pereira, M., 1980, Le crâne numéro 2 de Barra Honda. Museé de l'Homme. Paris. 18 p.

Rivier, F., 1973, Contribución a la estratigrafía de la cuenca de Limón. Tercera reunión de Geólogos de América Central, p. 40-41.

Rivier, F., 1983, Síntesis geológica y mapa del área del Bajo Tempisque, Costa Rica. Informe Semestral Ene-Jun. Instituto Geográfico Nacional. p. 7-75.

SNC-ACRES-TIL; 1979, Feasibility study for the Boruca Hydroelectrical Project. Instituto Costarricense de Electricidad. 8 vols+5 sets of maps.

Sprechman, P., 1984, Estratigrafía de Costa Rica. Manual de Geología de Costa Rica. Editorial Costa Rica, San José, 88 p.

Tournon, J., 1984, Magmatisme du Mesozoique á l'actuel en Amérique Centrale: l'exemple du Costa Rica; des ophiolites aux andesites. These de Doctorat Es-Sciences, Universite Pierre et Marie Curie, Paris. 335 p.

Wells, S., 1973, A geological reconnaissance on Barra Honda karst. Cave Research Foundation, University of Cincinnati, Ohio. Unpubl. report. 35 p.

THE NORTHERN KARST BELT OF PUERTO RICO: A HUMID TROPICAL KARST

JOSEPH W. TROESTER
U.S. Geological Survey
PO Box 364424
San Juan, Puerto Rico 00936
USA

INTRODUCTION

In association with the International Symposium on Tropical Hydrology and Fourth Caribbean Islands Water Resources Congress that met in San Juan, Puerto Rico in July 1990, the American Water Resources Association sponsored a field trip to the northern karst belt of Puerto Rico. The guidebook for that field trip (Troester and Rodríguez-Martínez, 1990) served as the basis for this chapter. The purpose of the field trip was to 1) provide the participants with an opportunity to observe a middle Tertiary limestone sequence that is typical of the Caribbean region, 2) to observe humid tropical karst landforms, and 3) to obtain an understanding of hydrogeology on a tropical island.

GEOLOGY

Puerto Rico is the smallest and easternmost of the Greater Antilles islands (Fig. 1). The island has a central mountainous area composed of Late Jurassic to Eocene volcanic and sedimentary rocks and Late Cretaceous granodiorite plutons. Most of these rocks formed in an island arc setting. A section of nearly horizontal middle Tertiary limestones and terrigenous sediments unconformably overlies the older rocks along the north and south coasts and composes the northern and southern karst belts.

The northern karst belt is 10 to 20 km wide and extends along the northwest and north-central coast of Puerto Rico for 110 km (Fig. 2). It is the largest and most extensively studied karst area on the island (Monroe, 1976; Giusti, 1978). The rocks consist of a thick sequence of Oligocene to Pliocene limestones that dip 2 to 4 degrees to the north. The sequence is described by Monroe (1980a) and is divided into six formations (Fig. 3). In ascending order these formations are the San Sebastián Formation (a mostly nonmarine, fine-grained clastic unit); the Lares Limestone; the Cibao Formation (a heterogeneous unit that includes the Montebello Limestone Member and an informally defined clastic upper unit); the Aguada Limestone; the Aymamón Limestone; and the Camuy Formation (a limestone with clastic units). These formation names have been debated: some authors prefer to use the names Los Puertos Limestone and Quebradillas Formation for the Aguada Limestone and Camuy Formation, respectively (Frost et al., 1983; Moussa et al., 1987). Regional geologic maps of the area have been produced by Briggs and Akers (1965), Monroe (1980a), and Giusti (1978) (Fig. 4). Geologic maps, drawn at a scale of 1:20,000, are available for most of the island. Similar sequences of middle Tertiary limestones can be found throughout the Caribbean, including in Florida and on Cuba,

International Contributions to Hydrogeology, Vol. 13 (1992)
© Verlag Heinz Heise, Hannover, FRG

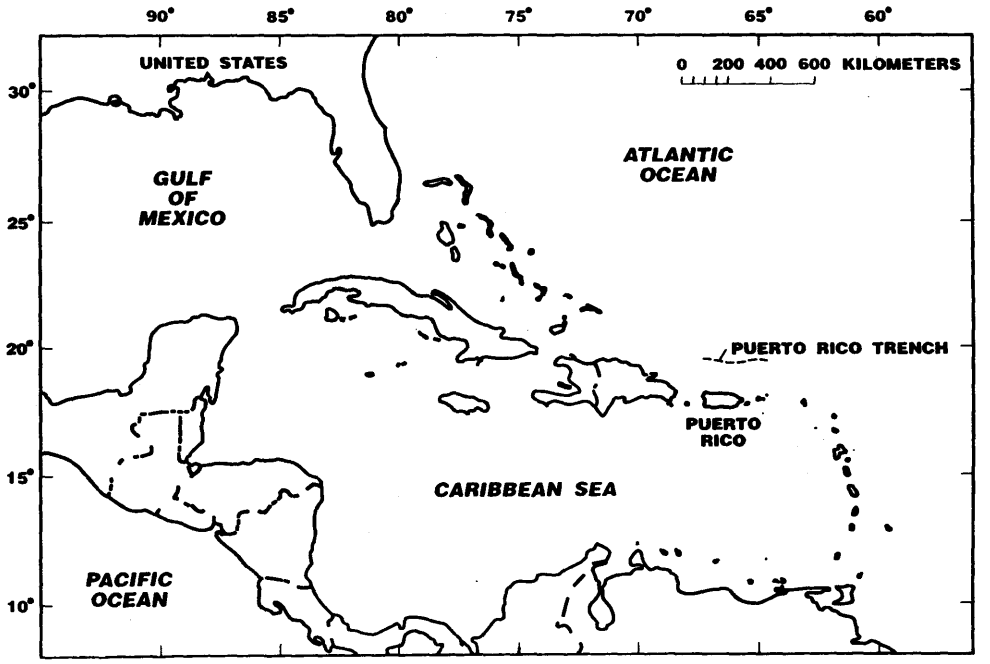

Figure 1. Map showing the location of Puerto Rico (adapted from Monroe, 1980b).

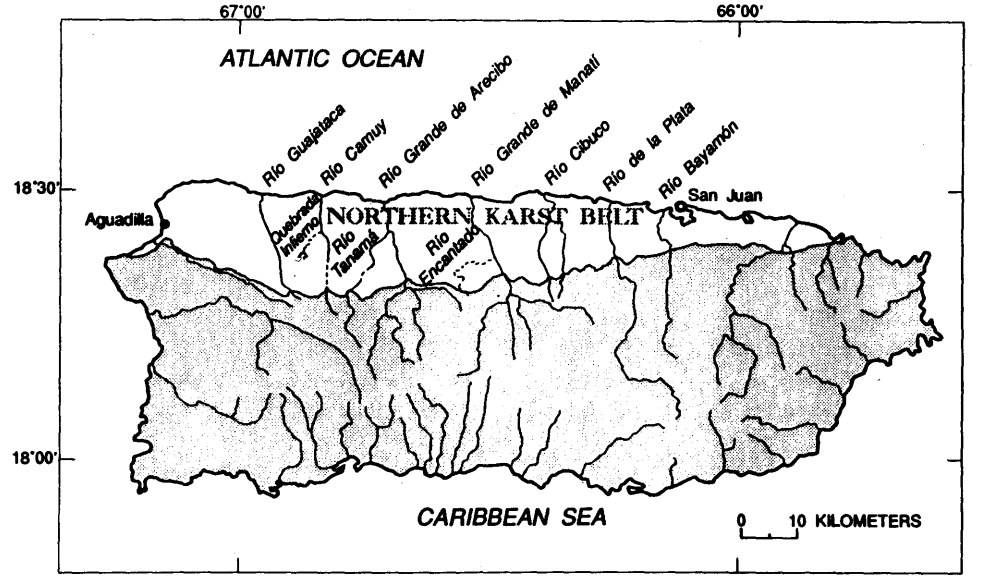

Figure 2. Map showing the northern karst belt of Puerto Rico (adapted from Giusti, 1978).

Hispaniola, Jamaica, the Yucatán Peninsula, and the limestone islands of the Lesser Antilles.

CLIMATE

Puerto Rico has a humid tropical climate, with nearly constant temperature and easterly trade winds. The average annual temperature in the northern karst belt is 26°C; the difference between the average temperature for the coldest month (February) and the hottest month (August) is less than 4°C. Precipitation is usually brief and intense. Precipitation patterns in Puerto Rico are a result of the orographic effect of the central mountain range on the easterly winds. Precipitation in the northern karst belt ranges from a low of less than 1500 mm along the northern coast to over 2500 mm at the southern edge of the karst. Precipitation occurs throughout the year, but a relative dry season occurs from January to April. Rainfall is normally heaviest in May, August, September, and October (Calvesbert, 1970).

GEOMORPHOLOGY

The northern karst belt of Puerto Rico is internationally known for its variety of karst landforms, including cone karst, tower karst, river caves, and deep gorges. These karst landforms have been described by Meyerhoff (1938), Doerr and Hoy (1957), Kaye (1957), Thrailkill (1967), Monroe (1976), Day (1978), Giusti (1978), Torres-González (1983), and Troester et al., (1984; 1987).

Cone and Tower Karst

Many different names have been proposed for the surface karst features in the humid tropics. Two main types of humid tropical karst landforms exist: cone karst (also known as Kegelkarst, cockpit karst, and fengcong) and tower karst (also known as Turmkarst and fenglin) (Sweeting, 1973, p. 273; Troester et al., 1987). This classification of humid tropical karst does not consider the shapes and genesis of the individual landforms. Cone karst is composed of many closely spaced cone- or tower-shaped hills separated by deep sinkholes with very little level ground (Monroe, 1970). Tower karst is composed of isolated limestone hills separated by flat areas often covered with alluvium or other detrital sand (Monroe, 1970; Yuan, 1985; Williams, 1987).

The cone karst with the highest relief in Puerto Rico is found on the Lares Limestone and on the Montebello Member of the Cibao Formation (Fig. 4). The cone karst in this area has been described by Monroe (1976) and Troester et al., (1987). The depressions are round or oval; have steep concave, sometimes vertical, sides; have a depth of tens of meters; and are separated by cone-shaped hills connected by sharp ridges (Fig. 5). The Arecibo Observatory, the largest radio telescope in the world, is built inside a depression in the cone karst (Fig. 6). The cone karst of Puerto Rico is similar to other karst areas in the Caribbean, including the cockpit karst of Jamaica (Versey, 1972), the Cave Branch karst in Belize (Miller, 1987), and the Cevicos karst region of the Dominican Republic (Palmer, 1983; Troester et al., 1984; 1987).

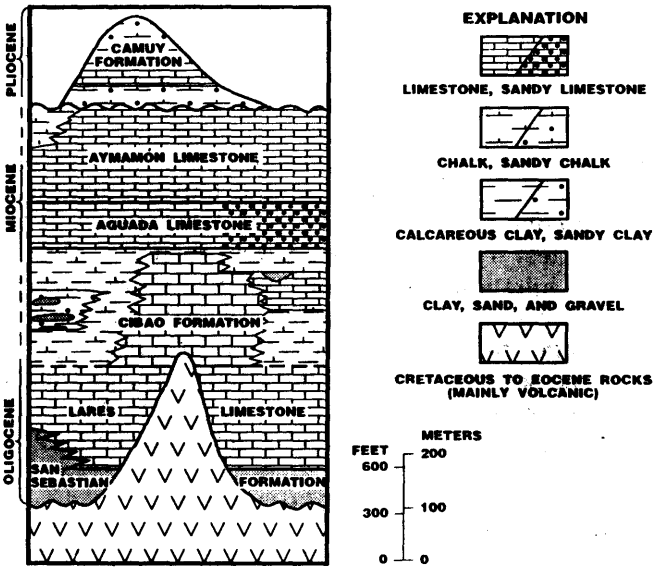

Figure 3. Columnar section of middle Tertiary rock in northern Puerto Rico (adapted from Monroe, 1976).

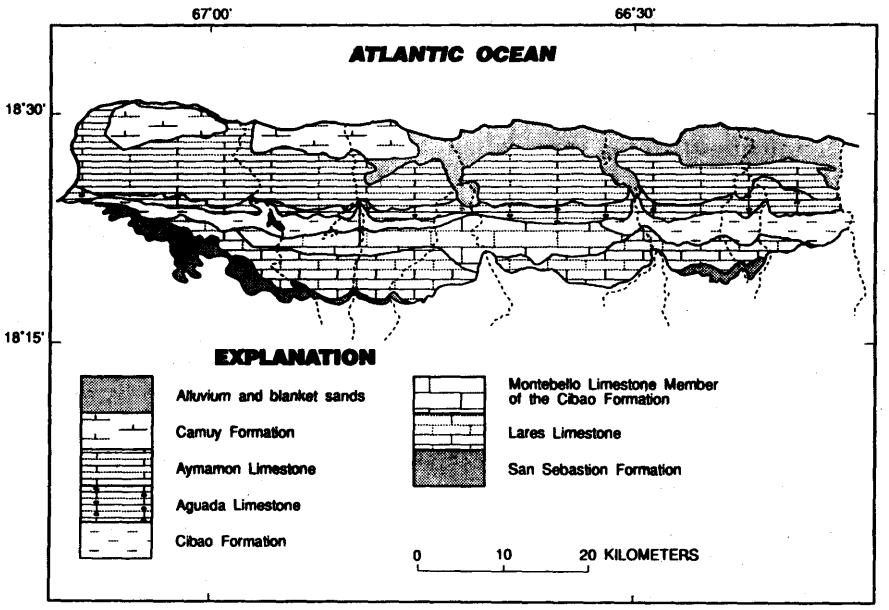

Figure 4. Geologic map of the northern karst belt of Puerto Rico (from Giusti, 1978).

Figure 5. A photograph of an area of cone karst east of Blue Hole, in Hatillo, Puerto Rico.

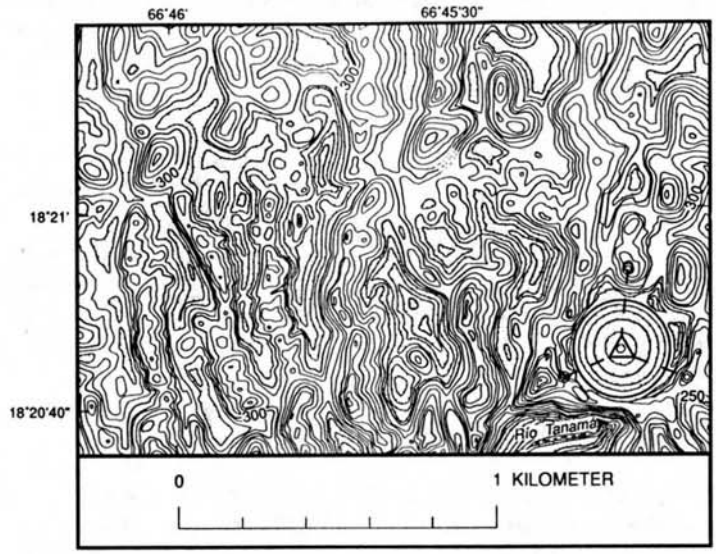

Figure 6. Topography from a section of the Bayaney quadrangle, Puerto Rico topographic map showing typical cone karst. The Arecibo Observatory is located in the lower right corner. The Río Tanamá flows into a cave south of the Arecibo Observatory. The areas inside of depression contours are shaded for clarity. The contour interval is 10 m.

The tower karst in Puerto Rico is best developed on the Aymamón Limestone (Figs. 7 and 8), but it is also developed on the Aguada Limestone (Fig. 4). In these areas, the isolated hills of limestone usually rise about 30 m above the blanket sands. The sides are very steep and rugged, but not vertical like the sides of some classic tower karst hills. In Puerto Rico and much of the Caribbean, the karst towers are usually called mogotes.

The blanket sands between the mogotes were probably deposited during the Pliocene, when dissolution had already begun in the underlying carbonate rocks. The blanket sands accumulated in the depressions and began to weather to their current composition of quartz sand and clay residuum (Briggs, 1966). This clayey soil provided a medium for plants, which produced CO_2 by root respiration. In addition, the clayey soil provided a reservoir for CO_2. Miotke (1973) found that the soil atmosphere in the wet, clayey, blanket sand ranged from 1.5 to 7 % CO_2. This level of soil CO_2 is much higher than is possible on the almost bare limestone slopes of the mogotes. Water that percolates down through the blanket sands becomes enriched in CO_2 and can dissolve more limestone than the water that soaks into the mogotes. As a result, more limestone is dissolved below the blanket sands than in the surrounding mogotes. As the limestone below the blanket sands dissolves, the sand and clay move down into the underlying cavities by piping, which occasionally causes catastrophic sinkhole collapses in the overlying blanket sands (Miotke, 1973).

In Puerto Rico, the sediment supply and the sediment carrying capacity of the underlying drainage system determine whether cone or tower karst will develop in a particular area. If the underground drainage system can remove all the insoluble sediment supplied to the sinkhole, then cone karst will develop. If the drainage system cannot remove all the insoluble sediment supplied to the sinkhole, gradually the sinkhole will fill with sediment and the area will develop into tower karst. The exact source of the insoluble material does not appear to matter. Most of the mogote karst in Puerto Rico is surrounded by blanket sand deposits. However in the area of San Juan, the mogotes rise out of more recent alluvial fan deposits. Monroe (1976) discussed an area called El Salto, where storm runoff from the Cibao Formation flows down dry stream valleys and carries insoluble material from the Cibao Formation into an area of cone karst developed in the Aguada Limestone. Evidently, the underground drainage system has been incapable of carrying this sediment out of the area. As a consequence, the depressions in the cone karst are slowly filling and the area is becoming tower or mogote karst.

River Caves, Deep Gorges, and Alluviated Valleys

Other significant geomorphic features of the northern karst belt of Puerto Rico include the caves and rivers that cross the karst from the interior of the island to the Atlantic Ocean. The caves of Puerto Rico have been cataloged and described by Monroe (1976). The rivers (Fig. 2) have formed caves, gorges, and valleys through which they flow by transporting large quantities of undersaturated, allogenic water onto the carbonate rocks. Four rivers currently cross the karst in caves or very narrow gorges or canyons: the Río Encantado Cave System (a tributary of the Río Grande de Manatí), the Río Camuy, the Río Tanamá, and the Río

Figure 7. A photograph of mogotes rising out of a pineapple field on the blanket sands, near Cruce Davila, Barceloneta, Puerto Rico.

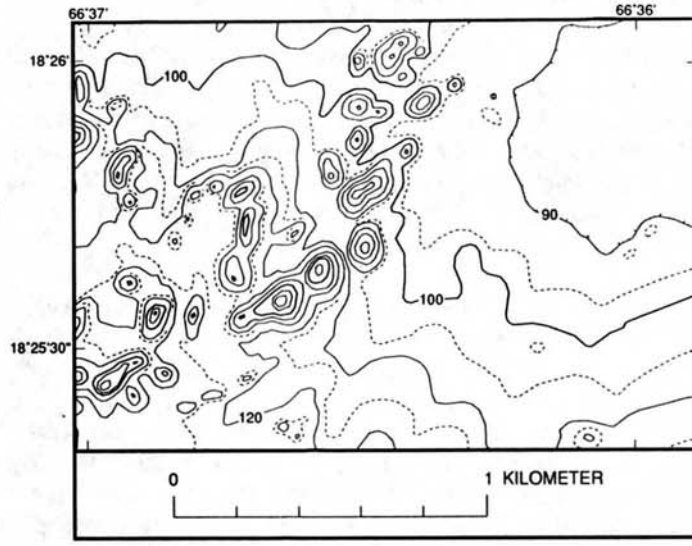

Figure 8. Topography from a section of the Barceloneta quadrangle, Puerto Rico topographic map showing typical mogote karst. The areas inside of depression contours are shaded for clarity. The contour interval is 10 m, supplementary contours at 5 m are dashed.

Guajataca. The remainder of the rivers, such as the Río Grande de Arecibo, and the Río Grande de Manatí, cut across the karst belt in wide alluviated valleys.

The rivers in the first group cross the limestone in systems of cave passages and narrow gorges (which may be collapsed cave passages). These cave systems often include older, upper-level passages that were formed by the same river and then abandoned as the area was uplifted and as sea level fluctuated. With time, the upper passages were dissected by surface lowering and collapse. Remnants of these passages are found in the hills around and above the active river passages and gorges.

One such cave system is the 20 km long Río Encantado in the northern karst belt, which has recently been explored and mapped (Courbon et al., 1989). The Río Encantado currently appears to have only a 4 km^2 catchment area on the insoluble rocks of the interior of the island. The river may have had a larger catchment area in the past, part of which has since been pirated by the Río Grande de Arecibo or the Río Grande de Manatí. The stream on this small catchment area sinks into a short cave in the Lares Limestone and has been dye-traced through two caves, to the Los Cafios valley, where it appears in the Río Encantado Cave System. The river continues north, in the direction of the regional dip, until it reaches the contact with the overlying Montebello Member of the Cibao Formation. From there, the cave turns east and follows the strike to emerge in the valley of the Río Grande de Manatí at a spring called Aguas Frías.

The Río Camuy begins in the interior of the island on pre-Oligocene rocks, where it has a 30 km^2 drainage area. As the river flows north toward the ocean, it enters the karst belt and follows a 3 km long, 150 m deep, alluviated, blind valley before it sinks at Blue Hole. It is not possible to follow the river into the cave at this point because the entrance is blocked by sediment and debris. About 1 km to the north the river appears inside the 10 km long Río Camuy Cave System in the Lares Limestone. The Río Camuy Cave System has been mapped and described by Gurnee and Gurnee (1974) and Torres-González (1983). Eventually, the cave is blocked and the river flows through a flooded passageway until it resurges 3 km to the north of the blockage. On the surface, the Río Camuy flows to the ocean in a deep, narrow gorge that Monroe (1976) suggests is a collapsed cave.

The Quebrada Infierno Cave System is the only major cave system in the northern karst belt that is not developed in the Lares Limestone. This cave system developed at the contact of the Cibao Formation and the overlying Aguada Limestone. The Cibao Formation near the cave system consists predominantly of marl and chalk and contains up to 36% insoluble residue. Because the formation contains a high percentage of insoluble material, caves seldom develop in the Cibao Formation. During heavy rains, water follows normally dry streambeds to the north, along the regional dip. When these streams reach the outcrop of the Aguada Limestone, which forms a low line of hills, the water follows the contact between the formations under the Aguada Limestone, often to reappear in a karst window or series of karst windows. These karst windows are floored by the less soluble Cibao Formation, and are surrounded by hills of the Aguada Limestone. There are many

different caves in this system that are separated by karst windows. The longest single cave is Quebrada Number 8, which is 1.5 km in length. "La Cueva de Camuy," a short portion of this cave system, has been opened to the public as a show cave. The final resurgence of the stream is at Boca del Infierno (the Mouth of Hell). At this point the stream, still following the contact between the Cibao Formation and the Aguada Limestone, flows into the Río Camuy gorge.

The rivers that cross the karst in alluviated valleys include the Río Grande de Arecibo, the Río Grande de Manatí, the Río Cibuco, the Río de la Plata, and the Río Bayamón. These rivers currently have higher discharges and sediment loads than the ones that flow through caves and narrow gorges. The larger rivers may have once crossed the karst belt in caves or narrow gorges like the smaller rivers, as indicated by the many old trunk passages scattered throughout the karst area that are now disconnected from the rivers that formed them.

During the Pleistocene, when the sea level was lower than today, most of the rivers of Puerto Rico cut deep valleys near the coast. As the sea level rose, these valleys were filled with alluvial material transported by the rivers from the interior of the island. This infilling is thickest (up to 70 m (Monroe, 1976)) and widest (greater than 1 km) near the shoreline. Therefore, most of the rivers in Puerto Rico have a much wider flood plain near the coast than they do only a few kilometers inland.

HYDROGEOLOGY

The aquifers in the limestones exposed in the northern karst belt are the most important ground-water reservoirs on the island of Puerto Rico. A hydrogeologic study of this area was conducted by the U.S Geological Survey in cooperation with the Commonwealth of Puerto Rico (Torres-González and Wolanksy, 1984; Rodríguez-Martínez, 1991). Fifteen test holes ranging in depth from 365 to 2,574 feet that penetrated most of the middle Tertiary sequence were drilled as part of this study. A dual-tube drilling method was used, which allowed retrieval of continuous lithologic cores, measurement of head, estimates of hydraulic properties, and collection of water samples and borehole geophysical logs. The paleontology, mineralogy, and petrology of the cores were analyzed by Hartley (1989), Schlarlach (1990), and Ward et al., (1991) at the Department of Geology and Geophysics of the University of New Orleans. The final phase of this hydrogeologic study is currently in progress and consists of developing a series of ground-water flow models. The hydrogeology of the northern karst belt has been defined by three main hydrologic units: an artesian aquifer, a confining unit, and an unconfined aquifer.

The artesian aquifer attains its maximum transmissivity in the area between the Río Grande de Arecibo and the Río Grande de Manatí, where it is mostly composed of the Montebello Limestone Member of the Cibao Formation and the Lares Limestone. East and west of this area, these limestones grade laterally into increasingly terrigenous sedimentary rocks that are less productive as aquifers. The recharge for this aquifer appears to be autogenic water, precipitation that falls in the outcrop area of the Lares Limestone and the Montebello Limestone Member of the

Cibao (Fig. 4). However the Río Encantado flows through a cave in this supposed recharge area of the artesian aquifer. The Río Encantado may be intercepting a portion of the artesian aquifer recharge and discharging it through a spring to the Río Encantado de Manatí. It is also possible that the Río Encantado is a losing stream and forms an integral part of the recharge to the artesian aquifer.

The confining unit is mostly comprised of the lower part of the informal upper member of the Cibao Formation. In northwestern Puerto Rico, the confining unit also includes strata in the middle and lower parts of the Aguada Limestone. The confining unit is composed of marl, claystone, fine-grained wackestone, and clayey, fine-grained sandstone.

The unconfined aquifer is mostly composed of the Aguada and Aymamón Limestones and locally includes surficial deposits, such as alluvium, that are Pliocene to Recent in age. A saline-freshwater interface is encountered at the base of the unconfined aquifer near the coast. Pumping has caused the saline water to move inland, and water supplies in some locations are threatened.

Most of the recharge for this aquifer comes from autogenic water, precipitation that falls on the outcrop area of the Aguada and Aymamón Limestones (Fig. 4). Some recharge may occur from the underlying artesian aquifer, although this recharge is normally minor because the permeability of the confining unit is low. Occasionally, flow from the artesian aquifer to the unconfined aquifer occurs through improperly constructed artesian wells.

Springs are frequent discharge points for the unconfined aquifer. Most of these are diffuse springs, such as La Cambija and Zanja Fría between the Río Grande de Arecibo and the Río Grande de Manatí (Zack and Class-Cacho, 1984; Guzmán-Ríos, 1988). However, conduit flow does exist in the unconfined aquifer, as evidenced by a few conduit springs, such as Ojo de Guillo and Maguayo (Guzmán-Ríos, 1988).

SUMMARY

The geology, climate, geomorphology, and hydrogeology of the northern karst belt of Puerto Rico are similar to many areas throughout the Caribbean and elsewhere. In Puerto Rico, researchers have had opportunities for study that have not been possible in other parts of the tropics. It is hoped that the work in Puerto Rico can help researchers understand the hydrogeology of humid tropical karst. Recently a joint project between the U.S. Geological Survey and the British Geological Survey has begin to compare the hydrogeology of the karst of Caribbean Islands.

REFERENCES

Briggs, R. P., 1966, The blanket sands of northern Puerto Rico: Third Caribbean Geological Conference, Kingston, Jamaica, 1962, Transactions: Jamaica Geological Survey Publication 95, p. 60-69.

Briggs, R. P., and Akers, J. P., 1965, Hydrogeologic map of Puerto Rico and adjacent islands: U.S. Geolgoical Survey Hydrologic Investigation Atlas HA-197, scale 1:240,000.

Calvesbert, R. J., 1970, Climate of Puerto Rico and U.S. Virgin Islands, revised: U.S. Environmental Science Services Administration, Climatography of the United States 60-52, 29 p.

Courbon, P., Chabert, C., Bosted, P., and Lindsley, K., 1989, Atlas of great caves of the world: Cave books, St. Louis, 369 p.

Day, M. J., 1978, Morphology and distribution of residual limestone hills (mogotes) in the karst of northern Puerto Rico: Geological Society of America Bulletin, v. 89, p. 426-432.

Doerr, A. H., and Hoy, D. R., 1957, Karst landscapes of Cuba, Puerto Rico, and Jamaica: The Scientific Monthly, v. 85, p. 178-187.

Frost, S. H., Harbour, J. L., Beach, D. K., Realini, M. J., and Harris, P. M., 1983, Oligocene Reef Tract Development: Southwestern Puerto Rico: Sedimenta IX, University of Miami, Miami Beach, Florida, 144 p.

Giusti, E. V., 1978, Hydrogeology of the karst of Puerto Rico: U.S. Geological Survey Professional Paper 1012, 68 p.

Gurnee, R. H., and Gurnee, J., 1974, Discovery at the Río Camuy: Crown Publishers, New York, 183 p.

Guzmán-Ríos, S., 1988, Hydrology and water quality of the principal springs in Puerto Rico: U.S. Geological Survey Water-Resources Investigations Report 85-4269, 30 p.

Hartley, J. R., 1989, Subsurface geology of the Tertiary carbonate rocks, northwestern Puerto Rico: M.S. thesis, University of New Orleans, New Orleans, Louisiana, 214 p.

Kaye, C. A., 1957, The effect of solvent motion on limestone solution: Journal of Geology, v. 65, p. 35-46.

Meyerhoff, H. A., 1938, The texture of karst topography in Cuba and Puerto Rico: Journal of Geomorphology, v. 1, p. 279-295.

Miller, T., 1987, Fluvial and collapse influences on cockpit karst of Belize and eastern Guatemala, in Beck, B. F., and Wilson, W. L., eds., Karst Hydrogeology: Engineering and Environmental Applications: Proceedings of the Second Multidisciplinary Conference on Sinkholes and the Environmental Impacts of Karst, A. A. Balkema, Rotterdam, p. 53-58.

Miotke, F. D., 1973, The subsidence of the surface between mogotes in Puerto Rico East of Arecibo: Cave and Karst, v. 15, p. 1-12.

Monroe, W. H., 1970, A glossary of karst terminology: U.S. Geological Survey Water-Supply Paper 1899-K, 26 p.

Monroe, W. H., 1976, The karst landforms of Puerto Rico: U.S. Geological Survey Professional Paper 899, 69 p.

Monroe, W. H., 1980a, Geology of the middle Tertiary formations of Puerto Rico: U.S. Geological Survey Professional Paper 953, 93 p.

Monroe, W. H., 1980b, Some tropical landforms of Puerto Rico: U.S. Geological Survey Professional Paper 1159, 39 p.

Moussa, M. T., Seiglie, G. A., Meyerhoff, A. A., and Taner, I., 1987, The Quebradillas Limestone (Miocene-Pliocene), northern Puerto Rico, and tectonics of the northeastern Caribbean margin: Geological Society of America Bulletin, v. 99, p. 427-439.

Palmer, R., 1983, The Dominican Republic, A brief study of the caving potential: Caves and Caving, no. 21, p. 25-27.

Rodríguez-Martínez, J., 1991, The hydrogeologic framework of the northern coastal province aquifer system of Puerto Rico: in Gómez-Gómez, F., Quiñones-Aponte, V., and Johnson, A. I., eds., Aquifers of the Caribbean Islands: American Water Resources Resources Association Monograph 15, p. 5-16.

Scharlach, R. A., 1990, Depositional history of Oligocene-Miocene carbonate rocks, subsurface of northeastern Puerto Rico: M.S. thesis, University of New Orleans, New Orleans, Louisiana, 242 p.

Sweeting, M. M., 1973, Karst landforms: Columbia University Press, New York, 362 p.

Thrailkill, J. V., 1967, Geology of the Río Camuy Cave area, Puerto Rico, in Gurnee, J., ed., Conservation through commercialization, Río Camuy development proposal: National Speleological Society Bulletin, v. 29, no. 2, p. 35-37.

Torres-González, A., 1983, Hydrologic study of the Río Camuy Cave System, Puerto Rico: M. S. thesis, Univeristy of Puerto Rico, Mayagüez, Puerto Rico, 115 p.

Torres-González, A., and Wolansky, R. M., 1984, Planning report for the comprehensive appraisal of the ground-water resources of the north coast limestone area of Puerto Rico: U.S. Geological Survey Open-File Data Report 84-427, 32 p.

Troester, J. W., and Rodríguez-Martínez, J., 1990, North coast karst limestone and ground-water characteristics, in Larsen, M. C., and Veva, T. D., eds., Field trip guide: International Symposium on Tropical Hydrology and Fourth Caribbean Islands Water Resources Congress, San Juan, Puerto Rico, July 1990, p. 1-19.

Troester, J. W., White, E. L., and White, W. B., 1984, A comparison of sinkhole depth frequency distributions in temperate and tropical karst regions, in Beck, B. F., ed., Sinkholes: their geology, engineering and environmental impact: Proceedings of the First Multidesciplinary Conference on Sinkholes, A. A. Balkema, Rotterdam, p. 65-73.

Troester, J. W., Back, W., and Mora-Castro, S. C., 1987, Karst of the Caribbean, in Graf, W. L., ed., Geomorphic Systems of North America: Geologic Society of America, Centenniel Special Volume Number 2, p. 347-357.

Versey, H. R., 1972, Karst of Jamaica, in Herak, M., and Stringfield, V. T., eds., Karst: New York, Elsevier Publishing Company, p. 445-466.

Ward, W. C., Scharlach, R. A., and Hartley, J. R., 1991, Controls on porosity and permeability in subsurface Tertiary carbonate rocks of northern Puerto Rico, in Gómez-Gómez, F., Quiñones-Aponte, V., and Johnson, A. I., eds., Aquifers of the Caribbean Islands: American Water Resources Resources Association Monograph 15, p. 17-23.

Williams, P. W., 1987, Geomorphic inheritance and the development of tower karst: Earth Surface Processes and Landforms, v. 12, p. 453-465.

Yuan Daoxian, 1985, New observations on tower karst: Proceedings of the First International Conference on Geomorphology, Manchester, England (also published by the Institute of Karst Geology, Guilin, China 14 p.)

Zack, A. L., and Class-Cacho, A., 1984, Restoration of freshwater in the Caño Tiburones area, Puerto Rico: U.S. Geological Survey Water Resources Investigations Report 83-4071, 33 p.

CHECKLIST FOR HYDROGEOLOGICAL ASSESMENTS IN KARST AREAS

CARLO F. BONI
Dipartimento di Scienze della Terra
Università degli Studi di Roma "La Sapienza"
C.N.R. - Centro di Studio per la Geologia dell'Italia Centrale
Piazza Aldo Moro
00185 Roma
Italy

INTRODUCTION

This checklist has been prepared as a guide to illustrate the hydrogeological characteristics of karstic regions. It is a selection of relevant items, all essential for the description of hydrogeological features. Each item can be developed according to the level of knowledge acquired. The aim of this list is: 1) to promote the standardization of regional studies in karst areas, in order to make any comparison easier and better and 2) to make the level of knowledge acquired clear and to stress the lack of information in certain fields. This checklist was prepared for large-scale regional studies and is not suitable for detailed studies or for demonstrating specific characteristics of small areas.

OUTLINE FOR CHECKLIST

Section A - GEOGRAPHY
Section B - CLIMATIC CONDITIONS
- Ba - Temperature
- Bb - Precipitation

Section C - MORPHOLOGY
Section D - GEOLOGICAL FEATURES
- Da - Stratigraphy and lithology
- Db - Structural features
- Dc - Fractures

Section E - HYDROGEOLGICAL SETTING
Section F - KARSTIC AQUIFERS
Section G - GROUND-WATER RECHARGE
Section H - BASE LEVELS
Section I - WATER-POINTS INVENTORY
- Ia - Quantity of data available
- Ib - Quality of data available
- Ic - Regime of discharge

Section L - WATER LEVEL
Section M - OVERLAND RUNOFF
Section N - HYDROGEOLOGICAL BALANCE AND WATER-RESOURCES ASSESSMENT
Section P - ADDITIONAL INVESTIGATIONS

International Contributions to Hydrogeology, Vol. 13 (1992)
© Verlag Heinz Heise, Hannover, FRG

DETAILED CHECKLIST

Section A - GEOGRAPHY

Basic information, such as these listed, are needed.

A1 - Nation, region, and more
A2 - Area (km^2)
A3 - Latitude
A4 - Orographic conditions (mountains, plateaus, coastal plains, and others)
A5 - Range of altitude (m)
A6 - Vegetation and soils

Section B - CLIMATIC CONDITIONS

It is advisable to describe the quantity and quality of basic data available, with special concern for the distribution of meteorological stations. The lack of stations in areas of high altitude commonly results in an underestimation of the amount of precipitation.

Ba - Temperature
  Ba1 - Mean temperature at different altitude
Bb - Precipitation
  Bb1 - Number of stations available and area covered (km^2)
  Bb2 - Approximate period over which data have been recorded (years)
  Bb3 - Range of mean annual precipitation
  Bb4 - Mean annual precipitation (mm) over the area
  Bb5 - Precipitation regime (% of mean annual precipitation)
    Spring (%) Summer (%) Autumn (%) Winter (%)
  Bb6 - Snowfall
  Bb7 - Additional information (rainy days, intensity of precipitation, insolation)

Section C - MORPHOLOGY

The morphological description is relevant to demonstrate the degree of surface and subsurface karst development. The description should reflect the level of understanding; therefore, the items listed below are generalized.

C1 - Surface karstic features
C2 - Subsurface karstic features
C3 - Any quantitative determination (index of cavern development index of excavation, index of subsurface karstification)
C4 - Paleokarst

Section D - GEOLOGICAL FEATURES

A description of regional geology is often overlooked. The lack of this kind of information makes the comparison between regions difficult and does not provide understanding of the role played by geology in karst processes. The basic information needed to have, at least, an approximate idea of the geological situation is listed below. If sectors characterized by different geological situations exist in the region concerned each sector should be considered separately.

D1 - Uniformity of geological features; specify whether geological features are uniform over the area or if they vary significantly.

Da - Stratigraphy and lithology

In regional scale studies, detailed description of stratigraphy may be unnecessary; however, it is always necessary to summarize the stratigraphy and lithology from a hydrogeological aspect. Special attention should be given to the existence of less permeable beds and to the sedimentological environment.

Da1 - Dominant lithology of carbonate rocks (dolomites, dolomitic limestones, micritic or bioclastic limestones, coral reef)

Da2 - Stratification: thin bedded (10/15 cm)
thick bedded (20/50 cm)
irregular or massive stratification (more than 50 cm)

Da3 - Interbedding of non-karstic sediments within the carbonate series (marls, shales, clays sandstones, etc.) given as % of the total thickness

Da4 - Thickness of carbonate series

Da5 - Age

Da6 - Stratigraphical relationships between karstic and non-karstic formations acting as aquitards or aquicludes (metamorphic basement, argillaceous flysches, volcanic, terrigenous covers, etc.)

Da7 - Sedimentological environment of the carbonate series

Da8 - Stratigraphical or lithological log

Db - Structural features

The structural setting resulting from: 1) the regime and intensity of tectonic forces and 2) the aptitude of rocks (plastic or rigid) to faulting or folding. A strain regime tends to stretch rocks and to give rise to faulted structures and to a large-mesh network of vertical fractures. A stress regime tends to compress rocks and to give rise to faulted and folded structures and a close-mesh irregular network of fractures. Structural features can, therefore, range from a simple homocline to complexly faulted, folded, and overthrusted structures.

Db1 - General description of the regional structural features

Db2 - Tectonic phases (age and regime of forces)

Db3 - Cross sections

Dc - Fractures

Fracture analysis has been standardized for special studies of structural geology and quantitative hydrogeology. In regional assessment only general information on fracture patterns is needed.

Dc1 - Fracture network. Mean mesh dimension (in meters):
- very close (less than one)
- close (from one to ten)
- large (from ten to hundred)
- very large (several hundred)

Dc2 - Regime of forces in tectonic phases. Specify whether fractures resulted from a stress or a strain or from alternative stresses and strains. Fracture pattern seems to have relevant influence on the process of infiltration and overland runoff. Where the mesh is close, infiltration, uniformly distributed over the recharge area, seems to prevail over runoff; as a result the karst landscape is usually not spectacular. Where the mesh is large, runoff seems to prevail over infiltration, temporary or ephemeral streams flow over the karst surface towards closed depressions where water disappears; as a result the karst landscape is often spectacular.

Dc3 - Relevant information about relation between the type of fractures and the type of karst development.

Section E - HYDROGEOLOGICAL SETTING

The hydrogeological setting reflects the structural relation between karstic and less permeable formations. If the original continuity of karstic rocks, both horizontal and vertical, is maintained, a unique large hydrogeological unit extends over the region. If the continuity of carbonate rocks has been cut and the karstic body partitioned into several sectors, separate hydrogeological units can be identified. A hydrogeological unit consists of: 1) a continuous body of karstic rock bounded by non-karstic terrains (therefore, ground-water exchange between contiguous structures is reduced to a negligible value), 2) an exposed karstic surface, corresponding to the recharge area, and 3) one or more base levels, where karst aquifers discharge. The area ranges from a few tens to several thousand square kilometers.

E1 - Relation between structural geology and hydrogeological setting.

E2 - Hydrogeological units. Specify whether or not several separate hydrogeological structures have been identified.

Section F - KARSTIC AQUIFERS

In a karstic region, and in each hydrogeological structure, one or more karstic aquifers can be identified. A basal aquifer collects most of the ground water. Separate perched aquifers or confined aquifers may occur. A karstic aquifer is a reservoir, fed by infiltration, which discharges toward the base level. Recharge and discharge conditions and the physical properties of the reservoir are the controlling factors of ground-water dynamics and regime. In a regional study, physical characteristics of karstic reservoirs are generally not investigated, but special attention is given to the recharge and discharge conditions.

F1 - Main basal aquifer
F2 - Minor aquifers

Section G - GROUND-WATER RECHARGE

Recharge normally results from precipitation on the recharge area, additional contributions to the recharge may occur by runoff from non-karstic areas. The recharge may be either uniformly distributed over the area or concentrated on particular points or sectors, due to localized and diffuse absorption of overland flow or to morphological factors. Effective infiltration, given in mm/a, is the amount of water that reaches the aquifer from the surface. In favorable conditions the simplest way to evaluate effective infiltration is to divide the mean annual discharge of a hydrogeological unit by its recharge area. Effective infiltration may also be evaluated by alternative methods.

G1 - Recharge factors. Specify whether the recharge is due to precipitation only or to additional factors.
G2 - Recharge distribution. Specify whether recharge is evenly distributed or concentrated in specific places.
G3 - Effective infiltration. Specify:
- the extent of the investigated area, the mean annual precipitation, and the method used
- range of values, according to local precipitation, geological factors, and morphological conditions.

Section H - BASE LEVELS

Base levels are where ground water discharges to the surface. A regional study must identify base levels. In coastal areas, base level corresponds to sea level; the identification of discharge points is often difficult and discharge measurements are virtually impossible. The base level may be localized along the outer limits of a hydrogeological unit or within the unit itself. In continental areas the base level may be indicated by 1) a spring, 2) a stream or lake, or 3) any man-made withdrawal from karst aquifers. When a spring acts as base level, the discharge point is easily observable, the discharge is concentrated and easily measurable. Rivers and streams may act as base levels when the hydrogeological unit has been so deeply eroded that the river bed lies below the ground-water level. If this is the case, the base level is not easily observable and measurement is difficult. This is why the importance of ground-water contribution to river discharge is often overlooked. Ground-water contribution to river flows may be easily detected by hydrograph analysis. If continuous discharge records are unavailable, a series of discharge measurements along the river course may be taken. Relevant withdrawals from karstic aquifers occur mainly in densely populated areas or in mining regions.

H1 - Types of base levels. Specify the types of base levels identified and their relative importance within the region.

Section I - WATER-POINTS INVENTORY

Ia - Quantity of data available

The inventory of the main water points may be complete or incomplete; it may include only springs or discharges to rivers and man-made withdrawal also. It is advisable to give information about the type and the number of water points and discharge ranges.

Ia1 - Quality of data available

Ib - Quality of data available

The quality of discharge data may be good or unsatisfactory. It is advisable to specify:

- the most common kind of record taken in the region:
  - long-term continuous record
  - periodical
  - occasional
- the period over which data have been recorded

Ib1 - Quality of discharge data available

Ic - Regime of discharge

The regime may be illustrated by graphs or by simple generic classification (as regular, irregular, etc.) according to the data available.

Ic1 - Regime of discharge

Section L - WATER LEVEL

In free conditions, the water table is the surface dividing the aquifer from the overlying unsaturated rocks. The position of the water table, with respect to the ground surface, the range of fluctuation of the water level, and the hydraulic gradient are relevant factors for theoretical and practical purposes.

L1 - Average depth to water level (in meters)
- one to ten
- ten to hundred
- several hundred
- (water-level fluctuation)

L2 - Hydraulic gradient
- range of variation

Section N - HYDROCHEMISTRY AND ISOTOPE ANALYSIS

Hydrochemistry is the result of the rock-water interaction; it is strictly related to the aquifer's hydrodynamics and lithology. Karst waters may be contaminated by water or gases of different origin (evaporites, hydrothermal activity, etc.). Isotope hydrology is a unique tool in a regional study, because it provides a wide range of information which no other method can supply.

N1 - Hydrochemistry and isotope analysis:
- range of total dissolved solid in karst water
- saturation index with respect to carbonate numerals
- seasonal variation of the above mentioned values
- contamination by non-karstic waters and gases
- isotope analysis

Section O - HYDROGEOLOGICAL BALANCE AND WATER-RESOURCES ASSESSMENT

The hydrogeological balance and the water-resources assessment are the final purpose of a regional study. Any information on the method used, the area concerned, the results, etc., are always of great interest.

O1 - Hydrogeological balance
O2 - Water-resources assessment

Section P - ADDITIONAL INVESTIGATIONS

Other investigations carried out, such as ground-water modeling and environmental problems, not included in the list may be discussed in additional sections.

William Back
U.S. Geological Survey
431 National Center
Reston, Virginia
22092 USA

Janet S. Herman
Department of
Environmental Sciences
University of Virginia
Charlottesville, Virginia
22903 USA

Henri Paloc
Le Ranc St. Sebastian
d'Aigrefeuille
F.30140 Anduze
France

At its inception, the Commission on Hydrogeology of Karst of the International Association of Hydrogeologists (IAH) accepted the mandate of developing a scientific understanding of the hydrogeology of karst regions. This is the seventh volume toward realizing that charge. The purpose of this book is to describe hydrogeologic situations in diverse settings around the world. In each study, the understanding of a local scientific problem is demonstrated. Collectively, the chapters in this volume provide us all a broader perspective on the fascinating features and special problems of the hydrogeologic study of karst terrains.

The scientific challenges presented in the study of karst are many. The scientific problems associated with karst phenomena focus on understanding the physical, chemical, and biological processes that control the hydrogeologic behavior of karst terrains. The approach evident in this book reflects the belief that understanding hydrologic phenomena of karst can be gained by comparative evaluation of the relative significance of the various processes that control the formation of karst features and the consequent occurrence and movement of ground water. Any serious coverage of the myriad of karst features and the range of processes necessitates a global study of karst hydrogeology.

The 32 chapters of this book are the result of contributions made by 44 authors in describing the processes of karst formation and their control on the occurrence and movement of ground water in 31 settings around the world.

ISSN 0936-3912
ISBN 3-922705-94-4

Verlag Heinz Heise GmbH & Co KG, P.O.B. 610407, D-3000 Hannover 61, Germany